UNIVERSITY OF SOUTHAMPTON

FAILURE MECHANISMS FOR SMALL DIAMETER CAST IRON WATER PIPES

By

Phillipa Jane O'Shea

A THESIS SUBMITTED FOR THE DEGREE OF DOCTOR OF PHILOSOPHY

FACULTY OF ENGINEERING AND APPLIED SCIENCE

DEPARTMENT OF CIVIL AND ENVIRONMENTAL ENGINEERING

SOUTHAMPTON

AUGUST, 2000

ABSTRACT

FACULTY OF ENGINEERING AND APPLIED SCIENCE

CIVIL AND ENVIRONMENTAL ENGINEERING

FOR DOCTOR OF PHILOSOPY

FAILURE MECHANISMS FOR SMALL DIAMETER CAST IRON WATER PIPES

By Phillipa Jane O'Shea

Water companies have received intense adverse publicity recently due to high levels of water wastage resulting in costs to consumers. Extensive surveys and research studies have shown that the majority of this water loss occurs due to burst water distribution pipes, during the winter months. Failure most commonly occurred in cast iron, 100mm diameter pipes with lead run joints. Several mechanisms for these failures have been proposed. It was believed that frost heave loading was the prime factor responsible for these failures. Much of this research was carried out in climates suffering from severe winters, which does not reflect the UK climate. Traffic loading was another popular theory for the failure of water pipes. However, none of the research carried out to date has been able to conclusively substantiate a single mechanism to be responsible for pipe failure. Until this study a combination of loading effects and various associated pipe defects had not taken place. It was the aim of this thesis to demonstrate that it is a combination of loading effects and associated pipe defects that is responsible for pipe bursts, rather than a single mechanism as proposed so far.

Four main mechanisms were investigated; in-pipe water temperature; internal pressure; traffic loading and frost loading. The strength characteristics of cast iron lead run joints were measured by carrying out axial tensile tests on joints exhumed from the ground. A finite element programme, (LUSAS), was then used to model the joints and connecting pipe lengths realistically. 3D, elastic computer models were generated in order to apply the four different loading mechanisms. The effect of each mechanism was then analysed and the maximum principal stress was compared to the ultimate tensile strength of the material. Each loading condition could then be examined to see if it brought the pipe close to failure or not. The different loading conditions and defects were then combined to obtain the overall effect. The results showed that a combination of loading and defects is necessary to bring cast iron pipes to failure.

Acknowledgements

This thesis would not have been possible without the advice and help from a number of people. The lessons I have learnt from them will continue to help me in the future.

First, I would like to thank Professor Clayton for his wisdom, patience and gentle but insistent persuasion to finish and keep on the right path. Without your support and criticism I would never have been able to complete this thesis. You taught me to focus in on problems and how to break them down in order to make the solution clear.

I wish to express my gratitude to Dr Vicki Hope for helping me get started on my literature review and her advice on searching for good references. I would also like to thank Brian, Tony, Lee and Peter for helping with the experimental work, which formed an important part of my work. I must offer my humble appreciation to Dr Mullord and Dr Will Marsden for their patience and understanding with 'Lusas'. Thanks also to Dr Mulheron for his expertise on materials and pointing me in the right direction for material properties.

I would also like to thank Claire Ashton, Kate Dixon and especially Jeff Whiter for their provisions of data and papers. Also thank you to all the people who helped me on the site investigations. Thanks must also go to Jason and my family for supporting me throughout my PhD.

LIST OF CONTENTS

LIST OF TABLES

LIST OF FIGURES

Figure 5.13: Section of 2 joint model showing stresses at mid span with temperature loading and thin wall.

NOTATION

E = Youngs Modulus (N/mm^2)

L = Length (mm)

W = Load (N/mm^2)

α = Thermal Coefficient/°C

σ = stress (N/mm^2)

ρ = density (g/mm^3)

ν = Poisson's ratio

D = Diameter (mm)

r_1 = outside radius (mm)

r_2 = inside radius (mm)

S1 = major principal stress (N/mm^2)

S2 = intermediate principal stress (N/mm^2)

S3 = minor principal stress (N/mm^2)

Sy = stress in the global y direction (N/mm^2)

Sx = stress in the global x direction (N/mm^2)

Sz = stress in the global z direction (N/mm^2)

CHAPTER 1

INTRODUCTION

CHAPTER 1 – INTRODUCTION

Over the past five years water companies have suffered from unfavourable press comments, on water shortages in the summer, floods in the winter, pipe bursts and water leakage. Although the actual rates of losses vary greatly between the water companies, the awareness by consumers of the scale of the problem has had a detrimental effect on the overall image of the privatised water companies. As well as benefiting the customers, cutting water losses due to pipe bursts would have direct economic advantages to the companies. When the risk of failure is reduced, a significant saving can be achieved through a decrease in capital investment in large storage capacities.

Water companies have begun to address the problem by investing in research programmes to reduce leakage and identify causes as to why water distribution pipes burst. A major water company has supported the work undertaken in this thesis.

There are many reasons as to why pipes may suffer bursts and leakages. For example:-

- poor design and workmanship in the manufacture and laying of pipes, leading to over-stressing under normal operating conditions
- high internal pressures
- as a result of corrosion and overall weakening of the pipe materials
- due to differential settlements, arising from poor backfilling beneath the pipe
- through settlement of the underlying ground, where pipes pass over compressible or collapsing ground, or over areas of mining subsidence
- as a result of seasonal shrinkage or heave in clay soils, perhaps exacerbated by the presence or removal of trees in the vicinity of the pipe
- through extremes of temperature, especially frost and in-pipe water temperature
- as a result of lateral or vertical movements induced by adjacent construction trenching or tunnelling, alongside or below an existing pipe
- from changes in stressing and induced vibration through increased trafficking.

Several issues had to be addressed before investigation could begin. Firstly, the huge variety of categories of water pipes, in terms of material, location, size, age, jointing, depth, construction, installation, backfilling, surrounding soil type etc., meant that many potential factors, acting severally and also in combination had to be considered. Secondly, it was vital that the detailed mechanisms of pipe failures were understood. The practical necessity was then to identify "problem" pipes in the distribution system, either before they burst or, after the event, to facilitate the location of chronic leaks.

This study progressed in three stages:

⇒ to carry out a literature review to postulate the key factors that lead to pipe bursts, and the physical parameters that may govern these factors

⇒ to measure a range of identified parameters from in-service cast iron pipes

⇒ to investigate in detail the mechanisms of pipe bursts, using numerical modelling techniques, incorporating measured parameters.

A particular aspect of the research was to assess the cumulative or combined influence of a series of events or factors which, taken individually, would prove innocuous but, when acting together, could trigger a pipe burst.

On carrying out the literature review, it was found that research had been carried out in detail in many areas, but that no one area had been labelled as being the primary mechanism for burst pipes. Pipes bursting with the highest frequency were found to be small diameter cast iron water pipes with lead-run joints. The four main categories associated with the bursting of these pipes were in-pipe water temperature, internal water pressure, traffic and frost loading.

In-pipe water temperature relies on the joints in the pipe line being rigid. Data on the pull out strength of small diameter cast iron lead-run joints did not exist and needed to be investigated. This became the parameter that was measured from in-service cast iron water pipes. Chapter 3 describes how several 100mm cast iron lead-run joints were

excavated from various sites and cut from the pipe section for experimentation. This chapter details how the joints were prepared for testing, how they were tested and what the results showed.

The results from Chapter 3 allowed the numerical analysis to take place, which is described in Chapter 4. The four main load categories mentioned above were analysed individually, on a model of two joints and 3 connecting pipe lengths, using the Lusas finite element package. Each load mechanism was modelled using perfect pipe conditions. The results were compared to see which one was the main contributory factor. However, perfect pipes do not generally burst. Bursts occur when a defect or anomaly is present. What is of concern is any deviation from the ideal of construction, installation and pipe state. Linkage between actual field observation and modelling was an essential aspect of this thesis to ensure the relevance of the numerical analysis and its validity. Defects were introduced to validate the analysis further, by creating more realistic parameters for the model to work with. Uneven supports, manufacturing defects, corrosion pits and general degradation (pipe wall thinning), were added to the four different load models and analysed. Again these analyses were done on an individual basis to see which had the greater contributory effect. An assessment of the cumulative influence of all loads and defects was made, to establish whether they could trigger a pipe burst.

The conclusions from the literature review, results from the pull out tests and results from the numerical modelling are then discussed in Chapter 5. Conclusions and recommendations are given in Chapter 6.

CHAPTER 2

LITERATURE REVIEW

CHAPTER 2 – LITERATURE REVIEW

2.0 Pipe-failure mechanisms for cast iron water pipes

The problem of water loss from water mains failures is significant. On average, water loss is thought to be around 30% of the total water supplied, which equates to 174 litres per property per day or 3552 Mega litres per day (OFWAT 98-99 report). In 1981 there were 8,000 bursts in the Severn-Trent Water Authority's water mains system (Newport 1981), which is equivalent to about one burst for every four kilometres of main. The direct cost of the repairs of the system (at 1981 prices) was reported to be over 1 million pounds a year. The indirect costs due to flooding and traffic disruption are difficult to quantify, but likely to be significant.

For the purpose of this thesis water loss can be separated into two categories; bursts and leaks. Bursts represent structural failure of the pipe resulting in a visible escape of water at the surface. Leaks represent continuous water leakage, for example from deteriorated joints and hairline cracks, which can go undetected for long periods. Water pipe bursts and leaks not only cause financial loss but also have a damaging environmental impact. As water loss occurs, demand for water is increased causing more water to be extracted from rivers and bore holes. This may cause rivers to shrink, which could lead to destruction of aquatic wild life which will then affect the animal food chain that relies on that water source. Water is one of the most important factors in the environment and the conservation of its quantity and quality and its protection against the impacts of human activities has been recognised as an important social problem (Yevjevich & Starosolszky, 1998).

A review of suggested pipe-failure mechanisms is undertaken in this chapter. The growing importance of burst pipes and their effects are described. Previously published statistical, experimental and theoretical results describing the mechanisms that cause burst pipes are compared and discussed.

2.1 Introduction

The Office of Water Services (OFWAT) monitors all water companies within England and Wales. This organisation determines the price of water and records the performance of all water companies, including leakage rates. OFWAT set mandatory leakage targets from October 1997 for each water company (OFWAT 1997 report). As a result of this, a limit on the amount of water a company can lose through leakage has been specified. Any water company failing to curb their leakage to within the prescribed limit will have to pay financial penalties. Active research to investigate the causes behind water pipe bursts is therefore being carried out. This thesis forms a part of these investigations.

The majority of water loss in the UK is generated by the bursting of water distribution pipes (OFWAT 1999), a high proportion of which occur during the winter months (Arnold, 1960; Monie & Clarke, 1974; Newport, 1981; O'Day, 1982; Bahmanyar & Edil, 1982; Needham & Howe, 1981 &1984; Ciottoni, 1983 & 1985; Wettering, 1985; Habibian, 1994; Rajani and Zhan, 1996; and Zhan & Rajani, 1997). The frequency of bursts over the course of a year, within the South East of England, is shown in Figure 2.1. It can be clearly seen from the Figure 2.1 that the burst rate peaks during the winter months. Water distribution pipes do fail at other times of the year, but statistics have repeatedly shown that there is a definite peak in the months of November, December, January and February in the Northern Hemisphere (Arnold, 1960; Morris, 1967; Needham & Howe 1981 & 1984 and Ciottoni, 1985).

It is typically observed that the water distribution pipes with the greatest frequency of bursting (highest value after normalisation by total length) are 100mm (4-inch) cast iron distribution pipes, as can be seen in Figure 2.2 and 2.3 (Monie & Clarke, 1974; O'Day, 1982; Bahmanyar & Edil, 1982; Ciottoni 1983 & 1985; Svensson, 1990 and Habibian, 1994). These small diameter cast iron pipes generally fracture circumferentially, which suggests failure in beam bending, shear fracture or axial tension (Bahmanyar & Edil, 1982; Edil & Bahmanyar, 1983), but sometimes the failures are longitudinal (Arnold, 1960; Newport, 1981; O'Day, 1982 and Ciottoni, 1983). The distribution of failure type can be seen in Figure 2.4. Figure 2.5 shows typical locations of failure type. The

distribution system is mainly made up from cast iron pipes (about 85%) with the remainder of pipes being a mixture of ductile iron, concrete and plastic pipes (Fry & Rumsey, 1984). Cast iron pipes have been laid since early 1825, but the majority of cast iron pipes in use today were laid between 1890 and 1960; after 1960 ductile iron pipes were introduced (Jones, 1983; Fry & Rumsey, 1984 and Atkinson & Whiter, 1998). Because of the considerable age of the existing pipe network it is important to look at the history of water pipes, their design, manufacture and installation, to establish the condition, properties, and the environment they were subjected to. Past conditions are likely to differ from today's. The history of the development and the properties of cast iron water distribution pipes are discussed in section 2.2.1 and 2.2.2 respectively.

2.2 Cast iron water pipes and joints

The water distribution network in the UK has undergone continual development and addition since the early 19th century. With the rise and growth of water companies came the developments in the methods of conveying and distributing water. Significant parts of the network have long exceeded what would now be considered their design life. Although much of the older pipe continues to function well, in terms of water quality and structural and hydraulic integrity, the proportion of such pipe requiring maintenance or replacement can be expected to increase with time, or as conditions deteriorate. The various components of the distribution infrastructure, including valves and meters, have all undergone considerable development during the growth of the distribution network. In this research, focus is given to the distribution pipe and its joints.

In London, lead pipes and earthenware pipes were first used to distribute water from London Bridge to consumer's houses (Jones, 1983). As the water industry grew, lead pipes became too costly and wooden pipes were used as an alternative. The pipes were made by drilling out the core of elm or fir trunks (M.W.B., 1948). Adjacent sections were joined by tapers and sockets; the taper was covered with white lead (Stanton, 1936), and the socket was reinforced against splitting using an iron hoop. Wood was used within the distribution system well into the 19th century, but the service it gave was not satisfactory. Great care was needed to produce tightly fitting ends, but the tapering gave it less resistance to decay and pipes began to leak. The Metropolis Paving Act of 1817 (Taylor's

Act) required new water mains to be cast iron. Under the act companies were permitted to repair, rather than replace, their existing wooden pipes. The use of cast iron gradually superseded that of wood, with wood disappearing by the 1850s.

Grey cast iron pipes have been produced in various forms, such as statically cast, spun chill-mould and spun sand mould (Fry & Rumsey, 1984; Jones, 1983). Vertical pit casting in sand was patented in 1846 (Stanton, 1936) and was one of the first methods used to produce cast iron pipes (Fry & Rumsey, 1984). From 1922 spun casting progressively replaced pit cast pipes particularly during the decade of 1930 to 1939. From then on centrifugal casting in sand-lined moulds was used, eventually developing to centrifugal casting in metal moulds (the Delavaud process). The Delavaud process produced pipe of more uniform wall thickness than did pit casting. Grey Iron was used exclusively for casting prior to 1965, but has been almost totally superseded by ductile iron since about 1970 (Fry & Rumsey, 1984). Methods of joining adjacent pipe sections were also developed from tapered ends with a lead seal, to lead caulked semi-rigid joints, and then to flexible rubber gasket joints. Cast iron pipes mainly used spigot and socket semi-rigid joints, whilst ductile iron pipes used rubber gasket joints.

It may well be that the properties of cast iron pipes and joint characteristics need to be established, since it is likely that these can influence the way in which the pipes fail. However, since cast iron pipes were first introduced into the water distribution system, many different types of cast iron and joints have been produced (Jones, 1983). Although most structural failures occur in the pipe barrels between joints (Figure 2.5), the mechanical properties of joints have a significant influence on the stresses and moments experienced by pipes (Pearson, 1977; Singhal & Meng, 1982 and Jones, 1983). The general properties of cast iron and its many varieties are described in section 2.2.1. The mechanical properties of various ferrous joints and their characteristics are described in Section 2.2.2.

2.2.1 Metallurgy of cast iron

Cast iron is essentially an iron-carbon alloy containing other important elements such as silicon, maganese, sulphur and phosphorous, which modify the structure and properties of the resulting alloy (Angus, 1976). Cast iron is sensitive to variations in its chemical constituents and to the rate of cooling during casting (Morrogh & Williams, 1947 and Laing & Rolfe, 1960). As a result, the durability of a given cast iron pipe may be more dependent on its foundry and 'vintage' of production than on its age. Cast iron can be produced with varying quality, from white iron to grey iron, where the varying quality depends on the state of the carbon. The carbon may occur in the free state, as graphite, or as carbide cementite. In most iron, carbon occurs partly in each state. When the carbon occurs mainly in the free state (graphite) it produces a fracture which is dark grey or nearly black in colour. This type of iron is referred to as grey iron. When the carbon exists as cementite it produces a fracture which is silvery white. This form is termed white iron. The mechanical properties and general behaviour of a cast iron are considerably affected by the quantity and type of graphite present (Laing & Rolfe, 1960; Morrogh & Williams, 1974 and Fry & Rumsey, 1984). In all its forms grey iron is characterised by low ductility fracture properties in which failure strain under tensile loading is usually less than 1% (Jones, 1983).

Large quantities of free graphite result in a relatively weak iron. However, two irons having the same quantity of graphite can still exhibit different strengths. Iron containing long straight flakes of graphite will be weaker than one with short curled flakes of graphite. For this reason the inside surfaces of pipes show less strength than the outside, as they contain larger coarser flakes of graphite resulting from slower cooling of the inside of the cast (Laing & Rolfe, 1960 and Morrogh & Williams, 1974). If the carbon present is cementite, then the iron produced will be much harder and stronger than grey iron. The process of graphitisation takes place mainly but not completely after solidification (Laing & Rolfe, 1960). The quantity of graphite can be controlled in two ways, by silicon content and the rate of cooling, each process entirely independent of the other (Morrogh & Williams, 1947). A higher silicon content or a slow rate of cooling will produce grey iron. A rapid rate of cooling or low silicon content produces a harder, white iron, which is closely grained (Morrogh & Williams, 1947 and Laing & Rolfe, 1960). In pumps and

engines it can be used to withstand high abrasion due to its hardness characteristics. White iron is not used in water pipes because of its lack of flexibility. For these reasons it will not be discussed further.

Ductile iron is another form of cast iron, which was used for water pipes from about 1960 (Jones, 1983). In grey cast iron, the graphite forms lamellar flakes, which cause brittleness in the material by interrupting the ferrite matrix. In ductile or nodular cast iron, the graphite forms spheriodal nodules. These nodules break up the continuity of the metal to a smaller extent than the flakes in grey iron. The nodules do not act as significant stress raisers, resulting in greater strength and ductility than in grey iron (Laing & Rolfe, 1960), and relatively good shock-resistance (Morrogh & Williams, 1947).

2.2.1.1 Grey Irons

Grey irons contain large amounts of graphite in the form of flakes or lamellae of various sizes, depending section size, rate of cooling and the melting procedure (Morrogh & Williams, 1947 and 1948). These graphite flakes confer upon the material its characteristic properties of non-ductility, non-malleability, good machinability and comparatively low strength (Fry & Rumsey, 1984; Rumsey & Dorking, 1984). The compressive strength of grey iron is three to four times its tensile strength (Salvadori & Singhal, 1977), and failure of these materials may occur in a brittle manner at all temperatures, because of the internal stress concentrations associated with the graphite flakes. Impact values (the ability to withstand shock load) are therefore quite low in grey cast iron, and decrease as temperature is reduced (Scholes, 1979). Grey cast iron never exhibits a truly elastic response (Fry & Rumsey, 1984 and Angus, 1976). At the first application of load, some plastic deformation takes place (Figure 2.6). During cyclic loading the stress-strain curves follow different paths during loading and unloading (hysterisis, Figure 2.7). The major reason for this behaviour is that the metal matrix is not continuous but broken up by the presence of graphite flakes which behave as voids in tension (Salvadori & Singhal, 1977). Pit cast grey iron is also susceptible to fissure corrosion. General corrosion is likely, resulting in a thinning pipe wall thickness.

2.2.1.2 Ductile Iron

As mentioned in section 2.2.1.1 cast iron is sensitive to variations in its chemical constituents and to the rate of cooling during casting (Morrogh and Williams, 1947 and Laing and Rolfe, 1960). An addition of cerium into molten grey iron results in a transformation of graphite type on solidification. Instead of lamella flakes of graphite forming, spheriodal nodules develop, creating ductile iron. Treatment with magnesium also results in ductile iron with a much wider range of composition than cerium treatment (Laing & Rolfe, 1960; Fry & Rumsey, 1984).

A practical means of producing ductile cast iron on an industrial scale was developed in the late nineteen forties, based on the addition of specific elements to the alloy (Morrogh and Williams, 1948; Gagnebin *et al.*, 1949). Ductile iron pipes began to be used in the water industry soon after the introduction of this production method, but only became widespread in the 1960s and 1970s (Newport, 1981; Fry & Rumsey, 1984; Lackington and Burrows, 1994). Ductile iron pipes had an advantage over grey iron pipes, as they could be produced at a lower cost without sacrificing strength, due to less material being used.

2.2.2 Joints

The role of efficient jointing is to link pipe lengths together and keep them watertight. Considerable attention has in recent years been given to the design and evolution of improved pipe joints. Joints fall into four categories, which can be classed as Rigid Joints, Semi-rigid Joints, Flexible Joints and Special Joints.

Rigid joints can be defined as those which are incapable of suffering any appreciable flexure or longitudinal movement without developing leakage or complete failure e.g. full turned and bored joints (Figure 2.8). Semi-rigid joints generally use lead as the sealing medium, the lead being introduced into the jointing space in the molten condition, or as lead wire or wool (Figure 2.9 & 2.10). Flexible joints provide for longitudinal as well as deflective movement without loss in joint performance (Figure 2.11). Special joints used in cast iron pipes include the lug type turned joints, bored joints, ball and socket joints and expansion joints, where they are used mainly on large diameter pipes.

Although many types of pipe materials have been used in pipe networks (cast iron, ductile iron, concrete and plastic are the most common) the most abundant pipe material is cast iron (Jones, 1983; Rumsey & Dorking, 1984; Fry & Rumsey, 1984). Systems incorporating cast iron pipes have been built up over many years, so that the pipes within them represent a variety of manufacturing techniques, strength and dimension specifications, and design criteria (Taki & O'Rourke, 1984). The majority of small diameter cast iron pipes use semi-rigid joints and for this reason the properties of semi-rigid joints will be discussed in more detail.

The most abundant joint used was the spigot and socket lead-caulked joint used on cast iron pipe (Bruzzon & Lonardo, 1996). The installation and characteristics of these joints are discussed in section 2.2.2.1. With the introduction of ductile iron pipes in the 1960's came another design of joint, the rubber gasket joint. Flexible rubber gasket joints were used in buried pipeline construction to improve its structural performance when subjected to differential ground movements arising from different causes. Rubber gasket joints are still manufactured and used for many sizes of pipe. Large diameter pipes still use flanged, bolted or welded joints. The majority of the existing network has lead-caulked joints on cast iron pipes or rubber gasket joints on plastic and ductile iron pipes. The behaviour of these two types of joint is very different and research has been carried out to highlight the differences between the two, which will be described below.

2.2.2.1 Lead Caulked Joints

From the introduction of the Metal Act in 1817 up to 1960, the Run or Molten Lead Joint was the most popular form of coupling for all types of cast iron main. The successful connection of a lead run semi rigid joint is a skilled and arduous job. These types of joints were manufactured both with flat spigot ends and ridged spigot ends. Boden (1936) has described the process of joint connection. The lead used was pure and sufficiently superheated to allow free running of the joint. Impure lead tended to give a hard metal that could not be caulked. The socket and spigot was prepared by cleaning the jointing surfaces. The spigot was placed in the socket and centralised when necessary with wedges. The wedges were removed once the inserted yarn supported the spigot.

Each strand of the oakum was cut several inches longer than the circumference of the pipe, so that the edges overlapped. The overlaps were staggered and the oakum pushed into the base of the caulking space by a narrow flat tool called a yarning iron. This was then compacted by hammering. For a 100mm (4-inch) diameter pipe, a depth of $1^1/_2$ to 2 inches was left for the lead. Boden (1936) describes the lead being poured into the joint along an asbestos lined metal clip around the mouth of the socket. Figure 2.12a, b, c, & d show the various stages of this process. Afterwards the runner was removed and the exposed lead face would be caulked using the specially formed tools of appropriate size (Figure 2.13a, b, c & d). It was said that if the yarn was not carefully introduced obstruction of the bore could occur (Boden 1936). If not properly compacted the yarn might allow the lead to run into the pipe and if unevenly caulked a lead space of irregular depth might result (Boden, 1936). It was recommended that jointing took place in the trench. It was suggested that making of the joints outside the trench then lowering them down into the trench could cause residual locked in stresses to occur (Jones, 1983).

Many old cast iron pipes use lead-caulked joints. The flexibility of these kinds of joints depends on the mechanical properties of lead. The behaviour of lead is strain-rate dependent and exhibits large amounts of creep at ordinary room temperatures (Salvadori & Singhal, 1977). Due to the non-linear time dependent (creep) behaviour of the lead, the deflection of lead-jointed pipes subjected to loads at the joints is also found to be non-linear and time dependent. The flow characteristics of lead allow the joints to sustain larger loads for brief periods than they can sustain over longer periods (Prior, 1935).

Prior (1935) carried out joint pull-out tests on pressurised large diameter cast iron pipes with lead-caulked joints. Two tests were executed on 150mm (6-inch) diameter cast iron pipes. The results showed the joints to have withstood about 90kN axial load before complete failure occurred, i.e. the joints could no longer maintain pressure. The smallest recorded failure movement was 1/32 inch, which suggests that the displacement results may not be very accurate due to inadequate instrumentation. Prior (1935) found that joints leaked after the initial slip, but once the joint displaced further the joints became water tight until complete failure occurred. From these tests Prior also established that a groove in the bell was more efficient than a bead on the spigot (Figure 2.14) for creating strength

and water tightness. These tests are the only axial pull out tests carried out on cast iron pipes that could be found in the literature search.

Salvadori and Singhal (1977) have shown that lead-caulked joints possess little rotational restraint against bending, which results in lower stresses developing in the pipe than locally in the vicinity of a joint. This was also observed by Hossein *et al.*, (1985). However, Salvadori and Singhal's (1977) tests showed that lead-caulked joints could sustain considerable rotation before structural failure occurred. The results suggest that the initial movement of the joint is influenced by the stresses in the caulking. Prior (1935) and Salvadori and Singhal (1977) conclude that lead joints become non-functional because of leakage long before they reach their ultimate joint rotation under a bending moment. Rotational rigidity of the joints depends on the caulking forces; the amount of lead in the joint; the internal water pressure; and the speed at which the load is applied to the joint.

Talbot (1926) pressure tested cast iron pipes with lead joints. The results showed the fracture of every pipe to occur at the least wall thickness. This was referred to as the 'thickness at break'.

2.2.2.2 Rubber Gasket Joints

Push-on rubber gasket joints are flexible joints, which can readily accommodate earth movements (Salvadori & Singhal, 1977; Singhal *et al.*, 1979 and Jones, 1983). Tests indicate that elastomeric gasket joints can undergo considerably more rotation than lead joints before leakage occurs (Salvadori & Singhal, 1977). Rubber gaskets are manufactured with various different types of cross-sections. When placed on the pipe, the rubber gasket exerts a slight pressure on the bell of the pipe. All gaskets are confined in an annular space in such a way that the movement of the pipe with hydrostatic or hydrodynamic pressures does not displace the gasket (Singhal *et al.*, 1979).

Singhal (1980 and 1984) carried out several tests on rubber gasket joints on ductile iron pipes, including axial pull out tests, bending tests, torsional tests, and buried pipe tests. Singhal's presentation of the results shows that pipes with rubber gasket joints behave as rigid links on a flexible chain. Singhal (1984) found the friction between the rubber

gasket and the pipe bell provides the resistance to torsional movement. When the full value of the frictional force is mobilised, the pipe joint begins to rotate freely without providing any additional resistance. This friction coefficient between the pipe and gasket also controls the start of slip during axial pull out or torsional tests, which prevents the joint from being easily pulled apart. With the buried pipe tests Singhal (1984) showed that the main influence of the soil is to provide additional friction forces against joint slippage. Singhal (1980 and 1984) concluded that the mechanical properties and behaviour of a rubber gasket joint is a function of several variables, namely the strength characteristics of rubber material, the geometry of the joint, the strength characteristics of the pipe material, operating pressure levels, buried depths and soil laying conditions. The geometry of the joint controls the axial, bending and torsional resistance of the joint. The rate of axial pullout was found to be load dependent. Bending of a joint beyond 4^{o} caused a metal to metal contact, giving very high stresses at the joint, and significantly increasing the chances of joint failure. Singhal (1980) concluded that a redesign of the joint geometry is necessary to avoid such situations.

2.3 Failure Mechanisms

It is widely believed that there can be several causes for a burst, often with several mechanisms acting in combination (Arnold, 1960; Morris, 1967; Newport, 1981; Bahmanyar & Edil, 1982 and Svensson, 1990), some of which cause a gradual weakening of the pipe, whilst others influence the timing of the failure. A defect-free cast iron pipe with no material faults or flaws is unlikely to fail when loaded, due to its tensile and compressive strength (110MN/m^2 and 280MN/m^2 respectfully, Stanton, 1997). However, in practice cast iron pipes are not "perfect", and experience both internal and external loads. It is therefore necessary to know how water pipes can be weakened, and how bursts are triggered. Suggested triggering and associated weakening mechanisms will be explained during this chapter.

2.3.1 Cold temperature failure mechanisms

Water pipes burst throughout the year but they have a relatively higher burst rate during the winter months than the summer (Arnold, 1960; Monie & Clarke, 1974; Newport, 1981; O'Day, 1982; Bahmanyar & Edil, 1982; Needham & Howe, 1982 &1984; Fry & Rumsey, 1984; Wettering, 1985; Habibian, 1994; Rajani & Zhan, 1996; Zhan & Rajani, 1997). During the months of November through to February, cold air temperatures can directly affect both ground temperatures and in-pipe water temperatures. It is important to look at both ground temperatures and in-pipe water temperatures and the effect each of these factors have on water pipes separately. Therefore this section has been organised into two parts. The first considers ground temperature effects and the second examines in-pipe water temperature effects.

2.3.1.1 Frost Heave

The phenomenon of frost heave has been widely investigated (Taber, 1930; Yoder, 1959; Tsyovich, 1975; Konrad & Morgenstern, 1980; Konrad, 1994; Eigenbord, 1996; Tester & Gaskin, 1996; Rajani & Zhan, 1996; Zhan & Rajani, 1997; Newman & Wilson, 1997; Peck & O'Neill, 1997). Past research mainly studied the effects of frost load on trenches, and frost penetration effects on road pavements. As a result of this research, much is known about how frost heave occurs in various soils and how it affects buried service pipes. The majority of the work has been carried out in North America, in places such as Ontario and Maine, where the winter temperatures can drop to around -35°C for periods of several months. This does not reflect UK winters, which are much milder, but it is valuable to examine the methodology used and to analyse the data obtained in these studies. This can then be used as a basis for understanding the possible influence of frost heave on underground water pipes within the UK.

Frost heave does not occur in all types of soils. The soils require certain properties for the creation of ice lenses. For example, if saturated clean sand or gravel freezes, the structure of the soil remains unchanged. The process of freezing merely increases the volume of each void slightly because of the 4% expansion of water contained in the void. Alternatively, if a saturated fine-grained soil freezes, the process involves the formation of

lenses of clear ice roughly parallel to the surface exposed to low temperature. The soil subject to freezing assumes the character of a stratified material consisting of alternate lenses of soil and clear ice (Taber, 1930; Figure 2.15). The distance between the ice lenses increases with increasing depth (Palmer, 1976).

The soil properties which control the degree of frost heave are the amount of fines contained within the soil (Tester & Gaskin, 1996), pore size distribution of both coarse and fine particles, and the mineralogy of the fines (Konrad, 1994). These properties collectively define the frost susceptibility of the soil. Using frost susceptibility values different soils can be compared. Silty and chalk soils are considered frost susceptible as they are fine grained (Konrad, 1994). Clay is not generally considered frost susceptible. This is because the natural permeability of clay is, in general, too low to allow significant upward migration of the water through the material during the typical period that the ground is frozen. This contrasts with silt and chalk, which have an intermediate permeability, and a fine enough pore size to maintain suction.

Water pipes buried in frost susceptible soils may be subjected to an increase in loading due to frost heave. As the near surface soil freezes ice lenses form, and the expansion of these ice lenses causes loading above the pipe to increase (Monie & Clarke, 1974; Smith, 1976; O'Day, 1982; Ciottoni, 1983; Fielding & Cohen, 1988). This is due to the unfrozen soil moving downward below the frost front (Zhan & Rajani, 1997; Figure 2.16). To investigate this suggestion Monie and Clarke (1974) carried out experiments monitoring the effects of frost heave on cast iron pipes in Maine, USA. They measured the load that the pipes experienced using stainless steel load cells placed underneath the pipe between supporting piers. Monie and Clarke recognised that these supporting piers caused the pipe to behave like a beam, which meant the load cells could not give a true reading of the load uniformly along the pipe (Figure 2.17). To overcome this, an extra load cell was placed in the trench, level with the crown of the pipe but to one side. This cell was therefore loaded only by the soil above it.

Monie and Clarke's results show that the vertical load approximately doubled as the frost front approached 1 m (3 ft), the pipe being 1.3 m (3.75 ft) deep. Smith (1976) carried out a similar investigation in Wheaton in Illinois. In this study an iron pipe was split longitudinally and load cells were placed vertically inside. The data obtained were

consistent with the results presented by Monie and Clark (1974). The load on the pipe approximately doubled from its usual 'soil load' value during the deepest frost penetration, which reached 0.9 m, when the pipe was buried at a depth of 1.2 m. Similar analyses carried out by Molin (1985) and Zhan and Rajani (1997), also show the load above the pipe approximately doubles when the frost penetration reaches about 1 m below ground level, for a pipe buried between 1.2 - 1.3 m. Figure 2.18 from Needham & Howe (1981), shows similar results for a pipe buried at 1m. The graph shows that the stress was retained when the ground was allowed to warm up, resulting in locked in stresses. Using graphical results from Fielding and Cohen (1988) approximations can be made of the load increase at various depths (Figure 2.19).

Frost does not penetrate below about 0.48 m during a UK winter (Glanville, 1951; Croney & Jacobs, 1967; Croney, 1977) and the ground temperature at 1 m depth does not vary significantly throughout the year in the UK (Needham and Howe, 1984; Figure 2.20). Most small diameter pipes are buried between 0.8 and 1.2m (Figure 2.21) so frost penetration reaching 0.48m would not seem that threatening. These typical burial depths are also reflected by site reports in Appendix B.

Rajani and Zhan (1996) and Zhan and Rajani (1997) produced mathematical models to predict frost load behaviour in trenches with sloping walls and vertical walls. Zhan and Rajani compared the theoretical results with field data collected in Canada. In a trench, the frost load develops primarily as a consequence of the different frost susceptibilities of the trench backfill and the sidefill, and the interaction of the backfill and sidefill, at the trench backfill-sidefill interface. Zhan and Rajani showed that the generation of frost load is affected by several factors including trench width, differences in materials, and the stiffness of the medium below the frost front. The latter suggests that frost loads will be higher on rigid pipes than on flexible pipes. Nixon (1992) showed that the initial ground temperature affects frost heave and the resultant frost penetration. The colder the initial ground temperature the deeper the frost penetration. Frost heave has been found to be dependent on frost penetration (Monie & Clarke, 1974; Smith, 1976; Fielding and Cohen, 1988; and Zhan and Rajani, 1997). Frost penetration has been shown to be dependent on type of backfill, with some soils acting as thermal insulators while others act as conductors (Peck and O'Neill, 1997).

2.3.1.2 In-Pipe Water Temperature

The temperature of the water within the distribution system varies seasonally. Distribution pipes can be fed by reservoir water or borehole water. The temperature of reservoir water falls in the winter due to air cooling. In the UK, the temperature of reservoir water can vary between 2 and 29°C during the course of a year, whilst borehole water temperature is generally quite stable at 12°C +/- 1°C (Figure 2.22).

There is some evidence to suggest that in-pipe water temperature has a role in winter pipe bursts. Wettering (1985) reported a study in which condenser cooling water, from a nearby electric generating plant, was used in lieu of Lake Michigan as the winter raw water source for a water distribution system. Normally the in-pipe water temperature would be around 1°C during the winter. When the generator water was used the in-pipe water temperature was 4°C. In two winter seasons of full-scale operation, the number of main breaks was significantly reduced (by 34%). Wettering suggests that cold water damage the pipes, causing them to fail. Wettering's study has indicated that there is a strong correlation between cold water temperatures and bursts, but the mechanism by which this operates has not been explained.

It has been suggested by some authors that the temperature of the in-pipe water, dropping suddenly or becoming constantly low, can increase the tensile stress within the cast iron water pipes causing them to break (Habibian, 1994; Ciottoni, 1983; Morris, 1967 and Arnold, 1960). It has also been suggested that cast iron pipes are prone to break when subjected to cold temperatures due to the brittle structure of cast iron (Angus, 1976 and Scholes, 1979). Although it has been shown by Arnold (1960), Morris (1967), Ciottoni (1983), and Habibian (1994), that there is much anecdotal evidence that an increase or decrease in in-pipe water temperature can be destructive to water pipes, the mechanism by which it operates has not been investigated.

Arnold (1960) noted that in Philadelphia the greatest number of winter bursts occurred the first time there was a rapid drop in temperature each winter. Habibian (1994) carried out statistical analysis of breaks in Washington (D.C) and found that when there is a drop in in-pipe water temperature below the previous minimum, there is a surge in the number of water pipe breaks. Arnold suggested that the sudden chilling of the water and the

surrounding earth resulted in shrinkage of the pipe metal. This could set up longitudinal stresses sufficient to fail the pipes, at points where it was already weakened. This mechanism requires that the pipe be constrained in the longitudinal direction, to allow thermal tensile stresses to develop in the wall of the pipe in the longitudinal direction. Rigid joints and/or frictional resistance between pipe and soil may cause this restraint (Fry & Rumsey, 1984). According to Rajani *et al.*, (1996) buried mains are restrained from movement by the frictional resistance between the pipe and soil. The stress induced by this restraint will be superimposed on the stresses that may already exist in the main, due to external loading and internal pressure. These combined loads may exceed the strength of the pipe (Ciottoni, 1983; Habibian, 1994; Rajani *et al.*, 1996). The process of prior weakening necessary for this model to apply could be caused by corrosion or material flaws within the cast iron pipe structure. Prior weakening mechanisms and their effects on cast iron pipes are discussed in section 2.4.

Habibian (1994) reported 18 circumferential water pipe breaks occurring when the in-pipe water temperature dropped from 20°C to 15°C. Similar burst rate peaks were observed during November and December. When the in-pipe water temperature dropped from 15 °C to 4°C there were 20 bursts. Further investigations carried out by Habibian showed that a sharper temperature drop, i.e. a greater rate of change of temperature, did not necessarily result in a higher number of breaks. Habibian speculated that there are a number of weak points in the water-main distribution system that are on the verge of failure. When there is a significant drop in temperature for the first time in a winter season, the weakest points may fail. This will cause a surge in the number of breaks. During the next period of cold weather, there will be another surge in the number of breaks when the temperature goes below the previous minimum. This process repeats itself each year as the distribution system ages and as pipes deteriorate over time.

Morris (1967) observed similar phenomena to Arnold (1960), in a statistical analysis of burst pipe data from Dallas over a 6 year period. Morris found that most pipe breaks occur in November, December and January. However, Morris reported that when the temperature dropped slowly few breaks occurred; most occurred when there was a rapid temperature drop (from 55°F to 35°F (12-2°C)). Morris calculated that this resulted in an additional axial stress of 1,390 psi (5.6 N/mm^2), making a total of 2,852 psi (19,668 kN/m^2). When these stresses are added to the hoop stress in the pipe due to the internal

working pressure and earth loads, the stress experienced by the pipe doubles from its initial value. If the water pipe is under stress from any other source, or is severely weakened by corrosion, or contains material flaws, failure is likely to occur (Morris, 1967). It is not clear from this paper whether the results are experimental or theoretical. For the purpose of this review they have been presumed theoretical.

The work carried out by Arnold (1960), Morris (1967), Ciottoni (1983) and Habibian (1994), illustrates several viewpoints. Arnold concludes there is a surge in pipe bursts the first time there is a rapid drop in in-pipe water temperature, whereas Ciottoni and Morris suggest there is a surge in pipe bursts whenever there is a rapid drop in in-pipe water temperature. Habibian suggests there is a surge in water pipe failures when the in-pipe water temperature drops below the previous minimum. This issue warrants further investigation, as it has implications for the prediction of cold weather burst events.

2.3.2 Other Suggested Pipe-Burst mechanisms

As mentioned in 2.3 water pipes burst at all times of in the year, and not solely at times of cold temperatures. Other bursts mechanisms could include:

- traffic vibration
- internal pressure
- movement during installation of other utilities
- tree roots and expansive soils

The effects of some of these mechanisms can be enhanced seasonally, and will be highlighted. The following section will discuss each of these mechanisms. No single mechanism operates in isolation: possible links between burst factors are described.

2.3.2.1 Traffic Vibration

Surveys of pipelines of small diameter have shown them to behave as beams, and therefore to be prone to transverse fractures (Rajani *et al.*, 1996). The risk of failure of

this type is greatly increased when the pipes are loaded, or if there is any unevenness or undermining of the support which the pipe receives from its bedding (Needham & Howe, 1979; Jones, 1983; Carder & Taylor, 1983 &1984). For this reason, the effects of traffic loading over pipelines have been investigated.

It is widely believed that the increases in traffic and axle loads on lorries over recent years are damaging water pipes buried underground (Arnold, 1960; Roberts & Regan, 1974; Needham & Howe, 1979; Jones, 1983; Fry & Rumsey, 1984). The majority of water pipes are made from cast iron, many of which were laid between 1900 and 1910 (Fry & Rumsey, 1984). The profile of these pipes would have evolved before there were significant traffic loads and may now be inadequate to support modern day traffic (Arnold, 1960; Jones, 1983 and Needham & Howe, 1984). This mechanism proposes stresses are not only caused by heavily loaded vehicles travelling along the road, but also by surface irregularities. Water pipes buried underground will experience strains due to these loads which they were originally not expected to endure and hence they may fail (Carder & Taylor, 1983 & 1984; Needham & Howe, 1984).

Current design procedures for buried pipelines place considerable emphasis on the ability of the pipe ring to resist load. When designing a pipe, it is not enough to know the magnitude of the static wheel load which the pipe will support; allowance must be made for any impact arising from the passage of the wheel travelling over an irregularity on the road surface. The impact factor is defined as the ratio of the load applied to the road surface (or the dynamic strain generated in the buried pipe) by the wheel travelling over the surface irregularity to that produced by the wheel when stationary (Page, 1966). In the past, an empirical impact factor has been used in pipe design. However the number of motor vehicles per mile has increased from 8.5 in 1925 to 95 in 1983 and is still increasing (source: TRRL). Therefore this empirical factor would no longer reflect present traffic flow. Presently lorries are allowed to load up to 38 tonnes and can have an axle load of 10.5 tonnes (Ministry of Transport - Legett, 2000 and Upsil, 2000), but in practice lorries may be carrying even larger loads than this (Carder & Taylor, 1984; Needham & Howe, 1984).

Page (1966) carried out investigations to measure the effects of loads on buried pipes, and what characteristics the magnitude of these loads depended on. Various lengths and diameters of concrete pipe were used, buried beneath seven different types of back fill. To induce surface irregularity, a wooden plank 12ft by 10 inches by $1^{3}/_{4}$ inches thick was laid at right angles to the direction of travel for all surfaces and pipes. Two of the pipes in each trench were fitted with eight 2-inch electrical resistance strain gauges and one inductive deflectometer. This deflectometer was used to measure change of vertical diameter at the centre of the pipe. The strain gauges were arranged in two sets of four, one set at the centre and one at the need to measure hoop strain on the inside wall of the pipe.

Page (1966) observed that greater strains developed in the pipes when vehicles travelled over surface irregularities on the road above the pipe, than when the vehicles made a smooth run. This strain was considerably reduced by employing concrete back filling instead of granular material or soil. This is due to the concrete acting like one body and spreading the load. This phenomenon was suggested but not investigated in research carried out by Arnold (1960). Page also showed that the relation between impact factor and vehicle speed is independent of the size of the pipe, its depth below the road surface, the type of bedding and the material used to backfill the trench. The strain on the pipe decreased with increase in depth, but the effect was less marked for larger diameter pipes. The rate of change of impact factor with vehicle speed decreased with increasing wheel load and with reduction of tyre pressure. The greatest strains under impact conditions resulted from heavily loaded axles, although the associated impact factors were smaller than for lightly loaded axles.

Carder & Taylor (1983) produced a mathematical model for analysing behaviour of pipes with different bedding conditions with superimposed traffic loads. The Boussinesq theory was used to determine the vertical stress distribution along the pipeline induced by traffic loading. They found that as long as small diameter, cast iron pipes are manufactured to the appropriate British Standards, and the trench and bedding is laid using the correct procedures (so that the pipe receives uniform support), then every pipe would have adequate safety factors against beam failure, due to heavy traffic. Carder and Taylor (1984) went on to confirm their mathematical findings with an experimental investigation. The results showed that maximum bending strains increased linearly with axle load. Strains in poorly bedded pipes were almost twice that for well-bedded pipes in granular

material. This contradicts the findings of Page (1966), who suggested that size of pipe, its buried depth, and type of bedding, does not contribute towards the failure of pipe due to impact loads from vehicles. In practice it is very hard to install a pipe with completely uniform support. It is the unevenness of the support, which the pipe receives from its bedding, in combination with heavy traffic that can lead to its failure (Figure 2.23).

It follows that if pipe breakage is so dependent on traffic, then a significant increase in bursts should have occurred as traffic loads increased between 1910-present day. New (1985) found bursts did not increase during this period. He suggests that this confirms results from investigations, which show that even the heaviest lorries are responsible for only very small strains in pipelines. This disagrees with both Carder and Taylor's (1983 &1984) and Page's (1966) experimental and mathematical findings.

Potter (1985) describes dynamic load induced by a vehicle as the static vehicle load multiplied by an impact factor, as defined earlier in this section. Potter (1985) found that live loads follow the Boussinesq stress distribution, as did Carder & Taylor (1983), for maximum stress with depth. The impact factor was found to be variable, and largest when vehicles crossed obstacles directly over the pipe. Potter observed that the condition of the ground could lead to greater compressions in some areas, creating surface irregularities. This causes the pipe to bend in various ways inducing localised stresses. Coupled with traffic loading these stresses may cause the pipe to fail. These localised stresses caused by surface irregularities were also found to occur by Needham & Howe (1984). Needham and Howe went on to note that bending strains progressively increase under repeated surface loading, which results in significant levels of stress being locked into the main. This locked-in stress may become a permanent feature of the main, making it more susceptible to failure by other loads.

Peters (1983) found that a higher incidence of leakage to occur on truck routes, which contradicts New(1985). Peters attributed this to soil settlements resulting from heavy traffic loads. However, despite several other statistical studies carried out in the USA, to correlate traffic loads with bursts, the relationship is still not clear. The studies do however, emphasis that cast iron pipes at intersections could be influenced by increased traffic loads, large temperature reductions and adjacent utilities (Arnold, 1960; Yie, 1968 and Saha, 1985).

2.3.2.2 Internal Pressure

Changes of internal pressure within the water distribution system of as little as 10 psi ($68kN/m^2$) can trigger bursts (Arnold, 1960). Sudden changes in pressure can be associated with pressure surges or water hammer. Water pressure fluctuations occur all year round. They are likely to increase somewhat in the winter, due to the higher pumping rates required to compensate for winter bursts. They may also peak in dry summer periods as pumping is increased to meet demand. Therefore pumping should be increased gradually to avoid over pressurising the pipe, perhaps causing it to fail (Newport, 1981). If the distribution system has already been weakened, even a small surge may cause a break. Pressure effects on water pipes can be separated into two groups, due to (1) pressure fluctuations and (2) air pockets.

Pressure fluctuations are due to operational factors and should therefore be capable of being monitored and controlled. Fluctuations of the internal pressure within water distribution systems can also be caused by mechanical devices (pumps, valves etc.). These fluctuations can cause strong vibrations and lead to failure of the pipe (Kartvelishvili, 1983). Kartvelishvili (1983), carried out studies showing that the main causes of rapid pressure fluctuations are; separation of eddies; blade impacts in turbines and rotating pumps; resonance of the units control system; cavitation in the turbine. Kartvelishvili describes a case when the range of these fluctuations reached 50% of the internal pressure. He suggested that internal pressure fluctuations can be dangerous even when they are less then the water hammer for which the design of the pipeline is calculated. However, this was not backed up by experimental evidence.

Air pockets are formed within the system, caused by environmental effects, which cannot be controlled. Air pockets can form in water pipes associated with low flow rates, mainly in areas of low incline. These air pockets can cause a build up of pressure behind them in the form of water waves. These water waves do not always flow in the same direction as the water flow. This can cause large pressures to build up due to constructive interference. Kottman (1995) suggests that these long turning water rollers concentrate the area of flow. Under these water rollers there are high speed sections where every speed change initiates

a big pressure wave. These pressure waves beat against the pipe wall and are reflected with double magnitude, similar to a ship's bow wave. Kottmann (1995) showed that these pressure waves are able to destroy pipes made out of brittle material. He suggests that one factor that contributes to these air pockets forming is the rise of in-pipe water temperature.

Degassing can develop air pockets, which happens when the ground temperature is very hot, or when the demand in the pipe is greater than the supply and air gets sucked into the system. High ground temperatures and in-pipe water temperatures will occur in the summer months. Therefore, one would expect more bursts to occur due to this mechanism in the summer months, which Kottman (1995) shows. Rajaini *et al.*, (1996) also suggests that higher ground temperatures contribute to surge pressures having a detrimental effect on water pipes.

2.3.2.3 Other Utilities

External activities include construction or the maintenance of other utilities. This often involves the excavation of trenches. The construction and backfilling of these trenches can create excessive forces on nearby water mains (Crofts *et al.*, 1977; Symons *et al.*, 1981; Rumsey *et al.*, 1982; Fry & Rumsey, 1883; Ciottoni, 1983; Taki & O'Rourke, 1984) which may cause them to fail (Arnold, 1960; Roberts and Regan, 1974; Needham & Howe, 1979; Jones, 1983 and Howe; 1984).

Trench excavation and its effects on adjacent buried water pipes have been widely researched. The effects on buried pipes of ground movement, due to trench excavation is dependent on the distance from the excavation site, depth of the excavation, its geometry, the type and properties of the soil, the method of excavation, ground support, standards of construction (Smith, 1976; Rumsey *et al.*, 1982; Rumsey & Cooper, 1982; Takagi *et al.*, 1984; Valliappan & Raja-Sekar, 1984; Rumsey & Dorking, 1984; Rumsey, 1984).

Symons *et al.*, (1981), investigated changes in bending strains in water pipes buried adjacent to trench excavations. They found small changes (about 80 μstrain) occurred both during the pipeline installation and subsequently during the excavation of the deep trench. Peak bending strains of $390*10^{-6}$ were induced by ground settlements during

backfilling. This is equivalent to 50MN/m^2 bending stress. Crofts *et al.*, (1977) also found that excessive strain occurred after backfilling. Crofts *et al.*, (1977); Carder *et al.*, (1982), Fry & Rumsey, (1984) and suggested that the subsequent bending was causing permanent locked in stress. This disagrees with Rumsey *et al.*, (1982) who said the bending strain was temporary and the locked in stress negligible. However, Chard & Symons, (1982) found peak bending strains only occurred during the backfilling stage if the process was poorly carried out. They found that generally peak strains occurred during excavation itself. Symons *et al.*, (1981); Rumsey, (1982); Jones, (1983); and Valliappan & Raja-Sekar, (1984) concluded that to avoid large lateral movements good compaction of the backfill is necessary. Ground movements could be minimised by having close contact between the support system and the adjoining ground (Rumsey, 1982 and Rumsey *et al.*, 1982). The excavation material should also be removed away from the site and not stockpiled on one side of the trench, as this tended to increase the lateral and vertical surface and subsurface movements (Chard & Symons, 1982; Toombs, *et al.*, 1982). Carder & Taylor, (1983) found that maximum strains were associated with continuous rigidly jointed pipelines, with most failures occurring in older pipes where the joints are locked by corrosion.

Trench excavation does not always occur parallel to buried pipes, sometimes it intersects existing pipelines. In these cases the pipe is often left unsupported across the excavation. Backfilling underneath the pipe can be difficult and good compaction may not take place. This results in the backfill underneath the pipe settling leaving the pipe acting as a load-bearing beam, supporting the soil above it (Casson, 1984). Trench walls, if not supported, may also move inwards and downwards. This movement of ground causes settlement which buried pipes may pass through and resist. If the settlement is great enough failure planes develop in the soil causing the pipe to hold up a much larger quantity of soil than designed for. This can lead to failure of the pipe (Casson, 1984). Casson (1984) found from carrying out field experiments, that variations in soil type did not appear to influence the pressure on the top of the soil, but the presence of a road surface tended to increase the loads on the pipe.

Blasting sometimes occurs near to buried water pipes. It was found by Esparza (1985) that the existence of a near-by trench in the line of blasting reduced the circumferential stresses in the buried pipes by as much as 87%. Greatest reductions were seen when long

and deep trenches were used. Esparza describes the increase in strain in pipes due to blasting but does not describe how this affects the pipes and whether they fail from it.

2.3.2.4 Expansive Soils and Tree Roots

In the UK there has been little research into the effect of soil shrinkage and swelling on water pipes. However, there has been considerable research to investigate the effects on building foundations. Expansive soils can severely damage structures constructed on, or within them (Clark, 1971; Elder, 1996), especially during periods of low rainfall. As water pipes are buried at similar depths and within the same vicinity as building foundations, it may be possible to learn how pipes are affected by looking at foundation research.

The types of soil which cause the most damage to building foundations are expansive clays. These clays often contain a high montmorillonite mineral content. This enables them to undergo substantial volume change when subjected to seasonal wetting and drying. This is because montmorillonite is made up of very thin platelets, consisting of two silica sheets, with an alumina sheet bound between by oxygen atoms. They have an average thickness of 10 nm, which are negatively charged and attract positively charged water ions. They also have a large surface area with which to attract this water. This can greatly expand the lattice, and as a result montmorillonite swells and shrinks to a high degree and exhibits a high plasticity and cohesion (Clark, 1971).

The only way in which volume change can occur in saturated clay, is through change in its moisture content. Constant wet or dry conditions cause little or no volume change, regardless of the potential of the soil (Elder, 1966). Change in moisture content can be brought about in one of two ways. First by moisture movement near the ground surface where moisture evaporates in dry weather and is replenished by rainfall and by upward migration of the water table; and secondly by removal of soil moisture from greater depths than the first process, through the action of the roots of vegetation. In general the larger the vegetation for a particular species, the greater will be its demand for moisture in dry weather. Certain species of deciduous tree (oak, willow) can lead to desiccation at depths of up to 4m.

Distribution water pipes are laid in all types of soils. Axial stresses, whether compressive or tensile, can be increased in water pipes if they are laid in expansive soils (Morris, 1967; Newport, 1981; O'Day, 1982; Needham & Howe, 1983; Ciottoni, 1983; Fry & Rumsey, 1984; Rajani *et al.*, 1996). Rigid pipes (e.g. cast iron pipes) are susceptible to damage, as they are not able to flex and rely on their strength to withstand external and internal loads (Clark, 1971). Kassiff *et al.*, (1962) describe the forces acting on water pipes laid in clay soils. Such forces are not considered in the usual design procedures, which take into account surge pressures, external loads, and internal pressures. As a consequence the pipes are subjected to unique stresses which may exceed the design strength of the pipes and cause it to fail.

Kassiff *et al.*, (1962) report on experiments in Israel to confirm that the shrink and swell of clay may cause water pipes to fail. They monitored the stresses along a water pipe made from asbestos cement, in a field of expansive clay. The field was exposed to seasonal changes and irrigation. The stresses were calculated by measuring the strain using vibrating wire strain gauges, at various sections along the pipe, in both horizontal and vertical planes. Measurements of soil moisture changes and soil movements were taken periodically during the investigation. Vertical and horizontal movements were measured using plates relative to fixed points in a basaltic rock.

Kassiff *et al.* (1962) and Clark (1971) suggest that rigid water pipes with small diameters may fail in beam bending, and large diameter pipes fail in ring crushing, due to expansive soils. Clark suggests that such damage is caused by high differential-soil pressure that develops on opposite sides of the pipe, vertically and laterally. Clark (1971) suggests a counter measure to reduce damage by differential-soil pressure, by deeper burial of the pipe. This should decrease the differential pressure by placing the pipe in more stable moisture conditions as well as placing more earth weight on the pipe to offset swell pressures from below.

Driscoll (1983) notes that removing trees from cohesive ground can lead to heave movements. As the trees are removed the soil swells as the moisture normally used by trees is soaked up by the soil. This causes the soil in the area where the tree previously stood to rise, causing foundations near by, and maybe water pipes, to fail. Many builders,

engineers, planners and landscape architects still do not appreciate the problem of volume changes in clay soil due to the drying action of tree roots. Research shows the risk appears to be greater when the trees are in groups or rows (BRE). Jarvis (1997) suggests that pipes laid along tree-lined streets are at risk from fracture from stresses induced by differential drying. This may be due to the significant contrast between the moisture content beneath the road pavement and the road edge where trees are growing. Significant clay shrinkage and swelling is confined to the top 1 m or so, which could affect water pipes as they are buried at depths between 0.7-1.0 m.

Tree roots can grow as deep as 4m and there are data (held by Thames Water) to suggest that they have affected sewer pipes, which are buried much deeper than water distribution pipes causing them to fail. The BRE found that large trees can create deep zones of dried and shrunken clay beneath them. In a dry summer, these zones will extend and when the wet weather returns, the slow rate of penetration of water into the more impermeable dry clay will be insufficient to replenish the soil before the next summer arrives. Thus the larger dry zones become permanent, reaching depths of up to 5 m. This could result in soil support failure for the water pipes that could lead to beam failure (Rajani *et al.*, 1996). Driscoll (1983) observed that soil deficits in the south-east of England usually reached a maximum during September and reduced to zero towards the end of December. Data held by Thames Water, show peaks of burst pipes in the months of August and September each year (Figure 2.1). Biddle (1983) found that these water deficits only reach a maximum depth of 1.5m, except where large trees are present.

Biddle (1983) found that the shrink and swell of soil was very dependent on the following: tree species; soil type; abnormalities in soil profile; soil permeability and permanent moisture deficits. Biddle observed that clay type makes little difference to the patterns of deficit but it is important in controlling permeability and amount of shrinkage. He also found that unless there are any abnormalities, the difference between individual tree species is insignificant. These findings suggest that water pipe should be buried deeper to avoid the damaging effects of clay shrinkage due to trees and vegetation.

Trees may also have a direct affect on water pipes by the movement and growth of their roots. Pressures are generated in root cells, which combine to give an overall pressure at the surface of the root, which can be transmitted to the soil (MacLeod & Cram, 1996).

Tree roots may grow near and along water pipes. The roots exert axial and radial pressures at the tip and just behind the tip respectively. MacLeod & Cram (1996) point out that radial pressure will be exerted over a relatively large area, whereas axial forces of root tips are applied at a point. Radial pressures therefore can generate a far greater total force than axial pressures. It is radial pressures exerted by secondary growth that may be a potential cause of structural damage to pipes and structures. Tree roots can not generate enough force to penetrate pipes or anything with a greater density of $2g/cm^3$, but they can raise or disturb paving slabs and small pipes (MacLeod & Cram, 1996). The raising or disturbing of rigid water pipes (e.g. cast iron) could lead them to beam failure, through differential ground movement along their length.

2.4 Weakening mechanisms

Cast iron pipes can be damaged and hence weakened by several different sources. The main ones to take into consideration are manufacturing defects, installation defects and corrosion. Manufacturing defects come in the form of inherent material defects e.g. graphite flakes, and casting defects such as blow holes, sand inclusions and slag voids. It is difficult to quantify manufacturing defects as they are generally located internally and their size and properties are unknown. It is only after the pipe has failed and has been examined internally at various sections that it becomes known that the pipe was defective (Stanton & Stauelet, 1963). The changes in strength properties of these areas can be given approximate values, but are dependent on type of defect, size and depth.

Installation defects are also not likely to be detected until after the pipe has failed and been examined. Installation defects arise from lack of conscientious care in handling and installing pipes. Ideally every precaution is taken to ensure that the pipe arrives on site to be laid as it left the foundry. Each length of pipe is examined, hydraulically tested and inspected before it is loaded for transportation (Stanton & Stauelet, 1963). Damage from rough handling during transit and unloading may occur, dropping the pipe to the ground is bound to cause damage (Stanton & Stauelet, 1963). Very poor pipe laying can lead to failure in a short time. Locked in stresses have been shown to vary from 3.5 to 20 MN/m^2 for a range of very good to very poor workmanship (Fry & Rumsey, 1984). Ideally a trench should always be prepared in accordance with engineers' specifications (Smith,

1976; Rude, 1983). The pipe bed should be level and free from protruding rocks and sharp edges. However, this does not always occur resulting in the pipe being subjected to unnecessary beam action and localised stress concentrations.

2.4.1 Corrosion

Once the pipe has been laid and backfilled, the pipe is then subjected to corrosion. The corrosion problem can be separated into two distinct areas, internal corrosion and external corrosion. For grey cast iron pipes stress corrosion also becomes a grave problem.

Corrosion is considered to be a principal cause of pipe failure (Roberts & Regan, 1974; Kirby, 1978; Needham & Howe, 1979). Ferrous water pipes suffer extensively from both external and internal corrosion (Lehmann, 1964; Morris, 1967; Kirby, 1978). External corrosion leads to perforation and failure of the pipe wall, internal corrosion leads to tuberculation, loss of carrying capacity and water discoloration. Different corrosive mechanisms create these two effects (Stadler, 1983). Each effect will be discussed separately. To understand the significance of corrosion and its potential danger, the various types of corrosion will be explained.

Corrosion may be defined as the destruction of a metal by an electro-chemical reaction with the environment. The majority of common metals are unstable or chemically active in most environments and tend therefore to revert to a more stable oxide, which destroys the original metal structure. A new pipe may resist the applied stresses but as it corrodes it strength falls, leaving it in a weakened condition causing it to fail under normal operating conditions (Figure 2.26). The rate at which corrosion occurs depends on many factors concerning both the metal and the environment, but the basic mechanism is the same for all systems.

2.4.1.1 External corrosion

External corrosion usually occurs on the surfaces of metallic pipes due to the action of aggressive soil. The majority of water pipes buried under ground are fabricated from cast or ductile iron. Unfortunately iron has a natural tendency to rust in the presence of water.

Anodic and cathodic sites develop on the surface of a buried pipe. In uniform conditions these sites may be very small and constantly change position, so that the resulting corrosion is evenly distributed over the pipe surface. If anodic and cathodic sites become separated on the pipe surface, pitting arises. In practice the corrosion reaction can be generated by a number of conditions, which include:

- Corrosive cells arising from variation in soil conditions.
- Galvanic corrosion arising from electrical bonding together of dissimilar metals.
- Stray current corrosion in which the separation of anodic and cathodic sites and the driving force for the corrosion reaction are induced by an electric current shorting onto a pipe.

The four main soil properties influencing external corrosion are:

- Soil moisture content: - water is essential for the corrosion reaction to take place, and soils with a moisture content above 20% are thought to be particularly corrosive.
- Soil acidity: - metal pipes usually dissolve more rapidly in acidic conditions, especially when the pH value falls below 4.0.
- Soil aeration: - poorly aerated (anaerobic) soils can promote corrosion, especially if they contain soluble sulphates.
- Electrical resistivity: - the resistivity of the soil gives a measure of the concentration of soil electrolyte, which is essential in the corrosion process. Soils with low resistivity will encourage corrosion.

Corrosive cells are often restricted to anodic sites on the bottom surface of the pipe. This is due to the fill placed above a pipe being slightly looser and better aerated than the undisturbed pipe bed, where the soil will be compacted and conditions possibly anaerobic. Under these conditions the bottom of the pipe will be anodic and thus more likely to corrode (Argent & Furness, 1985). Statistics reported by Argent and Furness (1985), show that pipe failures due to corrosion are three times more likely in clay soils than sandy soils (Figure 2.25). Jarvis (1997) also states that clay soils are considered highly aggressive and pipes laid in these soils are at risk from corrosion. Argent and Furness (1985), suggest that different soil conditions along a pipeline can also influence the distribution of corrosion. A pipe laid in lower resistivity soil is likely to corrode more

than a pipe laid in a high resistivity soil. This suggestion also comes from Reedy (1966), who points out that dissimilar soils produce concentration cells. Pipe sections located in sandy soils become cathodes, whilst and pipe sections in clay zones become anodes.

Galvanic corrosion is described as a chemical reaction which takes place when two dissimilar metals are used in the pipe network. Morris (1967) reported a bypass valve failing due to excessive internal corrosion occurring between the brass wedges and the cast iron housing. Arnold (1960) suggests that ferrous pipes suffer from stray current electrolysis corrosion. He notes that stray current electrolysis is becoming increasingly serious in cities where there has been partial abandonment of tram systems. Abandoned tracks, no longer used for trams, are paved over and may be used as a return path for the current supplying operating tracks. These old rails, being paved over, are not properly maintained, and open joints frequently develop resulting in discharge of large quantities of current to the ground and underground structures, such as pipelines. 1amp of current will remove 20lb of metal in one year, so that there is a good reason for concern when as much as 600 amp is found travelling on an underground piping system.

2.4.1.2 Internal corrosion

Internal corrosion is found in areas with an aggressive water supply, typically soft water areas. This type of corrosion is very much dependent upon the chemistry of the water flowing through the pipe. Water flowing through the pipes with low pH or dissolved oxygen is likely to corrode ferrous metals and can lead to failure (Reedy, 1966). pH adjustment, protective layering and chlorination can control chemical corrosion. Bacterial corrosion may be prevented by maintaining a chlorine residue throughout the water distribution system (Jarvis & Hedges, 1994).

In small diameter mains, tuberculation can form from the corrosion, which subsequently blocks the pipe completely or reduces the pipe bore by a significant percentage. This offers constraints to the flow in the mains and higher pressures are then required to overcome friction loss and to maintain sufficient pressures at the ends of the distribution system. This increase in pressure inside heavily corroded pipe is then likely to increase burst frequency and give rise to higher leakage in both mains and services (Reedy, 1996). If a cross section is cut through a tuberculation site, it can be seen that graphitic corrosion

has occurred beneath the tubercle (Kirby, 1978). These graphitised areas show up as darkened areas on the pipes cross section. It is thought that this material has some strength properties but has very low density and soft texture (Kirby, 1978). It is has been shown that the iron has been converted into iron oxide and is held together by the original graphite flakes which remain unchanged (Kirby, 1978). Kirby (1978) carried out strength tests on samples cut from pipes in the Severn Trent area and found that they were able to sustain high internal pressures but were extremely vulnerable to transverse fracture.

2.4.1.3 Stress Corrosion

Stress corrosion cracking occurs in many different alloy systems and environments through a continuous spectrum of mechanisms. Stress corrosion occurs due to the interaction of metallurgical, mechanical and electrochemical or chemical kinetic events under very specific conditions (Parkins, 1979 and Scully, 1983). Of all forms of corrosion, stress corrosion is considered to be the most highly localised. To achieve local corrosion the metal and the environment must react in a certain way. For this to happen the environment has to be in direct contact with the bare metal. However, most metals form a protective film around the outside. In order for stress corrosion to occur this film must be broken locally, either by mechanical or chemical means (Parkins, 1979 and Scully, 1983).

Mechanical film break down is caused by stress causing plastic deformation. The microstructure of spun cast grey iron is susceptible to stress corrosion. A threshold stress of approximately 40% UTS is required to initiate stress corrosion (Fry & Rumsey, 1984). The rate of growth of the cracking is dependent upon both the soil corrosivity and the applied stress (Fry & Rumsey, 1984). Chemical film breakdown may occur through penetration of the film pores. Once broken down the film can regrow and the rate of stress corrosion cracking will depend on the speed of film regrowth. Rapid film regrowth will result in crack arrest and slow film regrowth will cause crack blunting resulting in an elongated fissure or pit. When the film is broken the crack will extend due to anodic dissolution along a pre-existing active path or strain-induced path (Parkins, 1979). A pre-existing path may occur due to a grain boundary containing impurities resulting in

different electrochemistry to the rest of the matrix. Strain induced active paths occur by the rupturing of the protective film (Scully, 1983).

Cracking environments are specific and not all environments will promote cracking (Parkins, 1979). The environment needs to sustain a critical balance between activity and passivity. This balance can be altered by changes in the structure and composition of the alloy and the response of the alloy to stress. (Rankins, 1979 and Scully, 1983). Mechanical failure will occur at much lower stresses if stress corrosion is initiated than would otherwise be the case. The cracks formed will penetrate the wall with time, reducing the overall strength of the pipe section (Fry & Rumsey, 1984). Of all forms of corrosion, stress corrosion in cast iron and ductile iron, is likely to be accelerated by cold ground temperatures and in-pipe water temperatures, because these loading mechanisms may subject a pipe to additional stresses.

2.5 Discussion

A newly installed cast iron pipe laid in accordance with the correct specifications, has an ultimate strength 110MN/m^2 (Fry & Rumsey, 1983) and so is likely to be able to cope with the loads generated, for example, by frost heave or cold in-pipe water temperatures (Fielding and Cohen, 1988). However, cast iron pipe failure may occur if pipes have been subjected to prior weakening and/or additional loads from other sources. Prior weakening may occur from several sources, for example, poor manufacture, rough transportation and handling, inadequate installation and corrosion. Additional loads can result from traffic vibration, internal pressure within the pipes, tree roots and external utilities.

Several hypotheses have been identified in the literature. No single mechanism has been reasonably proven to be the sole mechanism for bursting a cast iron water pipe. Each mechanism seems to need other conditions to actually burst a water pipe. These hypotheses and their conditions are summarised below.

Previous investigations into the effects of frost heave and low in-pipe water temperature have mainly been carried out in North America. However, the winter climate of the UK is

not so severe as in North America; the UK experiences a much milder climate with less frost. Monie and Clark (1974), Smith (1976) and Molin (1985) have showed that in North America the load above the pipe approximately doubles when frost penetration reaches about 1m below ground level. However, Needham and Howe (1984) present field data which indicate that ground temperatures at 1.0 m depth do not vary significantly in the UK, whatever the air temperature (Figure 2.20). From these data it is difficult to see how frost heave can affect water pipe buried at 1m depth within the UK. Using the estimation methods presented by Field and Cohen (1988, Figure 2.19) loads of about 0.02N/mm^2 are obtained for water distribution pipes, for the maximum frost depth the UK experiences. These are unlikely to cause pipe failure.

Frost heave can only occur in silty or chalk soils. It does not occur in granular soils, and needs excessive freezing to occur in clays. UK winters are not sufficiently cold or long enough to allow frost to penetrate below 0.45 m, even with frost susceptible soils. Frost heave alone is unlikely to cause a cast iron pipe to fail if the pipe is experiencing no external or internal loads, has no material defects and is installed correctly. Frost heave and heavy traffic loads together may be adequate to fail a cast iron pipe, although data supplied by Monie & Clarke (1974) contradict this. A cast iron pipe may exhibit local weak points along its length due to substandard cast iron, corrosion, age and/or poor installation. These local weak points combined with increased loading due to frost heave may cause a cast iron pipe to fail.

This suggests that it is not just cold temperatures (frost) that have a destructive effect on cast iron pipes, but cold temperatures in conjunction with another factor. However the converse has been suggested by Rajani *et al.*, (1996), Rajani and Zhan (1996) and Zhan and Rajani (1997). They used results from a theoretical model and compared them to field data, which showed that cold ground temperatures alone could lead to an increase in circumferential water main breaks. They also suggested that brittle pipe materials, such as cast iron will be more prone to fail under these conditions, due to frost load being partly dependent on the stiffness of the medium below it; the stiffer the medium the greater the frost load. Further theoretical and field work needs to be carried out in this area within the UK, during a UK winter, to substantiate either suggestion.

The water that is fed into the distribution system is drawn from two sources; borehole supplies and river-fed reservoirs. The temperature of reservoir water falls in the winter due to cooling by the air and reduced solar radiance. In the UK the temperature of reservoir water can vary between 2 and 29°C (Figure 2.22), during the course of a year. Borehole water temperature is relatively steady at about 12°C +/- 1°C during a whole year (Figure 2.22). Geographical presentation of burst events suggests pipes fed by reservoir water have a higher frequency of bursting (Figure 2.27). This information in combination with the work carried out by Wettering (1985) suggests that water pipes supplied by reservoir water, which are exposed to greater variations in water temperatures, are more likely to burst than pipes supplied by ground water.

It would appear necessary to investigate how in-pipe water temperature varies during the course of a year within the UK, to see whether it is the absolute drop in temperature that is harmful, or the rate of change of temperature. Arnold (1960) and Morris (1967) suggest the latter is more harmful but that both will damage the pipes, whereas Habibian (1994) suggest that a sharp drop is not necessarily more destructive. Pipe damage may also occur due to the continual cyclic fluctuations in temperature, which would cause more frequent expansion and contraction of the cast iron, which could result in failure due to fatigue.

Frost heave coupled with cold in-pipe water temperatures may apparently also produce enough force to fail a cast iron pipe. Cold in-pipe water temperatures alone can have destructive effects on ferrous pipes in countries which suffer from severe winters. Rapid temperature drops have been suggested to have a greater destructive effect on water pipes (Arnold, 1960; Morris, 1967 and Ciottoni, 1983). It has yet to be shown that UK winters are sufficient to cause pipes to fail due to changes in water temperature alone. However in-pipe water temperatures in the UK in conjunction with a weakened pipe could produce a destructive effect. From the review of literature it has been suggested that ferrous pipes could be failing in one of three ways due to cold in-pipe water temperatures: increased axial stress due to sudden drop in temperature; fatigue due to continual expansion and contraction; and soil support failure in non-frozen ground due to increased pipe movement resulting from expansion and contraction. To carry out investigations within the UK the ground temperature profile, in-pipe water temperature, and source of water are critical parameters to record and log.

Traffic loads on roads have increased dramatically since the installation of the water distribution infrastructure. It has been suggested that these traffic loads cause a high frequency of water pipe failures buried underneath the roads, and that these loads are enhanced by road surface irregularities and uneven pipe beds (Page, 1966; Monie and Clark, 1974; Carder & Taylor, 1983; Needham & Howe, 1984). In normal pipeline installation, it is unlikely that uniform bedding would be achieved beneath the pipe. Monie and Clarke also suggested that (in the USA) in cold weather, frost penetration coupled with live loads is a major reason for the greater frequency of water-main breaks. This is in contrast with their data which suggests that with nearly 1 m (3 ft) of frost, the live load inflicted by a vehicle driving over the site, decreased the load by about 5% compared to frost free soil. This decrease may have been due to a wider distribution of the load by the stiff frost layer. The increased external loading due to frost penetration may cause beam (circumferential) failures where the bedding is not uniform, for example, where a stone is wedged beneath the pipe. Soft or unstable layers in the bedding could result in the same effect by permitting excessive deflection (Rajani *et al.*, 1996) enhanced by extra loading due to frost, live loads or both.

Water pipes could fail due to internal pressure in one of two ways. Firstly, from pressure surges or as a result of pressure fluctuations caused by the mechanical equipment used within the distribution system. These can be caused by human or operational error, or faulty equipment in need of maintenance. Secondly, air pockets may form within the pipe causing high speed water rollers to form underneath them, which may cause constructive interference. These air pockets may form from degassing due to high ground temperatures, and low pressures resulting from high demand. However many actions can be taken to avoid air pocket formation which Kottmann (1995) explains and has been described in section 2.3.2.1.

Tree roots can have a direct or indirect effect on water pipes. Tree roots may exert load on water pipes as they grow through the ground by raising or disturbing the water pipes when they cross their path of growth. This causes the pipe to fail as a beam, due to differential ground movement over its length (MacLeod & Cram, 1996). The load that the roots exert is due to the pressure inside the root cells (MacLeod & Cram, 1996). Tree roots can be expected to have a greater impact during the summer season, due to the majority of native trees being inactive during the winter in the UK. Trees can affect pipes indirectly, through

the swelling or shrinking of soil. These ground movements induce extra stresses within the pipe. The soil surrounding the pipes may shrink and swell due to seasonal changes in precipitation, irrigation, transpiration by vegetation, or any combination of the three. It has been shown by Driscoll (1983) and Biddle (1983), that soil desiccation penetrates to a depth of 1.5 m, and so can have destructive effects on building foundations. As water pipes are buried at similar depths, it may be assumed that soil desiccation could also affect water pipes.

Ferrous water pipes suffer extensively from both external and internal corrosion (Lehmann, 1964 and Morris, 1967). Corrosion occurs in many different forms and due to a variety of causes (Stadler, 1983; Argent & Furness, 1985; and Jarvis & Hedges, 1994), including varying environmental conditions, pipe material properties, and other utilities. Only three aspects of corrosion are relevant for this thesis: the weakening effects of corrosion, stress corrosion and tuberculation.

All types of corrosion affect the strength properties of ferrous water pipes. Structurally weakened pipes are less able to withstand load and stress, which increases the chances of pipe failure (Argent & Furness, 1985). Of all forms of corrosion, stress corrosion (Parkins, 1979 and Scully, 1983) is likely to be accelerated by cold ground temperatures and in-pipe water temperatures, because these loading mechanisms may subject a pipe to additional stresses which are not usually considered by industry operators. Tuberculation occurring from internal corrosion can have a significant affect on small diameter mains by blocking the water pipe completely or reducing the pipe bore significantly (Reedy, 1966 and Lackington & Burrows, 1994). This constrains the flow in the mains and higher operational pressures are then required to overcome friction loss and to maintain sufficient pressures at the ends of the distribution system. These elevated pressures are likely to increase bursts frequency and give rise to higher leakage in both mains and services (Lackington & Burrows, 1994 and Reedy, 1996).

2.6 Direction of Thesis Research

The literature indicates that in the UK small diameter cast iron pipes have the highest frequency of failure during the winter months and this is supported by burst data collected

by Thames Water. Previous researchers have suggested different failure mechanisms to explain this phenomena but no one mechanism has been validated. Collectively the research suggests that cold ground temperatures in conjunction with another load may be the reason for pipe failure in the UK. Low ground temperatures can lead to frost heave in certain soils that can increase the vertical load on the water pipe. This mechanism alone is not enough to fail a "perfectly" laid pipe but if the pipe has been subjected to prior weakening and/or additional loads from other sources, the pipe may fail. Other load sources may come from cold in-pipe water temperature; movement of surrounding soil; axle loads from traffic; tree roots; corrosion; external utilities or any combination of these factors.

Low in-pipe water temperatures on weakened pipes may cause a pipe to fail. In-pipe water temperature will have a direct effect on the pipe wall, changing its temperature. The pipe will contract or expand according to this temperature change. If the pipe is constrained longitudinally, by the surrounding soil or the pipe joints, it will not be able to move and longitudinal stresses will be induced in the pipe. This stress in addition to the load received by the cold ground temperature above may be enough to fail a previously weakened pipe. Experiments are required to investigate the relationship between soil loads (whether from frost or traffic, internal pressure, or in-pipe water temperature) various pipes defects and the effects each of these have on small diameter cast iron pipes.

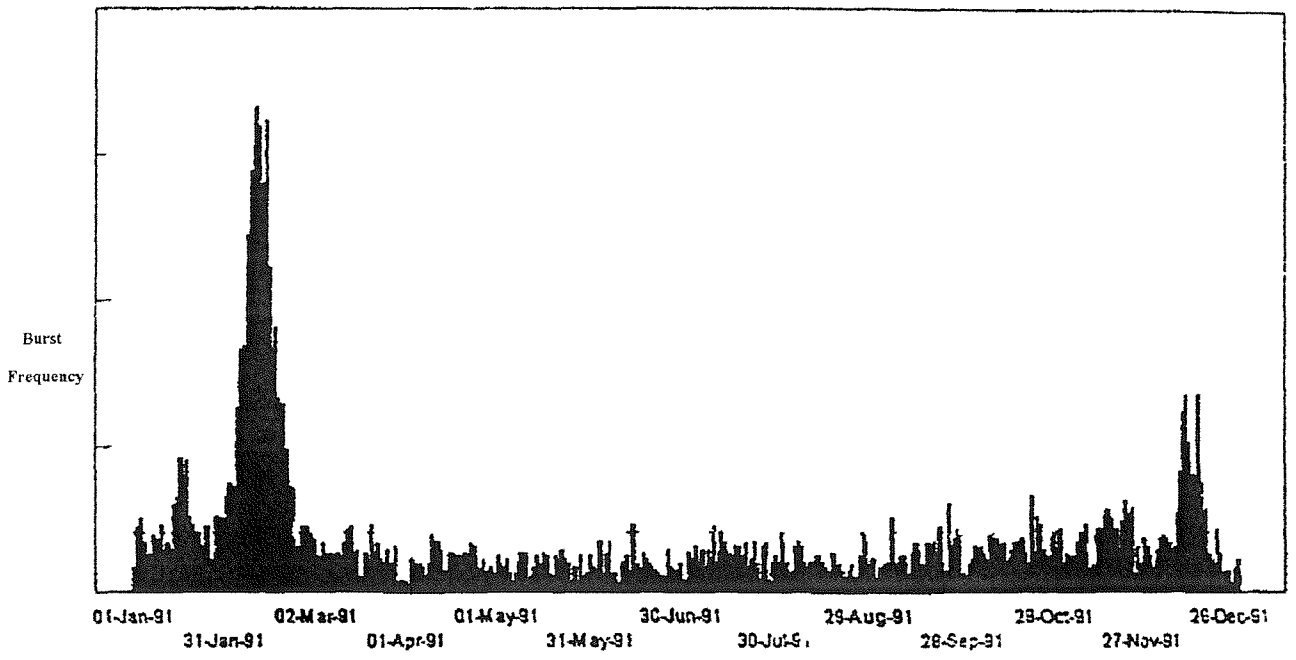

Figure 2.1: Graph to show seasonal burst patterns in South East England (Thames Water Utilities)

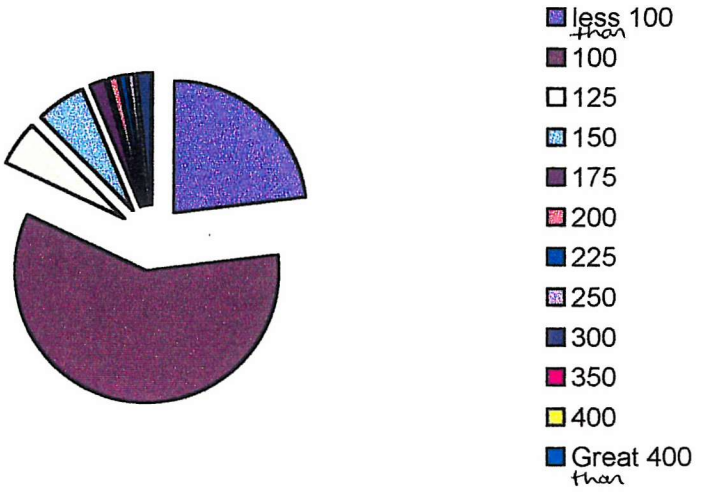

Figure 2.2: Chart to show burst frequency as a function of pipe diameter (mm), in South East England (Thames Water Utilities).

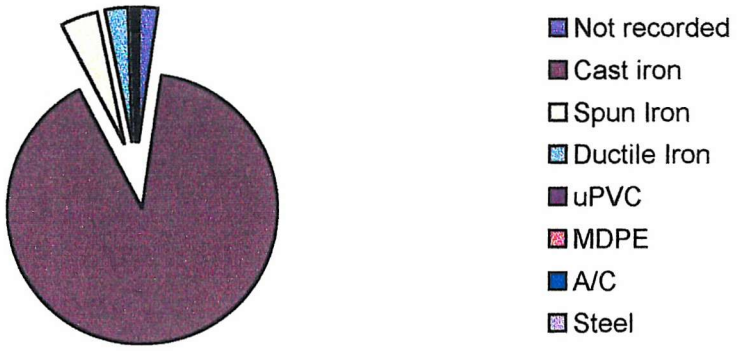

Figure 2.3: Chart to show burst frequency according to material type, in South East England (Thames Water Utilities).

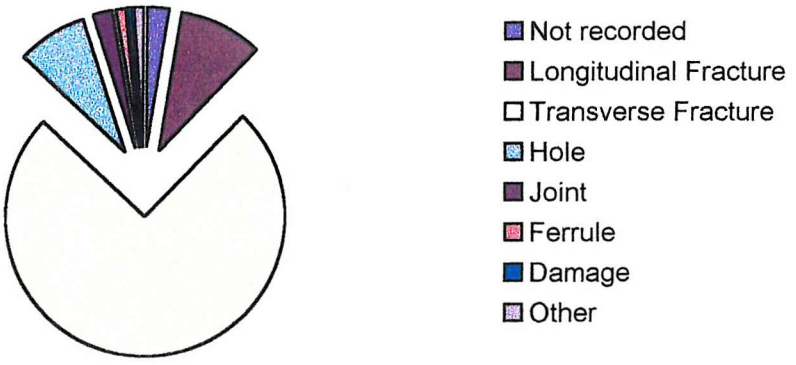

Figure 2.4: Chart to show frequency of failure type of burst pipe , in South East England (Thames Water Utilities).

Type of failure	Appearance	Cause	Preventive measures
(*a*) Overload fracture	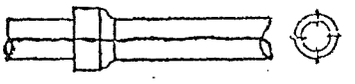	Excessive vertical load or inadequate bedding	Higher bedding class, or stronger pipe, or concrete surround
(*b*) Burst socket	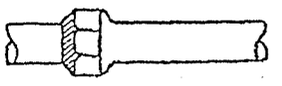	Differential thermal or moisture expansion of jointing mortar	Resilient jointing material which does not cause excessive radial pressure on the socket
(*c*) Distortion fracture	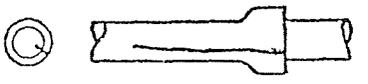	Differential heating or cooling or moisture content	Protection of uncovered pipes against sun or cold night (or drying wind, with concrete pipes)
(*d*) Beam fractures	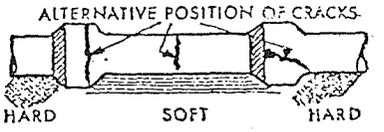	Uneven resistance of foundation, or soil movement, or differential settlement	Flexible joints and uniform hardness of foundation
(*e*) Pull fractures	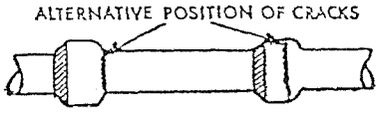	Thermal or drying shrinkage of pipe or site concrete, drying shrinkage of clay soil	Flexible-telescopic joints and gaps in site concrete at pipe joints
(*f*) Shear fractures	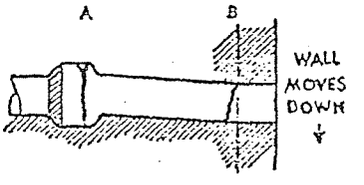	Differential settlement of wall relative to pipe or/vice versa	Flexible joints at least at A and B and making AB not more than 3 ft.
(*g*) Bearing fracture	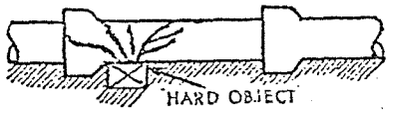	Hard spots in pipe bed	Elimination of hard spots
(*h*) Thrust fracture	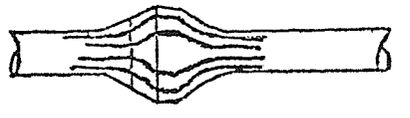	Restrained thermal or moisture expansion of pipe or compression due to subsidence	Flexible-telescopic joints which do not cause excessive radial pressure on the sockets. Spigot end not hard up in socket
(*k*) Leverage fracture	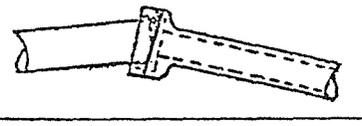	Excessive angular displacement	Avoidance of excessive slew when laying

Types of failure *b*, *d*, *e* and *f* may occur with rigid (e.g. cement mortar) joints.
Type *k* may occur with flexible (e.g. rubber ring) joints.
The other failures are uninfluenced by type of joint.

Figure 2.5: Typical locations of fracture type of burst pipes (Jones, 1983).

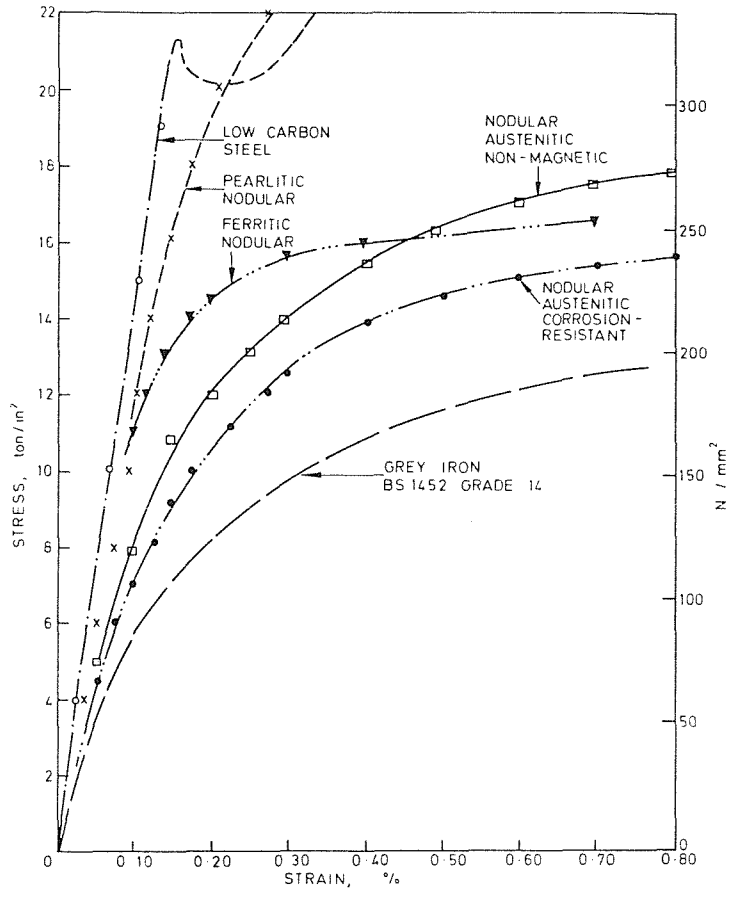

Figure 2.6: Typical stress/strain curves in tension for various cast irons (Angus, 1976).

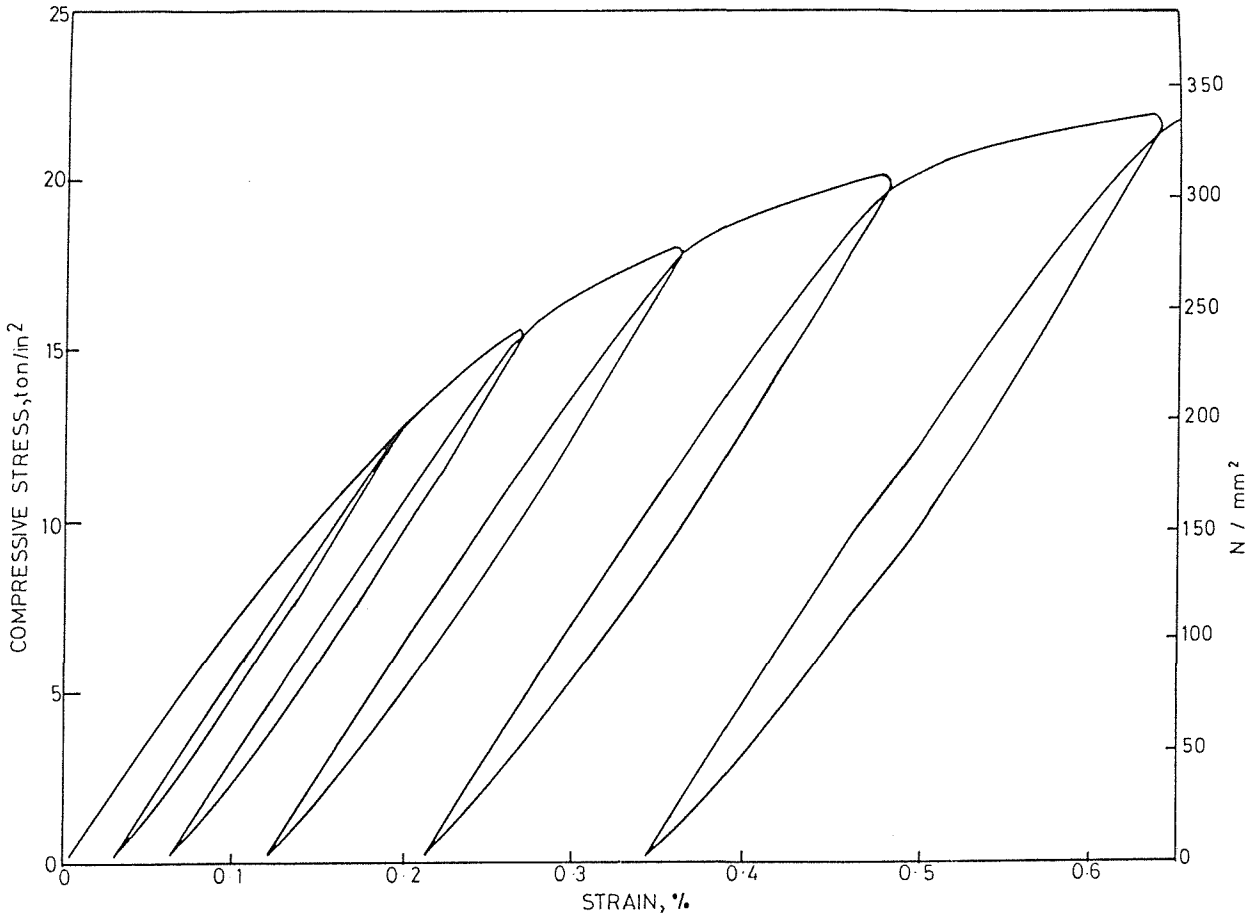

Figure 2.7: Cyclic loading and unloading stress/strain behaviour of cast iron (Angus, 1976).

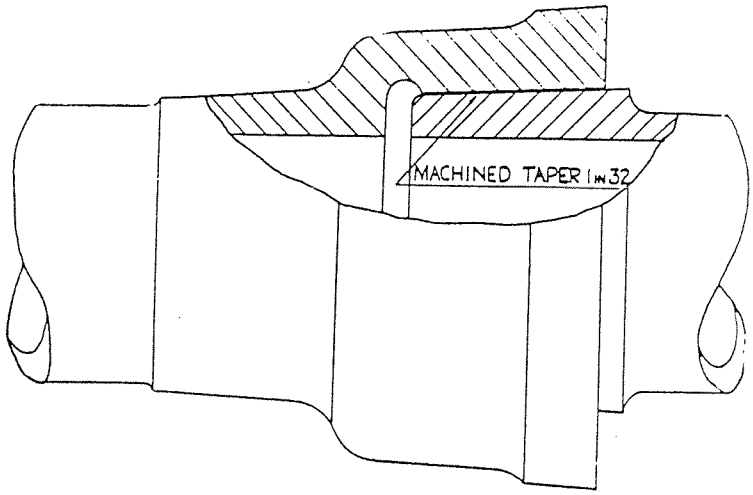

Figure 2.8: Rigid joint – full turned and bored (Boden, 1936).

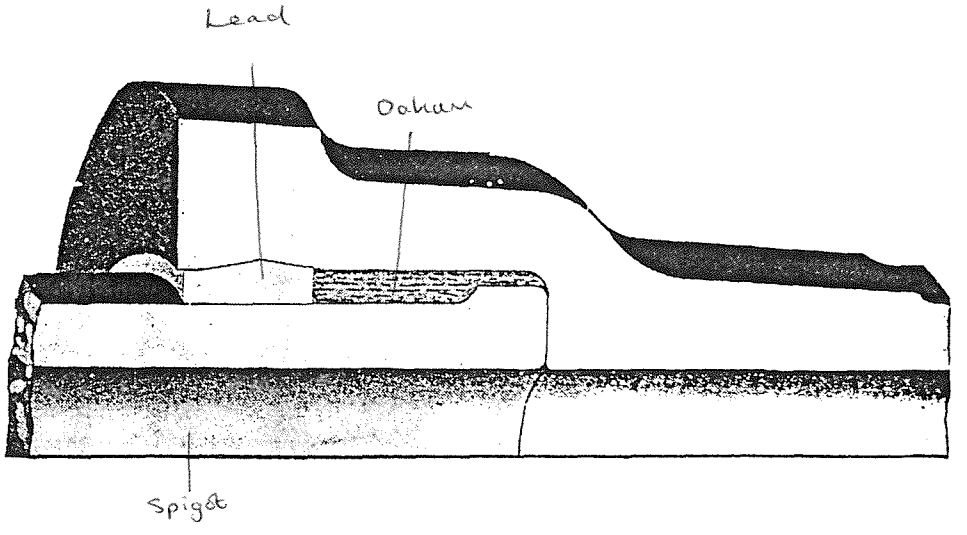

Figure 2.9: Semi-rigid joint – single collar joint (Boden, 1936).

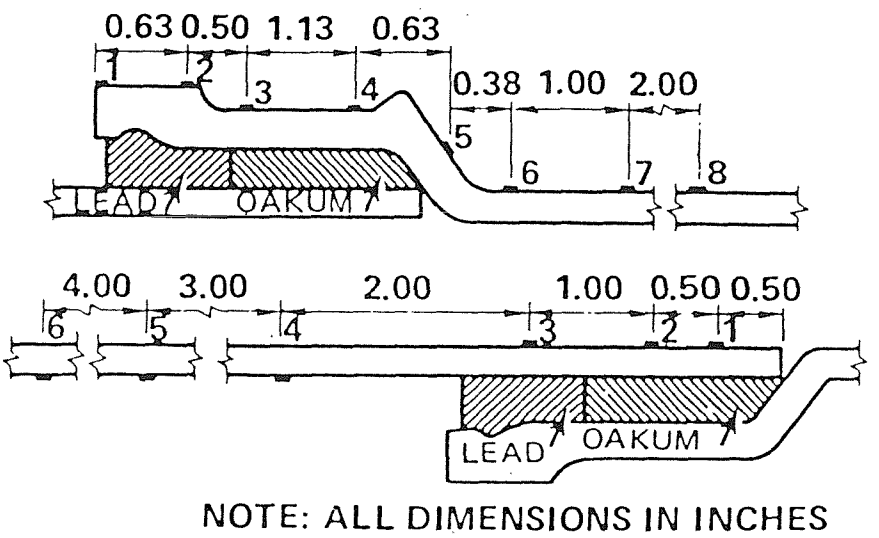

Figure 2.10: Semi-rigid joint – socket & spigot caulked lead joint.

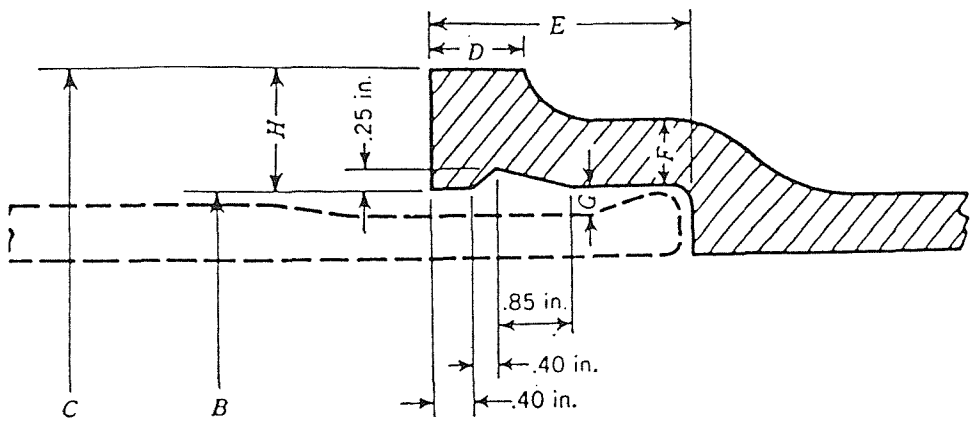

Figure 2.11: Diagram of flexible joint – rubber gasket joint

Fixing the asbestos rope runner

Sealing the runner with clay

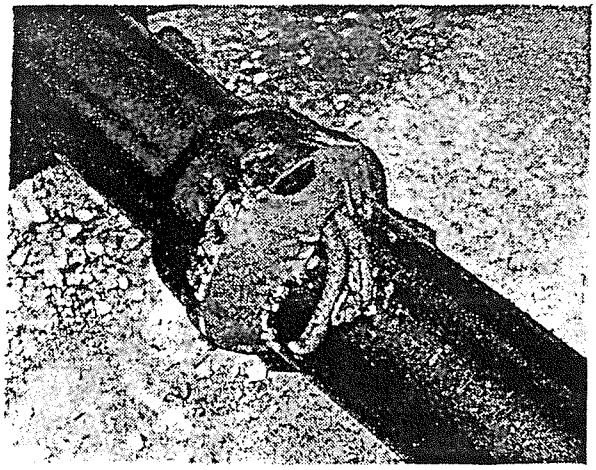

The runner sealed, and a pouring gate formed

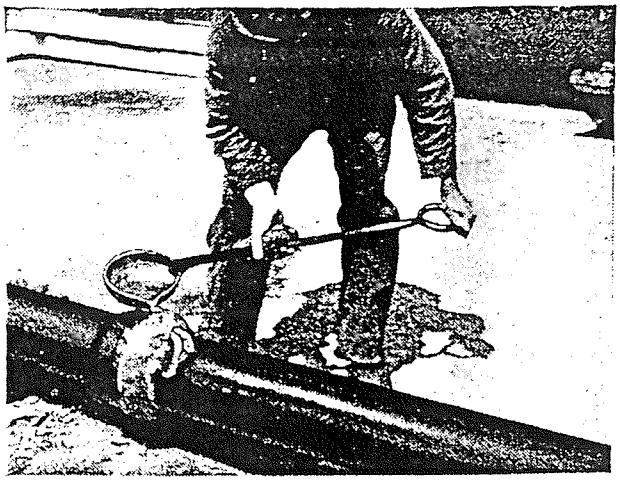

Pouring the joint

Figure 2.12a,b,c,d: Diagram of lead joint being prepared for lead to be poured (Boden, 1936).

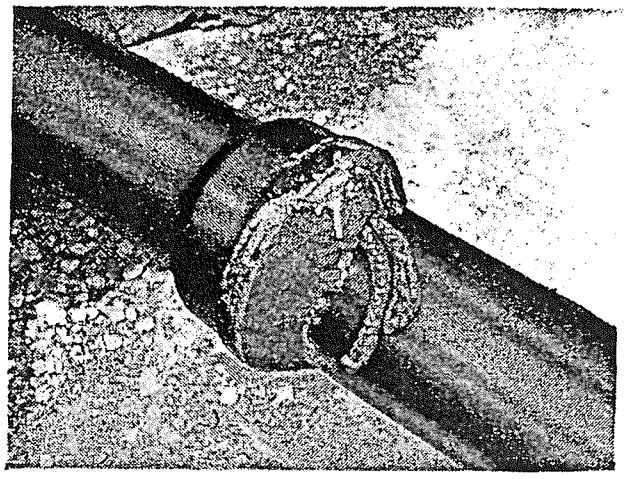

The poured joint

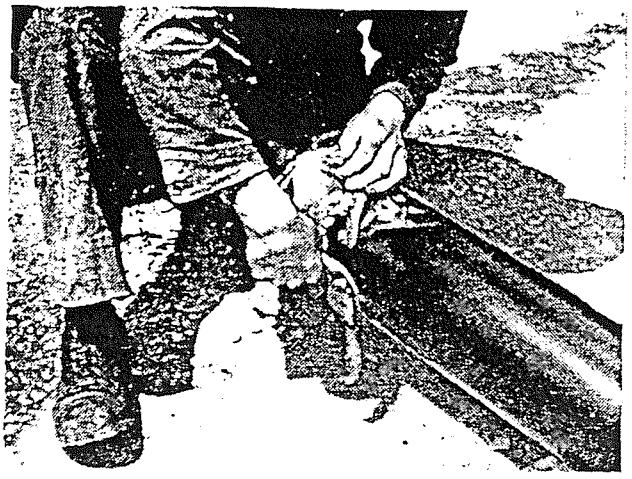

Removing the runner

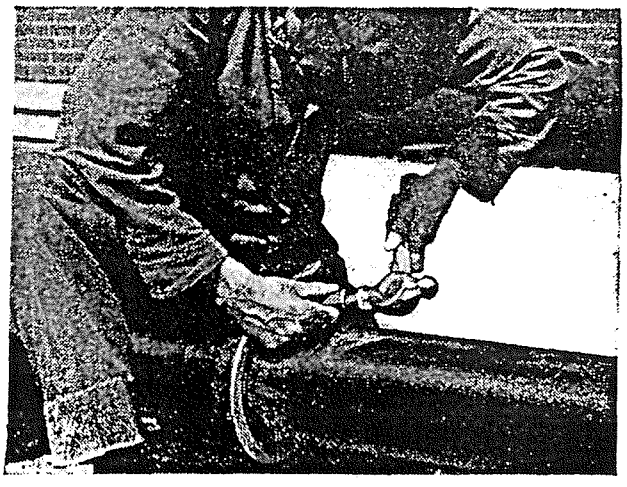

Caulking the joint

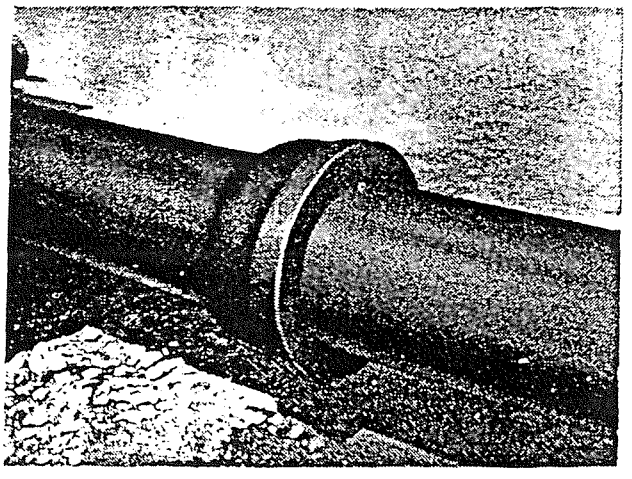

The finished joint

Figure 2.13a,b,c,d: Lead joint being caulked (Boden, 1936).

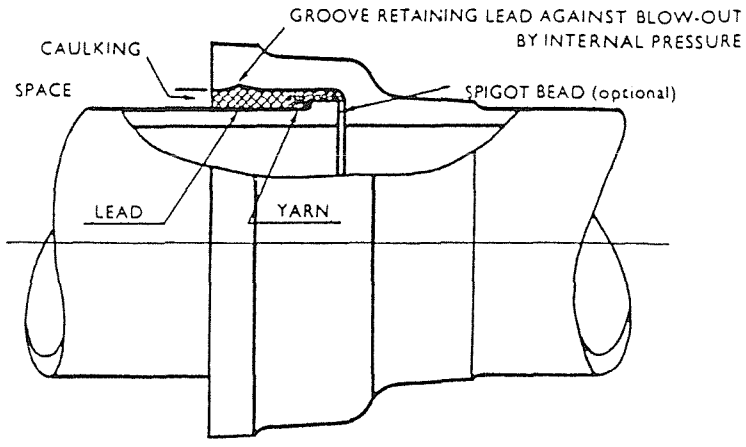

Figure 2.14: Diagram to show lead joint with groove and bead on spigot.

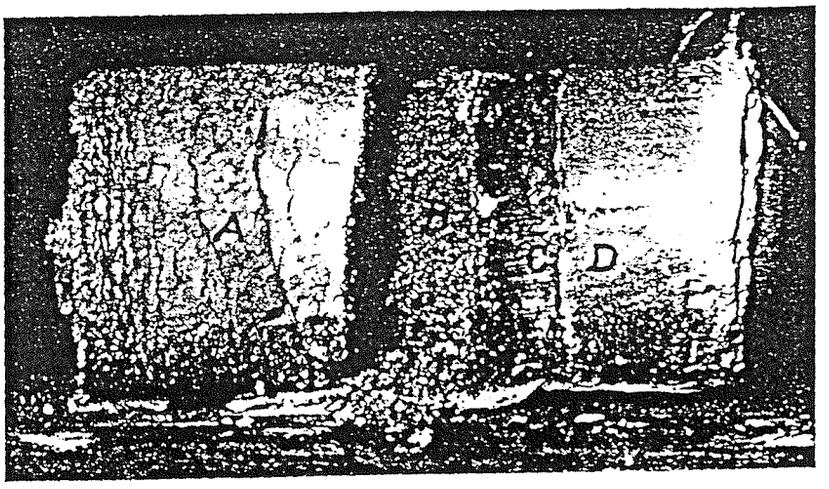

—Frozen clay cylinder with sand layer in middle. *A*, frozen clay; *B*, sand; *C*, ice; *D*, unfrozen clay.

Figure 2.15 Ice lens formation in clay soil sample.

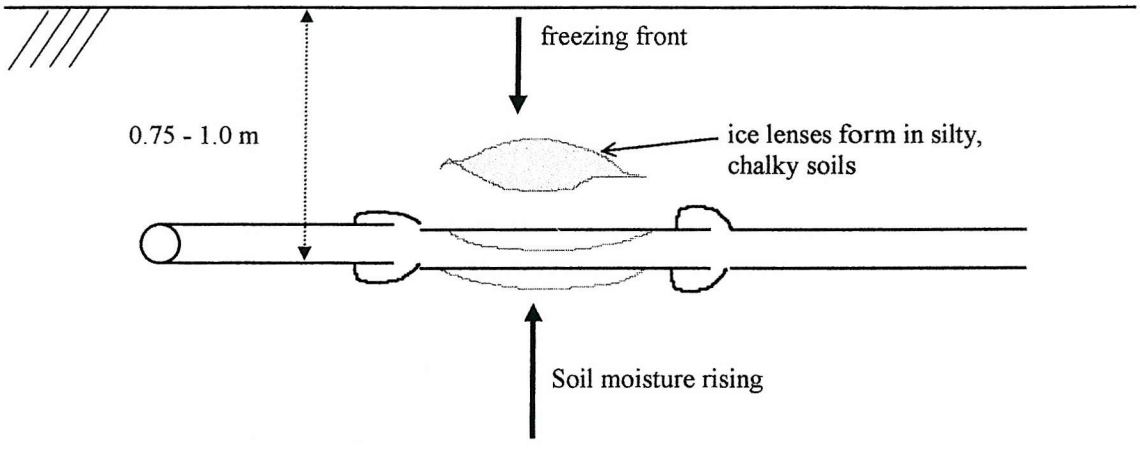

Figure 2.16: Diagram to show ice lens formation

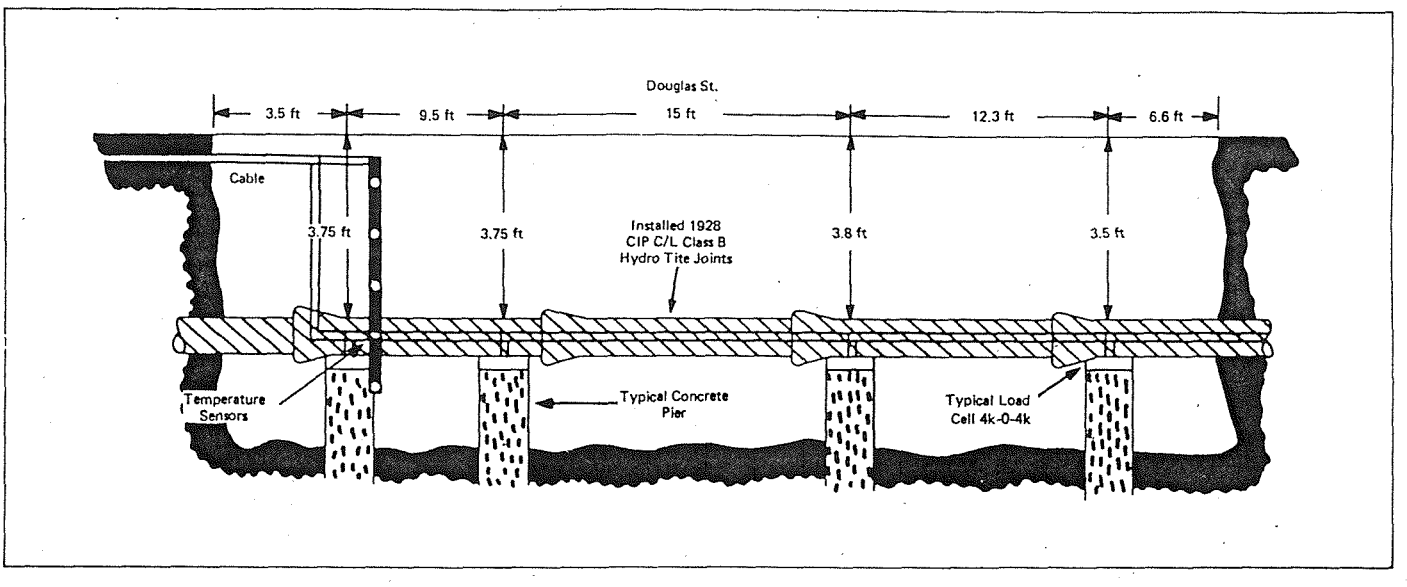

Figure 2.17: Diagram of experimental set of Monie and Clarke (1974).

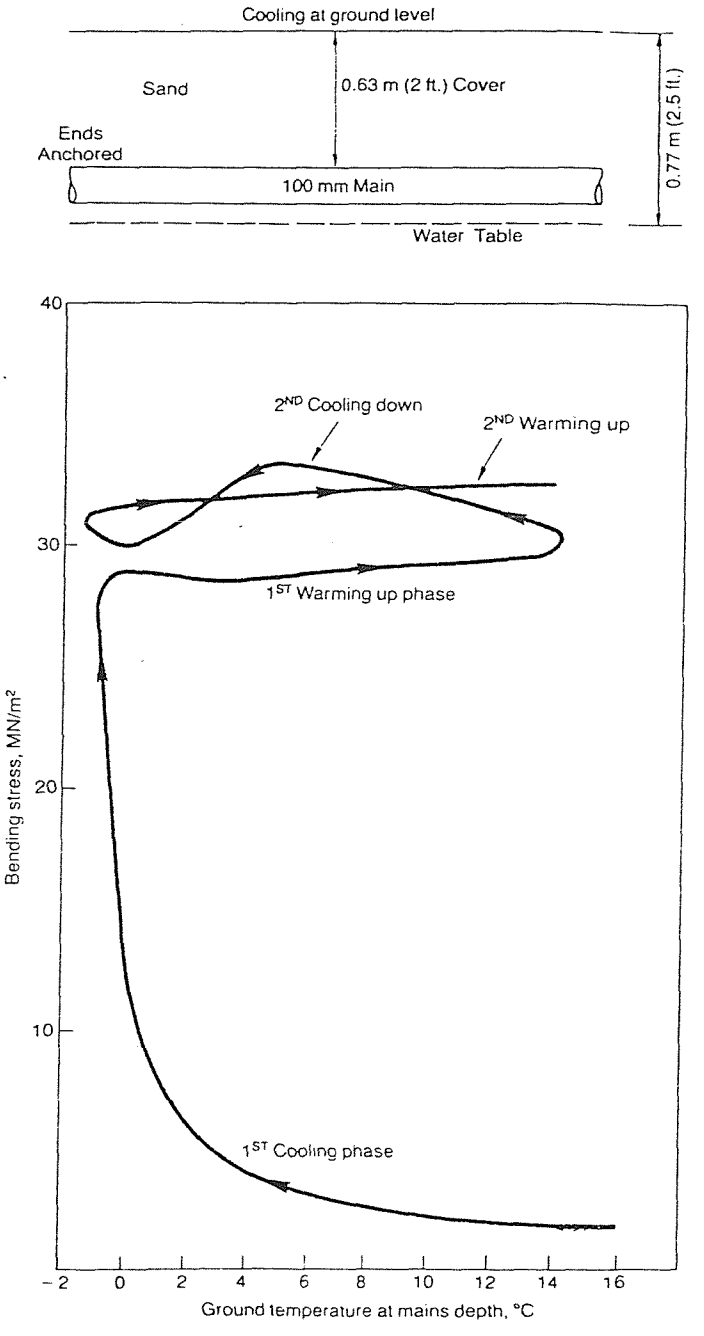

Figure 2.18: Experimental bending stress associated with ground freezing (Needham & Howe, 1981).

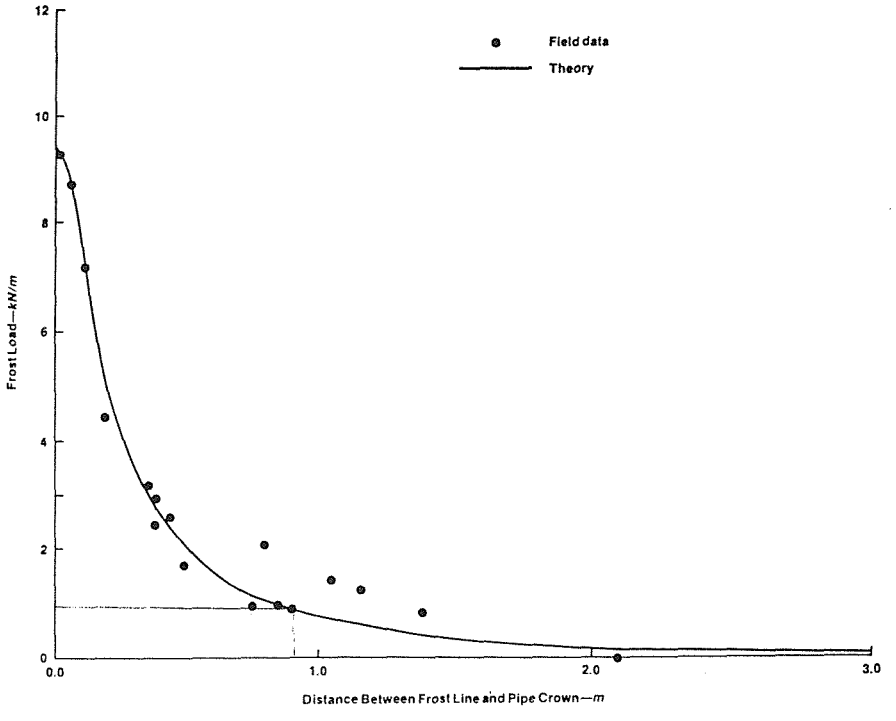

Figure 2.19: Graph to show ice lens load on buried pipe with varying frost depths, Fielding and Cohen, (1988).

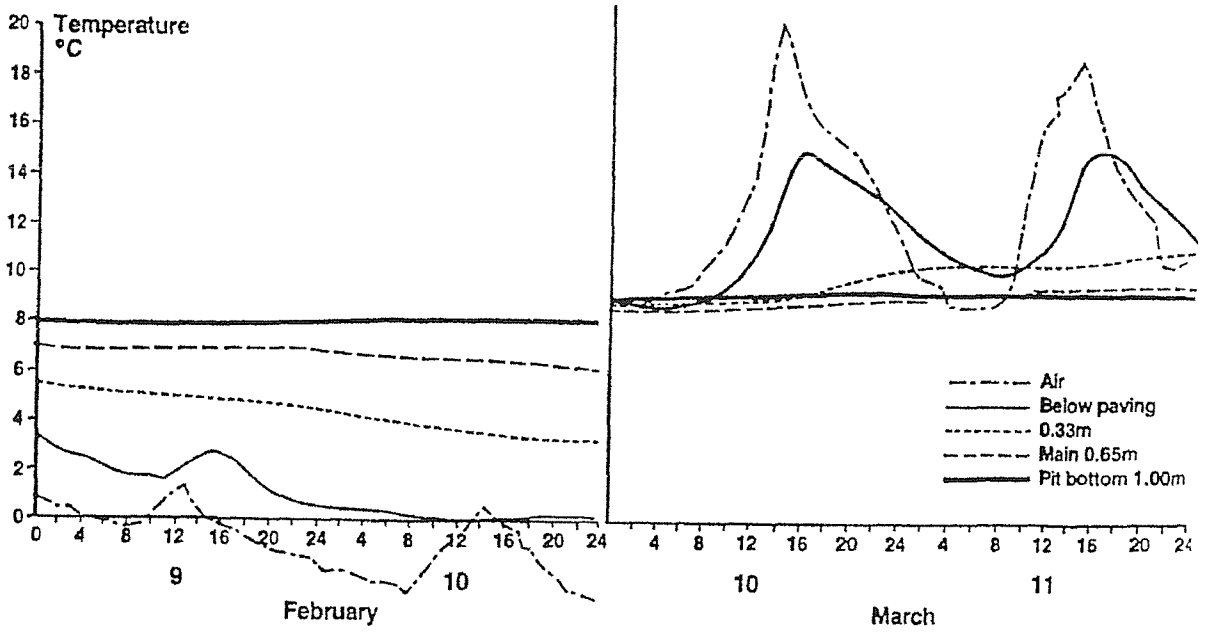

Figure 2.20: Daily temperature changes with depth (Needham and Howe, 1984).

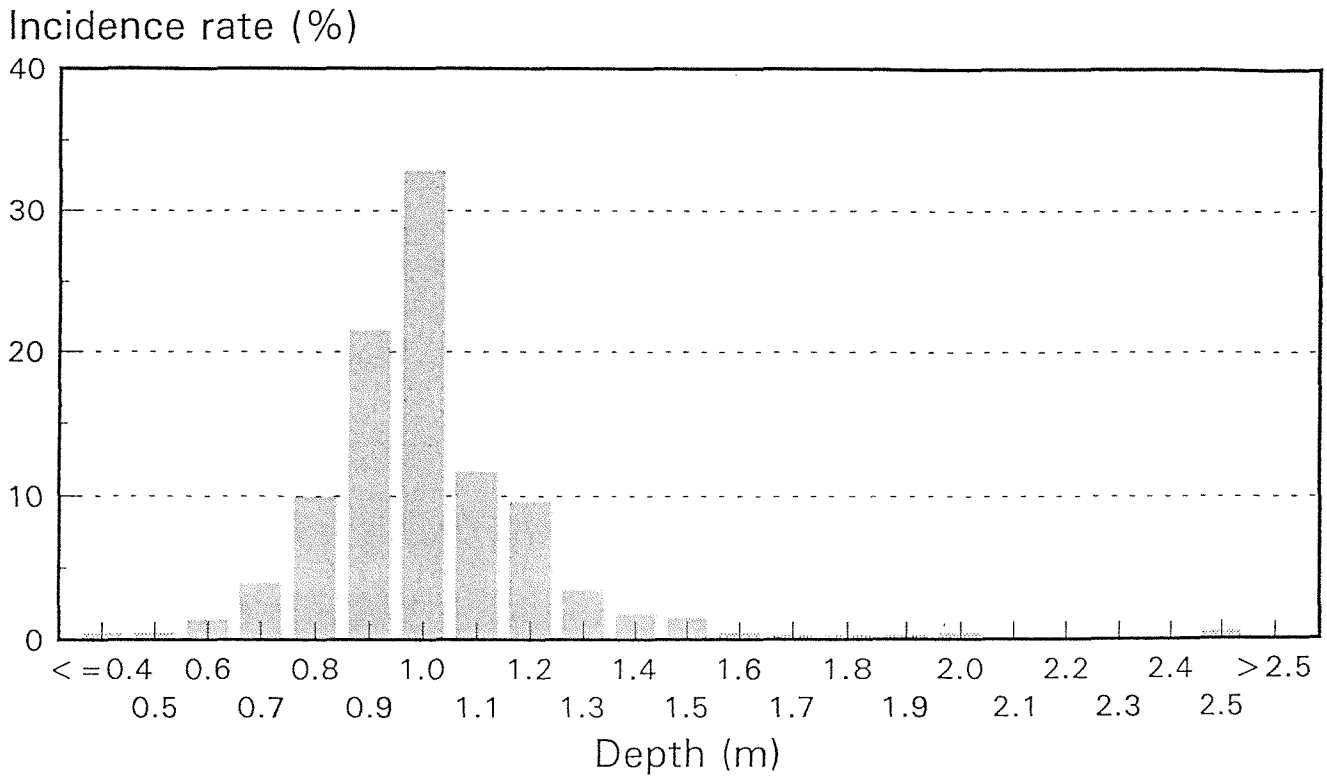

Figure 2.21: Burial depths of cast iron water pipes (courtesy: Thames Water Utilities).

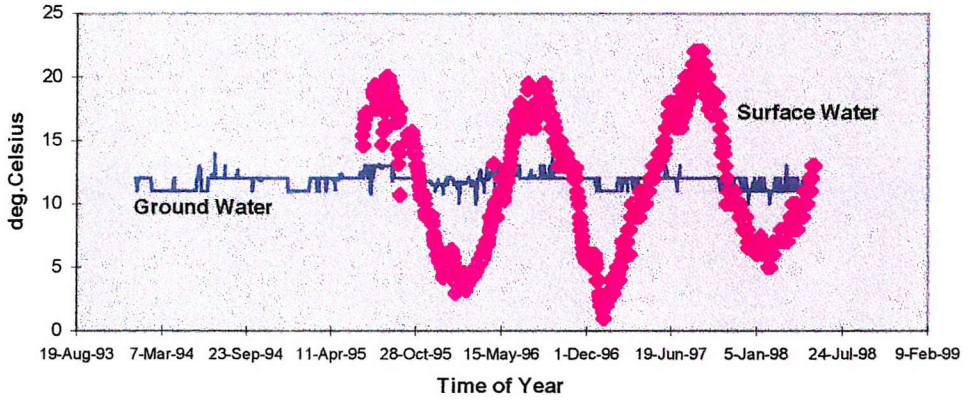

Figure 2.22: Graph to show water temperature variance over several years (courtesy: Thames Water Utilities).

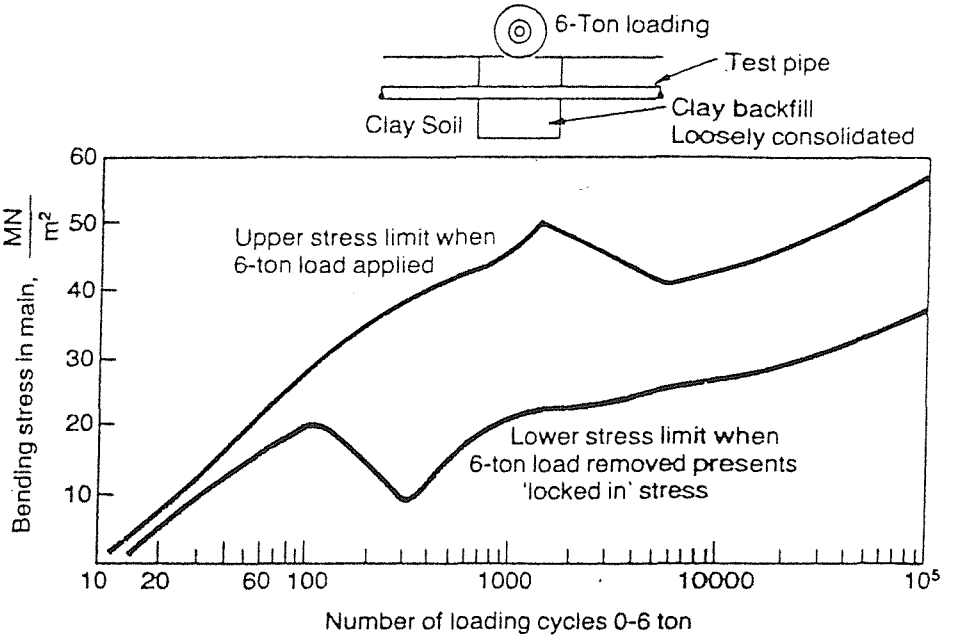

Figure 2.23: Bending stress induced by repeated surface loading on main with non-uniform bedding (Needham & Howe, 1981).

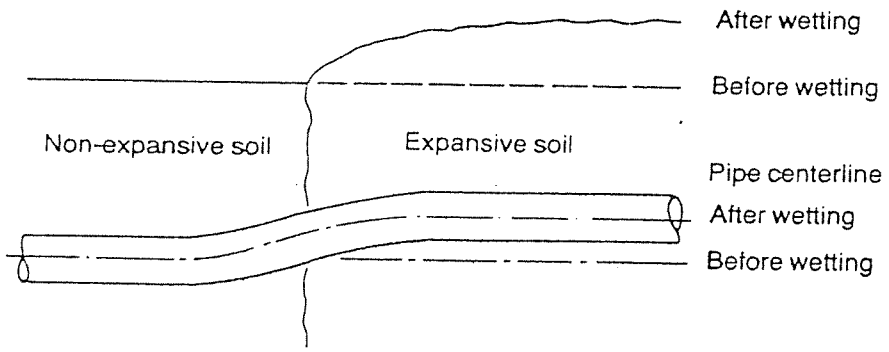

Figure 2.24: Diagram of the differential soil expansion effect on buried pipes (Needham & Howe, 1981).

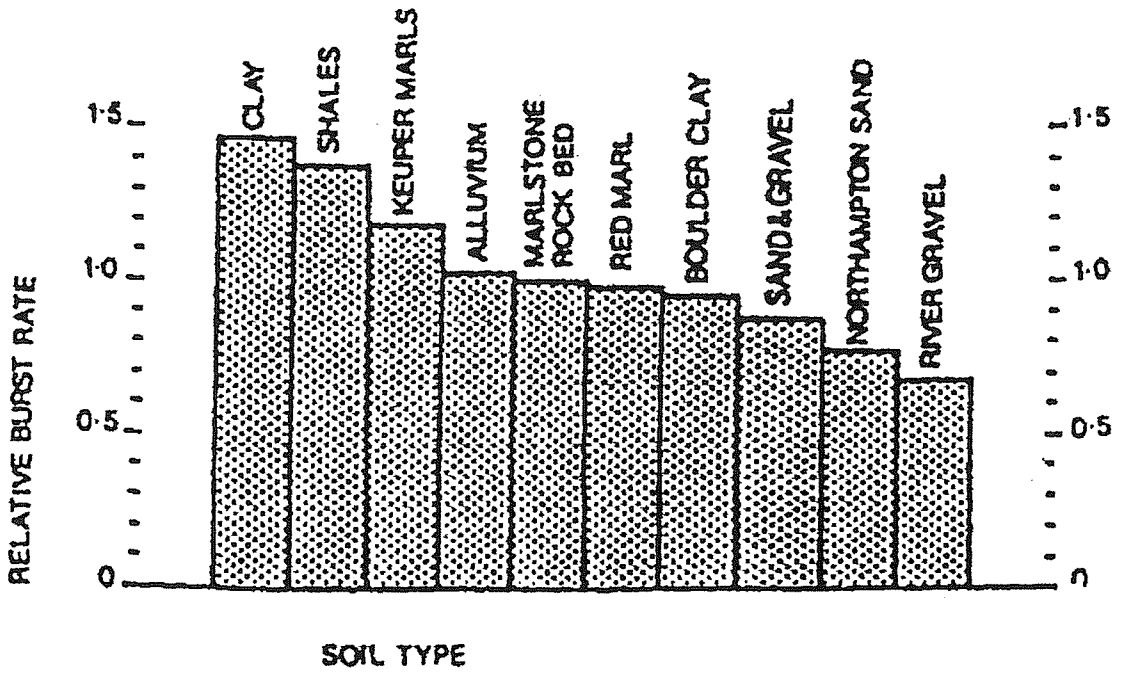

Figure 2.25: Burst rates of water pipes in various soils, South East England (courtesy: Thames Water Utilities).

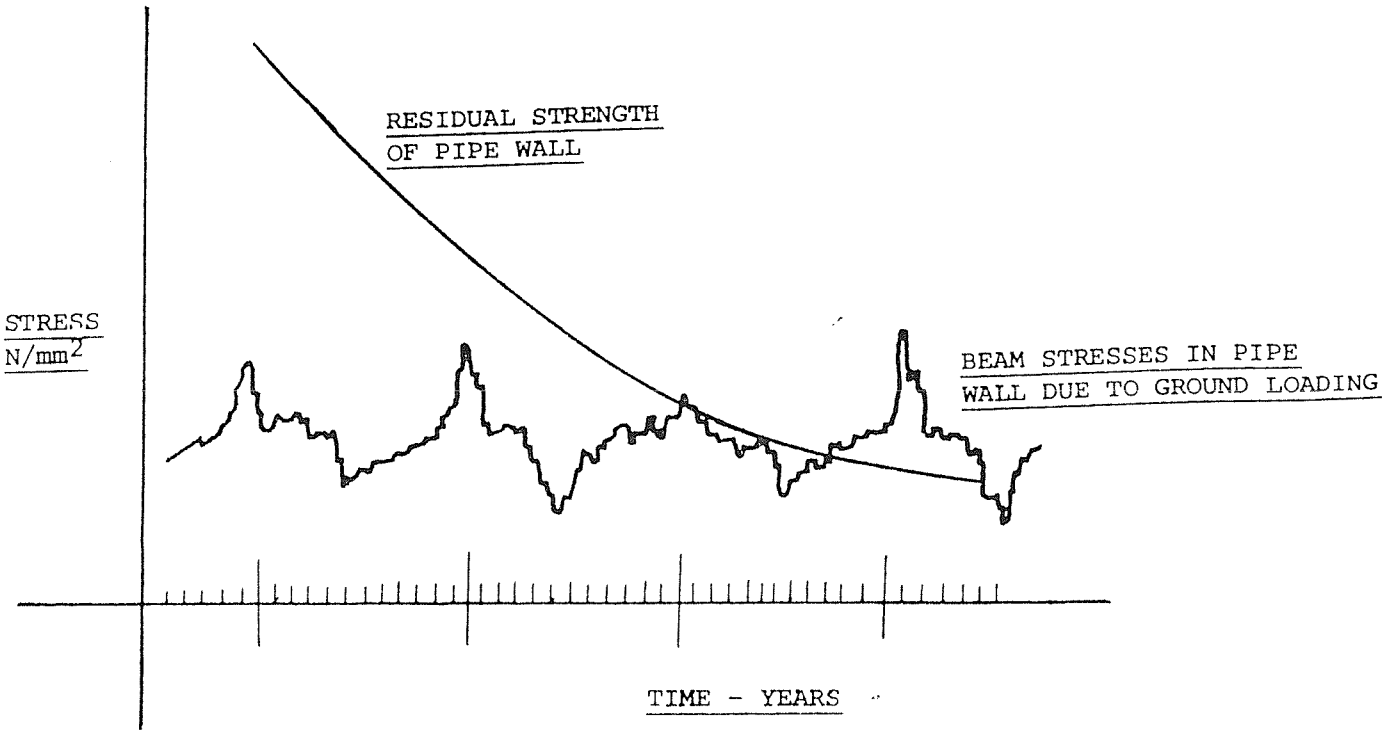

Figure 2.26: Interaction of the residual strength of pipe wall weakened by corrosion, with seasonally varying beam stresses.

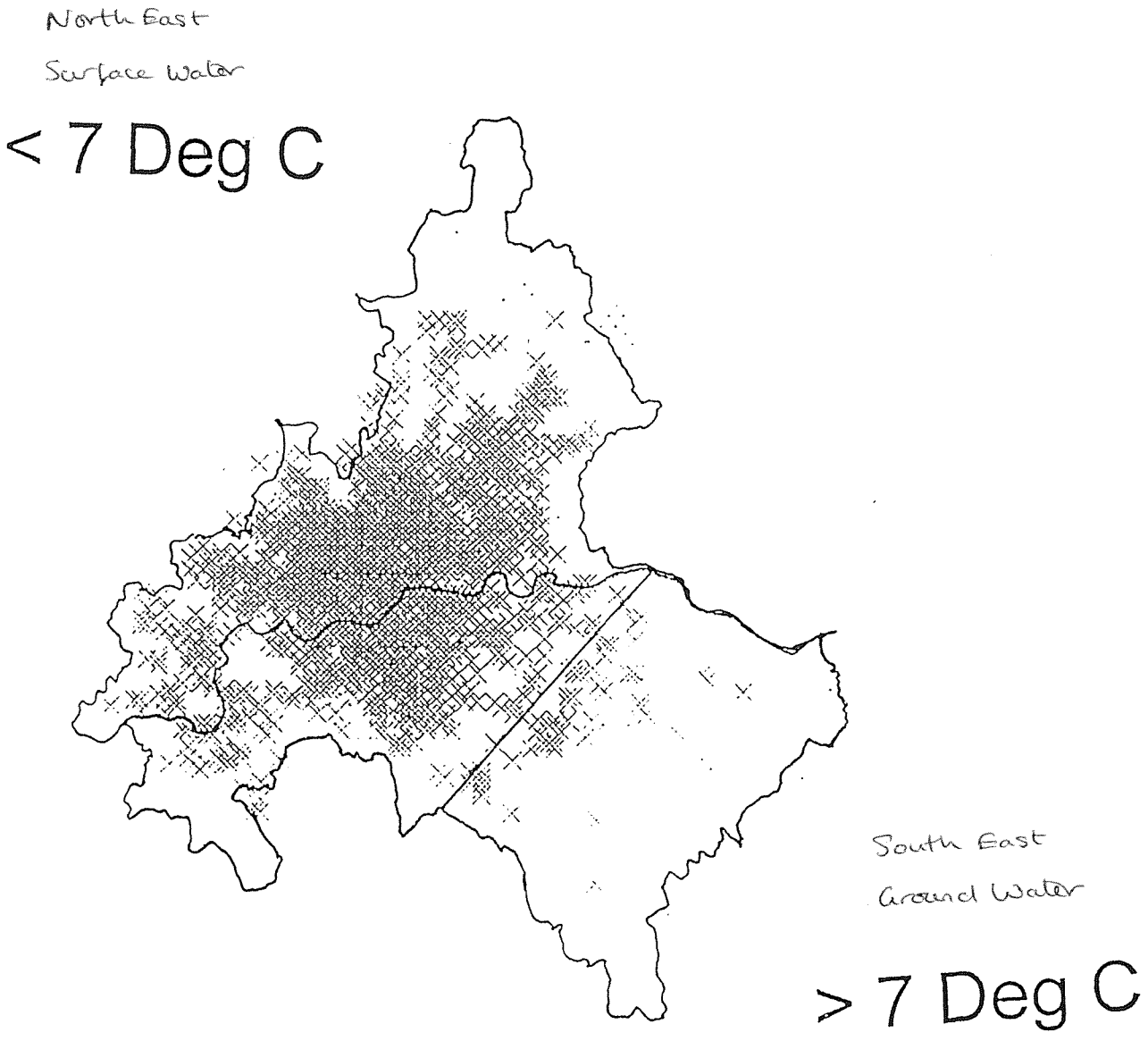

Figure 2.27: Regional map to show spread of pipe bursts to concentrate in surface water sourced areas (courtesy: Thames Water Utilities).

CHAPTER 3

AXIAL LOAD PULL OUT EXPERIMENTS ON 4 INCH CAST IRON WATER PIPES

CHAPTER 3 AXIAL LOAD PULL OUT EXPERIMENTS ON 4 INCH CAST IRON WATER PIPES

3.0 Introduction

The purpose of these experiments was to observe the pull out resistance of cast iron lead run joints in, 100mm (4 inch) diameter, to determine the longitudinal axial load required to fail the joints. The displacement of the joint during loading was to be measured until a significant displacement had been reached or until the joint failed, whichever occurred first. Particular emphasis was placed on movement at relatively small loads (40-80kN), as these loads would be experienced due to thermally induced stresses when the pipe is underground.

3.1 Methodology

Before any testing could take place collection and selection of cast iron pipes with lead run joints had to be carried out. Joints from various water pipe depots were collected and joints from known excavation sites were reserved and tagged in preparation for testing. At these known excavation sites, site investigations were carried out to obtain as much information as possible about the environment the joints had been laid in. Cast iron lead-run 100 mm diameter pipe joints were targeted as these joints and pipes statistically have the highest burst frequency (refer to Chapter 2).

Three cast iron joints were found from local pipe depots, in and around the Guildford area. Their history was uncertain. These were used for trial runs to ensure the procedure and equipment was optimised for tests on other joints with known backgrounds.

3.2 Selection and collection of joints

100 mm (4 inch) cast iron water pipes were selected with lead run joints. They could not be too heavily corroded, for otherwise the experimental preparation they had to undergo would break them, as their walls would be too thin for them to be adapted to the fixing mechanisms. It was important to know their source and the type of ground they were laid in, as certain ground types are said to be more corrosive than others are. This could then be noted when the condition of the joints was recorded. Three joints of unknown history were collected for the initial test runs. The rest of the joints were selected from three site investigations: Cedar Road, Embelton Road and Roupell Street, all of which lie within South East London districts. Seven 100 mm (4 inch) cast iron lead-run joints from Embelton road were tested, as these fitted the specification perfectly.

The site report for Embelton Road (Appendix B), showed the pipe to be located 1m west of the kerb of Embelton Road, running north-south. Figure 3.1 presents a sketch of the features and dimensions observed in the trench in plan view, and note the joint locations. The invert of the pipe was 0.82 to 0.89 m below the road surface. The back fill was varied ranging from sand at Joint#7 to clay at Joint#1. The joints found in the clay end (Joints#1 & #2), of the trench were much more corroded than those in the sand end of the trench. The joints had a date of 1910 stamped onto the rim of the bell. The surrounding housing was Victorian in style. At the north end of the trench on the road above was a stopcock marked "MWB", Metropolitan Water Board. These three observations suggest the age of the pipes and joints to be in the early 1900's, approximately eighty-eight years old. The trench was dry when the joints were taken, suggesting that the joints were not leaking.

3.3 Preliminary Trials

The purpose of carrying out trial pull out test on the three unknown cast iron joints was to:

- To establish likely ranges of failure load to assist in selection of instrumentation
- Develop the connections between the pipe and the testing machine.

3.3.1 Preliminary equipment specification

Figure 3.2 shows the set up of the equipment used to carry out the axial pull out tests, this equipment comprised of:

- 2 LVDT's - 2 MPE Transducers, LSC Type - HS, full bridge 350Ω, input 10V AC or DC (LVDTs), serial No. 2377-25.
- Loading rig - Instron tensile testing machine, model 1185
- Data logger - 1 Orion data acquisition system SI 3531D
- Calibration equipment - 1 micrometer, 1 digital multimeter (RS), Thurlby 1905a and 1 Farnell DC power supply, E15/2B
- Joint fixings - 2 cylindrical steel fixing bars and silver steel plugs

Measurements from the three 100mm (4 inch) joints were taken using a vernier calliper in the positions shown in Figure 3.3. Table 3.1 shows these measurements.

3.3.2 Calibration for preliminary trials

Using a 10 volt supply calibration of 2 MPE Transducers was carried out using a micrometer, a digital multimeter and a DC power supply. LVDT1 had a maximum error of 0.01mm over a range of 10mm, and an error of 0.02mm over a range of 15mm. LVDT2 had a maximum error of 0.01mm over a range of 15mm. The 2 LVDTs were then connected to an automatic logger (Orion) and a calibration was carried out on the combined system.

3.3.3 Procedure for preliminary trial axial pull out tests

The joint was prepared for the attachment of cylindrical steel fixing bars, collars and LVDT clamps. The outside of the joint invariably had corrosion deposits attached to its surface which had to be removed, to protect all equipment from loose debris. The corrosion deposits were removed using a hammer and chisel, until the surface was relatively smooth. If this was inadequate then the joint was placed in a shot blasting unit

for a few minutes to remove stubborn pieces of corrosion. The inside of the pipe was cleaned in a similar way. Holes were then milled into the joint in order to fix the steel bars and LVDT clamps. The milling machine was set up using V blocks to support the pipe joint. The pipe joint was positioned and clamped into place. One inch (25.4mm) holes were milled through the pipe joint 3" (76.2mm) in from each section (Figure 3.4). Two 2BA holes were milled at 90° to the 1 inch holes on the spigot end only, 3/4 inch in from the section (Figure 3.4).

LVDT clamps were attached to the spigot end of the pipe joint so that the LVDT's could be positioned at the midpoint of their length of travel when they touched the lip of the bell (Figure 3.5). The joint was installed in the loading rig using the steel bars and suspended by its bell end (Figure 3.6). The LVDT's were positioned in the steel clamps after the joint had been connected to the loading rig to protect them from any knocks during installation. The top and bottom of the joint were marked with the date and experiment number. The LVDT's were connected to the logger and initial readings were taken at zero load.

Readings from the LVDT's were taken with no load on the joint. The joint was then loaded with 0.1 tonne (1kN), and LVDT readings were taken. The load was then increased in 0.1 tonne (1kN) increments, with LVDT readings being recorded after each 0.1 tonne increment. The joint was loaded until either failure occurred or the joint was pulled apart by approximately15mm, or a load of 10 tonnes was reached. The failed joint was examined and signs of fracture were recorded, paying particular attention to corroded areas and their positions. The LVDT voltage readings were converted into displacement in millimetres using the calibration data. A graph of load against displacement was plotted using an Excel spreadsheet.

3.3.4 Results of preliminary trials

The LVDT's used in the Joint#1 experiment showed negative displacement for the initial part of the experiment. This can possibly be attributed to the sensitivity of the instruments and possible drifting until a certain displacement was obtained for readings to show movement in the positive direction. Referring to Figure 3.7 Joint#1 can be seen to be

responding to positive displacement when the load has reached 60kN. Displacement from this point continued to increase. However this displacement is minimal, reaching less than 0.02mm by the time the load had increased to 80kN. Figure 3.8 shows the displacement only to have reached 0.04mm in total even with 95kN of load. Further displacement with load could not be seen as we had reached the capacity of the machine. From Figure 3.7 Joint#2 showed initial slip at about 16kN. After this slip had taken place the joint slowly displaced itself reaching approximately 0.5mm at 70kN (Figure 3.9). After slippage the joint displacement shows generally linear behaviour with load. The load increments were halted and held at approximately 98kN as the machine had reached its maximum capacity. Displacement continued and the load began to drop as the joint moved apart, where the experiment was stopped.

From Figure 3.7 Joint#3 it can be seen that the LVDT responds in steps larger than that Joint#1 and Joint#2. The sensitivity has been decreased by a magnitude of ten. The original data gives displacements to two decimal places, whilst data from the previous tests gave displacements to three decimal places. The reason for this is unclear, but presumably resulted from operator error. However, the general behaviour of Joint#3 can still be seen, with initial signs of slippage around 38kN. The displacement-load relationship being generally linear up to 50kN (Figure 3.10). When the load reached around 68kN another slippage occurred which resulted in a large increase in displacement, approximately 2mm. When a load of about 73kN was reached the load began to drop but the displacement continued to increase. When the load had dropped to 55kN, the experiment was stopped and the LVDT's were realigned and reset, as their limit of travel had been reached. The experiment started again with the LVDT's at about 13mm. Load increased again with displacement remaining still, until a load of 55kN was reached, where the load began to fall and the displacement increased. When the load had dropped to about 40kN the LVDT's were realigned again. The load had dropped to approximately 11kN and displacement was reading about 18mm when the experiment was started again. Displacement and load re-engaged, with the load climbing back up to 40kN and displacement reaching 20mm. The experiment had to be stopped then as the Instron loading rig had undergone its maximum length of travel.

3.3.5 Observations from preliminary tests

Joint#1

Significant displacement of the joint did not occur during the whole experiment. Cracking noises were heard coming from the joint, but no movement was observed with the naked eye. The LVDT's recorded minimal displacement of approximately 0.04mm, even with 100kN of load. Corrosion was minimal and pitting was not seen over the surface of the pipe. Wall thickness was constant and the interior of the pipe was relatively clean and corrosion free.

Joint#2

Slippage of the joint started when the load reached approximately 16kN (Figure 3.9). As the load increased the joint appeared to significantly slip at approximately 28kN, resulting in a displacement of approximately 0.05mm. After this initial slip the load and displacement began to increase linearly. When 98kN had been reached the load began to drop off and displacement continued with a steeper gradient. The joint moved just over 1mm after nearly reaching 100kN. The joint showed strength and durability from this test. When examining the joint after the test, it was seen that a crack in the lead had occurred all around the rim of the bell on the inside. Failure of the joint had commenced. Further testing would have shown the spigot being drawn out of the bell end. The crack showed the joint had been weakened and it would have only taken more time to weaken it further rather than more load.

Joint#3

The pipe was heavily corroded externally on the spigot end, especially near the rim of the bell. The rim of the bell itself was also heavily corroded. From what could be seen of the inside of the pipe corrosion was minimal. Once slippage had occurred, the joint seemed to offer little resistance to displace itself further. However it did need more force to cause it to slip in the first place compared to Joint#2. This could be due to the corrosion binding the joint together, making the joint more rigid. After examining the failed joint, the lead could be seen to be striated, and it was heavily grooved as it had been gouged along its length as it was drawn out. From Figure 3.10a and 3.10b the stiffness of the joint at the two unload and load phases can be approximated, as 21kN/mm and 9kN/mm respectively.

3.4 Re-design of test Procedure based on outcome of preliminary trials

From the experiment observations during the preliminary tests it was concluded that:

1. Displacement measurements should be taken continuously to monitor slippage activity. This would show whether creep occurred.
2. LVDTs with a longer length of travel should be used to allow for complete measurement of the total joint displacement.
3. Load needed to be logged continually to be able to observe slippage activity. This could be done by changing the fixing shafts to fit onto the Instron loading rig, thus allowing automatic logging of the load.
4. The entire length of the joint would have to be limited to 800mm so it could fit inside the Instron loading rig.
5. Future tests required displacement control, instead of load control.
6. Joints needed to be marked where the bell lip initially lay, so that any movement during the experiment could be noted.
7. Protective plastic sheeting would be placed around rig, to prevent shattered pieces of pipe causing injury.
8. Future cast iron joint tests should initially be tested to 100kN, and if the joints had not failed at this load, then tested on a larger loading rig.
9. Tests should be left longer once the machine's full capacity had been reached, to give the joint time to fail and displace.

3.5 Final equipment specification

The equipment used to carry out the axial pull out tests on the Embelton Road joints comprised the same instruments as the previous trials except the loading rig. The Instron loading rig was not available for further tests, so a Satec Universal Screw Drive loading rig was used. No accuracy was lost in the change of loading rigs. A third LVDT was also installed on the head of the loading rig to monitor its travel. Feed rate was kept at 5mm/min.

It was acknowledged that the speed of the joints should be reduced, but time and resources were limited.

3.5.1 Embelton Road joint dimensions

All the dimensions were measured as shown in Figure 3.3. All the Embelton Road joints were 100mm (4 inch) cast iron lead run joints. Joint#1 was not measured and tested as it was badly corroded and not fit for experimentation (Figure 3.11). Photos of all the joints can be found in Appendix A from the Embelton Road site investigation report. Dimensions of Embelton Road joints can be found in Table 3.2.

3.5.2 Procedure for final axial pull out tests

The joint was prepared for the attachment of cylindrical steel fixing bars, plugs and LVDT clamps as described for the preliminary trials. LVDT clamps were attached on the spigot end of the pipe joint. The clamps were positioned to allow the LVDTs full length of travel to be in, just touching the lip of the bell. This was to allow for maximum use of the length of travel. A third LVDT was connected to the head of the loading rig so that the travel of the head could be monitored and checked against the readings (Figure 3.12). The joint was connected to the loading rig and the LVDTs were attached as discussed previously. The loading was set in motion and the results were monitored and plotted using an Excel spreadsheet.

3.5.3 Results of final trials

Embelton Joint#2

From Figure 3.16 it can be seen Joint#2 initially slipped at about 45kN. Displacement was minimal and Figure 3.17 shows Joint#2 remained rigid up to a load of about 60kN. Here one side of the joint began to displace as seen by LVDT2, and the other side remained fixed, as seen by LVDT1. Load continued to increase to 80kN when the uneven displacement of the joint caused the joint to be stressed on one side resulting in a crack in the pipe. This cracked propagated all the way round the pipe. The load dropped off to just less than 10kN with a displacement of 1mm on one side of the joint and 2.5mm on the other. Crack initiation occurred at the machined hole, into which the steel fixing bars were inserted to connect the joint to the loading rig. The external surface of the pipe in this area was heavily pitted, leaving the pipe wall thinner and weaker than elsewhere.

Embelton Joint#3

Figure 3.16 shows that the displacement of Joint#3 started to occur at 38kN, but the joint continued to take an increase in load. Figure 3.18 shows at approximately 95kN the joint had displaced about 1mm, then the load dropped sharply to 70kN resulting in a displacement of nearly 2mm. The load then began to increase again, with displacement continuing much slower. At 98kN the displacement increased sharply again with load decreasing to about 61kN causing an average displacement of 3mm. Load began to increase for a third time reaching 98kN when the joint slipped again, dropping the load to about 71kN and displacing now to about 4mm, where the experiment was stopped.

Embelton Joint#4

From Figure 3.16 it can be seen that Joint#4 initially slipped at 18kN but the movement was insignificant. Load continued to increase and only when 70kN had been reached had the displacement reached approximately 0.3mm (Figure 3.19). After 80kN the joint had moved 0.5mm and after 88kN this displacement had reached approximately 1mm. The joint peaked at 88kN of load where it failed and the joint began to displace rapidly. The load began to drop and by the time it had decreased to 65kN, the joint had displaced 20mm, where the experiment was stopped.

Embelton Joint#5

Figure 3.20 shows displacement of Joint#5 initiated the moment the load was engaged. Displacement was minimal and Figure 3.21 shows the displacement of Joint#5 did not begin significantly until the load had reached a value of approximately 55kN. At this load the joint significantly slipped. As the load continued to increase the displacement increased slowly at a relatively steep gradient, with the load peaking at about 100kN. The load began to fall and at approximately 88kN the joint must have failed as displacement accelerated. By this stage the spigot end of the joint began to slide out of the bell end. Movement was very slow and invisible to the naked eye. The load decreased to about 55kN by the end of the experiment and displacement was about 22.5mm.

Embelton Joint#6

Like Joint#5, Joint#6 began displacing the moment the load was engaged (Figure 3.20). From Figure 3.22 it can be seen that significant displacement of the joint started to occur when the load had reached 40kN. At 50kN the joint had moved about 0.8mm. Load and displacement continued to increase linearly at a gradient of 0.13. At a load of 70kN the joint had displaced about 5mm. Both load and displacement continued to increase, with load reaching a peak of 95kN and the joint displacing 23mm by the end of the experiment.

Embelton Joint#7

Again Figure 3.20 shows displacement was immediate but insignificant to begin with. From Figure 3.23 it can be seen that Joint#7 remained relatively fixed up to a load of about 50kN. Only after the load had reached 60kN did the joint begin to displace rapidly, with almost a horizontal line of travel. The load remained at about 65kN while the joint was displacing. The joint was left to displace further until it had completely separated. Figure 3.14 & 3.15 show Joint#7 pulling apart at a load of about 65kN and sitting completely apart at the end of the experiment, respectively.

3.5.4 Observations from final trials

Joint#2

After the joint had failed it could be seen that the crack initiated at the drilled hole, as it had been weakened. The hole itself would have reduced the strength across this section but it appeared to be the thinning of the walls due to corrosion pitting which was mainly responsible for weakening the pipe. Failure would have been caused by the uneven displacement causing stresses to build up at the fixing hole on the fixed side of the pipe. It can be seen from Figure 3.13 that the surface of the pipe is very irregular in this area because of the corrosion pits. These pits had reduced the thickness of the wall sufficiently enough to make this point the first point of failure under load.

Joint#3

Significant failure of the joint began once the joint at had been subjected to a load of 95kN. Total displacement was relatively small, only 4mm. Displacement of the joint was

due to the spigot end of the joint sliding away from the bell end. The lead remained intact and inside the bell end of the joint.

Joint#4

Failure of the Joint#4 occurred at 90kN and the joint continued to displace itself 20mm, while the load dropped off to 70kN. Displacement of the joint was due to the spigot end of the joint sliding away from the bell end. The lead remained intact and inside the bell end of the joint.

Joint#5, #6 and #7 all showed strength and displaced at loads of 70kN, 50kN and 60kN respectively. The lead remained intact in all cases. For Joint#7 it could be seen that the spigot end which was completely removed was still black from its original protective coating.

3.6 Conclusions

- A wide variety of load/displacement relations occurred.
- Initial slip occurred at 1 to 48kN. Significant slip occurred between 20 and 95kN.
- Unknown lead Joint#1 moves less than 0.04mm even with 100kN, resulting in a stiffness of 725N/mm.
- From unknown lead Joint#3, the first unload and load curve gives a stiffness for cast iron of 21kN/mm, the second curve gives a stiffness of 9kN/mm
- Post failure load decreased with displacement
- The state and condition of the lead, coal tar and cast iron is probably responsible for the initial slip load. The greater the corrosion the higher the load and the lower the displacement.
- A temperature drop of 20°C can raise the axial tensile load stress within the pipe to 84kN (24N/mm^2), if the pipe is held rigid. A displacement of 0.6mm in a 2.8m pipe length would relieve this temperature-induced stress. The tensile load built up between 47 and 92kN (13 N/mm^2 and 27N/mm^2 axial stress) in the Embelton Road joint tests before a displacement of 0.6mm occurred. This suggests that the joints are indeed allowing stress to increase throughout the pipe with a temperature change.

- Corroded joints increase the stiffness of the joint, which makes them require more load to displace which makes failure of the connecting pipes more probable.

	Joint#1			Joint#2			Joint#3		
Material	Cast iron pipe - lead joint			Cast iron pipe – lead joint			Cast iron pipe - lead joint		
A – Outside diameter (mm)	123	122	122	121	123	122	120	121	119
B – Inside diameter (mm)	112	110	111	110	114	112	109	111	110
C – Diameter of bell (mm)	200			200			200		
D – Wall thickness (mm)	10.4	11.2	10.5	11	9	10	11	10	9
E – Bell lip thickness (mm)	31	29	29	28	30	28	28	29	28
F – Length of pipe joint and fixings (mm)	550			800			800		
Origin	Unknown			Unknown			Unknown		
General state	Clean, non corroded			Lightly corroded with some pitting			Lightly corroded all over, heavy pitting around bell lip		
Test Date	30/09/98			27/11/98			27/11/98		

Table 3.1: Dimensions of preliminary trial joints.

	Joint#2	Joint#3	Joint#4	Joint#5	Joint#6	Joint#7
A – Outside diameter (mm)	117.9 117.9 117.8	124.0 124.1 123.8	124.5 124.0 124.0	124.8 124.3 123.6	125.4 125.6 126.5	125.5 125.7 125.5
B – Inside Diameter (mm)	97.3 97.1 98.8	102.0 102.0 102.0	103.5 103.0 104.0	102.2 101.9 102.0	99.9 100.2 100.4	102.4 100.5 100.4
C – Diameter of bell (mm)	204.2 206.1 206.4	216.0 212.5 212.1	209.5 210.8 211.4	219.1 217.4 217.8	219.6 217.7 217.5	217.9 219.0 217.6
D – Wall thickness (mm)	9.7 10.5 10.2	12.0 9.0 12.0	9.5 9.5 10.2	11.6 11.8 10.2	13.4 12.7 12.2	11.2 11.6 12.4
E – Bell lip thickness (mm)	33.5 36.0 34.1	34.0 34.0 33.0	33.0 32.0 34.0	35.5 34.9 35.0	33.9 34.0 34.6	34.9 35.0 35.7
F – Length of pipe and joint	600	600	600	600	600	600
Test date	19/01/99	27/11/98	27/11/98	19/01/99	19/01/99	19/01/99

Table 3.2: Dimensions of Embelton Road Joints

Figure 3.1: **Plan of Embelton Road Trench showing joint locations and excavation sample locations**

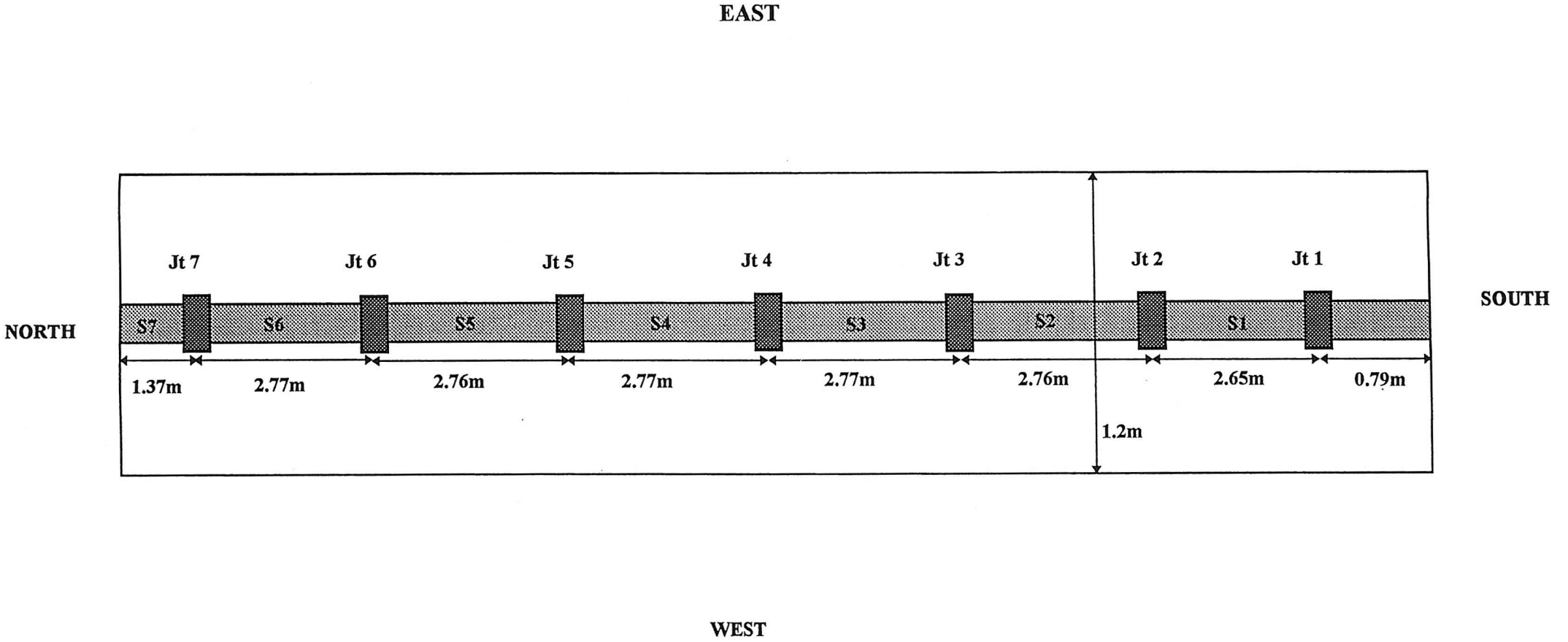

Figure 3.2: **Photo to show set up of loading rig and joint**

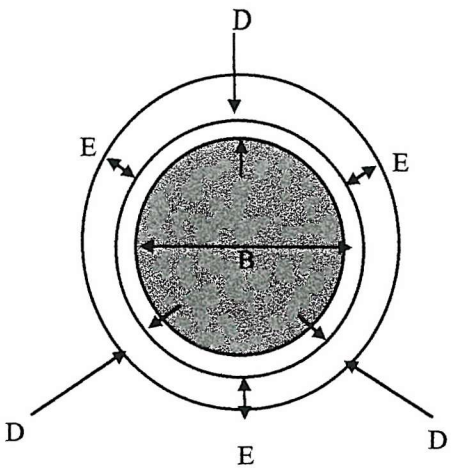

Figure 3.3 Section AA of joint

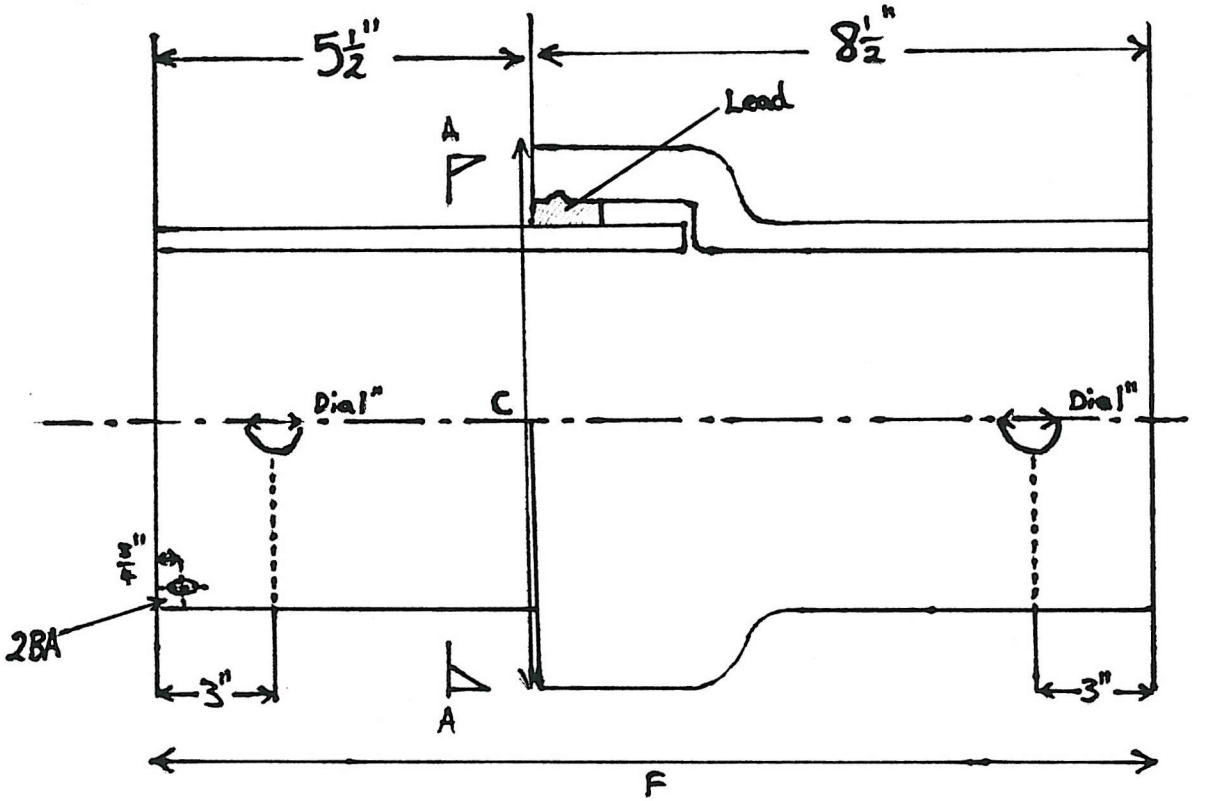

Figure 3.4: Pipe joint preparation dimensions

Figure 3.5: **Joint#1 showing the fixing of the LVDT to the test specimen**

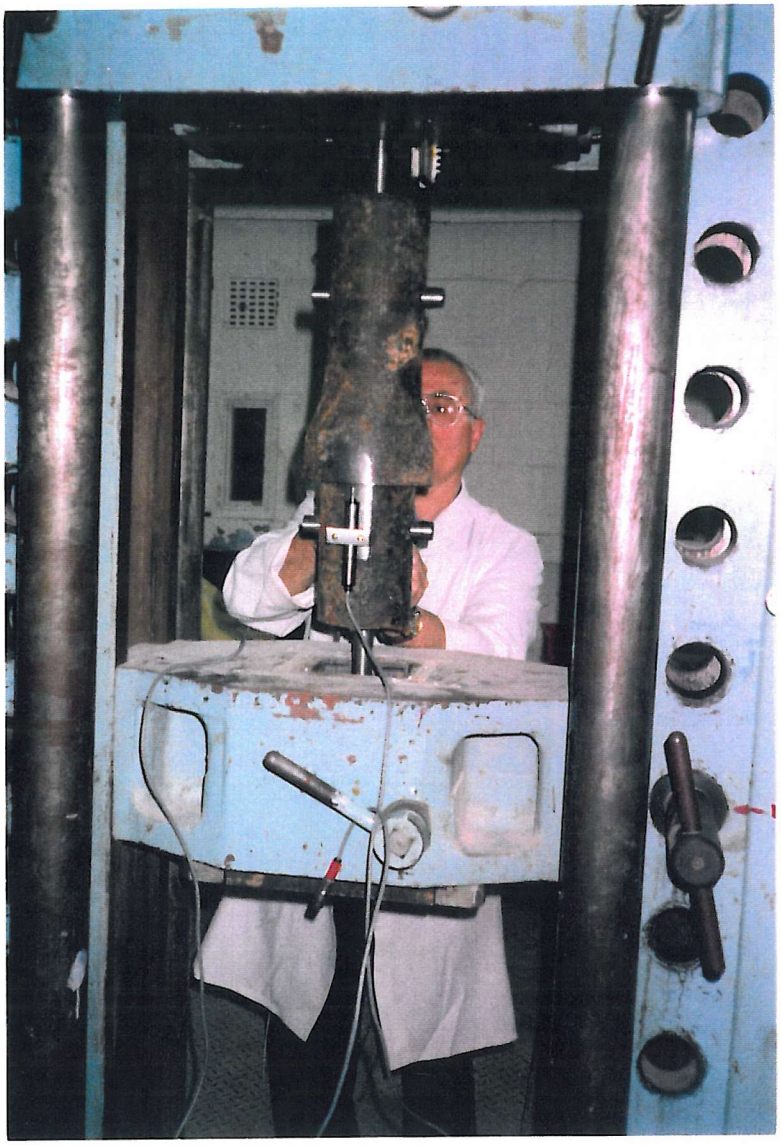

Figure 3.6: **Joint#1, showing the installation of the test specimen in the loading rig.**

Figure 3.7 Average displacements of unknown lead joints detailing initial slip loads

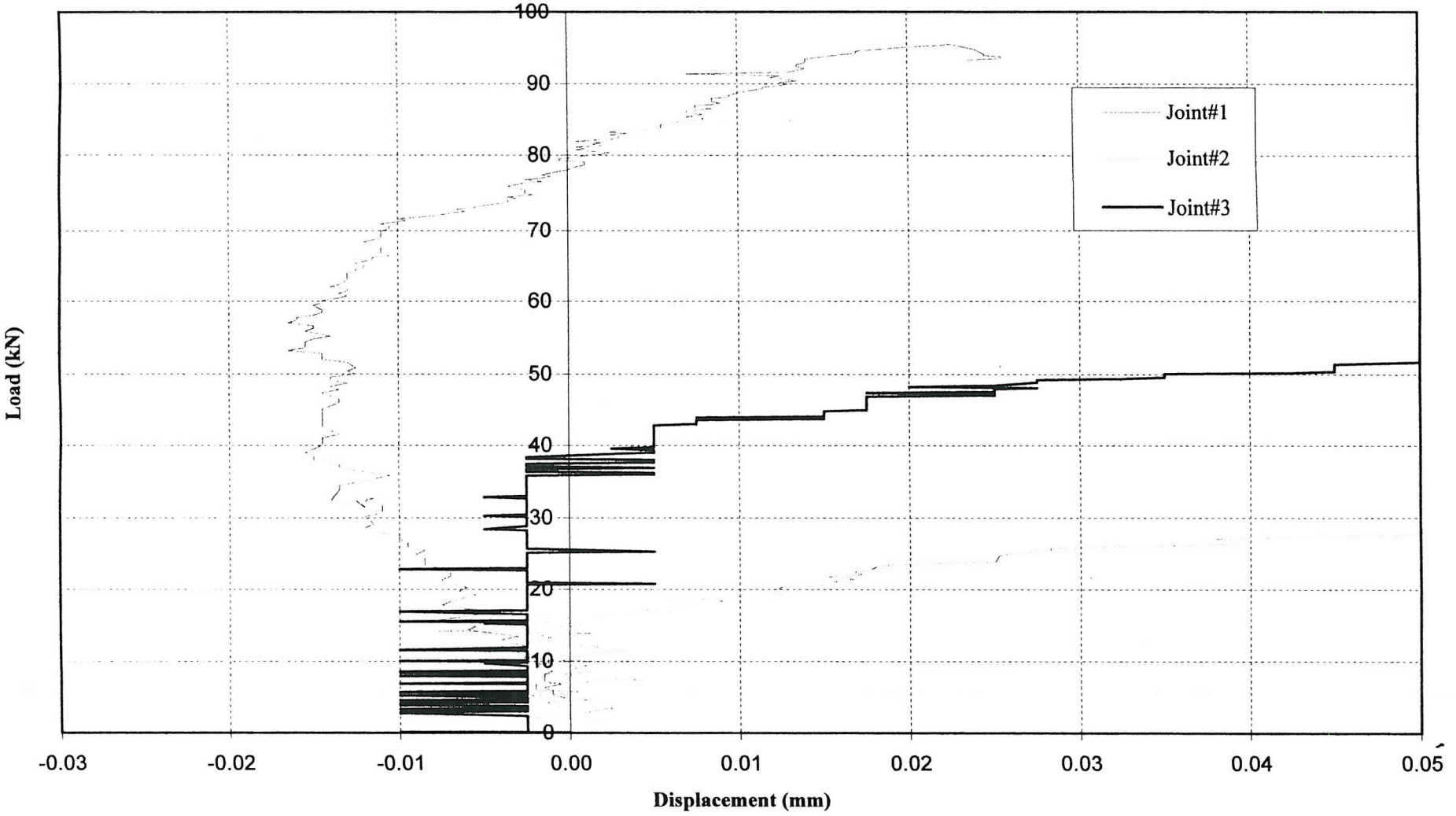

Figure 3.8 Displacement of unknown lead Joint#1

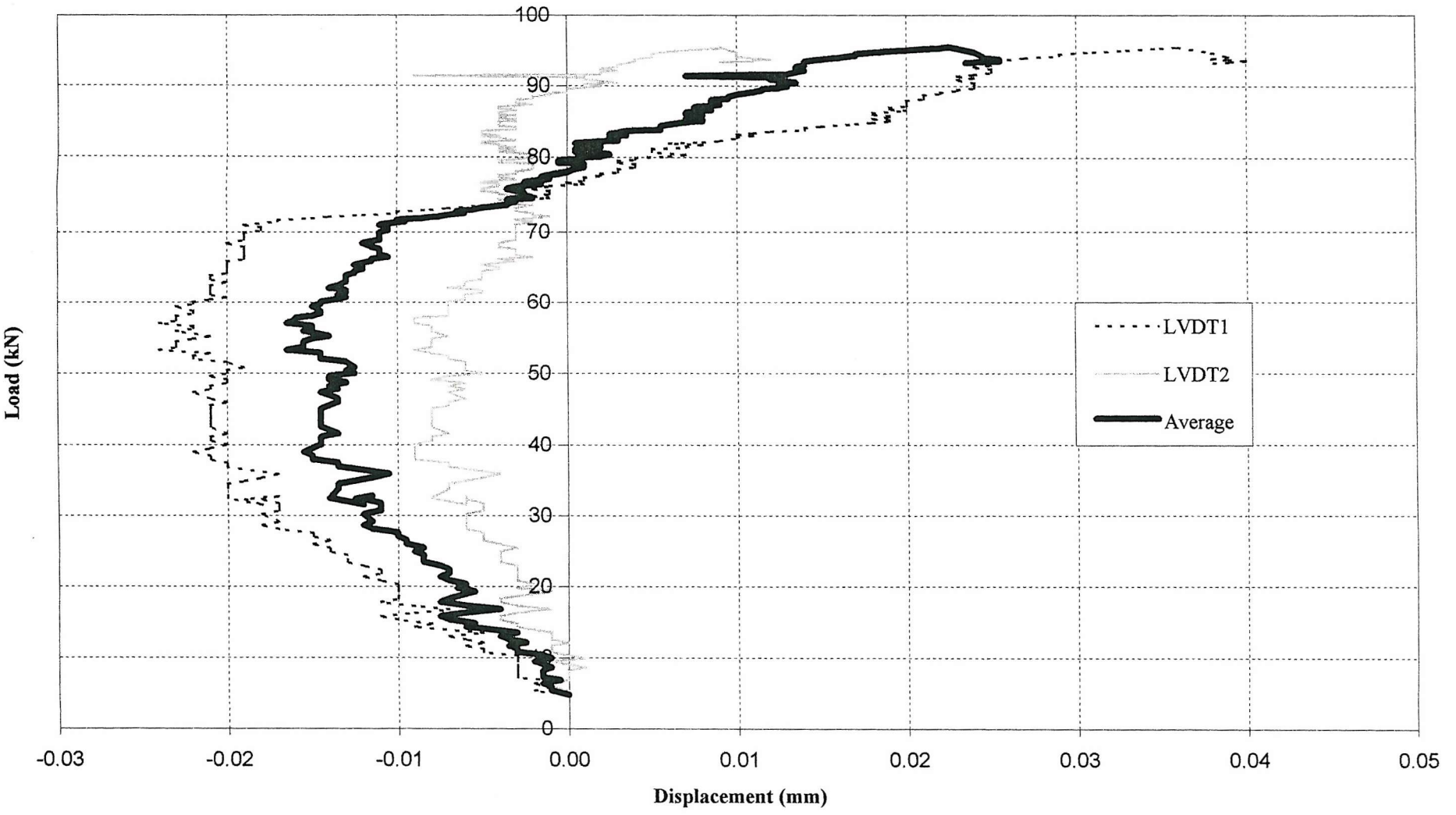

Figure 3.9 Displacement of unknown lead Joint#2

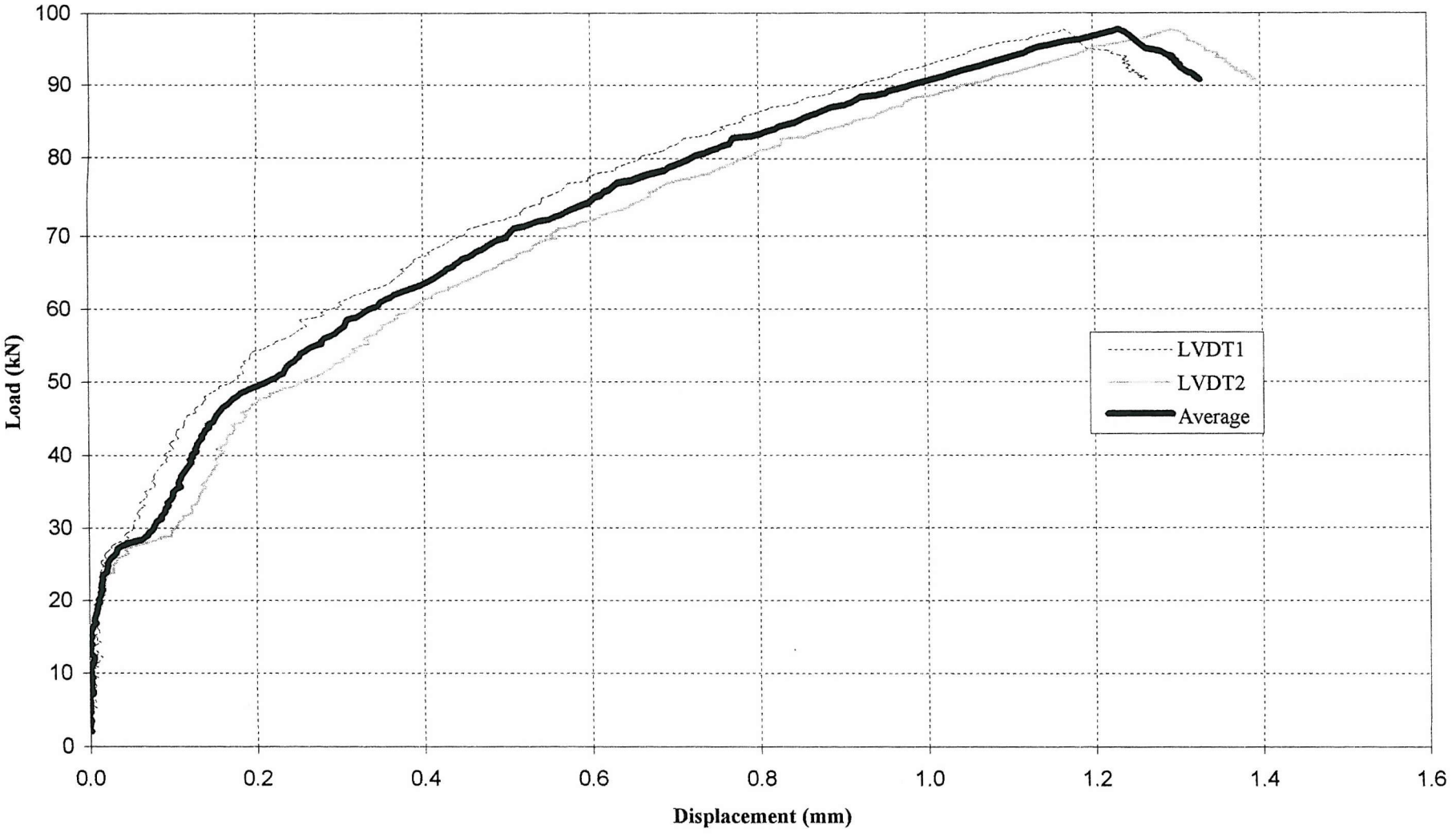

Figure 3.10 Displacement of unknown lead Joint#3

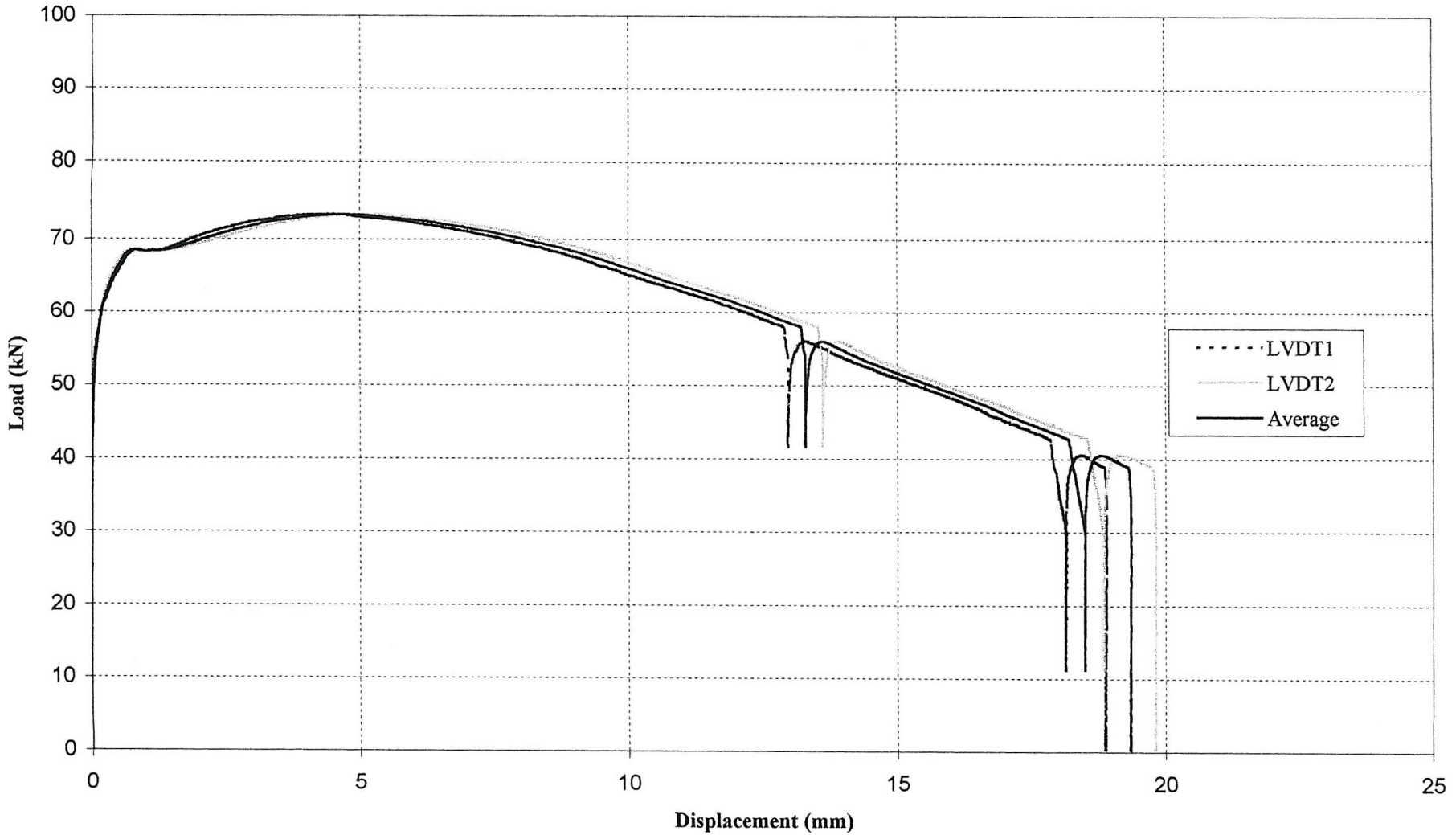

Figure 3.10a Displacement of unknown lead Joint#3 (part of figure 3.10)

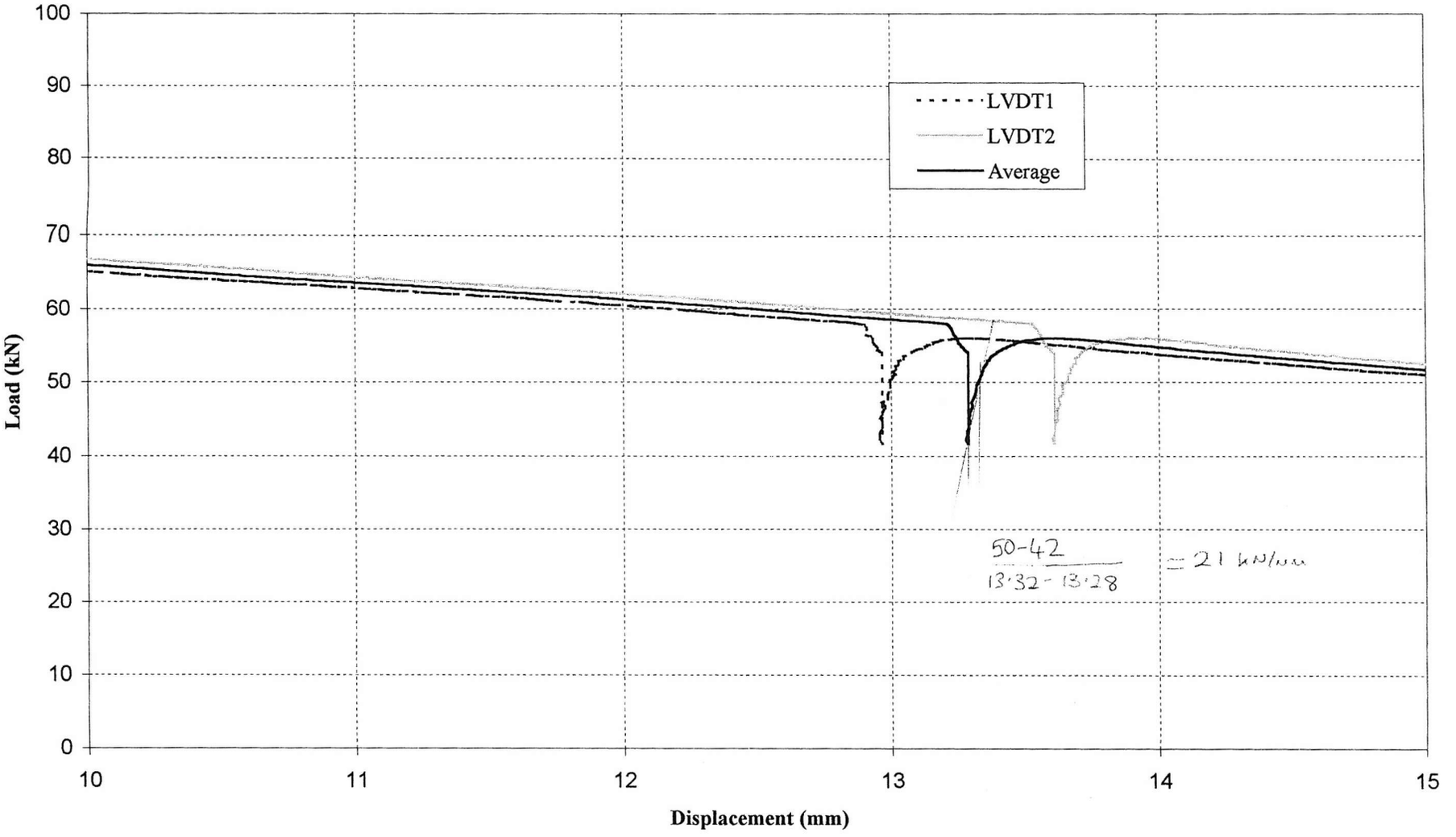

Figure 3.10b Displacement of unknown lead Joint#3 (part of figure 3.10)

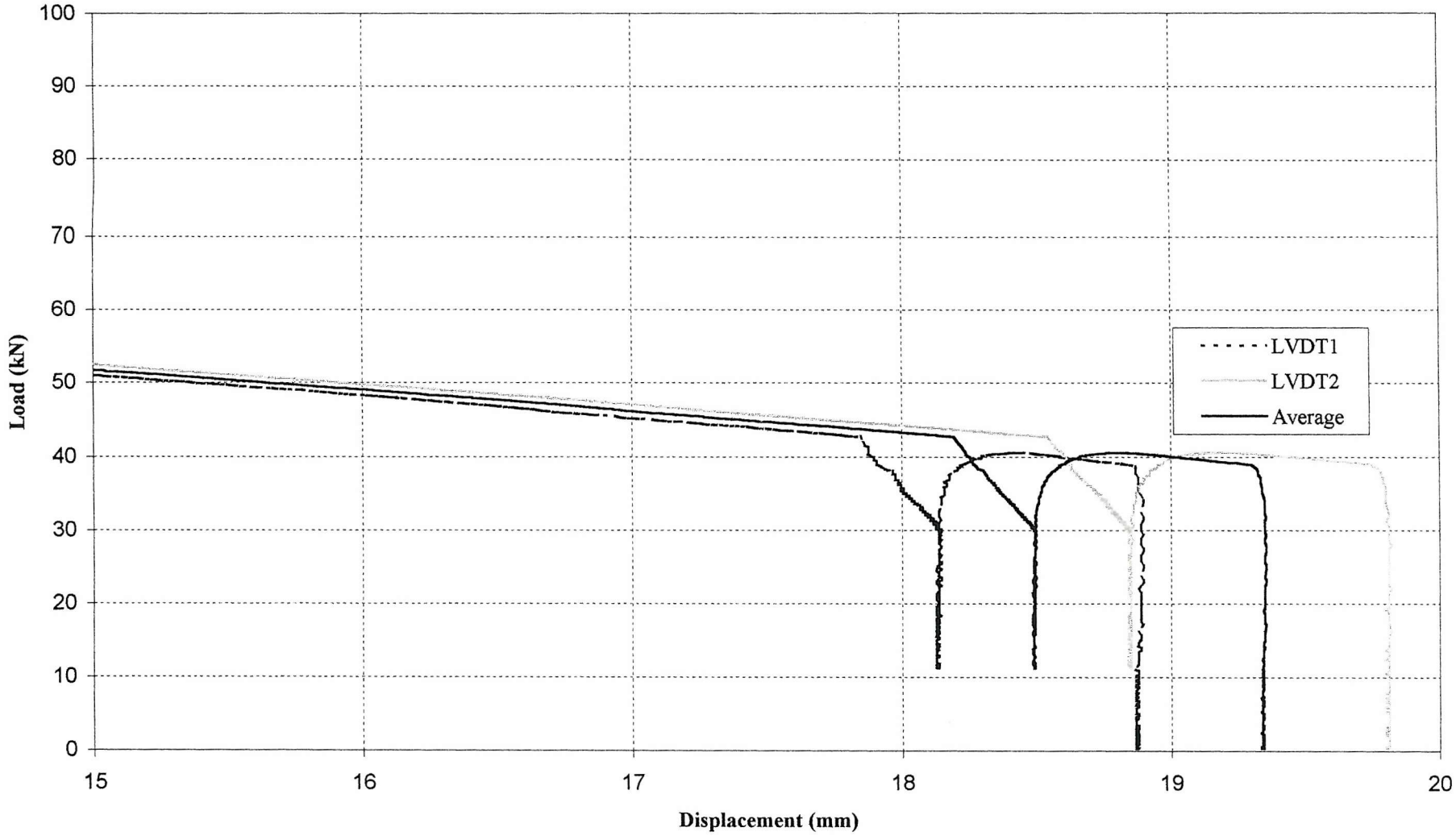

Figure 3.11: **Photo of Embelton Road Joint#1 showing extensive corrosion pitting.**

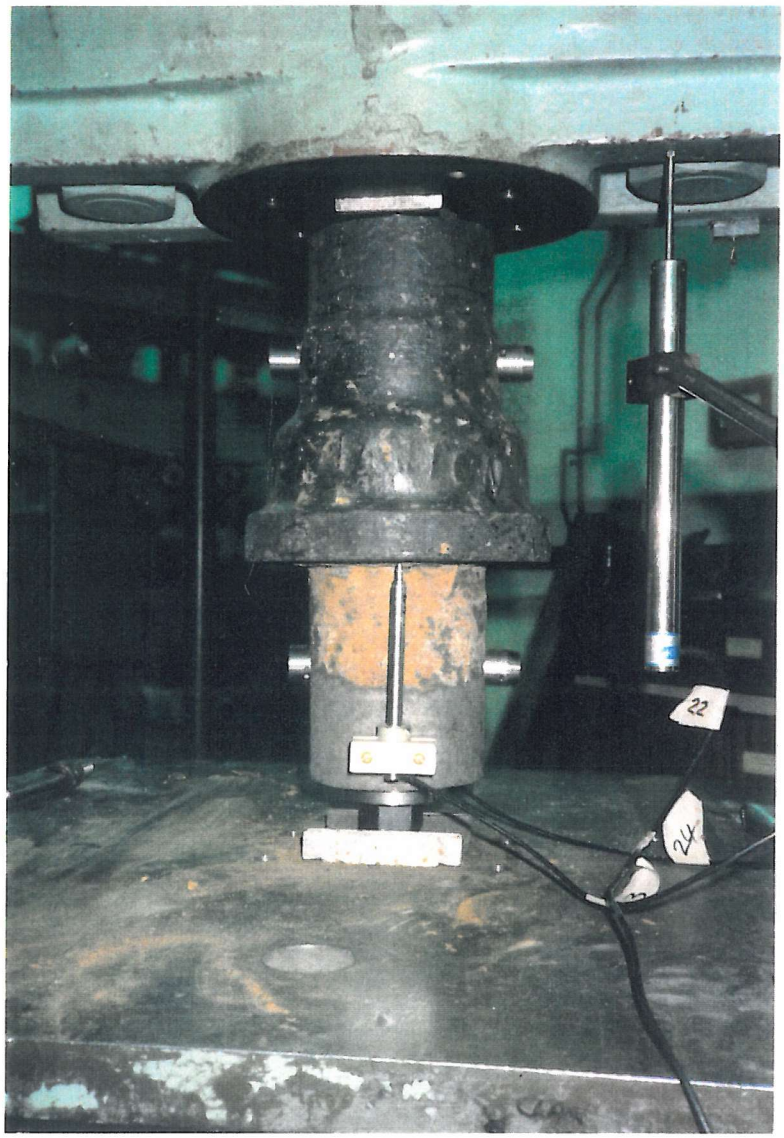

Figure 3.12: Photo of Embelton Road Joint#2 showing set up of LVDTs in screw loading rig.

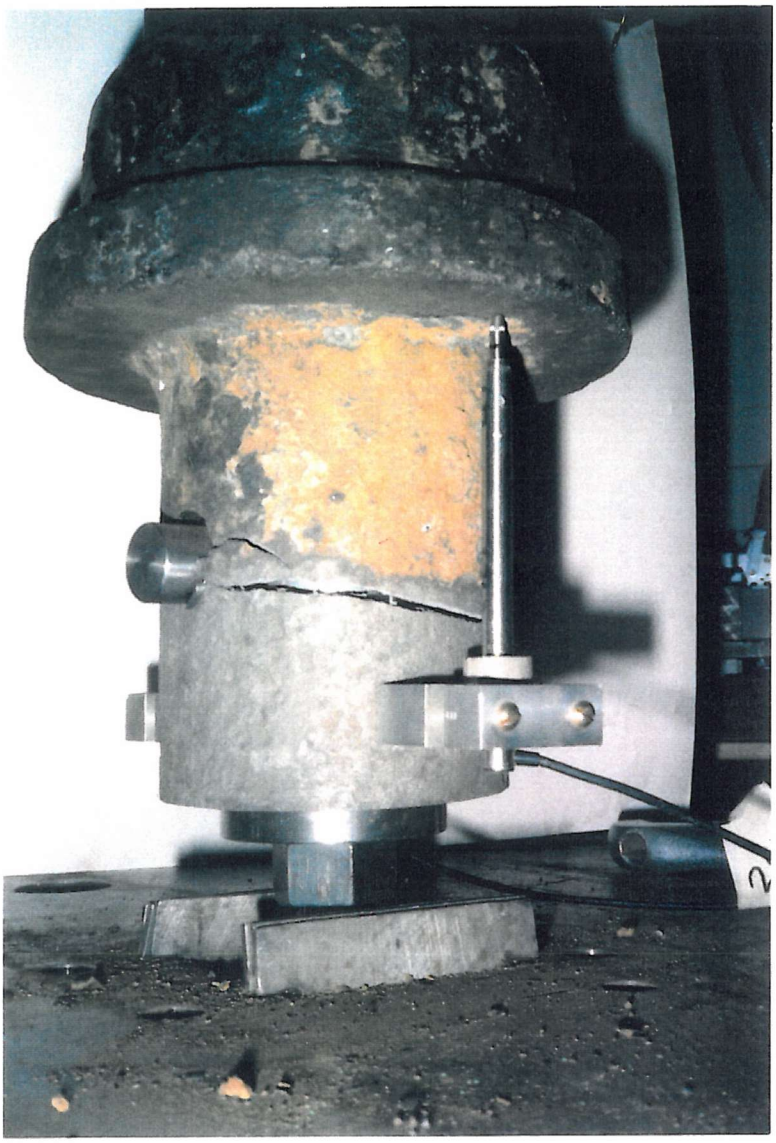

Figure 3.13: Photo of Embelton Road Joint#2 showing crack initiation of joint failure.

Figure 3.14: Photo of Embelton Road Joint#7 showing displacement of spigot from bell.

Figure 3.15: Photo of Embelton Road Joint#7, showing complete separation of spigot from bell.

Figure 3.16 Average displacements of Embelton Road Joints, showing initial slip points

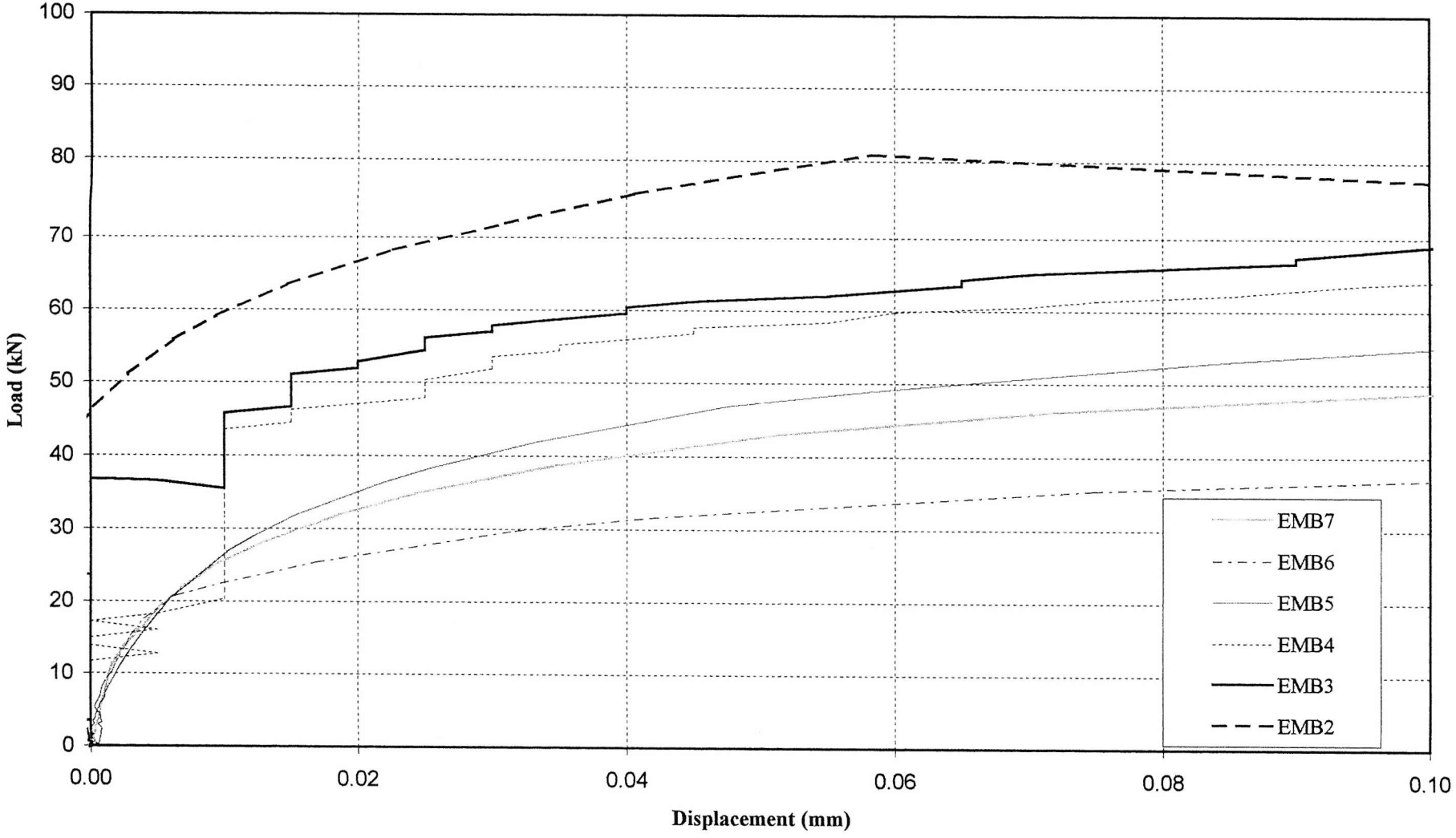

Figure 3.17 Displacement of Embelton Road Joint#2

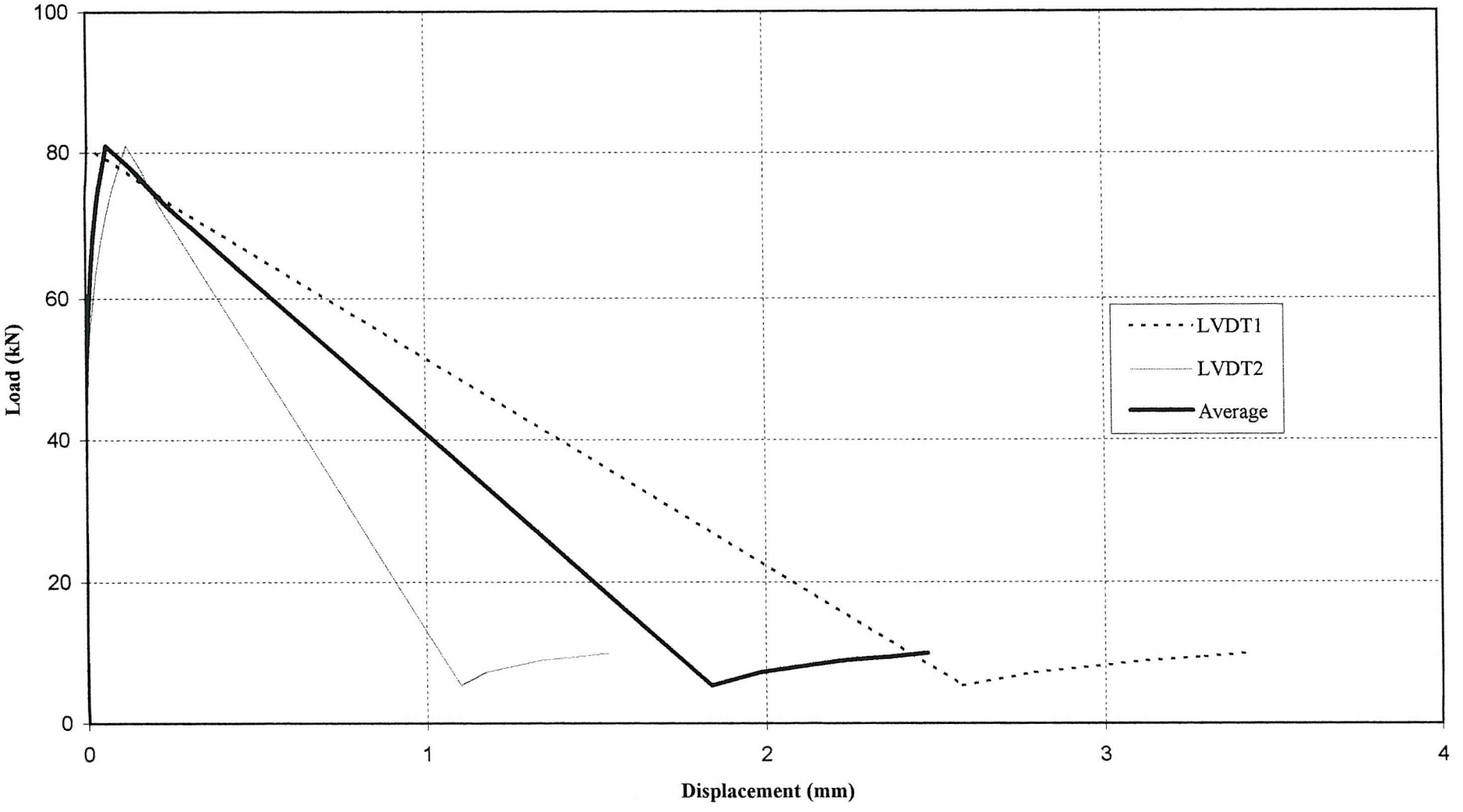

Figure 3.18 Displacement of Embelton Road Joint#3

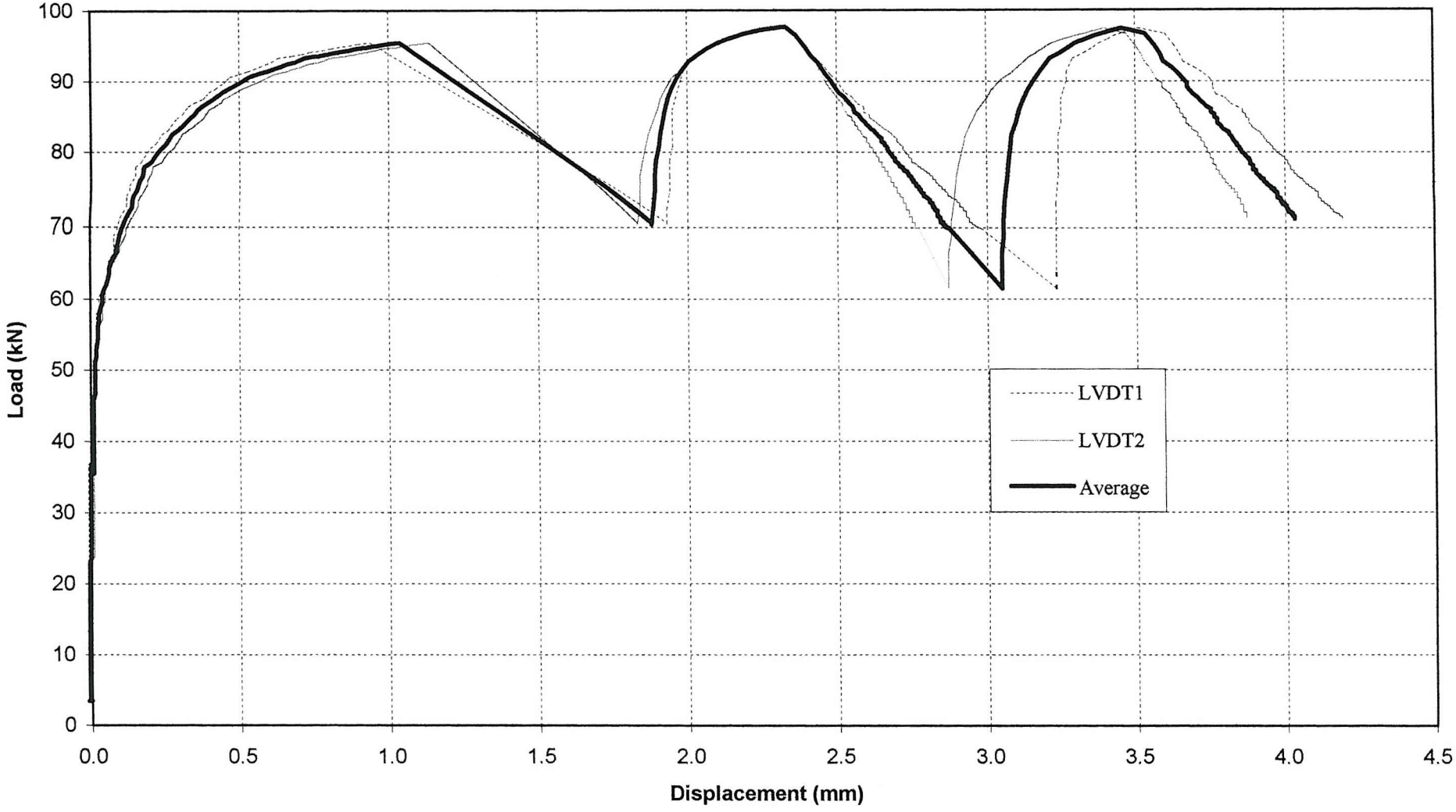

Figure 3.19 Displacement of Embelton Road Joint#4

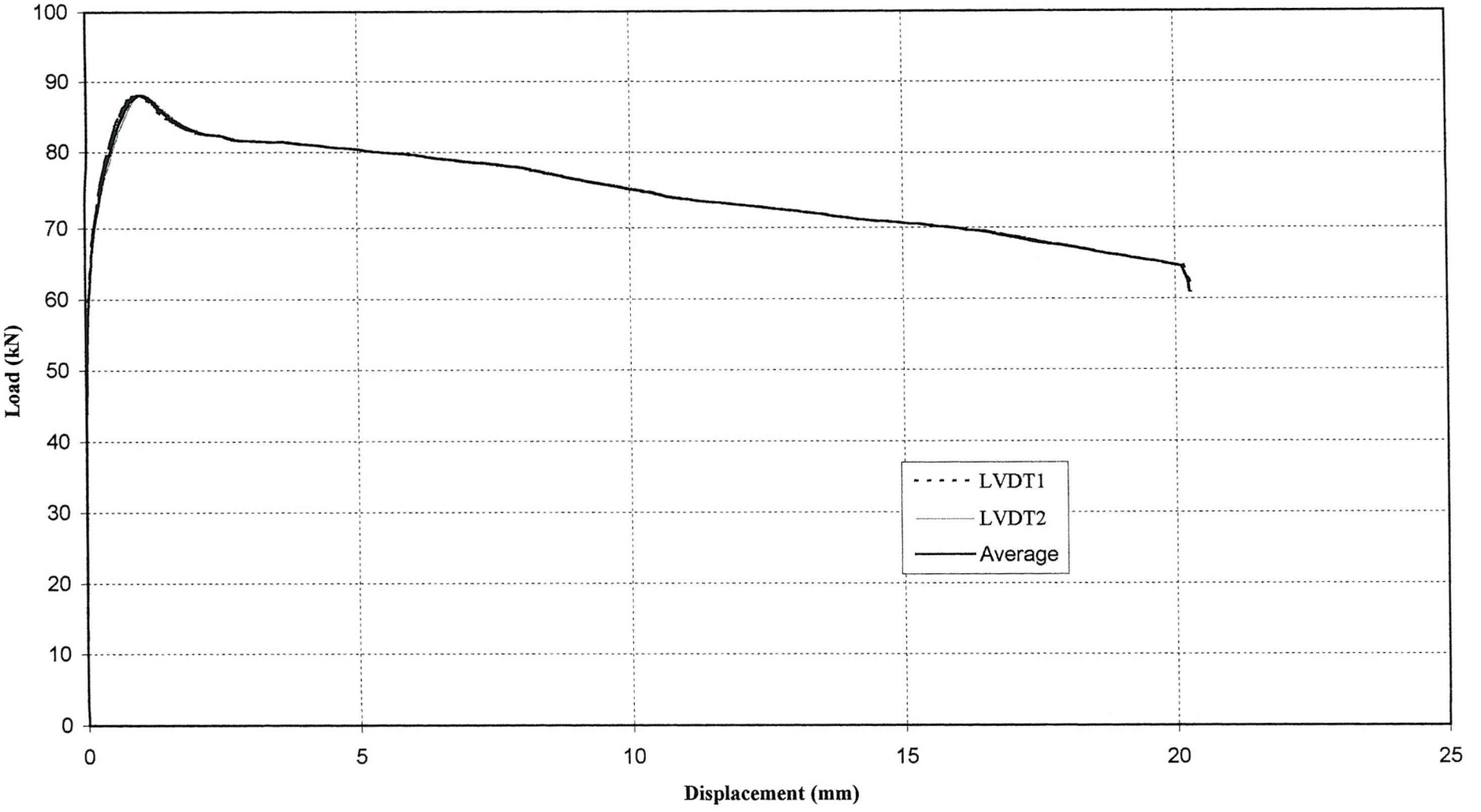

Figure 3.20 Graph to show initial slip loads for Embelton Joints 5, 6 & 7

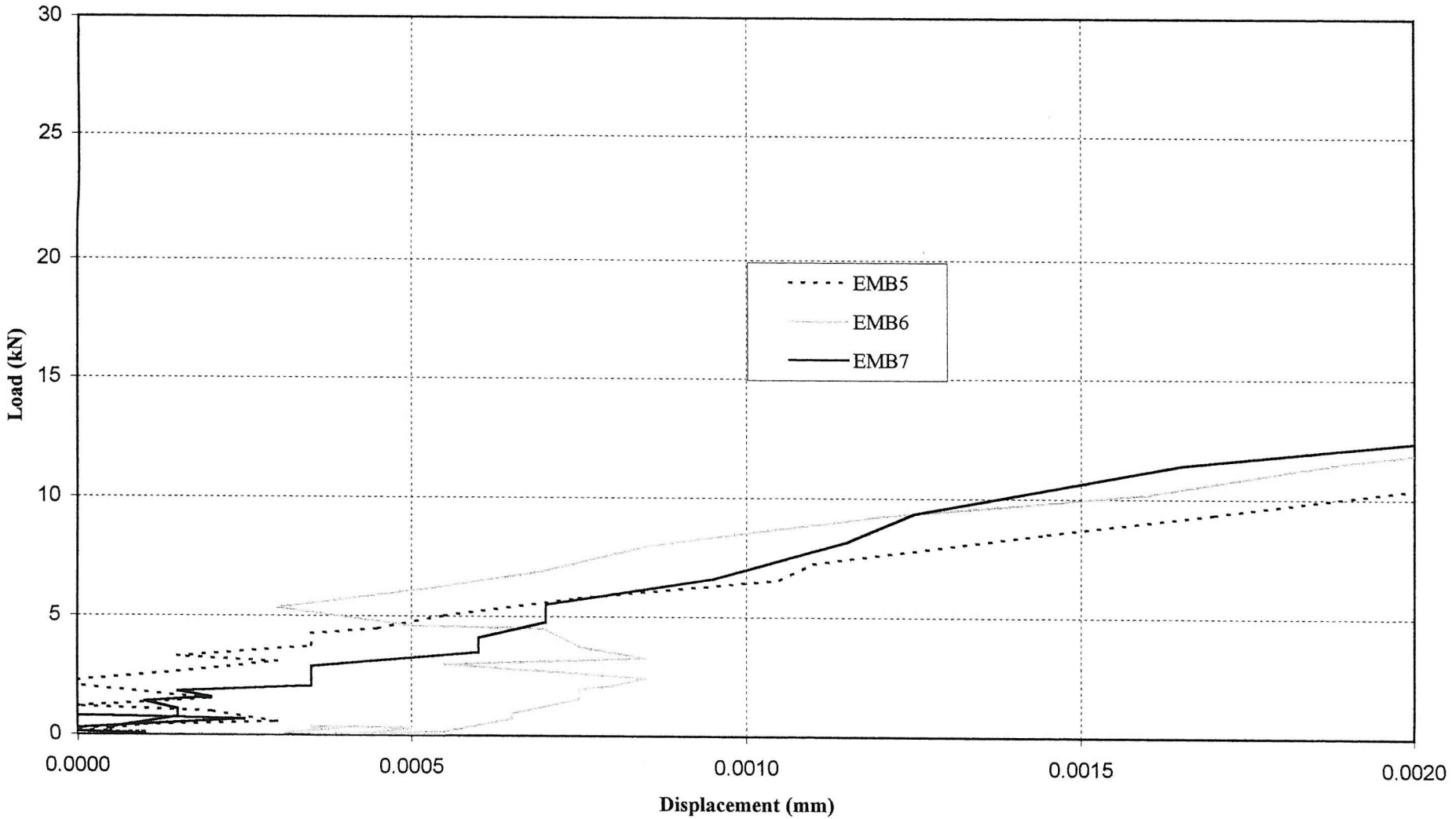

Figure 3.21 Displacement of Embelton Road Joint#5

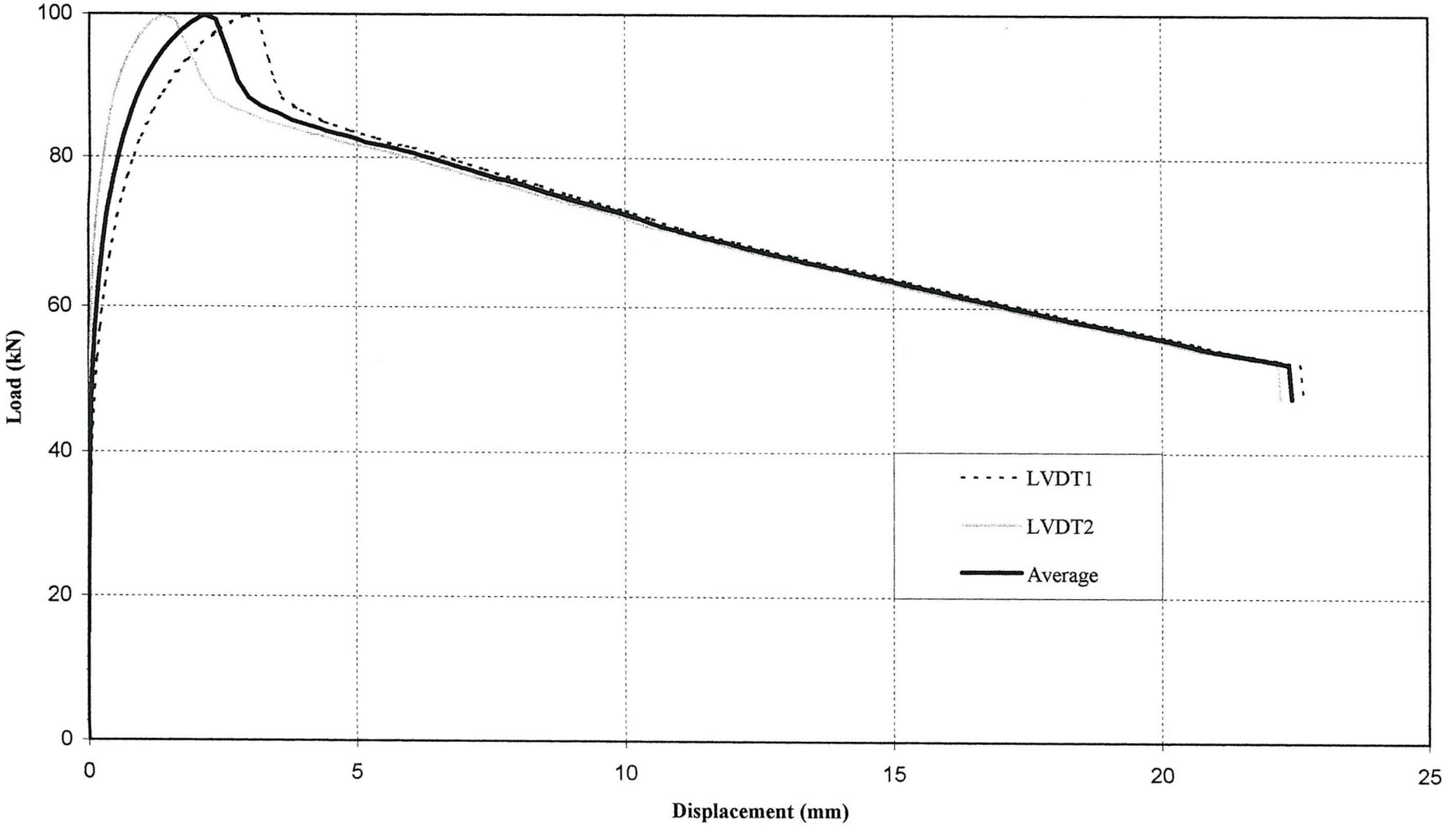

Figure 3.22 Displacement of Embelton Road Joint#6

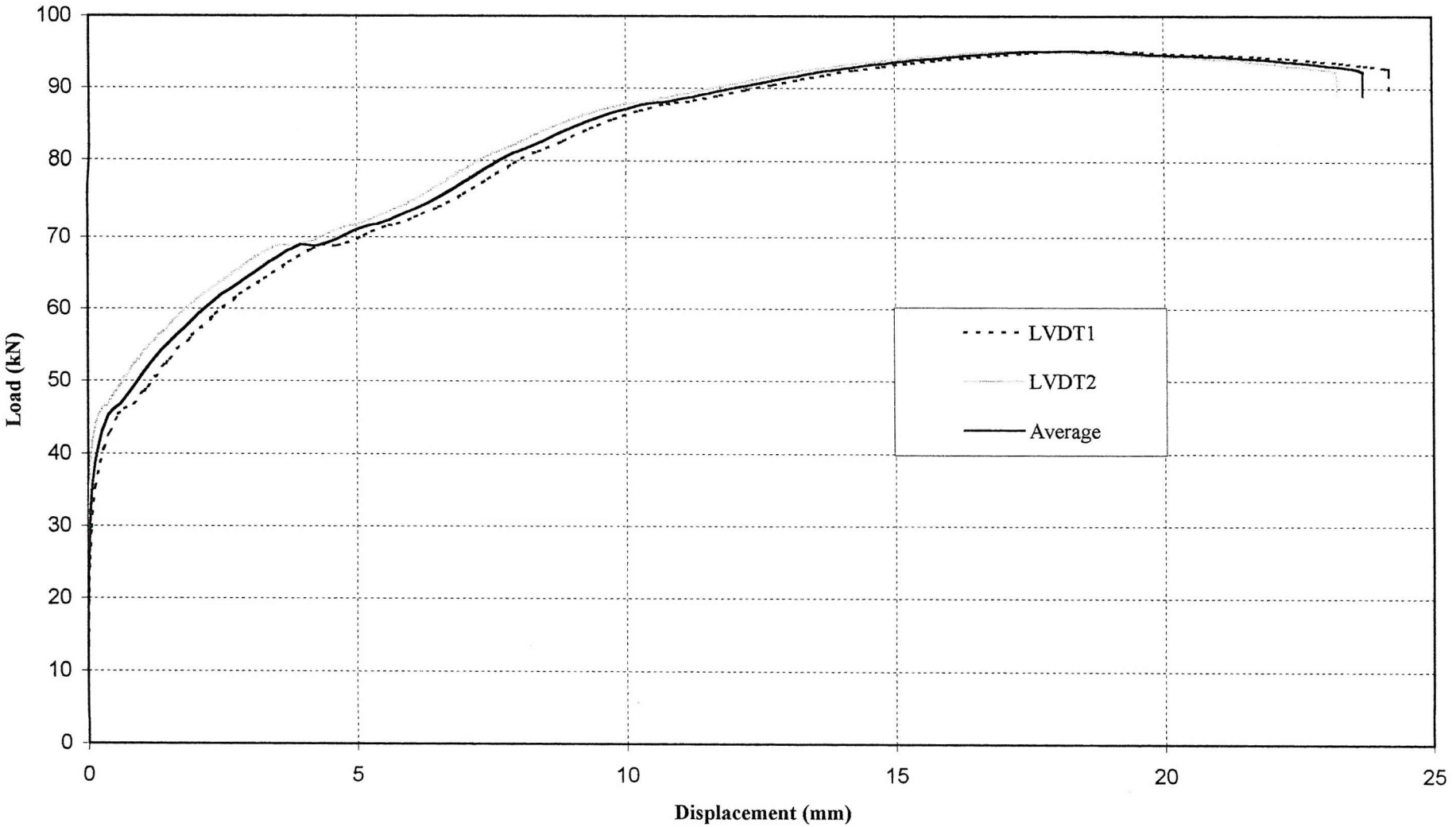

Figure 3.23 Displacement of Embelton Road Joint#7

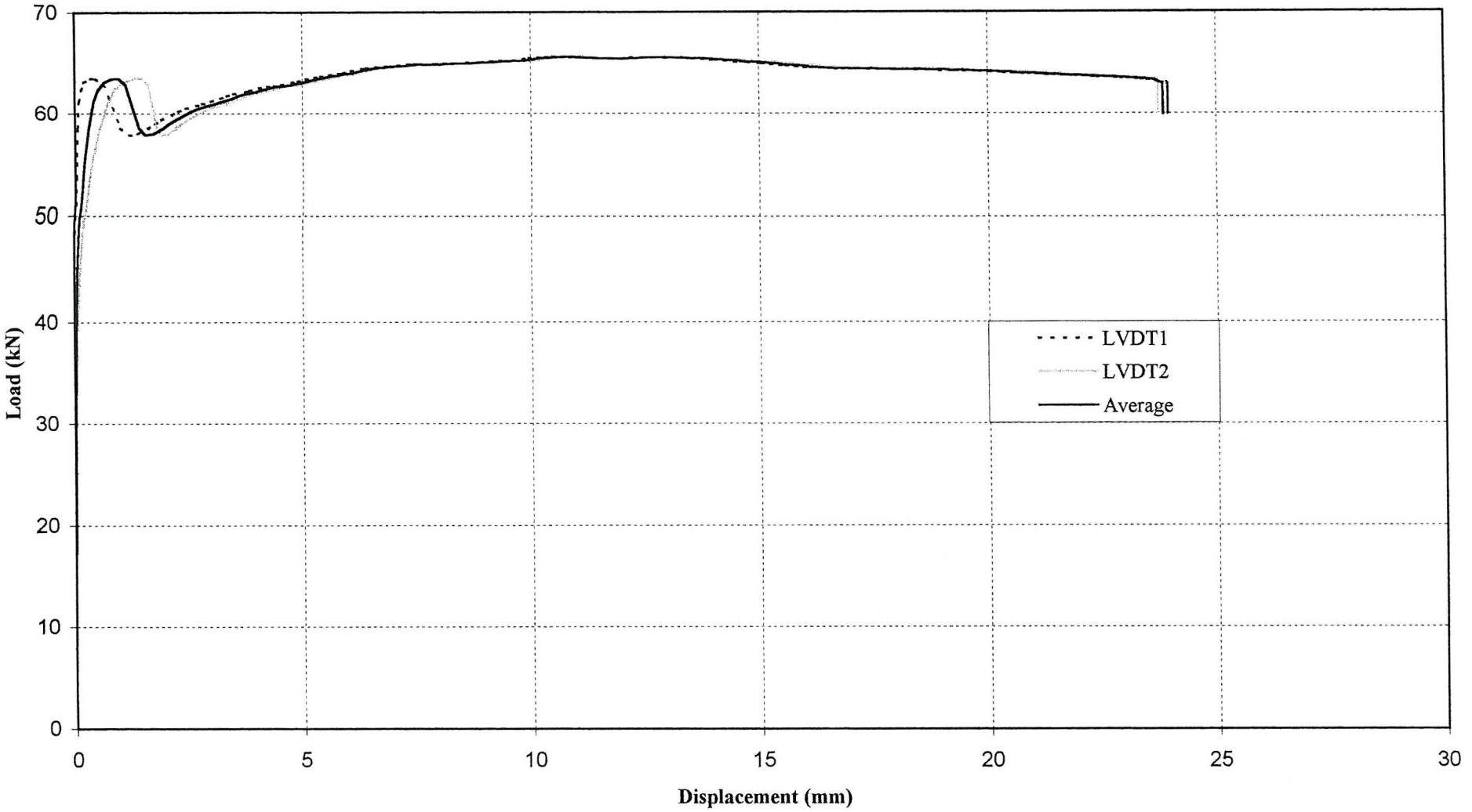

CHAPTER 4

FINITE ELEMENT ANALYSIS OF PIPES UNDER VARIOUS LOADING CONDITIONS

CHAPTER 4 FINITE ELEMENT ANALYSIS OF 2 JOINTS UNDER VARIOUS LOADING CONDITIONS

4.0 Numerical Analysis

As reported in Chapter 2; buried water pipes are subjected to many different loads including; frost, traffic, internal pressure, tree roots and near-by trench excavations. They are also subject to corrosion of many different types. Some of the above mentioned loading mechanisms have been studied in detail, for example frost load and traffic loading (Page, 1966; Carder & Taylor, 1983 &1984; Fielding & Cohen, 1988; Zhan & Rajani, 1997). None of these studies have fully demonstrated that any of these mechanisms are solely responsible for bursting water pipes. There is much speculation that water pipes burst from a combination of load effects but experiments have not been carried out to show this. To carry out a controlled field experiment simulating all the varying loads on a buried pipe would be a huge task. An easier method to investigate the load combination theory is to simulate the pipe with all the different load cases using numerical analysis.

By using numerical analysis the water pipes and their joints can be modelled. The different loads can be simulated individually to see the effect directly on the pipe and pipe joints. The model may then be loaded with any combination of loads and results seen almost immediately. This process of numerical experimentation enables many different load cases to be investigated and the results seen instantly, without the expense and time restrictions of a field experiment and all the potential problems they can produce.

Numerical analysis gives an approximate solution and cannot, without significant validation, be relied on for the exact answer. However, it is a good indicator to show which loading mechanisms have the greatest impact and which combination could result in failure of the pipes. In this case some validation has been done to make the results as realistic as possible.

Analyses were carried out using Lusas Version 13. The main assumptions made are detailed in Appendix C.

4.1 Pipe material properties

Cast iron lead-run joints contain both lead and grey iron. The lead can be originally of different forms: lead wool, lead wire or poured lead. The most common forms of lead joints are made from poured lead, poured in on top of oakum layers (see Chapter 2). The grey iron used is lower class ferrite iron. The properties of these two materials can be found in Table 4.1. These material properties are estimates found in the literature (Angus, 1976) for joints of the age (dated 1910) used in experimental work. However, they are not completely accurate as real data for pipes and joints made before 1920 could not be found (Fry & Rumsey, 1984). British Gas ERS have tested samples of pipe of this age recovered from mains and determined the range of tensile strengths to be approximately 95-125MN/m^2. An average value of 110MN/m^2 was taken for the finite element analysis. Therefore the actual values of design strength, etc., are likely to be lower than values used here. The values used were also supported by values found in a Stanton handbook (Stanton 1997), who were the main manufacturers of the time. Discussions held with Stanton also confirmed these values.

Initially only one joint was modelled, for simplification, and to keep the memory requirements low and disk space at a minimum. The joint modelled used both lead material properties and grey iron. The joint was modelled in 3D, with the lead modelled as sandwiched between layers of grey iron, see Figure 4.1. The joint was loaded with a load of 70kN on one end, while being fixed at the other end with supports, to produce a longitudinal tensile force (Figure 4.2). The results of this model were then compared with that of a joint using solely cast iron. This was done to establish if the absence of lead had an effect on the position and value of maximum stress. Table 4.2 shows that the absence of lead did not produce significantly greater errors when compared to force equilibrium values.

Although the presence of the lead did have a local effect on the sections of pipe it lay between, it did not affect the position of maximum stress or its value. The position of maximum stress appeared on the neck of the joint where it turned into pipe (Figure 4.3). It was therefore decided to eliminate lead from the rest of the model runs, to further simplify the model and to reduce memory needs.

Later in the analysis material defects were introduced. It is known from the literature review that grey iron pipes are open to many types of defects. Cast iron pipes can include production defects, such as slag voids, sand inclusions and others. Once manufactured these pipes may be damaged by careless transportation and rough installation, which can produce hairline cracks, nicks and notches promoting corrosion when buried. This corrosion can then lead to thinning walls and/or corrosion pits. It is impossible to determine transportation and installation defects and as such these defects were not modelled. The defects that were modelled were; thin walls, corrosion pitting and slag voids. Corrosion and thin wall defects did not require material property changes, only geometrical, and are discussed in section 4.3. Slag voids used property changes, the values of which were obtained by an engineering judgement. From the material books used and discussions with Stanton, the maximum tensile strength of a grey cast iron pipe when new is 110kN/mm^2. This value was reduced to 50kN/mm^2, approximately half the original strength, which was considered reasonable. Poisson's ratio and coefficient of thermal expansion were kept the same. Density was reduced to 6.0g/cm^3, as it was thought this material would be less dense than grey iron.

4.2 Loading conditions

The loading conditions modelled were chosen on the basis of the literature review in Chapter 2. The loads were imposed by water temperature, frost, traffic and internal pressure. All these loading conditions have been suggested as being sole causes for bursting water pipes. The purpose of the numerical analysis was to see whether each one could possibly burst a grey iron water pipe on its own, or whether a combination of some or all loads would be needed. Each loading mechanism was investigated and is discussed below. The origin of each load value is detailed in its own sub section.

4.2.1 In-pipe water temperature

According to data held by Thames Water, water distribution pipes are fed by two sources. These sources are either ground water supplied by boreholes, or surface water supplied by reservoirs. Sometimes pipes have a mixture of the two flowing through them. The data

show that ground water remains at a steady 12°C with minor fluctuation of +/- 1°C throughout the year (Figure 2.22). Surface water, however, fluctuates from 2 to 29°C (Figure 2.22). Taking into consideration the ambient water temperature, it was decided that a typical temperature change the pipes would undergo was of the order of 20°C. A temperature load of 20°C was assigned to all nodes on the model, which can be seen in Figure 4.4, representing half of the complete model.

Given a Young's Modulus of 110GPa, a coefficient of linear thermal expansion of $11*10^{-6}$/°C, and a temperature drop of 20°C, a cast iron pipe without joints, rigidly clamped at either end, will be subjected to a longitudinal tensile stress of 24.2N/mm^2. This is equivalent to 8.4 tones of tensile load in a pipe with an internal diameter of 100mm and an external diameter of 120mm. Calculations can be found in Appendix B.

The pull out tests described in Chapter 3, have shown that some joints begin to displace significantly around 8-10 tonne loads, whilst others did not pull out even under the maximum load that could be applied. Therefore some joints are capable of resisting the load applied by a temperature drop of 20°C.

4.2.2 Internal pressure

The normal operating pressure for pipes is difficult to establish as it is always changing due to demand, repairs in the system and operational effects. On discussion with Thames Water operators, pressure within the pipes varies but normally does not exceed 14 bar. Under normal operating conditions 14 bar is the maximum operators like distribution pipes to be subjected to. This value of internal pressure was used to represent pressure loading in the numerical models and was assigned to all the internal surfaces of the model (Figure 4.5). With the value being the optimum pressure operators would like pipes to experience, it was thought that it represented the normal impact internal pressure had on the pipes. It was considered that if the models showed that 14 bar had little effect on the pipes then it could be presumed that internal pressure was not a significant factor in producing failure.

4.2.3 Traffic loading

Much research has been carried on the effects of traffic loading on buried pipes and pavements (Page, 1966; Needham & Howe, 1979 & 1981; Nath, 1981; Jones, 1983; Carder & Taylor, 1983 & 1984; New, 1985 and Potter, 1985). Originally the pipes were not designed for traffic loading. Over the years traffic loading has increased significantly beyond any anticipated loads the water pipes were expected to experience. The Ministry of Transport, the maximum load that a HGV may carry today falls into four categories, 38, 40, 41 and 44 tonnes, each using a different number of axles and varying number of wheels. However, it is generally known that sometimes the load exceeds the legal requirements, especially vehicles coming over to this country from the rest of Europe. Therefore the actual values may be much greater than this.

A finite element model was used to calculate the load at the pipe crown. The worst legal case of loading was used to establish the load at the pipe crown. Legally the worst load is given by a combination of 38 tonnes, 5 axles and 12 wheels. This gives a load per wheel of 31.1kN, using an impact factor of 1.3 (BS153, 1954) this increases to 40.43kN per wheel. Three different types of wheels can be used to carry this load, single, twin and super single. The inflation pressures of these wheels are 120, 100 and 125 lb/in^2 respectively. However, on further discussions with a heavy goods driver it was found that a pressure of 120 lb/in^2 is generally used for all tyres. For the worst load case described above single wheels would be used. With a wheel load of 40.43kN and a wheel pressure of $0.822N/mm^2$ ($120lb/in^2$), assuming the walls of the tyre take no load, the contact area would be a 0.222m square or a 0.125m circle.

Using an axisymmetric model, a volume of soil was loaded with a face load of $0.822N/mm^2$ (Figure 4.6). Due to the limitations of the finite element program a model using a square contact area was run to find what the stress would be at various depths and distances. This model was then further divided into two models to simulate different soil types, one using one average soil property for the whole volume, the other with layers of Asphalt, Bitumen, Gravel and Sandy Clay. The properties of the soils and layers can be found in Table 4.3, the results in Table 4.4 and Figure 4.7 & 4.8. The results compare to

those stated by Jones (1983). In Figure 4.7, the maximum load the pipe crown experiences was 74kPa at a depth of 0.5m, using the circular contact area and one soil property throughout. A load of approximately half this value (Traffic load(1), 33kPa) was applied at mid section along the model across a surface area of width 1200mm, as the graph in Figure 4.7 indicates. For the multilayer soil model the stress seen by the pipe was much smaller. This load was modelled by traffic load(2) 12kPa across a width of 1900mm as the graph in Figure 4.8 indicates. Figure 4.9 show a schematic diagram showing how the load was applied to the top surface of the pipe crown.

4.2.4 Frost loading

Many investigations into burst pipe events have been carried out in North America, where the winters can be harsh. Monie & Clarke (1974), Smith (1976), Molin (1985), Fielding & Cohen (1988), Zhan & Rajani (1997), and have shown that water pipes can be damaged by frost heave, if the frost front penetrates to at least 1m depth. At this depth the load the pipes experiences from the soil has been shown to double, increasing the strains on the pipes (Monie & Clark, 1974 and Smith, 1976). However, even during extreme British winters e.g. the winters of 1991 and 1993 where temperatures of -10°C were reached, with long periods below zero, the ground did not freeze to a depth of more than 0.48m (Glanville, 1951; Croney & Jacobs, 1967 and Croney, 1977). This makes it unlikely that frost heave is a significant failure mechanism for British water pipes, but it remains one that needs to be investigated. The majority of water pipes are buried within the range of 0.75-1.00m (Figure 2.21).

From Fielding and Cohen (1988) we can estimate the load a 100mm-diameter cast iron pipe will experience due to frost load alone, if the frost penetrates to a depth of 0.45m.
If a cast iron pipe is buried at 1.0m and the frost depth reaches 0.45m, then from the graph in Figure 2.19 the frost load the pipe crown experiences is 1.7kN/m. For a 100mm diameter pipes this equates to 0.0017N/mm^2. If the pipe is buried at 0.75m then this load increases to 0.033N/mm^2 (33kPa) for the same pipe. As a buried depth of 0.75m gave the worst load case, these assumptions were used in the joint model and a frost load of 0.033N/mm^2 was applied at mid section of the model. As this load condition was equal to

the traffic load model and likely to be spread over the same area, the results for the traffic loading were repeated for the frost loading models.

4.3 Geometry

The geometry of the joints was based on measurements taken from joints found at the Embelton Road site (Table 3.2). The measurements of these joints and design were similar to those described in Bode (1936). The model of the joint went through several changes before the final geometry was established. It was found that the shape of the joint was very important for establishing or eliminating stress raisers. Each small change had a significant effect on the stresses in the joint.

The geometry was first modelled in axisymmetric 2D using the shape shown in Figure 4.10. It can be seen from the Figure 4.10 that the neck of the joint leading the joint into the pipe has a smooth, round but steep incoming corner. This produced a significant stress increase within the numerical analysis. In order to reduce this effect the corner was drawn out to give a gentler profile.

The size of the lead section (modelled as iron) also had an impact on the stress results. Initially the lead was modelled as covering the whole length of the inside of the joint. The lead was modelled in this way as it was not clear how large this section should be. On closer inspection of the Embelton Road joints, it was found that the lead was only about 25 mm long (1 inch), (Figure 4.11). The joint was remodelled using this length. The results showed the stress on the rounded outside corner of the joint to reduce, and the stress at the interface between the lead and cast iron to increase.

At first it was assumed that the thickness of the joint wall was uniform throughout its length. On closer inspection this was found to be incorrect. From Figure 4.10 it can be seen that the inside of the joint was assumed to follow an "S" shape bend with uniform thickness, when in actual fact the joint has two sharp 90° bends with extra thickness across the wall (Figure 4.12). The model was changed to represent this joint more closely and was analysed. This small change had a large effect on maximum stress levels. Nearly all stress disappeared on the outside bend of the joint.

Once all these geometrical differences were resolved, the 2D axis-symmetric model was developed into a 3D whole joint (Figure 4.13). The model was again run with a simple tensile axial load with fixed supports on the ends in the longitudinal direction only. The results were compared with those obtained from the 2D axisymmetric model to make sure they were the same. The result proved to be similar and stresses were of the same magnitude, which enabled the model to be further developed.

The next stage was to model 2 joints connected by a length of pipe. The same loading and checks were repeated. A model was then built with 2 joints and 3 pipe lengths. Here memory capacity problems occurred. To combat this the 2 joint, 3 pipe length model was sliced in half along the length of the model (Figure 4.14) and roller fixity was applied to the plane of symmetry. The new model was run without problems. The geometry of the model had now reached its final design stage. This model was then used for the rest of the analysis.

4.4 Mesh

The mesh size and shape was originally investigated using only one joint with no pipe lengths, in 3D. The joint was loaded simply using solely an axial tensile load of 70kN with fixed end supports in the longitudinal direction (Figure 4.2). Six models were run. Three had a Hexahedral mesh and three had a Pentahedral mesh, (Figure 4.15). Mesh divisions of 2 and 4 elements per super element were run with each mesh shape. The purpose of this was to establish whether the model was sensitive to mesh size or shape. The results of each model were taken through a force equilibrium check at various sections along the joint, to judge their accuracy. There were minor differences between results (Table 4.5). For different mesh shapes the maximum percentage difference was 17% for a Pentahedral, 2-element division mesh. The Hexahedral mesh showed slightly more accurate results with a percentage difference of 6%. This difference was considered acceptable, and it was concluded that the model was not sensitive to mesh shape. The Hexahedral mesh was chosen for the rest of the model runs. Mesh divisions showed even less difference with a maximum of 3% between 2 and 4 divisions. At this stage it was

decided to run further models with 4 mesh divisions with a Hexahedral mesh, as this size did give slightly better results.

The model was then built up to two joints with a connecting pipe length. The model used a Hexahedral mesh with 4 element divisions, as concluded earlier, and loaded with a basic temperature load of 20°C. The computer failed due to insufficient swap space and it was recommended that an additional hard drive be installed to resolve this. The element divisions were reduced to 3 to reduce the memory requirements as well.

On closer inspection of the mesh and how it moulded the corners of the model, it could be seen that the mesh did not curve around the bends. It was thought that the stress created at these corners could be further refined if the mesh could be curved, allowing reality to be represented more closely. A 2D axis-symmetric model was used in order to find a satisfactory curved mesh more quickly. A curved mesh proved to reduce the maximum stress slightly, but not significantly. The change of geometry of the corners as mentioned in section 4.3, allowed the mesh to be made more simply. It was this change in geometry that reduced the errors significantly. The curved mesh was then compared to a non-curved mesh with the new geometry model. The maximum point of stress showed equal reduction and both gave similar errors when subjected to a force equilibrium check. From this it was decided not to use a curved mesh as it used much more memory. The maximum horizontal equilibrium errors were 10% in the pipe lengths and 18% at the pipe joint interface, which was considered a reasonable approximation, given the uncertainties inherent in the analysis

The mesh structure, shape and element divisions had now been chosen. The 2D model with 2 joints and connecting pipe length was then swept into 3D and analysed. As mentioned in section 4.3 the model was split along its vertical plane of symmetry, in order to reduce memory requirements. It was possible to do this, as all the load cases were symmetrical. The model was then built up to its final stage with 2 joints and 3 pipe lengths. The mesh was made coarser in the pipe lengths and in the joints, to further reduce memory requirements. To simplify the mesh in the joints the lead was removed, which enabled the groove to be removed (Figure 4.12). The mesh was simplified considerably around this area but the errors when checked were still between 10-20%. The final model (2 joints, 3 pipe lengths, 3D and half the volume) required 320 MB of RAM to run.

4.5 Supports

The type of supports required for the analysis were established following the same pattern as all the other properties discussed so far. A simple axial tensile load of 7t was applied to one end of a 2D axisymmetrical joint, while being fixed at the other end in the x direction only. The results were analysed by subjecting them to a force equilibrium check. The errors found in the force values were within 5% of the correct value. The model moved onto the next stage with a temperature loading of 20°C being applied to all elements and both ends of the joint were fixed in the x direction only (Figure 4.16). No fixing was applied in the z and y directions. The model now represented a fixed joint held rigidly at its ends, with the temperature loading providing a tensile axial load. It was expected that the results from this would be similar to those of the first model run.

The 2D axisymmetrical model was swept into 3D to develop the supports needed to represent the soil support around the joint. Spring supports with a stiffness of 0.3N/mm^2 were assigned to all the outside surfaces of the joint (Figure 4.17). The value of stiffness was obtained from simple elasticity assuming a Young's modulus for the soil of 50MPa, and assuming the pipe to act as an infinitely long. The stiffness being 300 MPa/m, calculations can be found in Appendix B.

The model was expanded to include two joints and three pipe lengths. The support conditions were assigned with the same temperature load of 20°C. By using the same loading mechanism the results could be compared with the previous models, as they should be the same. However, due to capacity problems the model would not run. The models mesh and geometry and mesh were altered as described in the previous sections but the model still would not run. By halving the model the size was reduced but further support conditions were created. The exposed edges of the model now needed to be fixed to simulate the other half of the joint. This was done by assigning a fixed support in the z direction on each edge surface in the spring mode (Figure 4.18). This allowed the support to be compatible with the other supports and they followed the axes of each element. The model was then run successfully and support conditions were finalised for final analysis.

4.6 Defects

Several types of defects can be found in cast iron pipes. Manufacturing defects can produce slag voids or sand inclusions in the metal matrix. These can cause local weak spots and can occur anywhere along the pipe. Installation defects can occur as a result of transportation and the burying of the pipes in the ground. If the pipes are not handled carefully they can produce hairline cracks from impacts against each other and underlying bedding. This can then aid corrosion along the crack, weakening the pipes faster than would normally occur. Corrosion itself is another cause of defects, which can occur internally and externally, in many different forms as described in Chapter 2, section 2.4.

All of these different types of defects are difficult to measure and some can not be measured at all. This is partly due to the fact that they cannot be located and/or measured without destruction of the pipe itself. Slag voids can not be measured but an educated guess can approximate the loss of strength in that area, how large the area can be and what shape it is.

For the purpose of the numerical models, the strength of material for a slag void was halved to 50kN/mm^2 and the density was reduced from $7*10^{-6}$ kg/mm^3 to $6.0*10^{-6}$ kg/mm^3. This change of material property was assigned to a volume at mid section of the model (Figure 4.19). Transportation and installation defects should not really occur if care is taken. It has been assumed for the purpose of the numerical models that defects do not occur during transportation and installation, as measuring their magnitude would be impossible. Corrosion can be recorded on pipes, which have been exhumed. Thames water has carried out extensive research on the extent on internal and external corrosion (Dixon, 1999). Pipes have been exhumed, shot blasted to remove the corrosion deposits, and the size and depth of the corrosion pits recorded. This database gives a good idea of the extent of corrosion found, its position, and the damage it has caused. The data shows that the largest pits occur externally, generally on the pipe invert. Figure 4.20 shows an example of a corrosion pitting and its dimensions. From the measurements of the pits the maximum size tended to be several pits joined together to form a rectangular shape, 3.5mm deep, 20mm across and 15mm wide. This size of pit was used to represent a

corrosion defect in the numerical models and was placed at mid section of the pipe (Figure 4.21).

Corrosion also results in graphitisation, which significantly reduces the strength of the cast iron. It often occurs uniformly all round the circumference of the pipe. This results in a thinning wall effect. The pipe wall thickness from the Embelton road joints were recorded and it was found that in most cases the wall thickness had reduced by 4mm. This defect was also modelled numerically, as it would give a significant increase in the effect of temperature loading. The mid section pipe wall was reduced along its length between the two joints, with it reaching a minimum at mid span (Figure 4.22).

Ferrule holes were also modelled on a straight pipe section with no joints. It is generally believed that ferrules have an influence on pipe failure. Each load case was analysed on this straight pipe section with a ferrule hole at the top in the centre of the pipe length (Figure 4.23). The purpose was to investigate the stress changes and concentrations with the ferrule hole present and compare those to the stresses found without the hole.

It has been suggested that uneven bedding often contributes to pipe failure (Carder & Taylor, 1984), for example when the pipes are loaded with traffic loads above ground. To investigate the significance of these claims, models with vertical loading from traffic and frost were given uneven supports and analysed. The point supports were placed in positions to give the worst case scenario, which was underneath the bell of each joint (Figure 4.24). This simulates the pipes acting like beams supported by two pillars. The results from these analyses were compared with those achieved from even supports.

4.7 Boundary conditions

The final numerical models used to obtain all the results were based on using two joints and three pipe lengths. The lengths of the pipe sections were taken from average measurements from the three site reports, which can be found in Appendix A. The number of joint and pipe lengths was also chosen so as not to affect the loads being analysed. Temperature loading, internal pressure and defects are not dependent on the number of joints or total length of pipe. The stress effects, frost load and traffic loads and

their distribution are dependent on finite lengths, but the total length on the models is sufficient to contain the effect of the loads.

Body force was a parameter that had to be present in all load cases. A body force resulting from gravitational acceleration ($9.81m/s^2$) was assigned in the y direction uniformly along the model, to represent the effects of gravity (Figure 4.25). Normal soil loading also had to be considered. The surrounding soil supports the pipe from the side and bottom as well as loads the pipe from the top. A uniform soil loading of $0.02N/mm^2$ was assigned to all the outside surface areas to represent this boundary condition (Figure 4.26). The soil was modelled using both spring supports ($0.3N/mm^2$) "to represent the support the soil gives to the pipe" and soil loading to represent its overburden ($0.02N/mm^2$).

4.8 Typical results

Each model was analysed and stresses produced were viewed in several different directions. The maximum stress was noted for each model and which direction this occurred in so as to obtain an idea of failure mode. The stress contour pictures were sliced to view the stresses inside the pipe wall as well as along the inside and outside surfaces.

Each load case was modelled separately to establish its effects as a possible failure mechanism. The results were analysed and recorded. The analyses were then repeated but this time with one defect present: slag void, corrosion or thin wall. The models were run until each defect had been modelled with each load case. Traffic and frost loading were also modelled with point supports as described earlier. They were both modelled without defects and then with defects separately. Frost and traffic loads were then used together with slag voids and point supports. This model was then compared to the two loads used together and point supports only. The results from all of these load combinations are described in section 4.8.1 to 4.8.4. Each contour plot for each case uses the same scale to show the reader which load case had the greatest effect.

4.8.1 In-pipe water temperature

Each model gave a maximum principal stress of approximately 54N/mm^2 (Table 4.6). This is up to 50% of the total strength of the pipe when in new condition. The introduction of each defect did not have a significant effect on the maximum stresses found. Only the thin wall defect doubled the stress in the horizontal direction. Looking at Figure 4.27 and 4.28, it can be seen that with basic temperature loading, the maximum stress occurred at the neck of the bell on the outside and the inside corner of the bell. Referring back to Figure 2.5, this is a typical location for failure fractures in cast iron water pipes. Throughout the rest of the pipe the stress reached approximately 24N/mm^2, which reflects the results from a straight pipe section (Table 4.9). For temperature loading the maximum stress was always found to act in the axial direction. This suggests that this loading condition would fail the pipe in axial tension as originally thought.

Out of all the defects modelled, the thin wall had the greatest effect on the stress results. It can be seen from Figure 4.29, that the presence of the thin wall at centre span is beginning to increase the stress in the pipe section. Again this increase in stress acts in the axial direction. This increases the chance of pipe failure at this point.

4.8.2 Internal Pressure

Table 4.7 shows that internal pressure does not produce high stresses within the pipes or joints. With basic pressure loading the maximum stress was approximately 8.7N/mm^2. This stress tended to act in the vertical and horizontal direction with equal magnitude, which is to be expected. Figures 4.30 and 4.31 show that compared to temperature loading, pressure loading has little effect.

The influence of the slag void and corrosion are minimal and could be considered insignificant (Figure 4.32). The thin wall increased the maximum stress to 11.54N/mm^2 which, occurred equally in the vertical and horizontal directions. The origins of this maximum stress shifted from inside the joint at the spigot end, to the area of thin wall (Figures 4.33 & 4.34). The influence of joints in the pipe sections is also minimal, as the maximum stress in pipe sections only is 7.72N/mm^2 (Table 4.9). Therefore the pressure in

the pipe is uniform throughout regardless of the joints (Figure 4.35). None of the maximum stress values come close to the maximum strength of the pipe, which would suggest pressure is not a sole cause for pipe failure.

4.8.3 Traffic and frost

Both traffic and frost loadings were placed at the centre of the pipe length on the crown across half the pipe circumference. The impact of the loads on the stress levels in the pipe was significant depending on the support conditions used. If the pipe was supported well with soil supports around its entire surface then the load caused by traffic and frost were insignificant (Table 4.8). These loads could not possibly be failing the pipes on their own or even together. Without the presence of defects or point supports, the maximum stress reached at mid span was 0.65N/mm^2 for both traffic and frost. Once the soil supports and end supports were taken away to simulate poor bedding conditions the stresses increased approximately 24 times to 15.3N/mm^2. With the addition of defects this stress increased to 25.7N/mm^2. Poor bedding conditions resulted in traffic and frost loading having the second largest effect on stresses in buried pipes. Used in conjunction together with a corrosion defect, the proportion of stress inside the pipe at mid span would equal half the ultimate tensile strengths of 55N/mm^2.

Traffic load models with simple point supports were compared to theoretical calculations for a simply supported beam. This was done in order to check that Lusas was modelling what was expected of it. Two straight pipe models of varying lengths with uniformly distributed loads of 0.033N/mm^2 were compared to theoretical calculations. It was found that the two methods varied by a factor of $\pi/2$. This was due to the fact that Lusas used the entire surface area to calculate the load effect and not the projected area as the theory uses. In order to correct this the Lusas models had to be run with a factored load i.e. 0.033N/mm^2 divided by $\Pi/2$. The results are shown in Figure 4.36. This comparison was also made with varying lengths of pipe but fixed load widths, these results can be seen in Figure 4.37. Is can be seen from the graphs that factoring the results of the previous models which used 0.033N/mm2 gave accurate results with errors of 6% or less for straight pipe lengths and 13% for a 2 joint model. This showed the Lusas was modelling correctly and accurately compared to theoretical analysis.

4.8.4 Pipe length

Analyses of the plain pipe length models were carried out for each load case to judge the influence of the presence of joints on the stress levels and concentrations. Although the maximum stress levels in the given direction in most cases did not change, the value of stress increased slightly in other directions. However, the maximum stress for temperature loading more than doubled from 24N/mm^2 to 54N/mm^2, but it did not occur in the same place (Table 4.9).

The addition of a ferrule hole in the pipe length had a significant effect on the stress levels reached and on the concentration of the stresses (Table 4.10). For temperature loading the stress increased up to five times the previous maximum, equating to 134N/mm^2 (Figure 4.38). This value of stress is greater than the ultimate strength of the pipe, but statistics show that pipes are not failing at ferrules. For pressure loading the maximum stress increases three times to a value of 23N/mm^2 (Figure 4.39). Stresses under traffic and frost loading were unaffected by the ferrule hole. These results suggest ferrule holes cause a weakness in the pipe, but in reality this is not the case. This may be explained by the fact that ferrules are on top of a pipe, in the zone where bending stresses are compressive.

4.8.5 Combination of load and defects

On reflection of all these results it was decided to load the model with all the different load conditions together with slag void, thin wall and corrosion defects, to observe the effect of combined loads on the pipe joint. The results were significant, showing an increase in stresses in all directions, especially in the horizontal direction. The stress contour plot shows a stress concentration in the centre of the pipe length at the invert of the pipe. The maximum stress is found in the longitudinal direction suggesting failure in axial tension, the concentration of which suggests failure in the pipe length. This would give a circumferential fracture, which reflects how the majority of small diameter pipes fail. Figure 4.40 show the stress contour on the whole of the pipe.

Poperties	Grey Iron	Lead
Young's Modulus	110 kN/mm^2	18 kN/mm^2
Poisson's ratio	0.27	0.44
Thermal expansion	11 * 10^{-6}/°C	29 * 10^{-6}/°C
Max tensile strength	110 N/mm^2	15 N/mm^2
Max compressive strength	280 N/mm^2	-
Beam strength	100 N/mm^2	-
Bursting	55 N/mm^2	-
Shear strength	90 N/mm^2	-
Ring Bending	110 N/mm^2	-
Density	Grade 10-26 6.9-7.2 g/cm^3	-

Table 4.1 – Material properties of grey iron and lead

	Force (kN)	
Distance along pipe (mm)	3D Cast iron only	3D Cast Iron with lead joint
55	70	70
114	74	74
200	70	72
275	70	70

NB: force at any section should equal 70kN.

Table 4.2: Force equilibrium check results for cast iron v cast iron with lead, using 3D model.

Construction layer	Material	Thickness (mm)	Elastic Moduli (kPa)	Poisson's Ratio
Wearing Base	Rolled Asphalt	111	$1.7*10^6$	0.35
Base	Dense Bitumen	222	$0.82*10^6$	0.35
Sub base	Gravel	222	$0.48*10^6$	0.4
Sub grade	Sandy Clay	-	$6.55*10^4$	0.4

Table 4.3: Properties of layers in soil load multilayer model.

	Distance along surface from middle of loaded area (mm)		
Depth (mm)	**Multilayers with circular loading, stress (kPa)**		
	0	0.5	1.0
0.5	27	12.5	5
0.7	18.5	12	5
1.0	14	10.5	4.9
Depth (mm)	**One soil layer with circular loading, stress (kPa)**		
	0	0.5	1.0
0.5	74	15	2
0.7	41	16	3
1.0	23	14	4

Table 4.4: Traffic load results on different types of soil and layers.

	Force (kN)			
Distance along joint for each section (mm)	**Hexahedral mesh 4 element divisions**	**Hexahedral mesh 2 element divisions**	**Pentahedral mesh 4 element divisions**	**Pentahedral mesh 2 element divisions**
55	70	70	69	69
114	72	74	72	72
200	73	72	77	82
275	70	70	70	70

NB: force at any section should equal 70kN.

Table 4.5: Force equilibrium checks for mesh shape and number of elements

Stress (N/mm^2) – max 0.01%	2 Joints basic	2 Joints with slag void	2 Joints with thin wall	2 Joints with corrosion
Sx	48.28	48.26	46.79	48.29
Sy	23.09	23.08	22.28	23.10
Sz	23.07	23.04	22.25	23.07
S1	54.46	54.44	52.55	54.48
S2	21.31	21.31	20.56	21.32
S3	6.39	6.39	6.16	6.39
Se	47.39	47.37	46.32	47.39
S1 at mid section	24.06	30.72	34.13	43.18
Defect Factor		1.28	1.42	1.79

Table 4.6: In-pipe water temperature maximum stress values for all models.

Stress (N/mm^2) – max 0.01%	2Joints basic	2 Joints with slag void	2 Joints with thin wall	2 Joints with corrosion
Sx	4.89	4.91	4.92	4.91
Sy	8.62	8.62	10.47	8.62
Sz	8.63	8.79	10.47	12.14
S1	8.71	8.87	11.56	12.15
S2	3.85	3.87	3.88	4.87
S3	1.02	1.03	1.03	1.02
Se	9.66	9.66	10.43	10.76
S1 at mid section	7.72	8.05	10.56	12.15
Defect Factor		1.04	1.37	1.57

Table 4.7: Maximum stress results for internal pressure models.

Analysis	Pipe type	Loading	Support	Defect	Major principal stress (N/mm^2)		Position of stress at mid section	Factor effect
					Bell & spigot	mid span		
1	2 Joints	Temperature	Uniform with end supports	None	54.46	24.06	Uniform	-
2	2 Joints	Temperature	Uniform with end supports	Slag void	54.44	30.72	At defect	1.28
3	2 Joints	Temperature	Uniform with end supports	Thin wall	52.55	34.13	At defect	1.42
4	2 Joints	Temperature	Uniform with end supports	Corrosion pit	54.48	43.18	At defect	1.79
5	2 Joints	Pressure	Uniform with end supports	None	8.71	7.72	In bell and spigot	
6	2 Joints	Pressure	Uniform with end supports	Slag void	8.87	8.05	At defect	1.06
7	2 Joints	Pressure	Uniform with end supports	Thin wall	11.56	10.56	At defect	1.37
8	2 Joints	Pressure	Uniform with end supports	Corrosion pit	12.15	12.15	At defect	1.57
9	2 Joints	Traffic load (1)	Uniform with end supports	None	1.01	0.65	At bottom inside pipe	
10	2 Joints	Traffic load (1)	Point supports only	Slag void	24.59	14.44	At bottom outside pipe	0.94
11	2 Joints	Traffic load (1)	Point supports only	Thin wall	23.98	21.44	At bottom outside pipe	1.4
12	2 Joints	Traffic load (1)	Point supports only	Corrosion pit	28.91	25.77	At defect	1.68
13	2 Joints	Traffic load (1)	Point supports only	None	24.64	15.36	At bottom inside pipe	
14	2 Joints	Traffic load (2)	Point supports only	Slag void	16.00	6.46	At bottom outside pipe	0.96
15	2 Joints	Traffic load (2)	Point supports only	Thin wall	15.28	8.71	At bottom outside pipe	1.3
16	2 Joints	Traffic load (2)	Point supports only	Corrosion pit	19.20	12.09	At defect	1.8
17	2 Joints	Traffic load (2)	Point supports only	None	15.98	6.70	At bottom inside pipe	
18	2 Joints	Combination	Point supports only	All	112.00	155.00	At concentration of defects	

Table 4.8: Summary of maximum stress results for all models

Analysis	Pipe type	Loading	Support	Defect	Major principal stress (N/mm^2)		Position of stress at mid section
					At support	mid span	
19	Single pipe length	Temperature	Uniform with end supports	None	24.17	24.17	Uniform
20	Single pipe length	Temperature	Uniform with end supports	Ferrule	65.23	65.23	At defect
21	Single pipe length	Pressure	Uniform with end supports	None	7.72	7.72	Uniform
22	Single pipe length	Pressure	Uniform with end supports	Ferrule	25.64	25.64	At defect
23	Single pipe length	Traffic load (1)	Uniform with end supports	None	0.41	0.41	At bottom inside pipe
24	Single pipe length	Traffic load (1)	Uniform with end supports	Ferrule	0.45	0.32	At bottom inside pipe
25	Single pipe length	Traffic load (1)	Point supports only	None	53.88	8.38	At bottom outside pipe

NB: Traffic load(1) = $0.021N/mm^2$, Traffic load(2) = $0.0095N/mm^2$
Frost equates to traffic load(1), so this load is used twice in the combination model, as frost covers approximately the same area as traffic.

Table 4.8: Summary of maximum stress results for all models.

Stress (N/mm^2) – Max 0.01%	Temperature load		Pressure load	
	Pipe length	2 Joints	Pipe length	2 Joints
Sx	24.17	48.28	1.78	4.89
Sy	-0.004	23.09	7.65	8.62
Sz	-0.004	23.07	7.65	8.63
S1	24.17	54.46	7.72	8.71
S2	-0.003	21.31	1.78	3.84
S3	-0.081	6.389	-0.15	1.02
Se	24.22	47.39	7.80	9.66
S1 at mid section	24.17	24.06	7.72	7.72

Table 4.9: Maximum stress results for pipe length v pipe lengths with joints

Stress (N/mm^2) – Max 0.01%	Temperature load		Pressure Load		Frost Load (middle)		Traffic load (middle)	
	Ferrule hole	Pipe length	Ferrule hole	Pipe length	Ferrule hole	Pipe length	Ferrule hole	Pipe length
Sx	134.0	24.17	6.68	1.78	0.13	0.12	0.88	0.71
Sy	5.44	-0.004	17.85	7.65	0.15	0.12	0.79	0.61
Sz	12.60	-0.004	22.70	7.65	0.30	0.26	0.69	0.72
S1	134.0	24.17	23.40	7.72	0.31	0.26	0.88	0.72
S2	12.79	-0.003	6.68	1.78	0.11	0.12	0.73	0.71
S3	2.49	-0.08	0.62	-0.15	0.008	-0.001	0.04	0.02
Se	128.2	24.22	22.40	7.80	0.12	0.55	5.31	1.12

Table 4.10: Maximum stress results for pipe length v pipe length with ferrule hole.

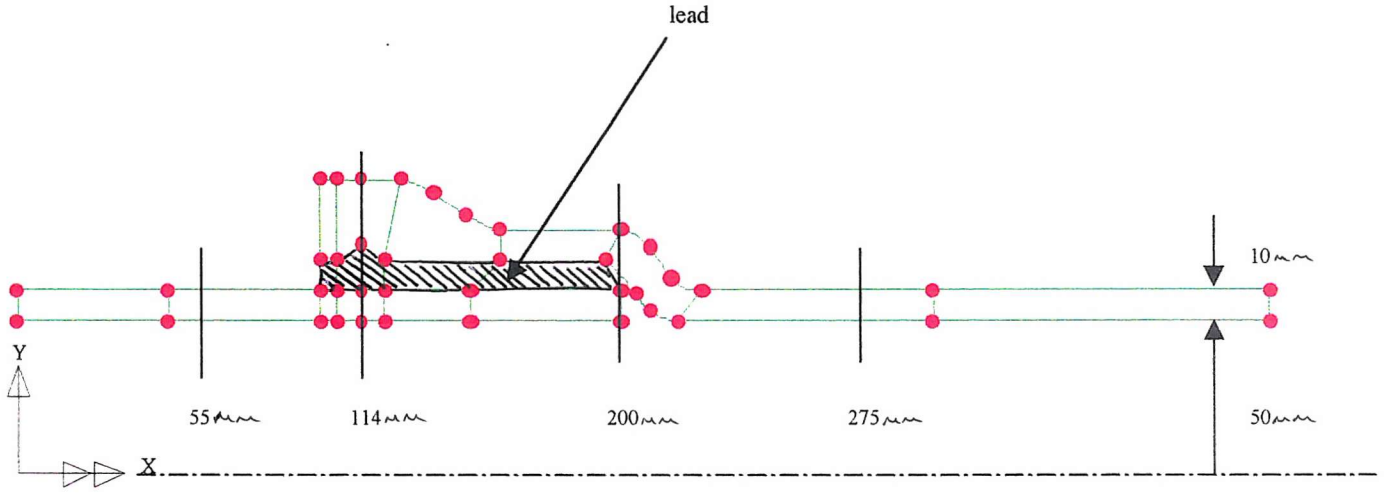

Figure 4.1 **Diagram of lead joint, showing position of lead and sections where equilibrium checks were taken.**

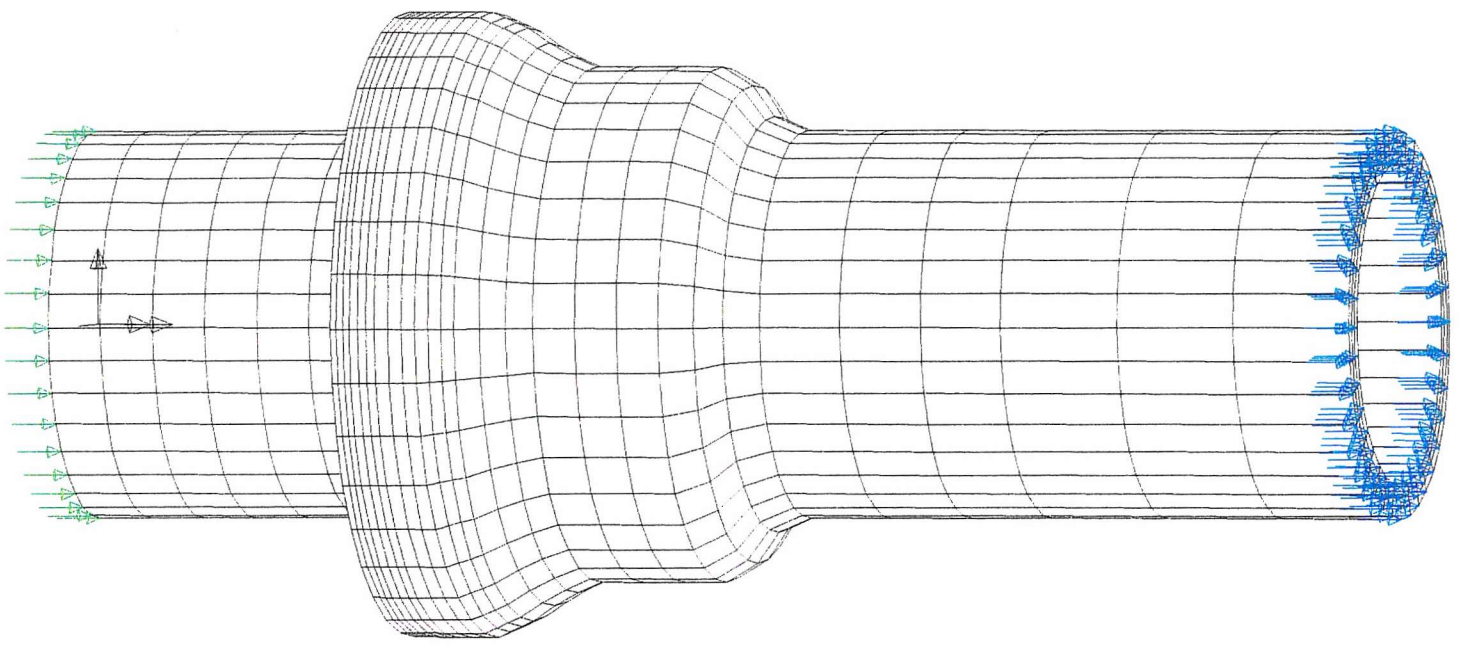

Figure 4.2: 3D plot of joint showing rigid supports and tensile load assignments.

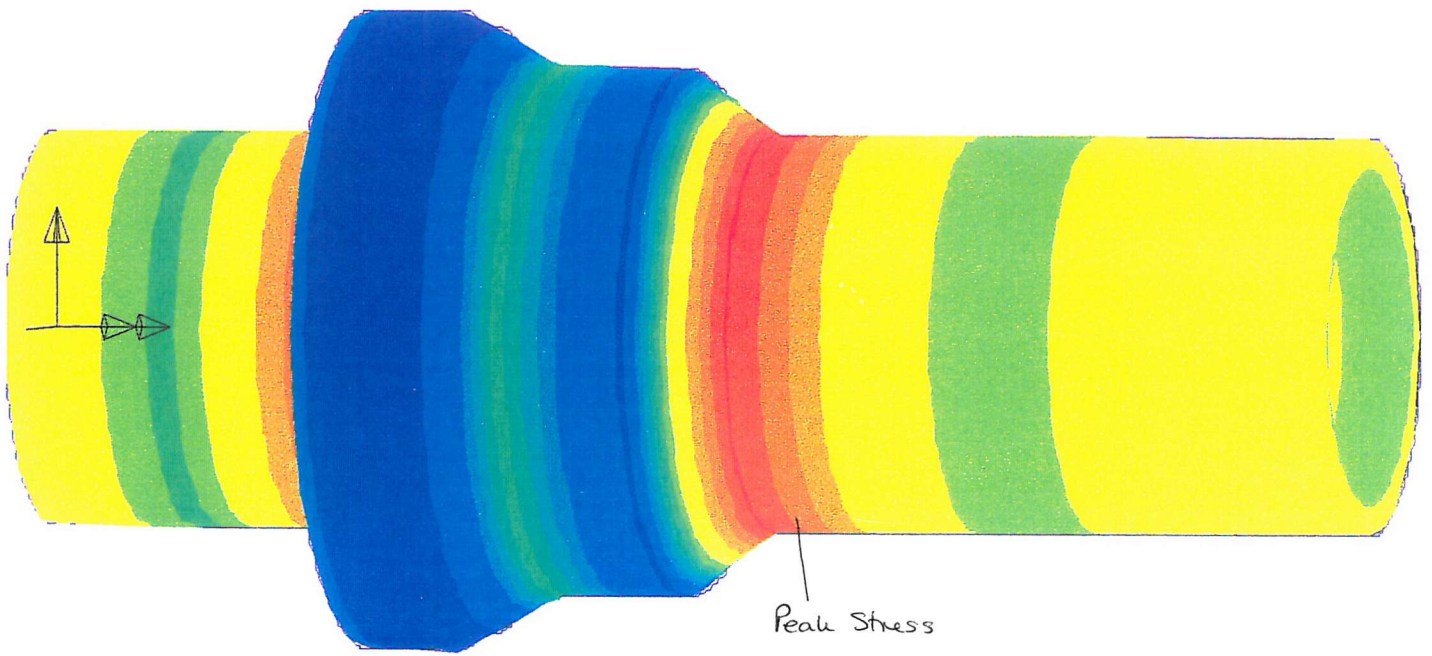

Figure 4.3: Contour plot of initial lead joint showing stress concentrations at the neck.

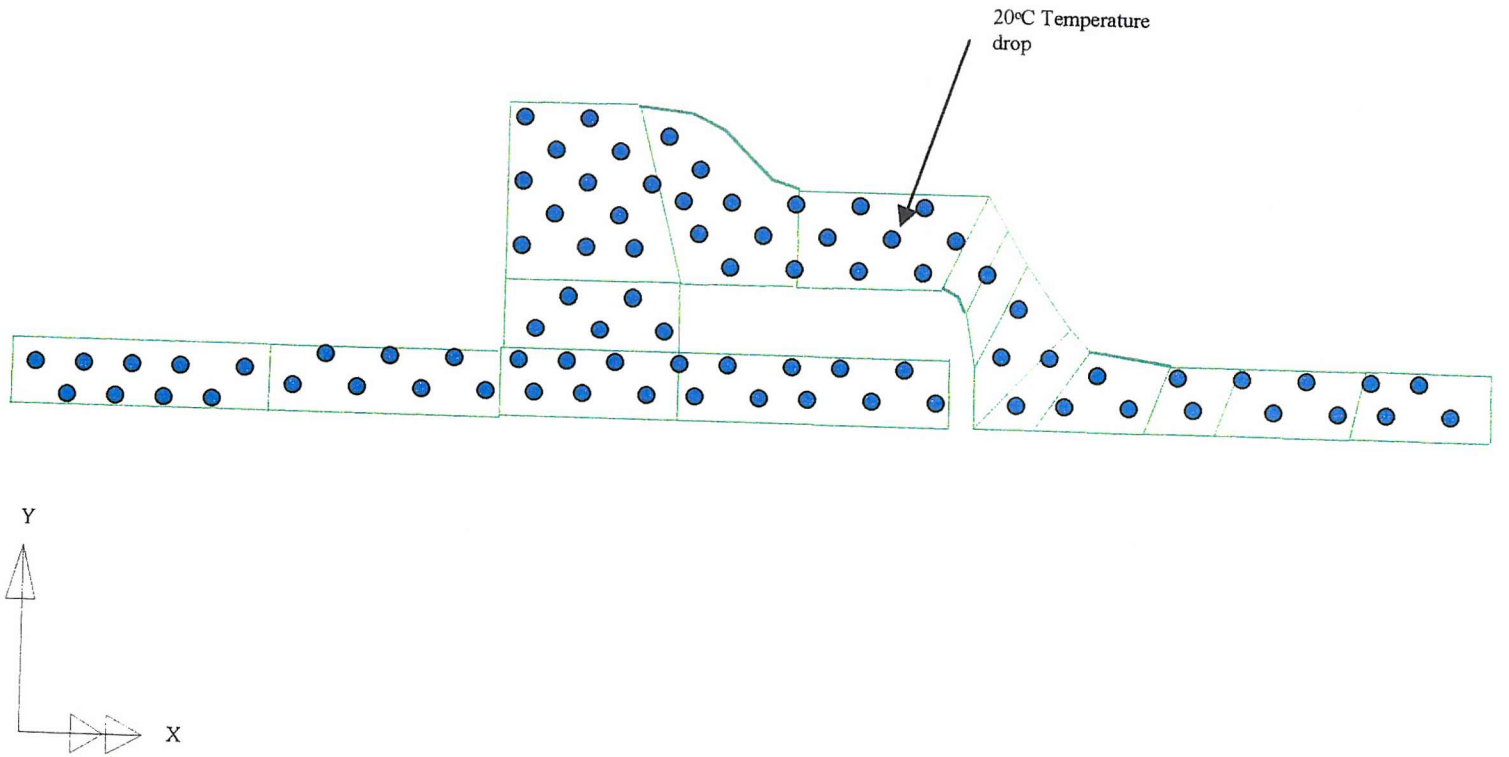

Figure 4.4: Section of complete model to show temperature load assignments.

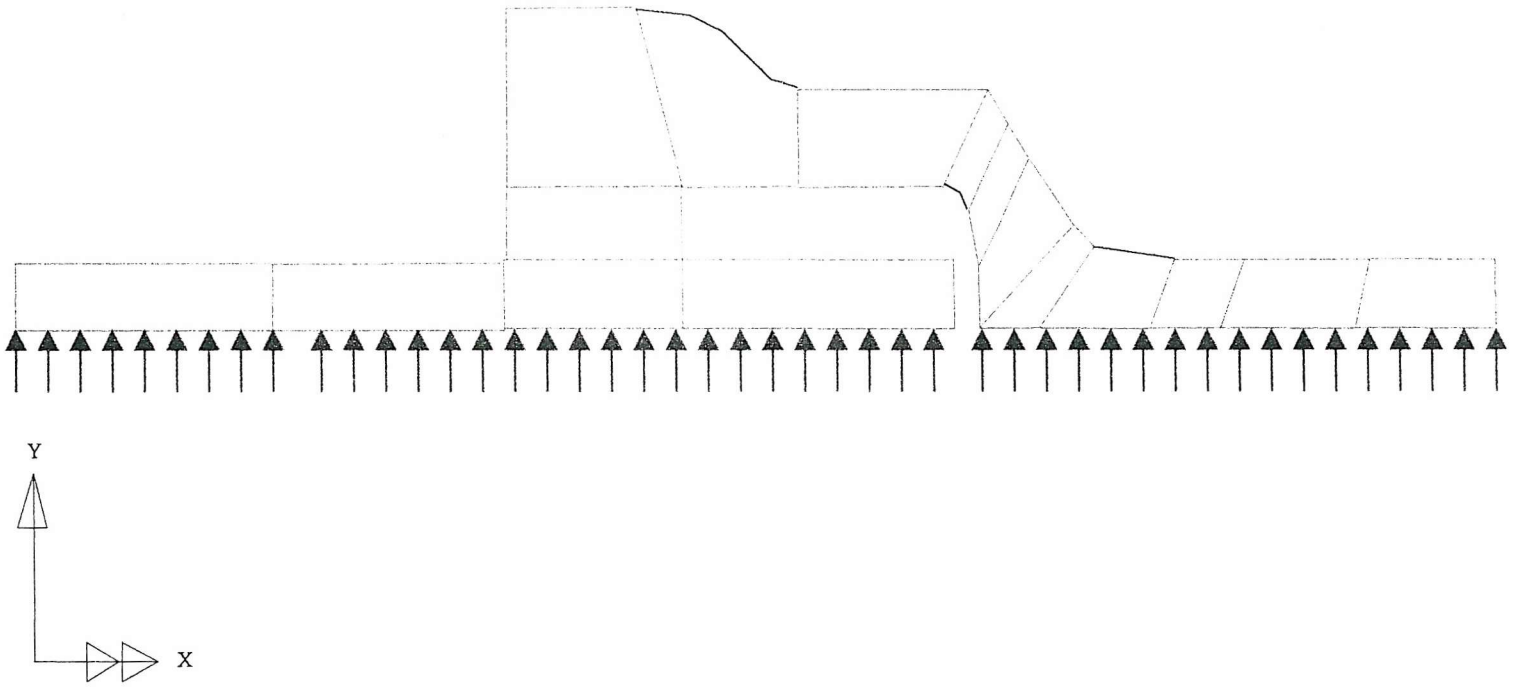

Figure 4.5: Section of complete model to show pressure load assignments.

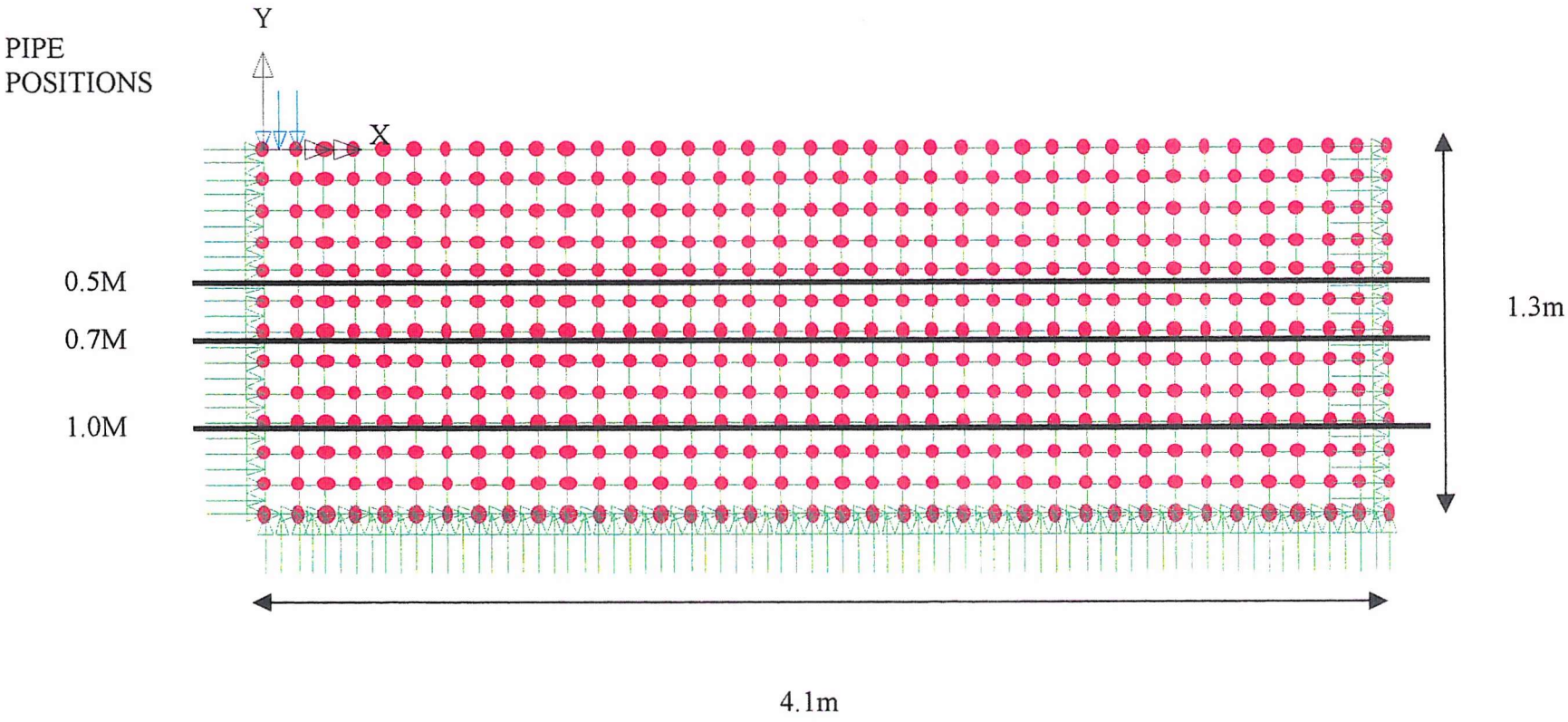

Figure 4.6: Set up of soil load model to determine traffic load at pipe crown.

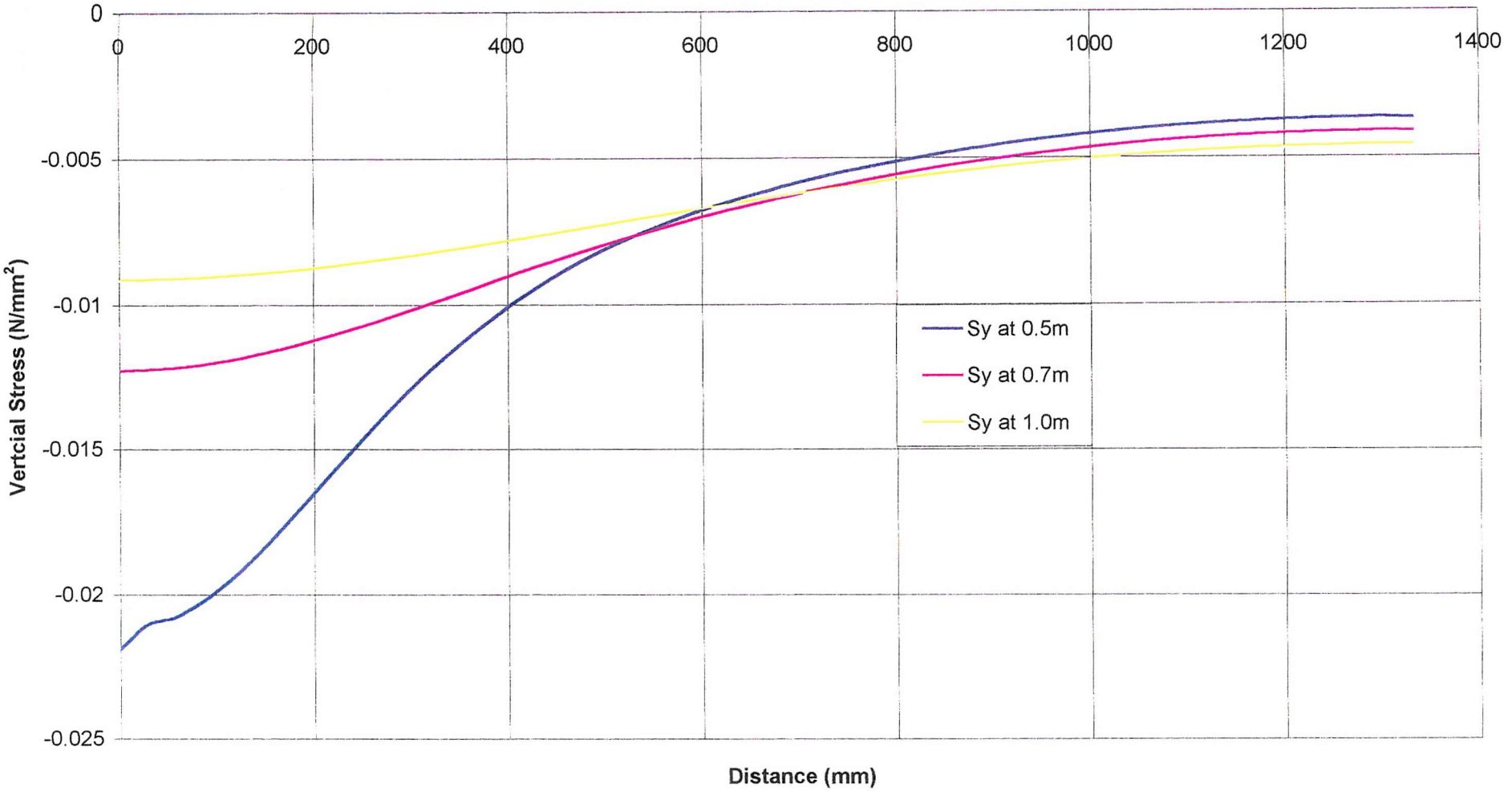

Figure 4.7: Stress distribution results of soil model with multilayers.

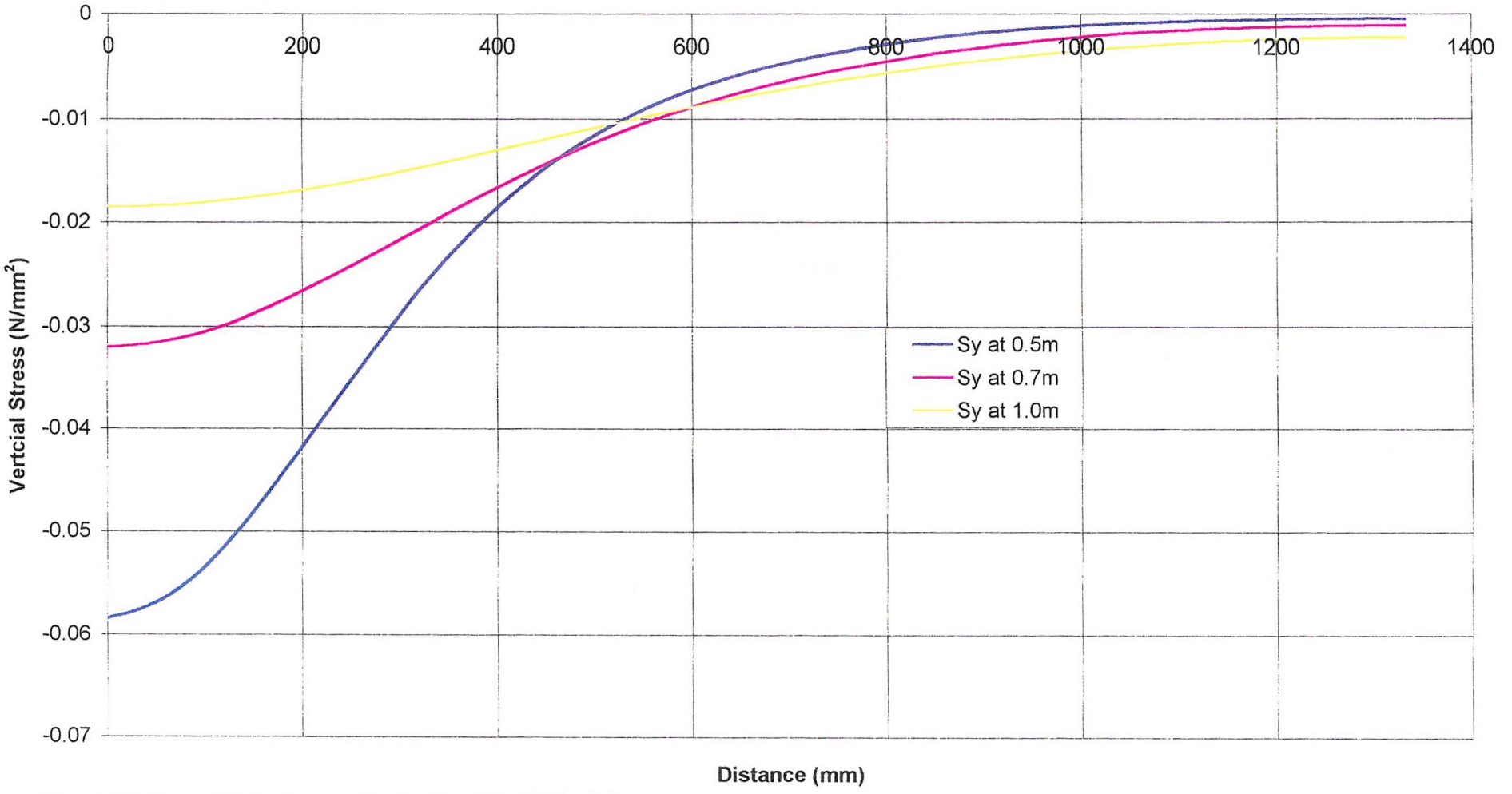

Figure 4.8: Stress distribution results of soil model with single layer.

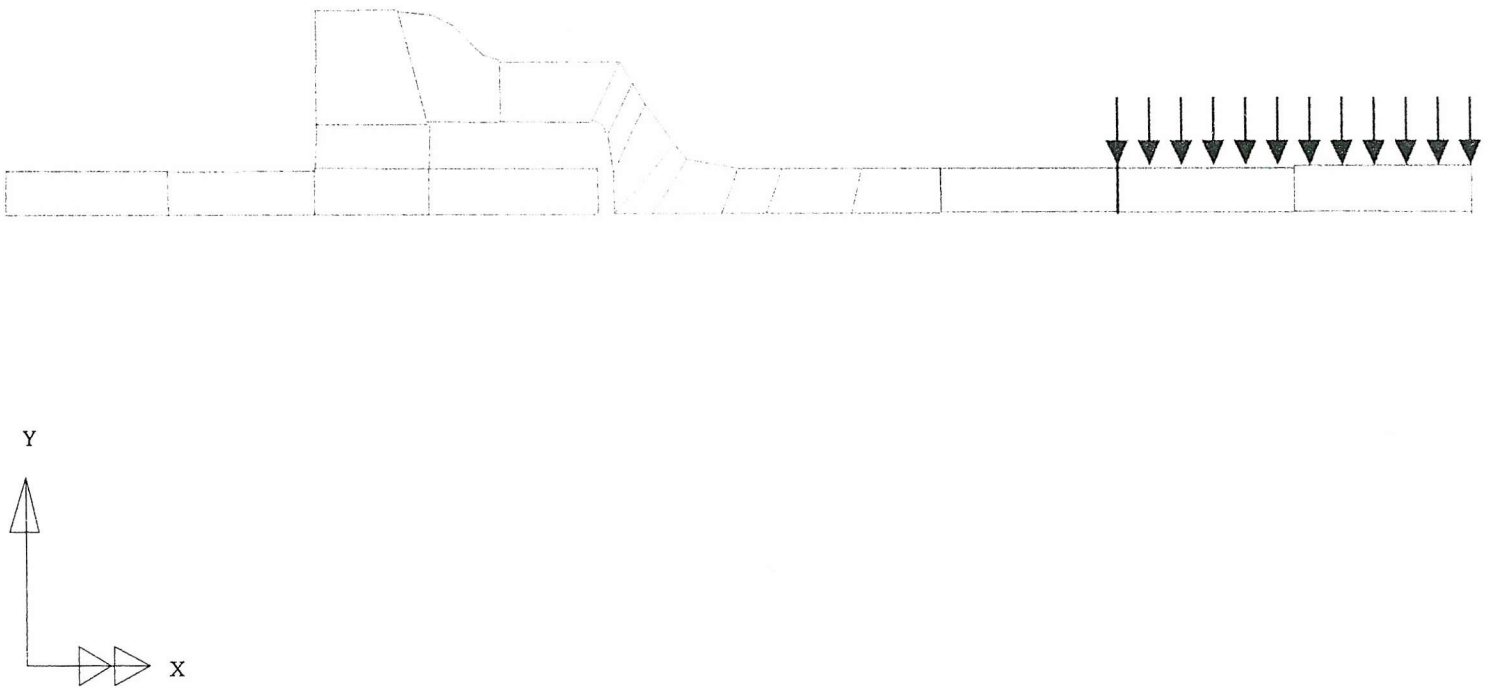

Figure 4.9: Section of complete model to show traffic load assignments at mid section.

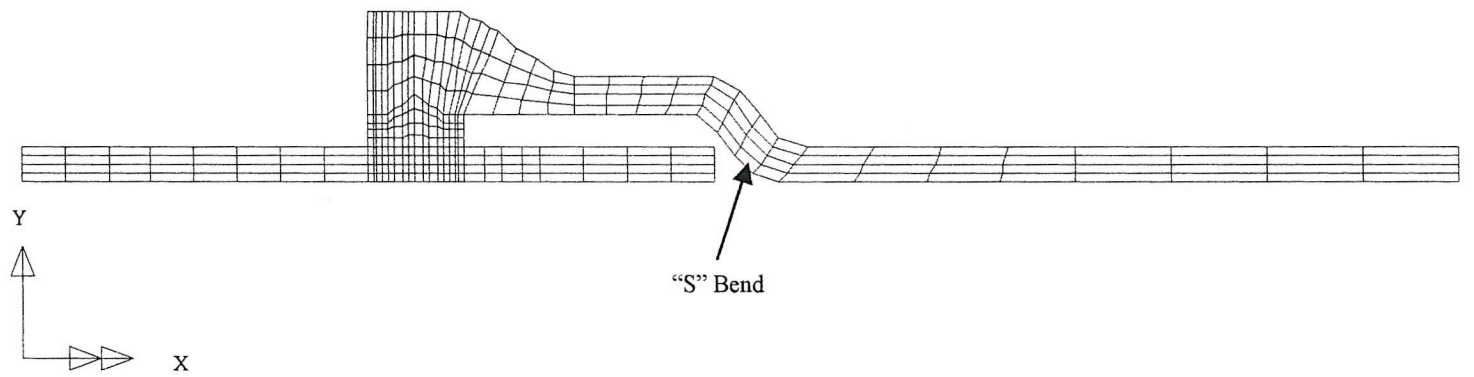

Figure 4.10: Initial lead joint with 'S' shape internal corner.

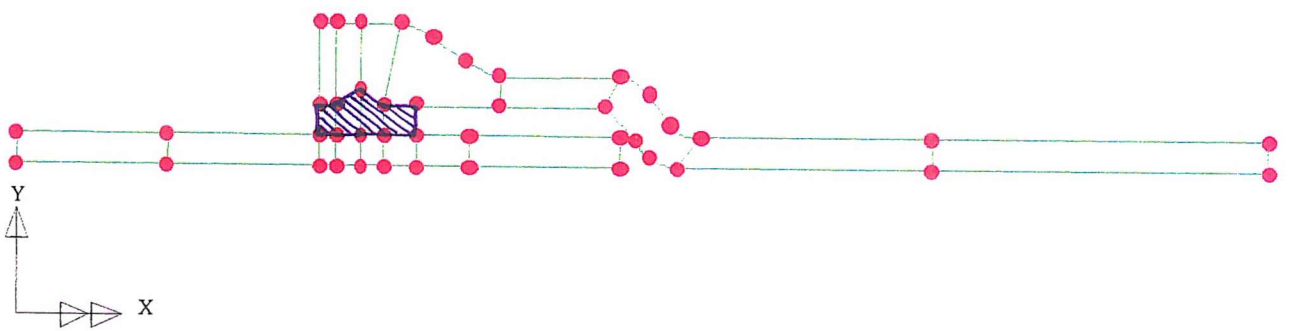

Figure 4.11: Original lead joint with shortened lead length.

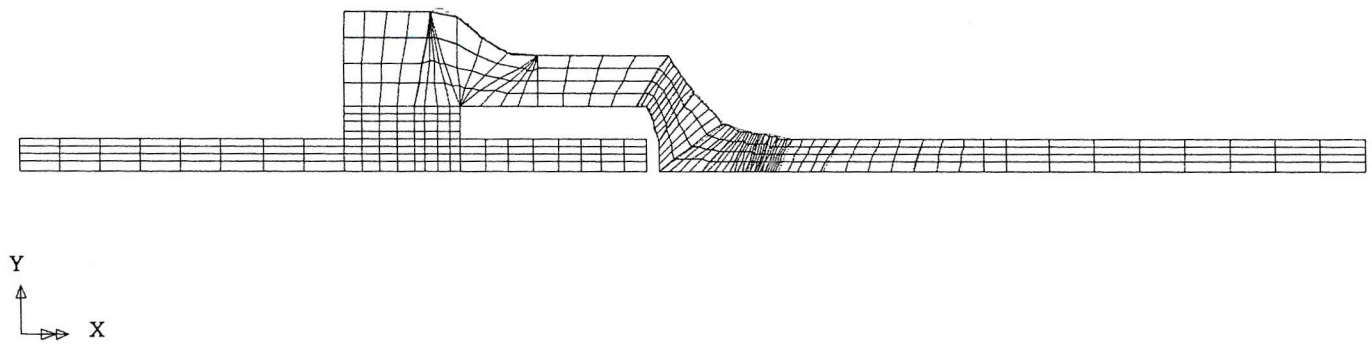

Figure 4.12: Lead joint with revised 90° internal corner.

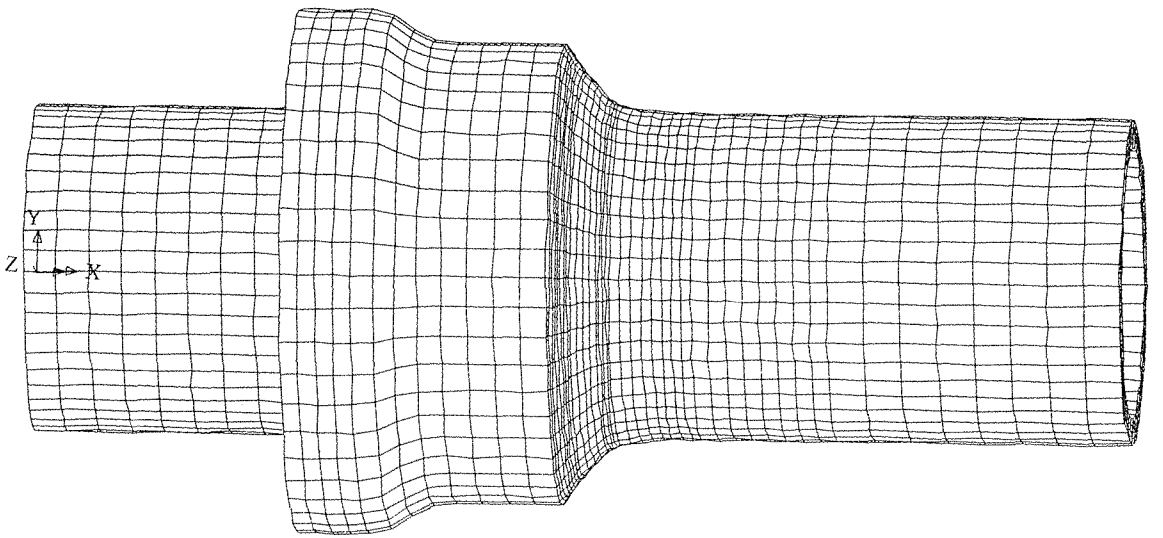

Figure 4.13: Diagram to show full 3D joint.

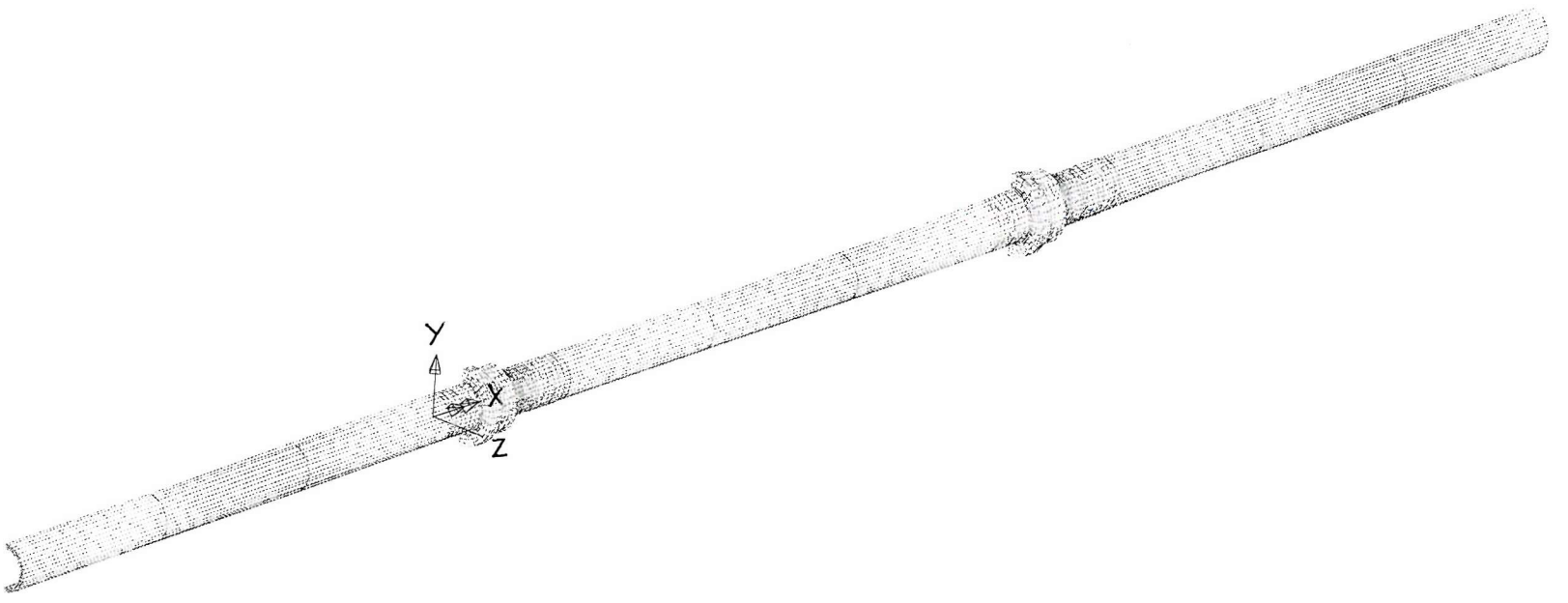

Figure 4.14: Diagram to show halved section of final model

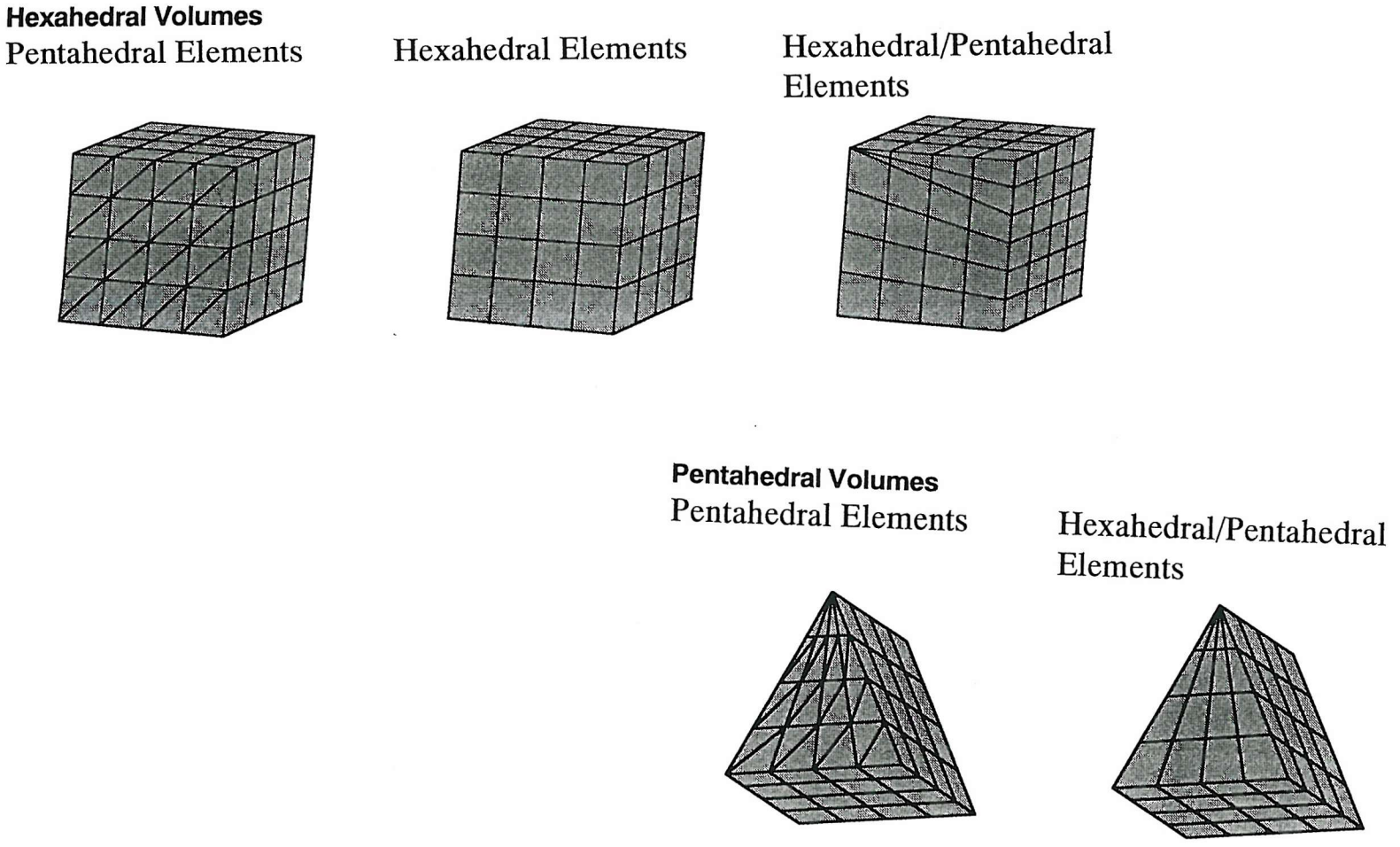

Figure 4.15: Mesh shapes, hexahedral and pentahedral.

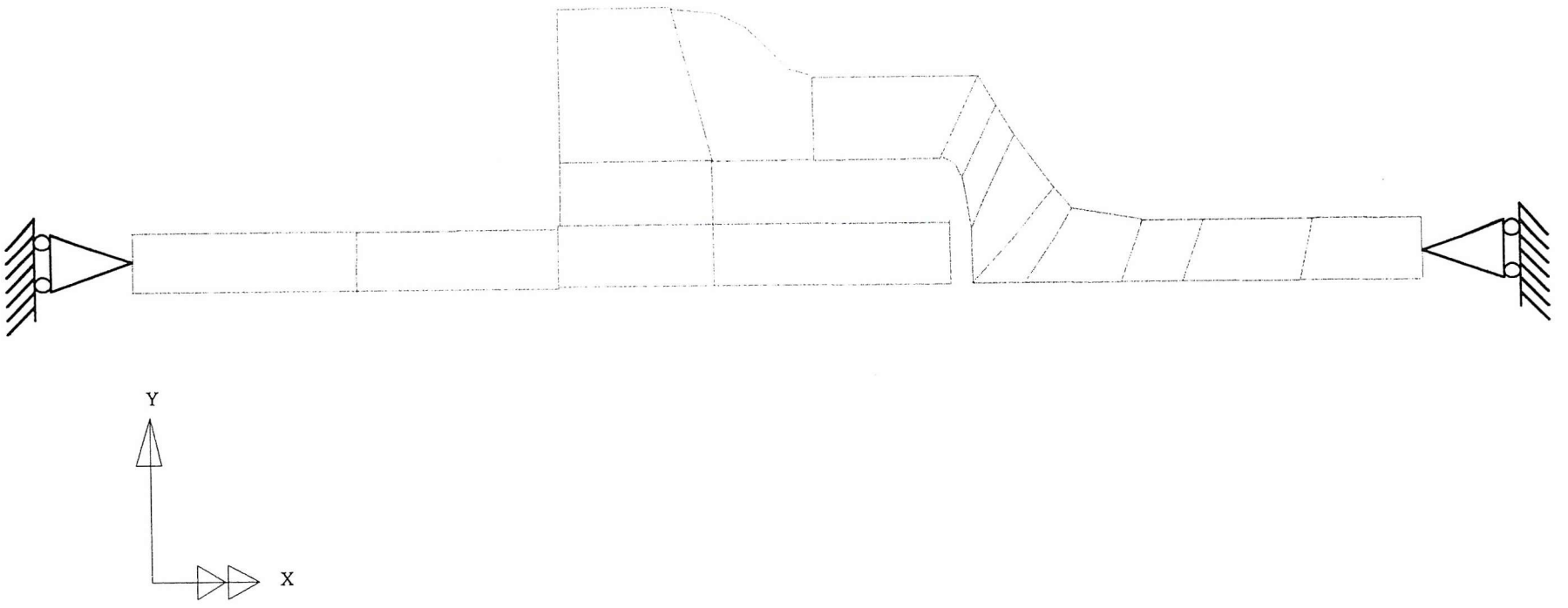

Figure 4.16: Section of final model showing type and application of end restraints.

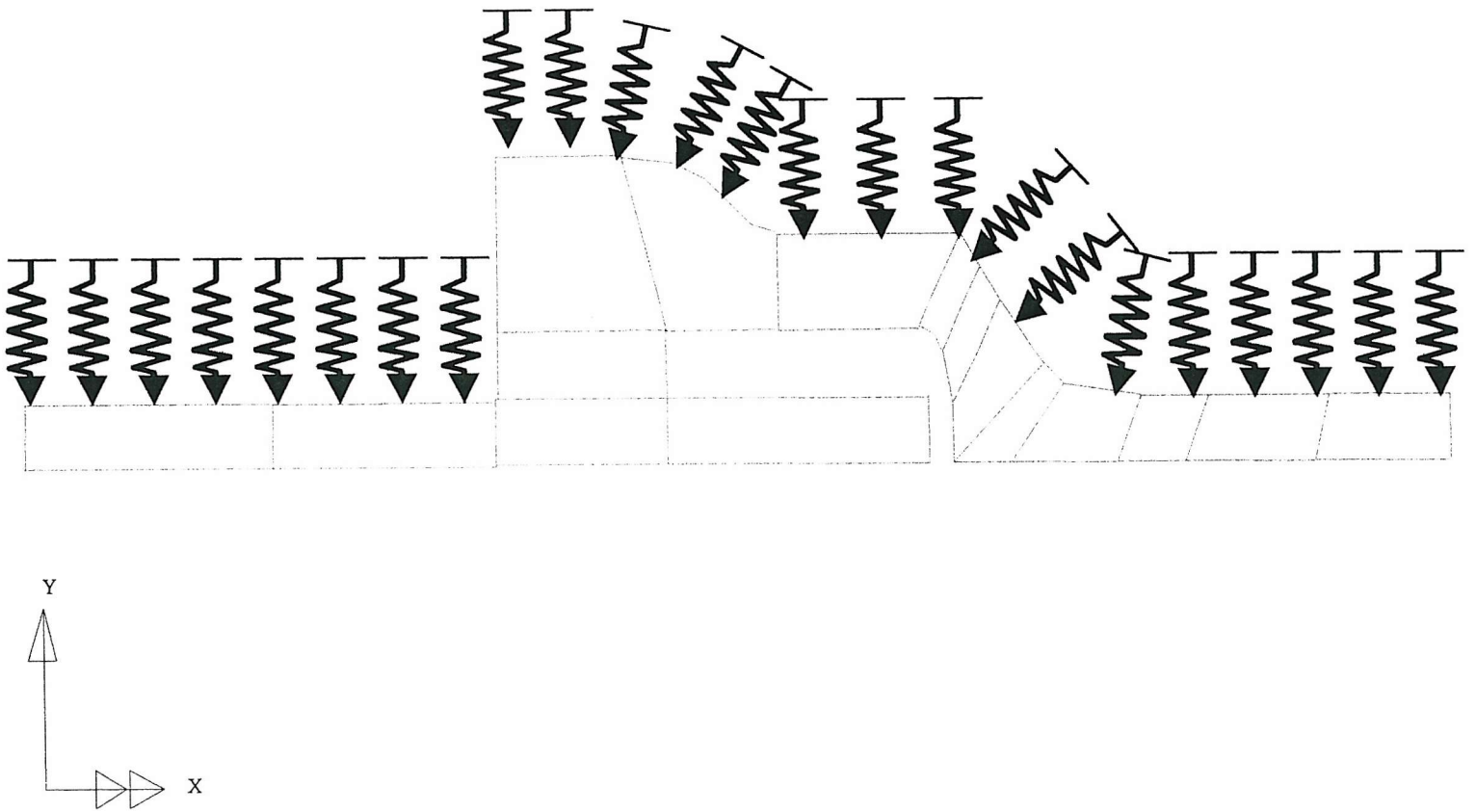

Figure 4.17: Section of final model showing soil spring supports along outside surface of pipe.

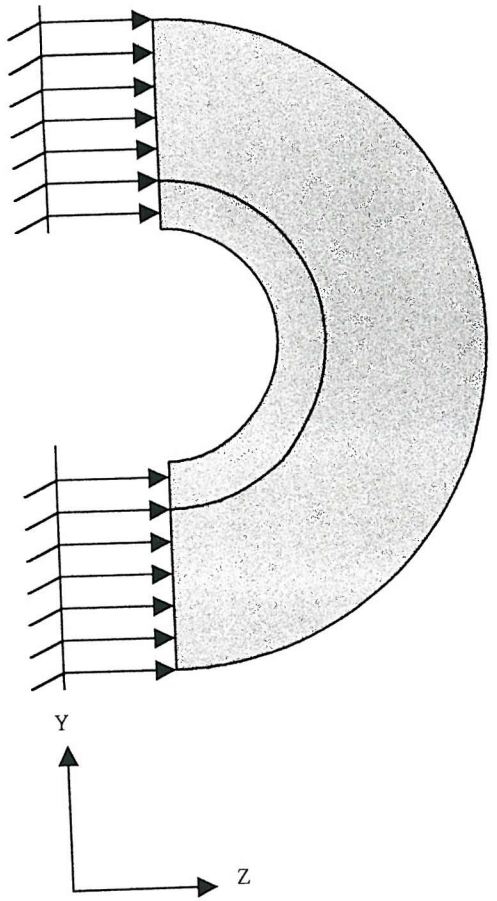

Figure 4.18: Section of final model showing surface edge supports, used to mirror symmetry.

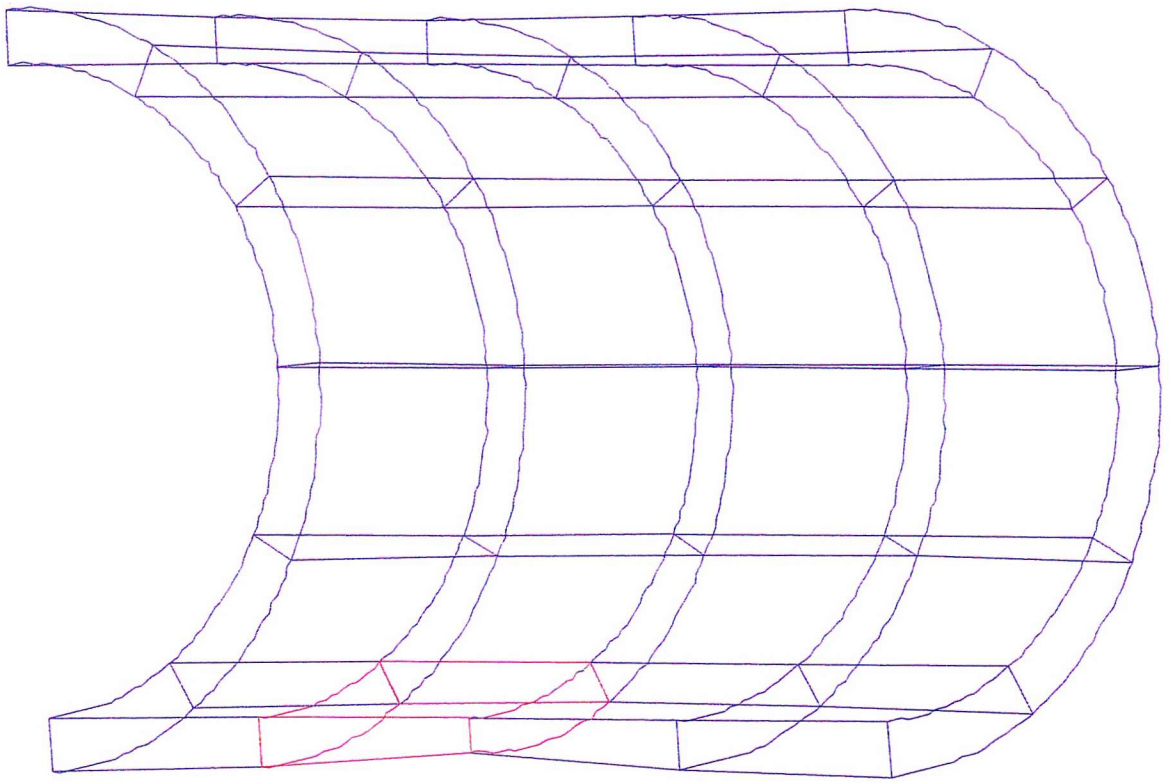

Figure 4.19: Enlarged mid section to show position of slag void.

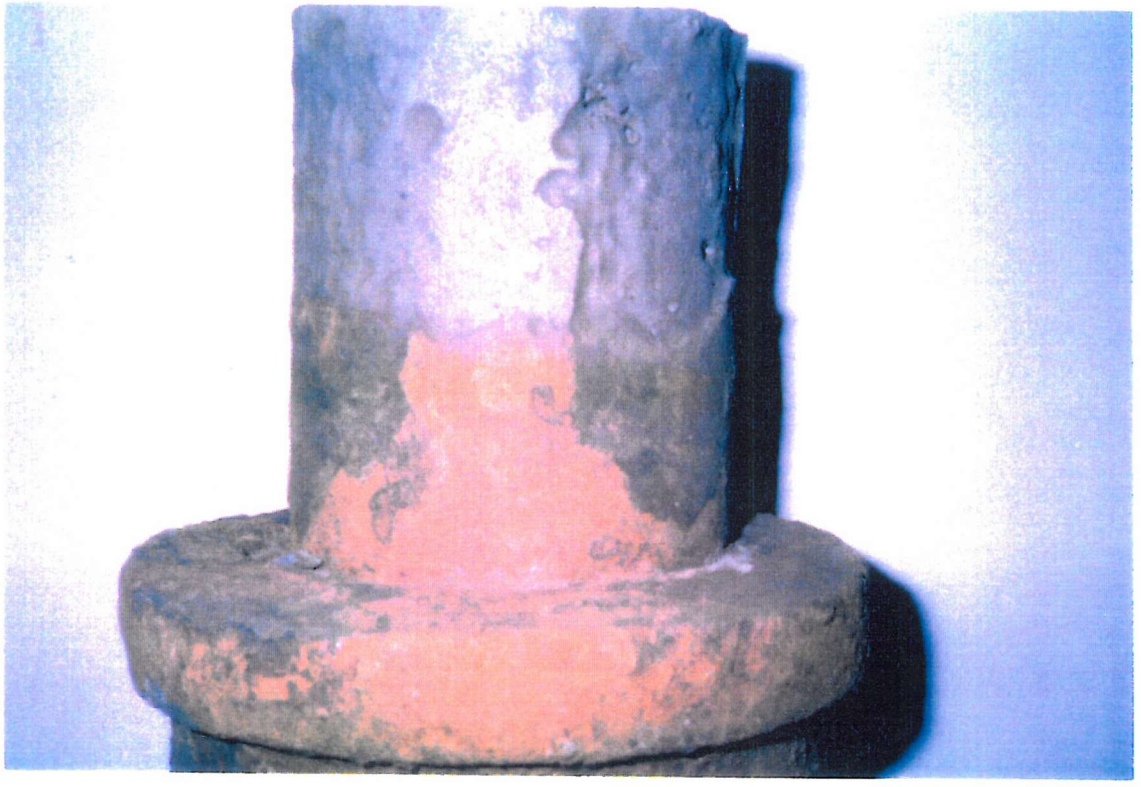

Figure 4.20: Photo of cast iron pipe with corrosion pitting

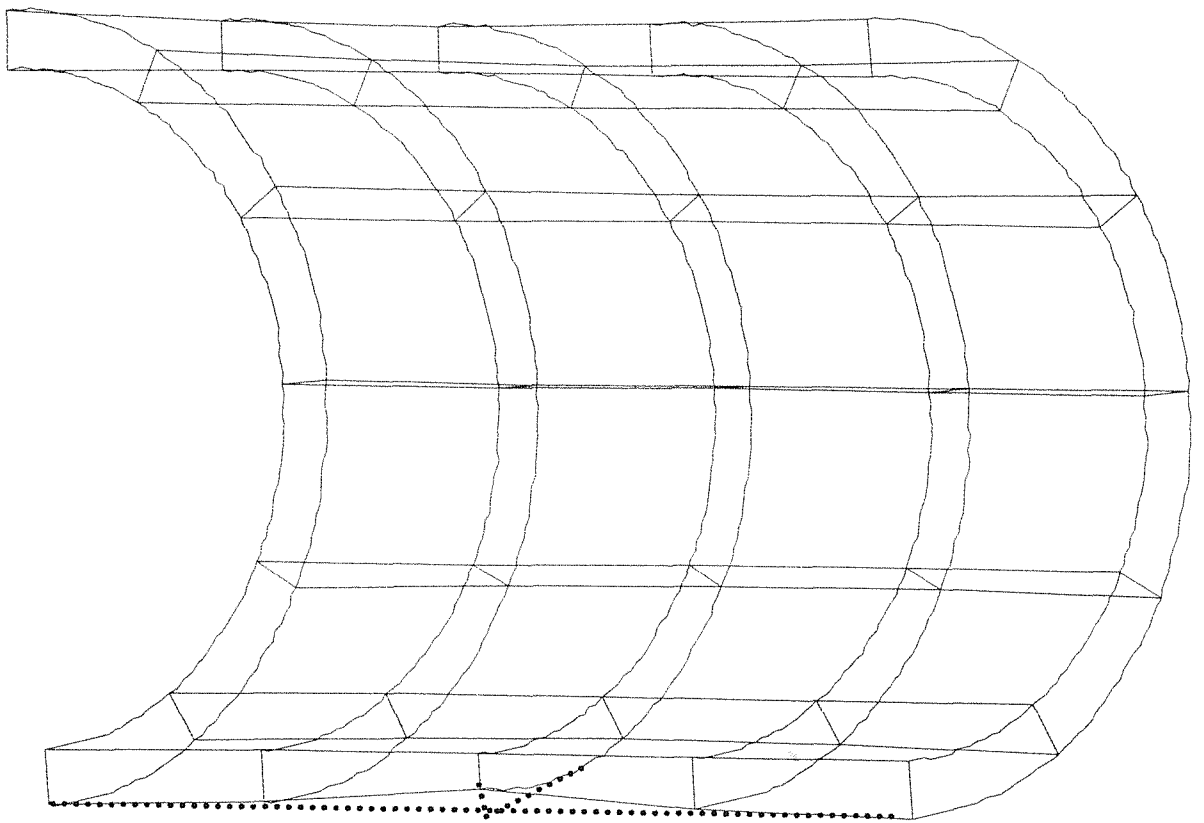

Figure 4.21: Enlarged mid section to show position of corrosion pit.

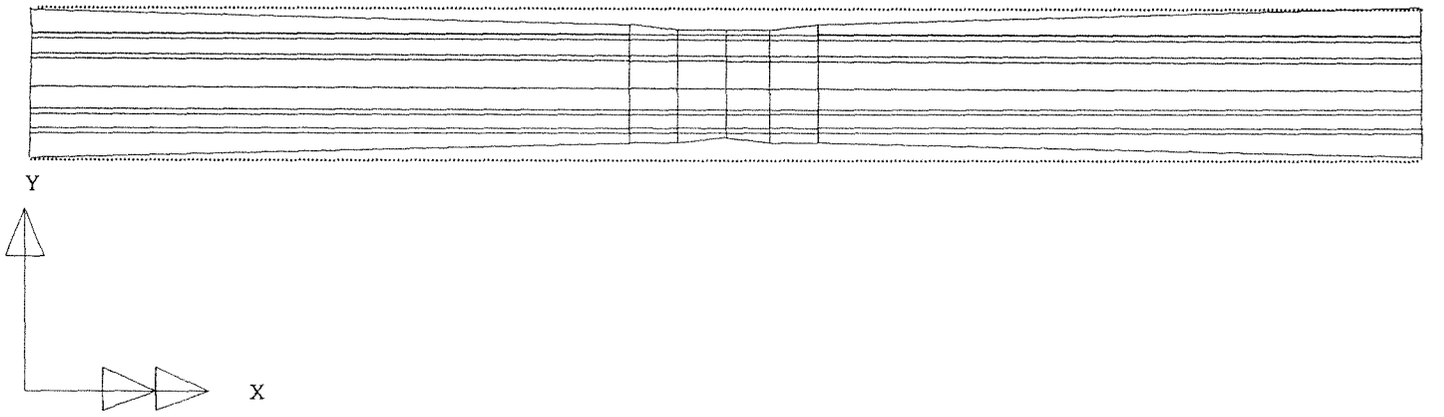

Figure 4.22: Enlarged mid section to show thin wall and corrosion pit.

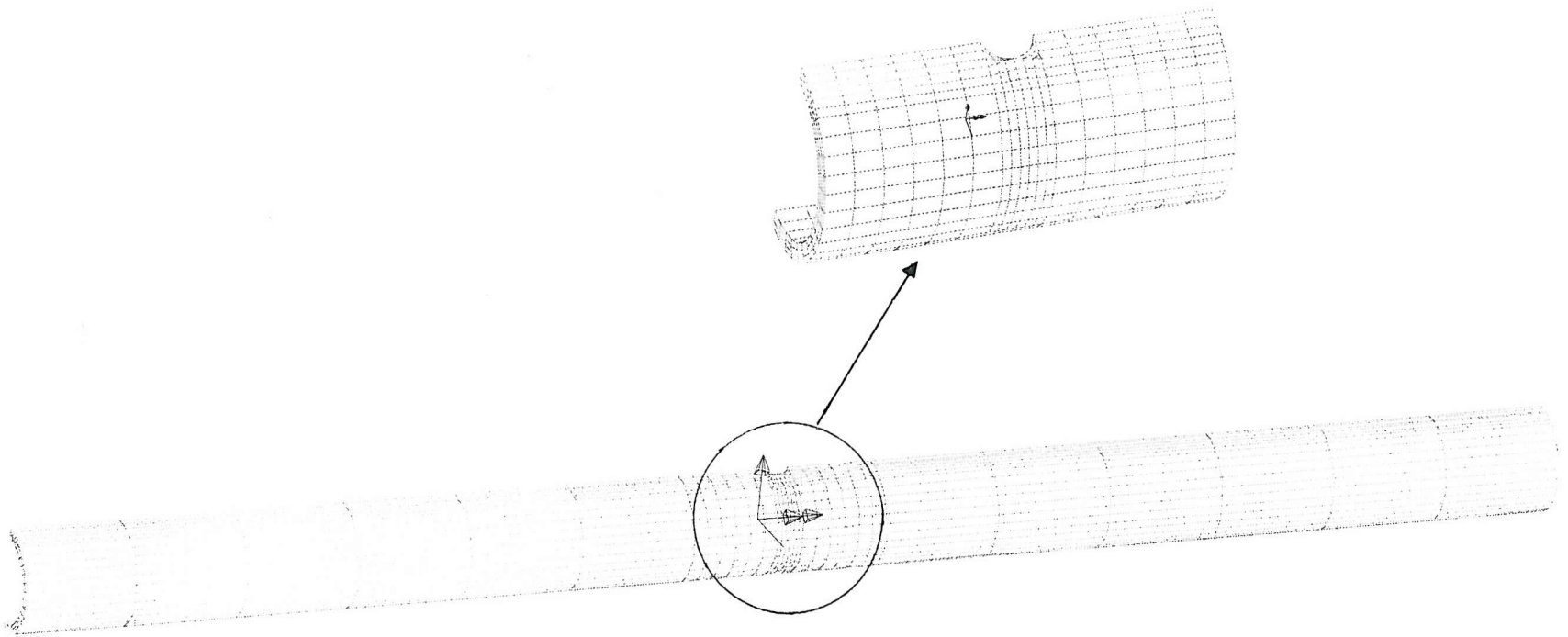

Figure 4.23: Pipe length with hole, representing ferrule in the crown of the pipe.

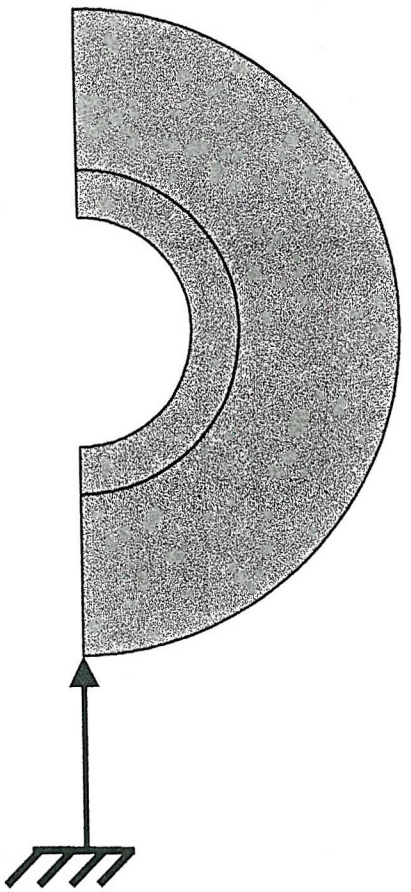

Figure 4.24: Diagram to show point supports assigned directly underneath each bell of the joints.

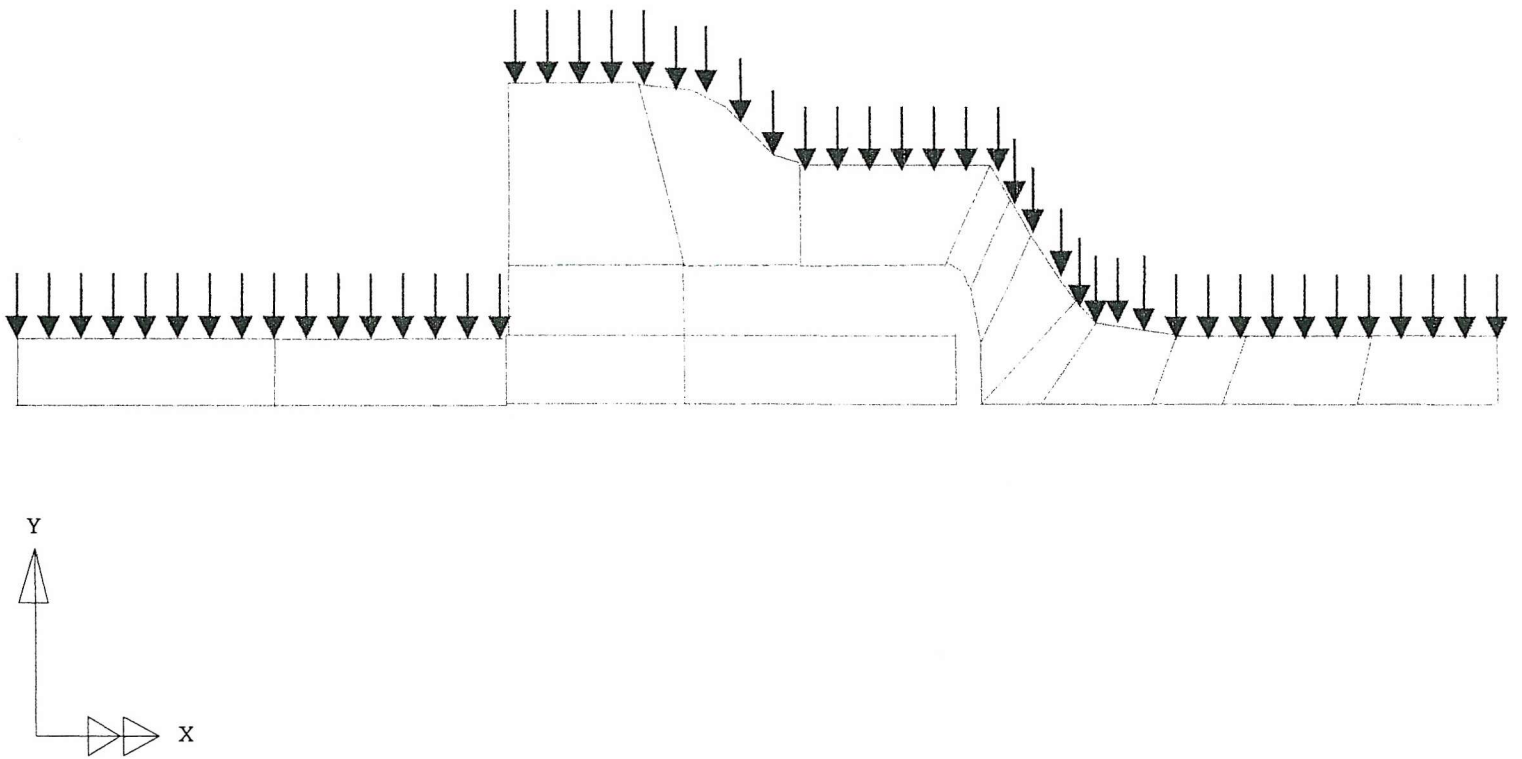

Figure 4.25: Section of final model to show assignments of body force.

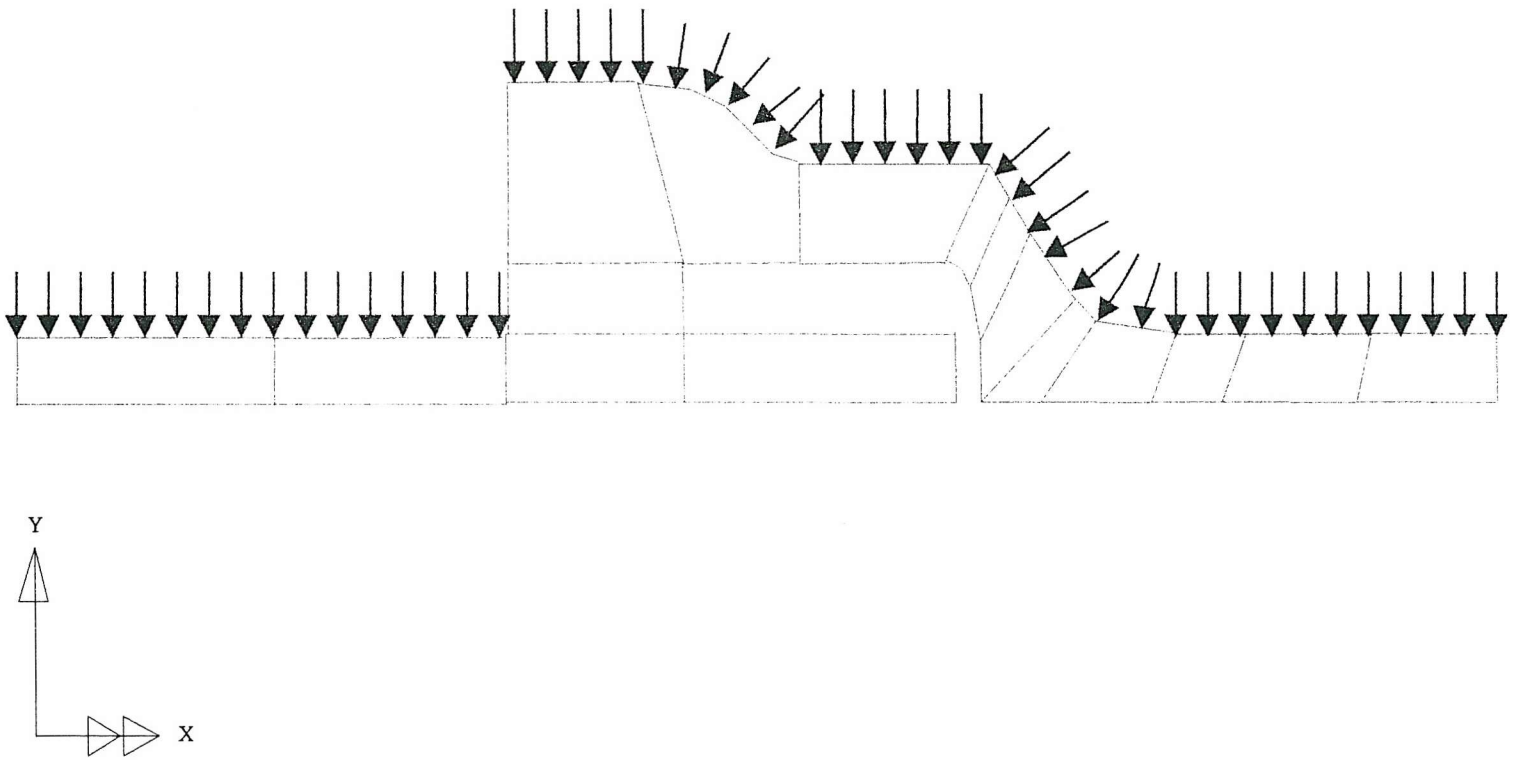

Figure 4.26: Section of final model showing assignments of soil load.

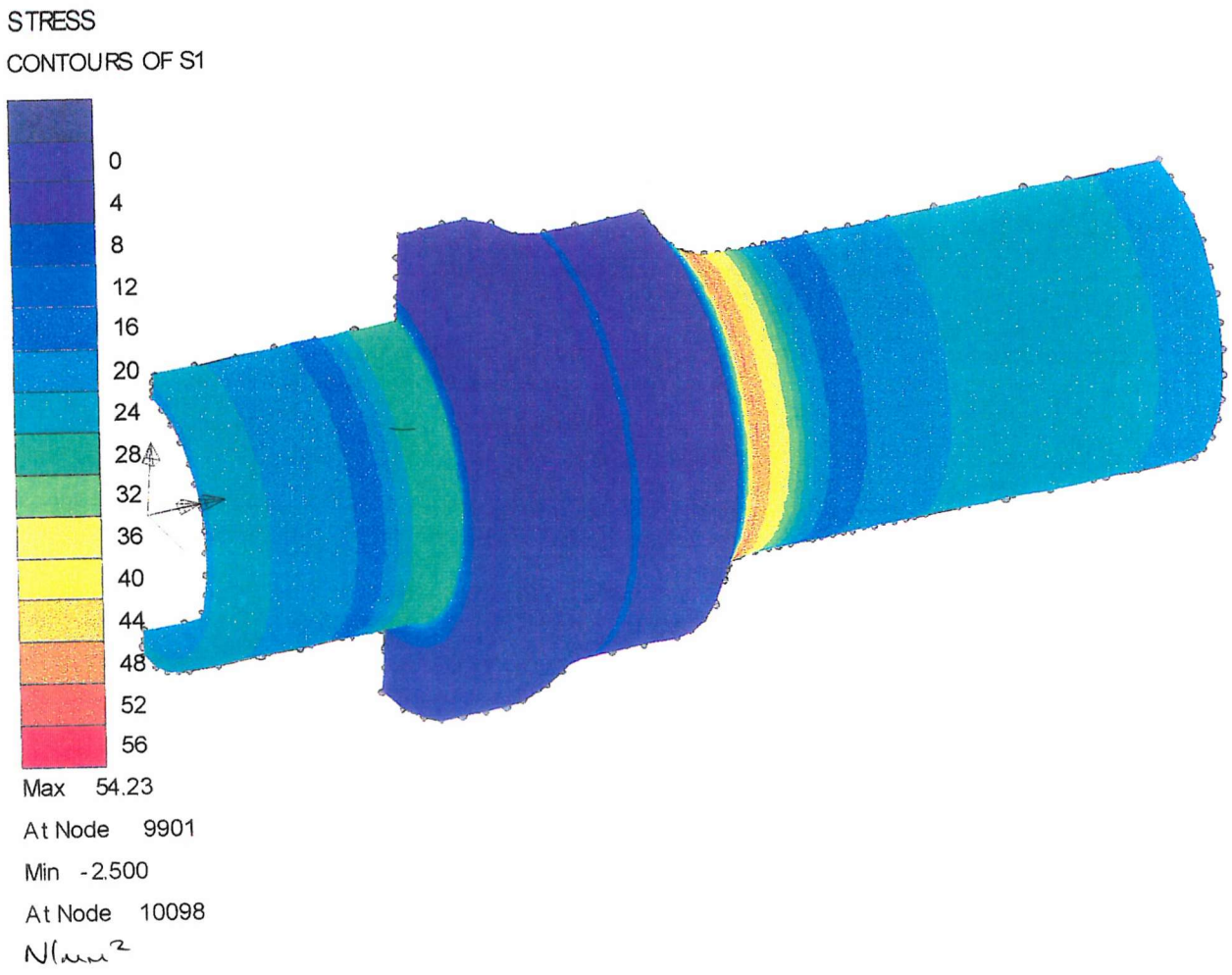

Figure 4.27: Stress contour plot of a section of the model, showing basic temperature loading effects on the outside of the pipe, using S1.

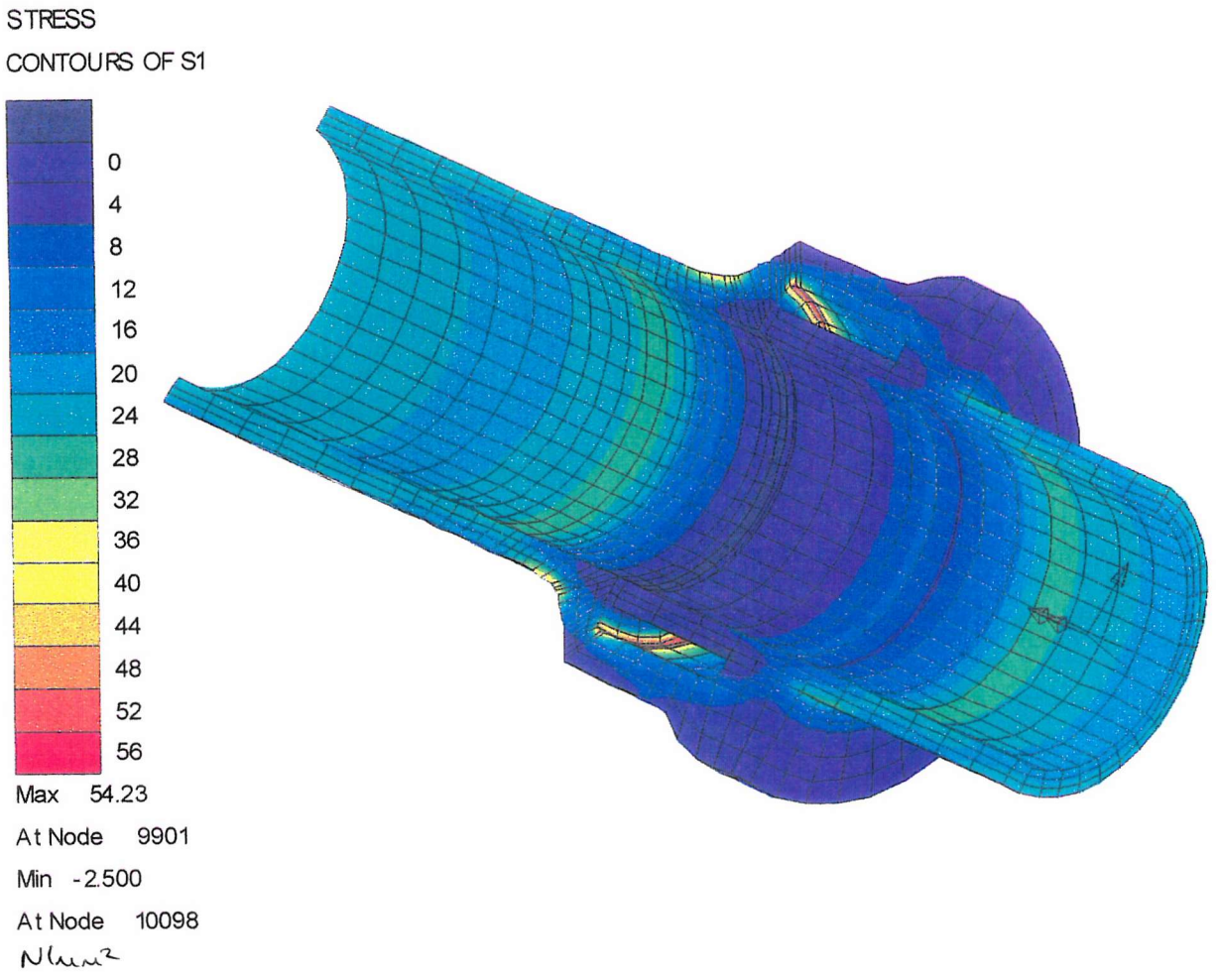

Figure 4.28: Stress contour plot of a section of the model, showing basic temperature loading effects on the inside of the pipe, using S1.

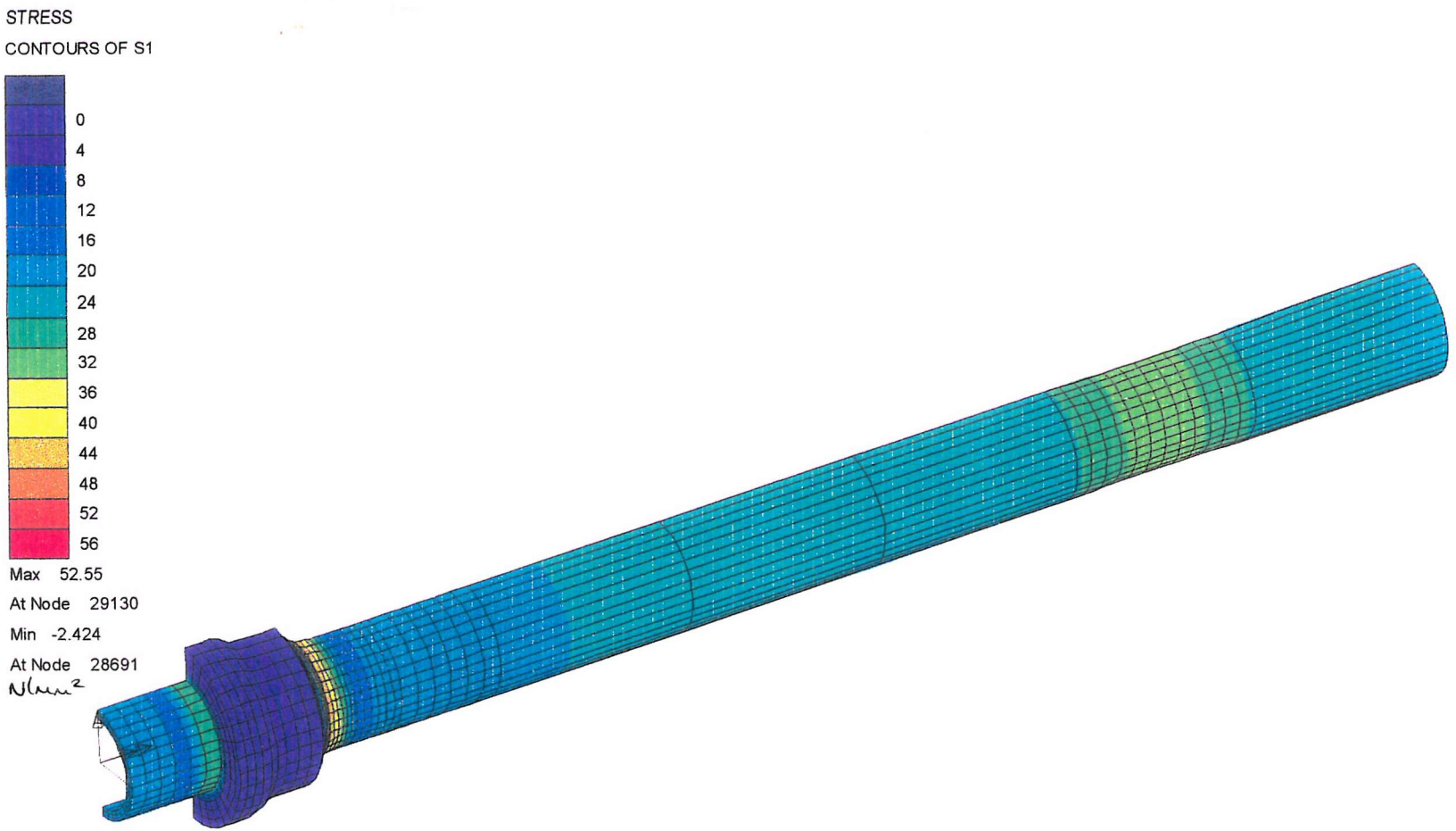

Figure 4.29: Stress contour plot of a section of the model, showing basic temperature loading effects with thin wall on the outside of the pipe, using S1.

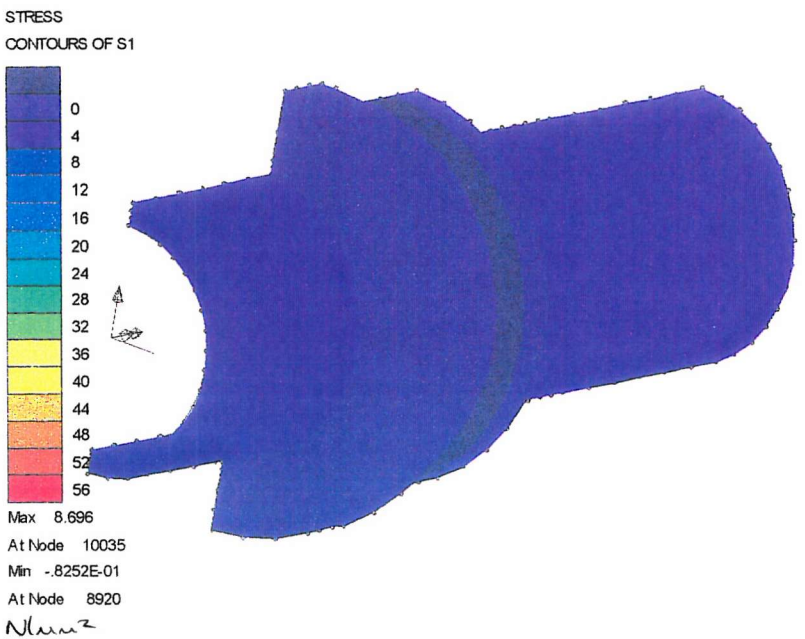

Figure 4.30: Stress contour plot of a section of the model, showing basic pressure loading effects on the outside of the pipe, using S1.

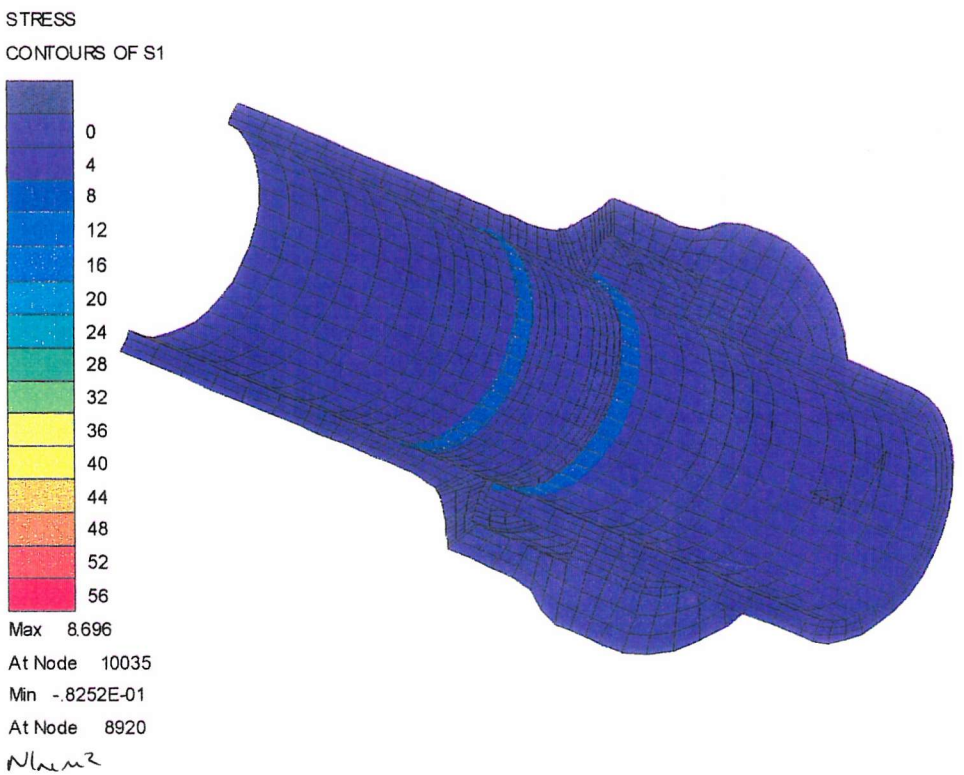

Figure 4.31: Stress contour plot of a section of the model, showing basic pressure loading effects on the inside of the pipe, using S1.

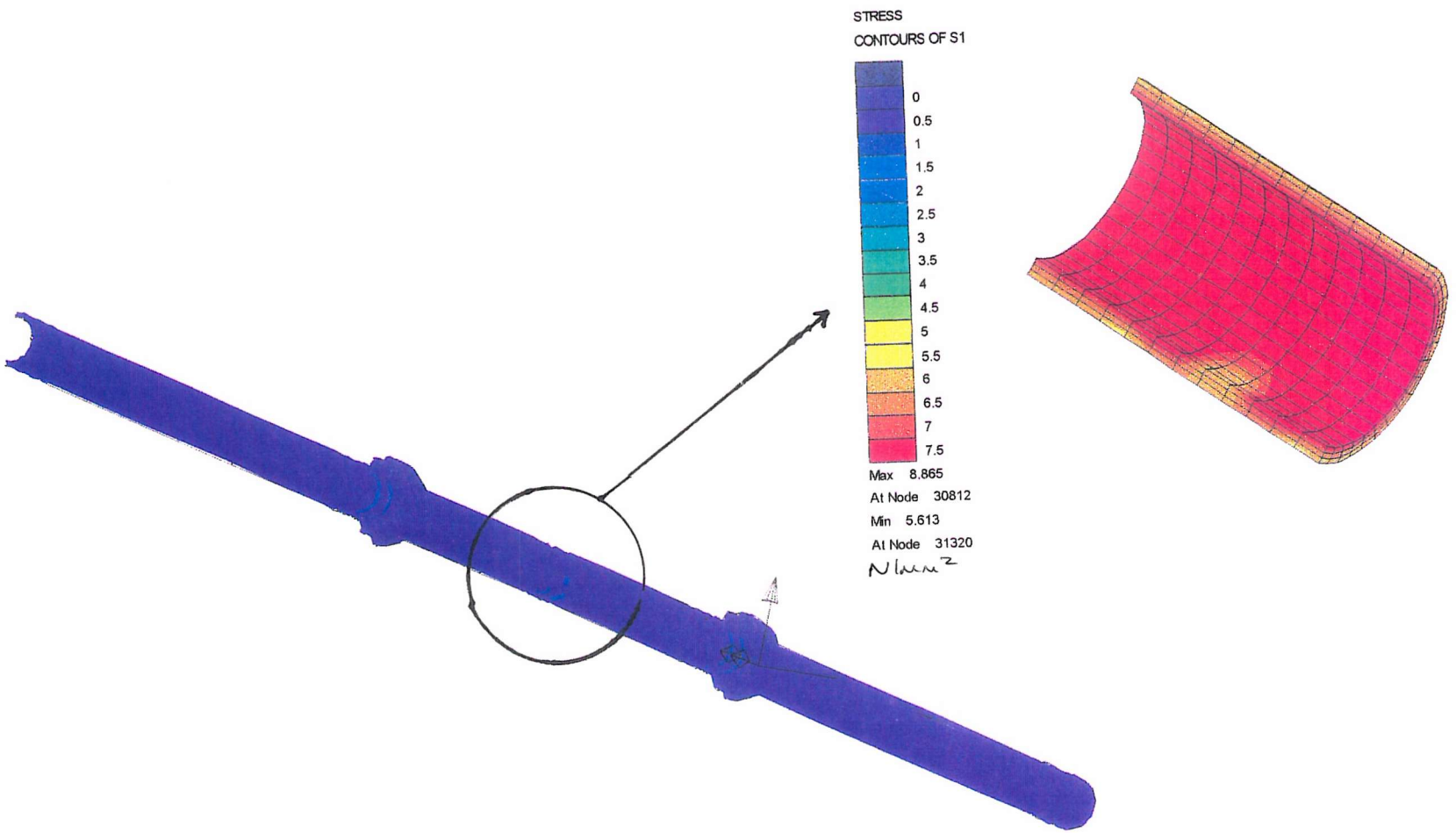

Figure 4.32: Stress contour plot of a section of the model, showing basic pressure loading effects with slag void, on the outside of the pipe, using S1.

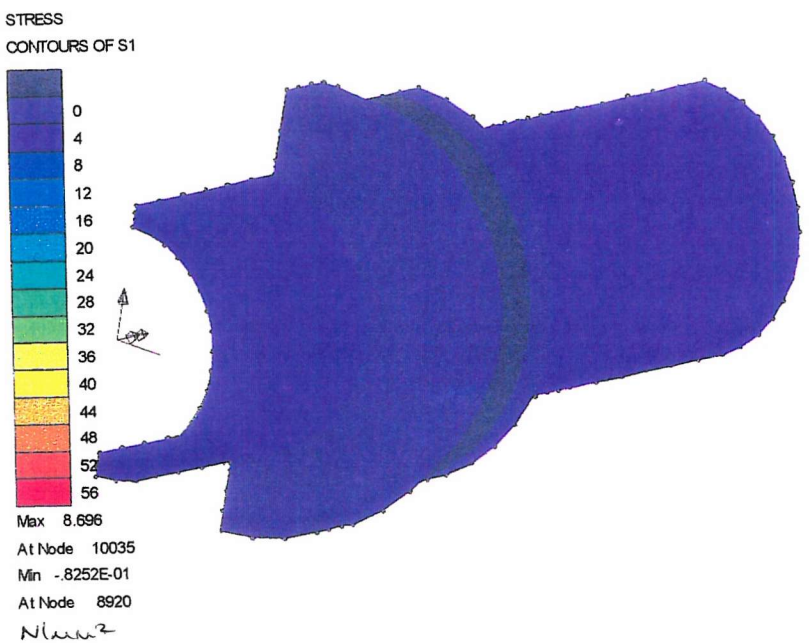

Figure 4.33: Stress contour plot of a section of the model, showing basic pressure loading effects with thin wall, on the outside of the pipe, using S1.

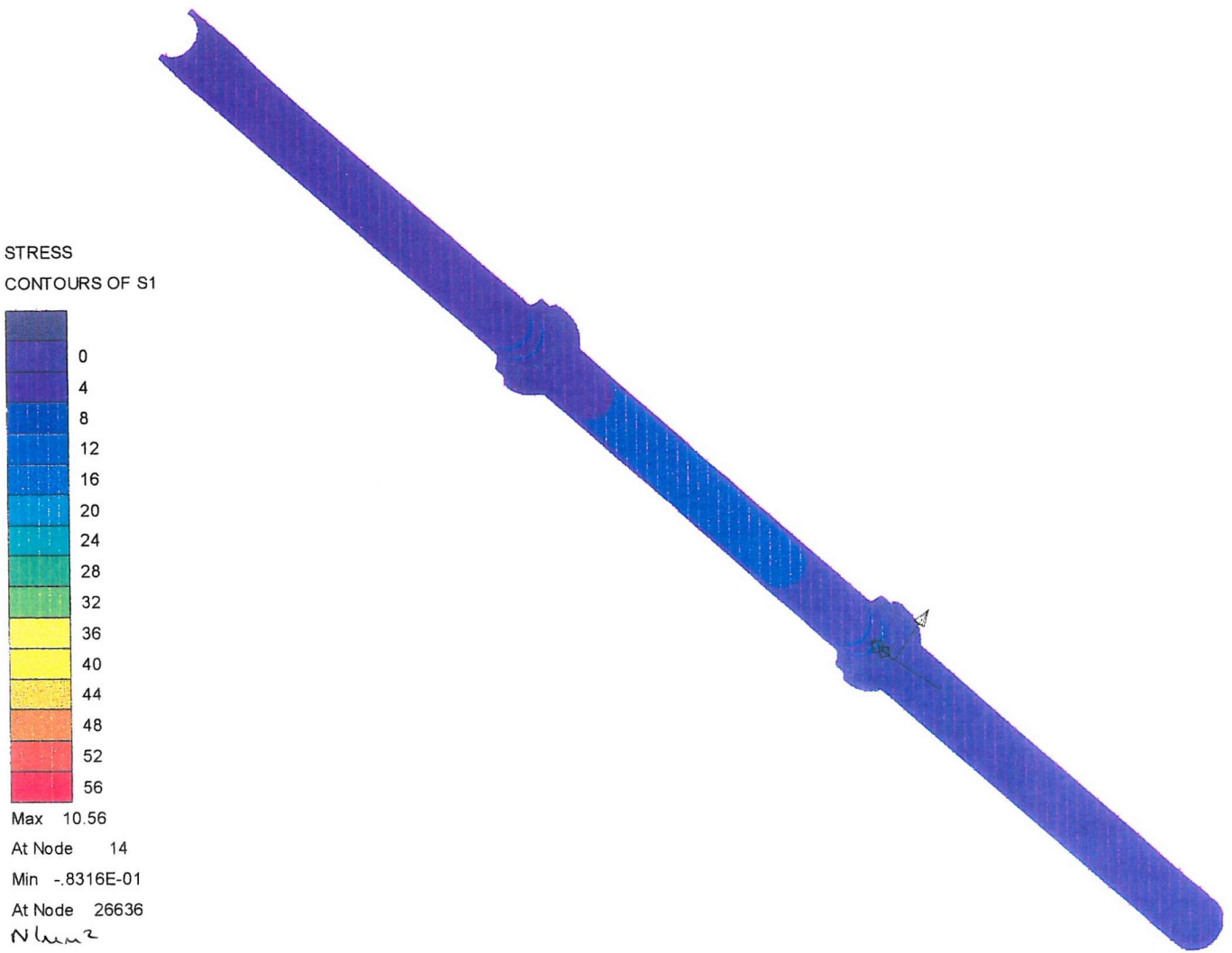

Figure 4.34: Stress contour plot of a section of the model, showing basic pressure loading effects with thin wall, on the inside of the pipe, using S1.

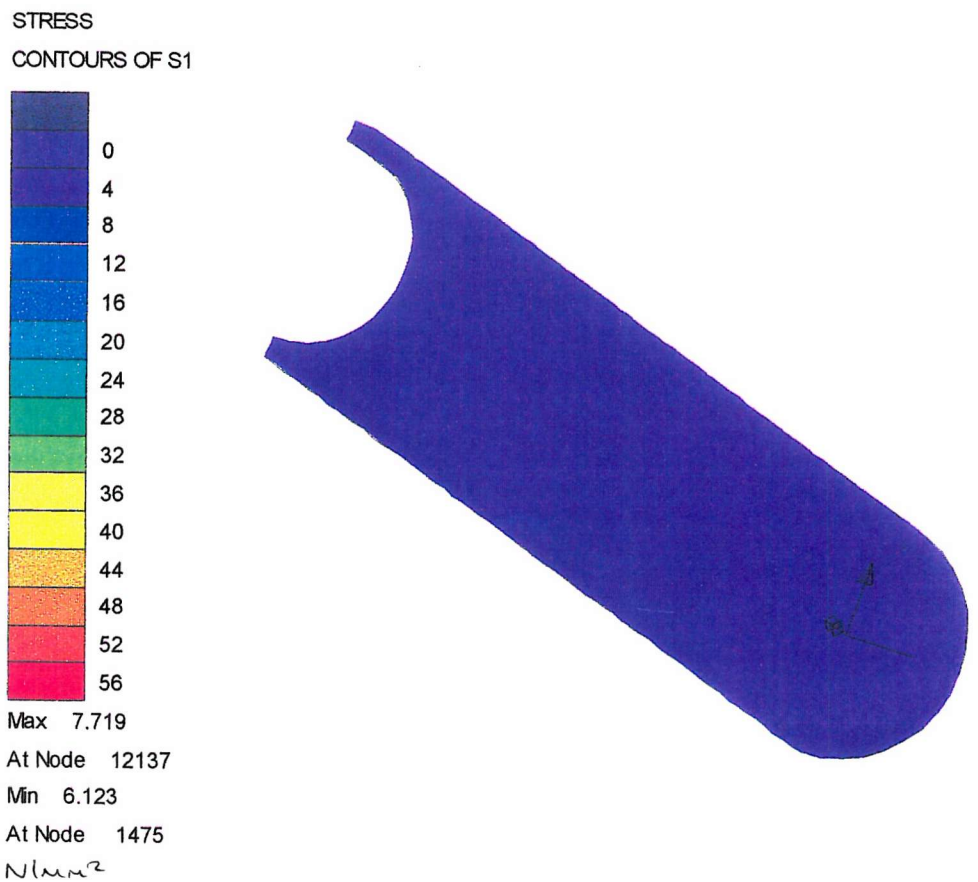

Figure 4.35: Stress contour plot of pressure loading in pipe length, using S1.

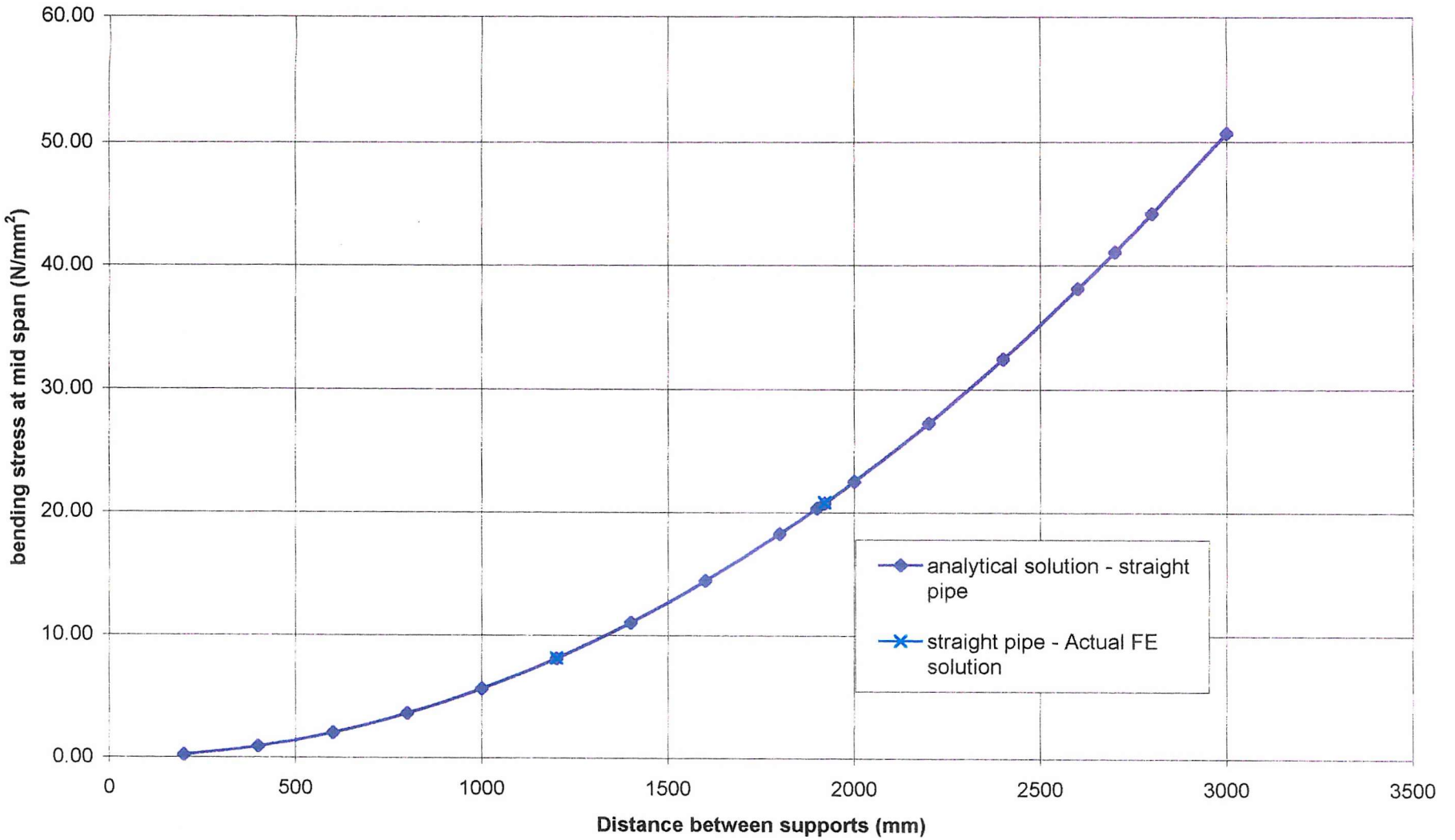

Figure 4.36: Graph comparing theoretical calculation to Lusas results for UDL.

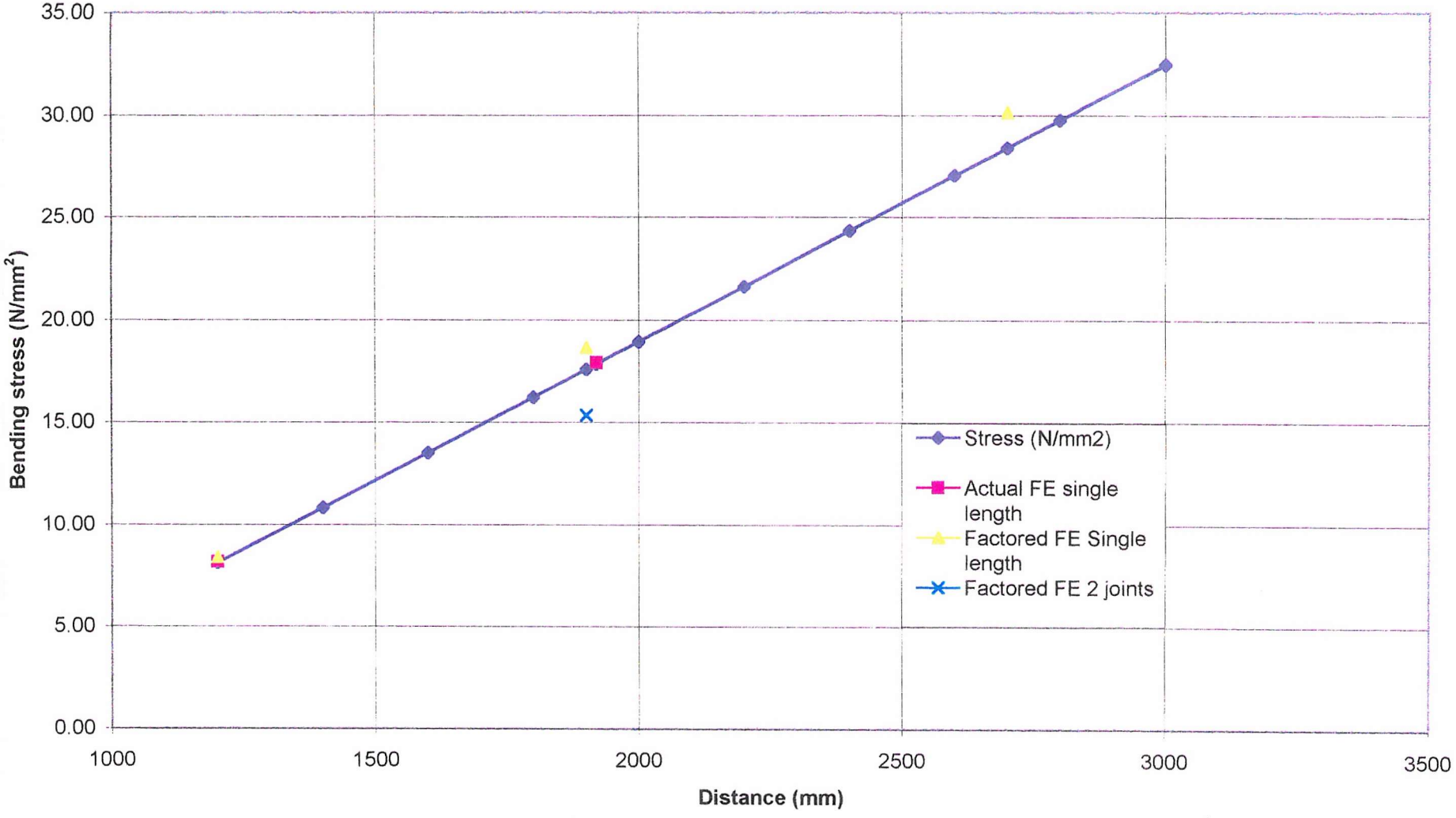

Figure 4.37: Graph comparing theoretical results with Lusas for a fixed width load.

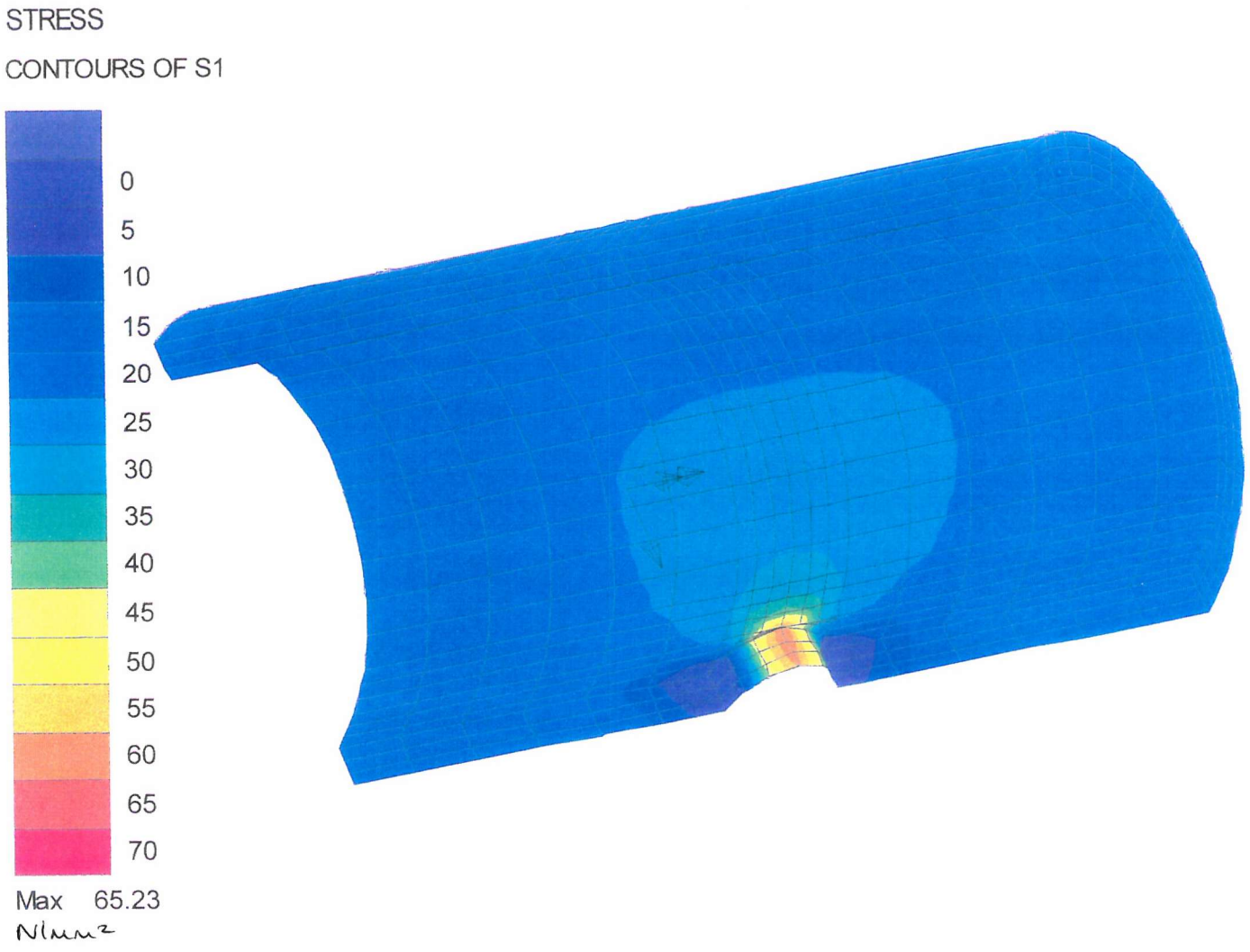

Figure 4.38: Stress contour plot of temperature loading in pipe length with ferrule hole, using S1.

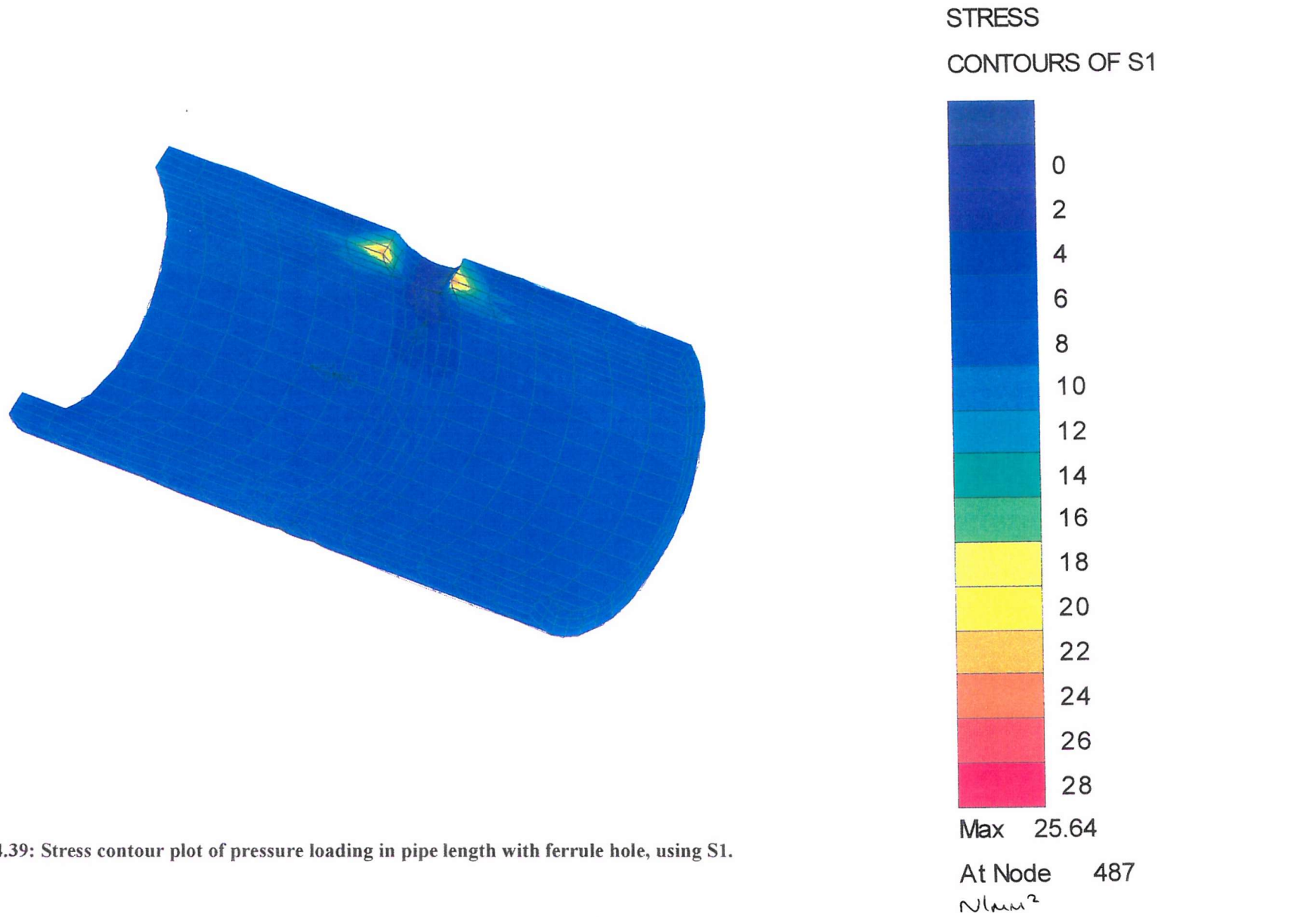

Figure 4.39: Stress contour plot of pressure loading in pipe length with ferrule hole, using S1.

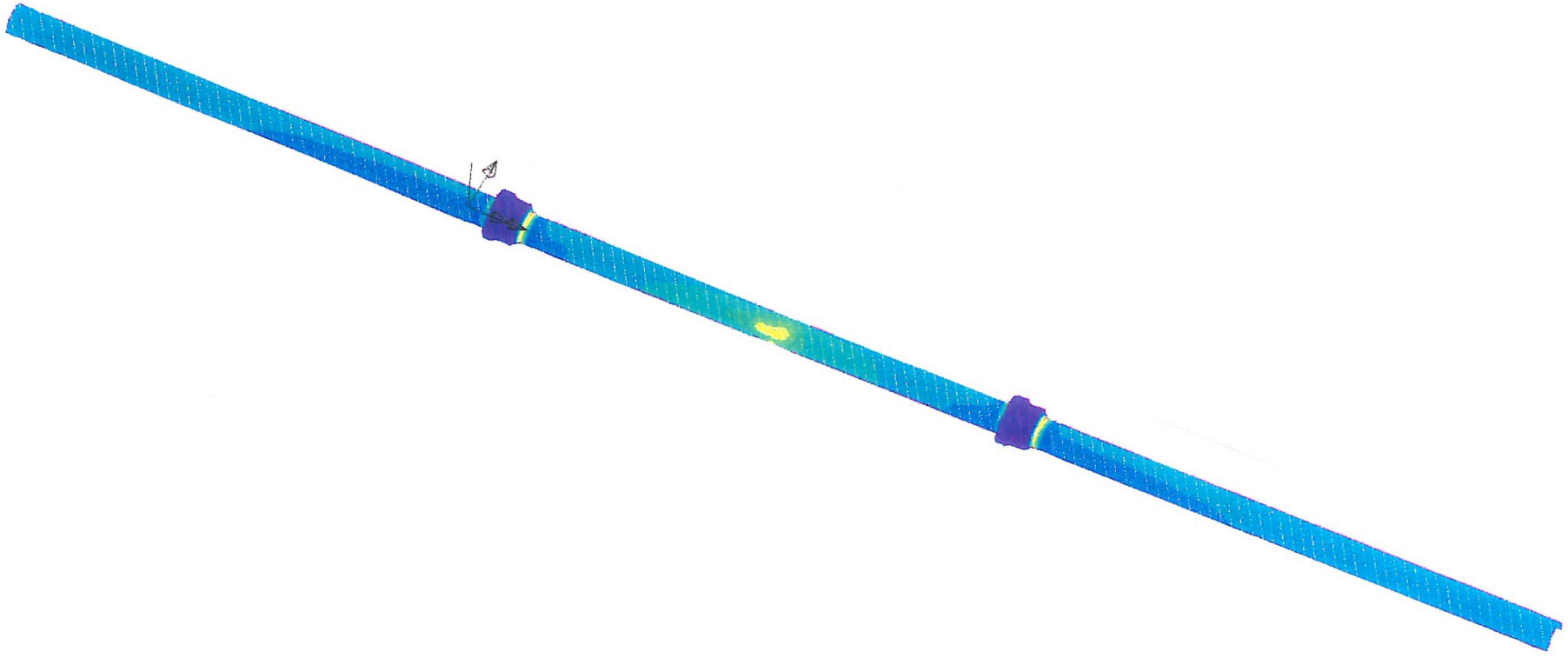

Figure 4.40: Stress contour plot for combination loads without spring supports, using S1.

CHAPTER 5

DISCUSSION

CHAPTER 5 - DISCUSSION

Discussion of the results of this research has been split into three sections; literature review, experimental work and finite element analysis. However, the results from each part of the research link together, and it is the aim of this chapter to make these connections clear, in order to draw overall conclusions from this work

5.1 Literature Review

Water leakage is a growing and on going concern. It causes environmental as well as financial problems for both the water companies and their customers. Bursts occur all year round but data collected by water companies and information from the literature review show the highest frequency of bursts to occur during the winter months of November through to February. Of these bursts, after normalisation for length of installed pipe, the majority occur on small diameter pipes of 100mm, made from cast iron connected with lead run joints. The failure pattern in these small diameter pipes is frequently that of a transverse fracture. This suggests failure due to bending, axial tension or axial shear. In contrast, large diameter failures generally have longitudinal fractures or blowholes. Cast iron is four times stronger in compression than in tension. Therefore cast iron is much more likely to fail in tension which can result from bending or contraction, giving a transverse fracture. The majority of small diameter pipes show this type of fracture, suggesting failure due to bending or axial tension.

Buried pipes have a variety of loads acting upon them. The main load conditions reported in the literature are due to internal pressure; in-pipe water temperature changes; frost loading; traffic loading; ground movement due to nearby trenches; tree roots; soil desiccation; and normal soil loading. In conjunction with these conditions, pipes also suffer from material defects and corrosion, which reduce their section and their strength. The literature review has shown that failure mechanisms have generally been investigated in isolation. For instance, the loading effects of frost heave and traffic loading have been investigated individually and never as a combined loading. Previous research has been unable to establish any of these load conditions as being the sole or primary failure mechanism for buried water pipes. This suggests that the pipes are failing due to two or

more load conditions acting together. It appears that until this thesis, the effect of combined loading conditions on buried water pipes had not been investigated.

Much of the previous research has also been carried out in countries that are subjected to severe winters (e.g. Canada or the north USA). The findings from these investigations may not be relevant for UK pipe bursts, as the UK does not suffer from extreme winter conditions. Because the UK does not suffer from severe frost, it can be expected that water pipes used within the UK will not experience large frost loads.

The literature review revealed anecdotal evidence to suggest that a change in in-pipe water temperature may be a contributory factor causing pipes to burst due to constraint of the surrounding soil and/or their joints, but until this thesis no research had been carried out to explain this mechanism. The behaviour of joints would have a significant effect on the workings of this mechanism. Rigid joints would allow the cast iron to be subjected to axial stress when the pipes contract and expand, since only a long length of pipe can develop sufficient anchorage in the soil. However, the pull out force of cast iron lead-run joints for small diameter pipes until now had not been investigated. It was postulated that changes in in-pipe water temperature (20°C) in pipes fixed by rigid joints could contribute significantly to the axial tensile failure of the pipe section. This type of failure could explain the transverse fractures found on many burst pipes.

In-pipe water temperature can vary as much as 20°C in a year, if fed by a surface water source in the UK (Figure 5.1). Ground water remains mostly constant at 12°C all year round. Data from the Greater London area has shown that pipes fed by surface water areas have a higher number of bursts than pipes fed by ground water (Figure 5.2). Again no past research had been carried out to further develop this theory.

Even with all the various load conditions acting on a pipe, it might be expected that a perfectly made pipe, laid according to the correct specifications would have a design strength capable of supporting these loads without failure. A perfectly made pipe would have a design tensile strength of approximately 110N/mm^2. If laid well, the combined loads of traffic, frost, internal pressure and in-pipe water temperature do not produce stresses that reach half the design strength. However, cast iron pipes have been manufactured and laid for well over a century and generally do not follow these

conditions. Manufacturing processes introduce defects that produce weak points throughout the pipe length. Transportation and installation processes can create further weaknesses in the pipe through lack of care and attention. Most cast iron pipes still in use today are likely to be between 50-100 years old. The strength properties of these pipes are likely to have decreased compared to the original strength when brand new. The strength of cast iron is very dependent on its chemical constituents. As a result of the different foundries used, the range of strength properties of cast iron can not be known and only estimated, and therefore the strength properties of cast iron might be much lower than anticipated. It is suggested that pipes need to be weakened for them to fail by today's loading mechanisms. This weakening may result from corrosion, graphitisation and/or defects from manufacture, transportation and installation.

5.2 Joint Experiments

As noted above, in-pipe water temperatures are known to vary by as much as 20°C in areas fed by surface water. A 20°C change in temperature in a fixed length of cast iron pipe (coefficient of thermal expansion = $11*10^{-6}$), will induce a stress of some 24N/mm^2 (c.f. yield stress of cast iron 110N/mm^2) in its pipe length. This is equivalent to a tensile load of 8.4 tonnes for a 120mm outside diameter, 100mm inside diameter pipe.

Joints tested were found to show a wide variation of pull out forces, between 37kN and 80kN (Figure 5.3). Half the joints tested were heavily corroded while the other half still showed the tar coating on the surface of the pipe to be intact. It could be seen from the results that the more corroded joints (Embelton #2, #3 & #4) required larger forces to produce significant displacement, compared to non-corroded joints (Embelton #5, #6 & #7). It is thought that the tar coating gave the joint some lubrication to enable the joint to be pulled apart easily. These non-corroded joints started pulling apart as soon as the load was applied (Figure 5.4), suggesting that these joints would not set up significant tensile axial stresses if loaded slowly. The corroded joints required much larger forces to initiate displacement, which would increase the chance of the pipe failing, due to the increase in axial stress in the pipe section.

The results from these experiments suggest that it is only corroded cast iron pipes connected with lead-run joints that are susceptible to failure from changes in in-pipe water temperature. Non-corroded pipes are able to contract and expand with the water temperature changes, therefore eliminating the build up of axial stress. It appears that one solution to network replacement would be to target pipes in corrosive soil areas and replace these pipes first. However, as seen in the Embelton road site, the soil can change from corrosive to non corrosive in a matter of a few metres, even along the same line of pipe.

5.3 Lusas 3D model experiments

As discussed in Chapter 4, section 4.3, results from the finite element program were sensitive to the geometric shape of the joint. A smooth "S" profile (Figure 5.5) produced higher stresses than one without (Figure 5.6) due to a lack of material supporting the re-entrant corners. This is discussed in greater detail in section 5.3.1. Different mesh shapes using both pentahedral and hexahedral elements, did not alter the results significantly, which showed that the model was not mesh-type dependent. A quadrilateral mesh with eight nodes per element was chosen for the final model, as the model was limited by the memory capacity of the computer. The longitudinal stress was integrated with respect to the cross sectional area, and the resultant force checked for equilibrium errors. This check showed the finite element result to differ from the theory by 10%, on the pipe lengths and all other sections except the bell face, where the results differed by 20%. These differences are likely to have resulted from the averaging effect of the integration points.

5.3.1 Load only models

Initial model runs were carried out on a single cast iron pipe with no joints, and a length of 2m. A temperature load was applied to the model uniformly by assigning the temperature change to all of the nodes in the model. The pipe was held rigidly at both ends with fixed supports in the axial direction. This scenario simulated the pipe being stressed by impeded contraction. The outside surface of the pipes was supported uniformly by spring supports and loaded uniformly by soil load. The maximum stress was found in the axial

direction, with the vertical stress and stress in the horizontal direction near to zero. For a 20°C temperature drop the maximum axial stress was equal to 24N/mm^2, which is just over 1/5 of the anticipated tensile strength of cast iron. This result shows that a perfectly made pipe laid according to the correct specifications is unlikely to fail under a temperature load of 20°C, as suggested by the findings in the literature review.

The straight pipe length model was then increased to a 2 joint model with three pipe lengths. The same support conditions and loading conditions were applied. It was found that the longitudinal stress in the straight pipe length section of the model equalled that in the single pipe length model (24N/mm^2, see Figure 5.7). This showed the Lusas program to be consistent suggesting the mesh, geometry, material, support and load conditions to be appropriate. The maximum stress was not found at mid span however, but rather at the joint. The two re-entrant corners inside and outside the joint showed high maximum axial stresses, of about 54N/mm^2. As pipes do not frequently fail at the joints, these stresses may be unrealistically high. This is evident when all the loading and defect conditions are applied to the same model, as the maximum stress occurs at mid span and not the joint (Table 5.1). The mesh at the re-entrant corners is not very refined for the geometry it is trying to model, therefore there are likely to be many errors involved in the calculation of stress at these points. Re-entrant corners are natural stress raisers, and the material at these points is almost twice as thick as elsewhere on the pipe, perhaps because of experience. The Victorians would likely have improved the performance of their water pipes by trial and error, resulting in over engineering of the joint profile. This area of the joint would need to be studied in greater detail to achieve a more appropriate mesh, etc. Since this Thesis was about establishing which loading mechanism and defect type had the most effect on cast iron pipes, further analysis was not carried out to refine the mesh in these areas.

The temperature load was then removed from the model and an internal pressure load added. This pressure load was applied as a surface load and assigned to all the internal surfaces of the pipe. Pressure loading was analysed as the literature review highlighted the fact that internal pressure causes failure when pressures surges occur in weakened pipes, causing blowouts. The finite element analysis showed that a typical operating pressure at the higher end of the scale recommended for use (14 bar = 1.4N/mm^2) has little effect on the stresses within the pipe. The longitudinal stress was minimal (1.8N/mm^2)

while the vertical stress and horizontal stress were equal, but only reached a maximum of 7.7N/mm^2. The major principal stress showed a maximum of 7.7N/mm^2. This suggests that pipes with no defects are certainly not failing due to internal pressure. When the single pipe length model was replaced with the 2 joint model, at mid span the maximum stress was found to be the same.

Pressure loading was then removed and frost and traffic loading were analysed. The amount of frost loading to be applied to each model (single pipe length model and 2 joint model) was calculated from the findings of Fielding and Cohen (1988). This equated to 0.03N/mm^2 vertical stress on the surface of the pipe crown, when the frost reached a depth of 0.75m. A simple finite element analysis was carried out to model the application of a tyre load to the surface of a multilayer and single layer elastic system. The soil conditions modelled were uniform clay for the whole of the depth and multilayers of asphalt (E=1700MPa), gravel (E=820MPa), sand (E=480MPa) and clay (E=65.5MPa). The uniform soil condition gave the highest pipe stresses, as would be expected. At 0.7m depth, the stress that the pipe crown would experience if buried could be approximated to 0.033N/mm^2 along a length of 1.2m (Traffic Load(1)) Figure 5.8. The multilayer soil model gave a load of 0.012N/mm^2 at the same depth, less than half that of the uniform soil model (Traffic Load(2)). As the maximum traffic loading and frost loading values were similar, it was decided that for simplicity to model the traffic load alone, since the frost loading would give similar results.

A simple plain pipe length model with no spring supports or soil load conditions had traffic load(1) assigned to the upper half of its surface along a length of 1.2m. This model was run and the results compared to those from theoretical calculations for simple beam bending. The results compared very well with the finite element results lying directly on the theoretical curve. The single pipe length model used for previous load conditions was then used with traffic load(1). These finite element results, as well as those for the 2 joint model results showed reasonable agreement with the analytical results (Figure 5.9), with differences of only 3% and 12.6%. This was considered a reasonable result especially as the theoretical calculations did not take into consideration soil load and gravity etc., which the finite element models did. When a uniform load was used along the whole length of pipe and the supports were 1.2m apart, the bending stress was about 8N/mm^2. This increased to about 21N/mm^2 when the supports were placed 1.9m apart.

The 2 joint model was run with two joints 1.9m apart but from site reports (Appendix A), joints average 2.5m apart. From the theoretical curve in Figure 5.9, supports a distance of 2.5m apart could be expected to produce a bending stress of about 35N/mm^2. But when the load remains at a fixed width of 1.2m and the supports are moved further apart (Figure 5.10), the stress when the supports are at 2.5m is only about 26N/mm^2.

Point support conditions were only used on frost and traffic load models, as these are the only loading conditions that would be affected by them. Past research has concentrated on the effects of these two mechanisms individually. The past research fails to show that either mechanism is capable of failing pipes on their own. The results from the finite element analysis confirms this, with the highest stress only reaching 15.4N/mm^2 with traffic load(1) and only when the pipes were not supported uniformly and are buried in a uniform clayey soil. The stress is reduced to 6.7N/mm^2 with traffic load(2), if the pipes were buried under a road, making the traffic load less damaging than internal water pressure. When these results are extrapolated to a joint spacing of 2.5m, the stress can increase to 26N/mm^2 when using traffic load(1).

Both the single pipe length model and 2 joint model, when uniformly supported with spring supports and loaded with traffic or frost loads, stresses are minimal. The maximum principal stress at mid span was only about 1N/mm^2. This confirms conclusions drawn from the literature review that traffic and frost loadings do not cause pipe failure if the pipe is installed correctly and well bedded.

The stresses found underneath the point supports were higher than those at mid span. Theoretically these stresses should be infinite but the finite element results can not accurately simulate such a condition. Therefore the results at the point supports have been ignored, as they do not reflect reality.

When traffic load(1) and frost loading for the UK were combined, the net effect on the mid span stress was increased to approximately 32N/mm^2 (Table 5.1). This value is considerably less than the ultimate tensile strength used for this pipe model, therefore unlikely to fail it.

5.3.2 Defect conditions

Three defect conditions were modelled to simulate changes in the material properties and geometric properties of the model. These were corrosion, a slag void and thin wall (graphitisation – causes the pipe wall to thin). Both corrosion and a thin wall changed the geometric properties of the model, while the slag void reduced the strength properties of the model. Each defect had the effect of increasing the stresses resulting from each load condition.

When a corrosion pit was inserted into the temperature loaded 2 joint model, the mid span stress increased from 24N/mm^2 to 43N/mm^2 (Figure 5.11), showing the corrosion pit to have a stress increase factor of 1.79. The high stress concentrated around the outline of the pit, reaching a peak at the maximum depth of the pit. Comparing this stress to the ultimate tensile strength expected for cast iron, the stress reached about 50% of the ultimate. If this pit had increased diameter or depth the stress increase would be wider spread and greater, which would result in a transverse fracture starting at the pit. The research has shown that many transverse fractures do show initiation at a corrosion pit (unpublished data). The addition of the slag void defect had the least impact on the stress results out of the three defects modelled, multiplying stresses by a factor of 1.28. The stress at mid span increased to 30.7N/mm^2 (Figure 5.12). It can further be seen from Figure 5.12 that the stresses in the actual area of the slag void are low, causing the rest of the material to take on additional stress due to arching around the slag void area. The introduction of a thin wall (graphitisation) increased the stress to 34.1N/mm^2, increasing stresses by a factor of 1.42 (Figure 5.13). The increase in stress was uniform across the thickness of the pipe section as would be expected. If all defects were used together with temperature loading, the resultant stress at mid span would be 78N/mm^2, which is approximately $^3/_4$ of the estimated maximum strength of good quality cast iron. This increases the chance of transverse fracture in the pipe section, where the majority of the failures are found.

When internal pressure loading models were subjected to the individual defects, the multiplying effects of each were similar to those found for temperature loading. The multiply effects were 1.06, 1.37, and 1.57 for slag void, thin wall and corrosion respectively (Table 5.1). Even so, the stresses due to internal pressure were still not

significantly high. It is suggested that pipe failures due to internal pressure only happen when the pipe is highly corroded and operational error has occurred causing abnormally high pressures for a short time period. These could perhaps be lessened by targeting and replacing corroded pipes and tightening up on operational procedures.

If a corrosion pit is introduced into the pipe structure, the net effect of the two loading conditions rises to 50N/mm^2, which is half the maximum strength in this case. If all three defect conditions are present the net effect is increased to 68N/mm^2, bringing the total stress close to the approximate maximum strength of the pipe (110N/mm^2), hence closer to failure. These results would then suggest that pipes buried in corrosive soil, close to or under busy roads with no appropriate bedding are more likely to fail with transverse fractures due to bending.

5.4 Summary

When all loads are used in combination the principal stress at mid span increases to 155N/mm^2 which is greater than the expected ultimate tensile strength of the material. This increase in stress is shown as a stress concentration in the middle of the pipe length at the invert. This would imply that the pipe fails due to bending in the pipe length, producing a transverse fracture, as is so often seen. The major component of this stress was the water temperature loading, which would only apply if the joints were corroded and could not displace without significant force.

Many of the above mentioned load conditions rely on defects to increase stresses to the level necessary to fail the pipe. The defect producing the largest increase is corrosion. The joints exhumed for the experimental tests had the ground they lay in described. For the Embelton road joints the trench appeared to be of two main types of soil, changing from one to the other half way along the trench. Joints#1, #2, #3, #4 were found to be corroded and were buried in the clay end of the trench. Joints#5, #6, #7 were less corroded and lay in the sandy end of the trench. Clay has a corrosive effect, weakening the pipe with corrosion pits and thinning the pipe walls, but also leads to locking of pipe joints.

The material properties of an old buried cast iron pipe will not be the same as a new pipe. The design strength values do not take into consideration the corrosion factor, the slag void factor and any other defects introduced by transportation and installation procedures. The average multiply effects of the defects are 1.06, 1.37 and 1.71 for slag void, thin wall and corrosion pit respectively (Table 5.1).

To reduce pipe bursts or to predict burst locations, the state of the pipe and its joints as well as internal pressure and in-pipe water temperature need to be monitored. Provided that operational procedures are in place and followed correctly, internal pressure effects can be reduced. Pipes fed by surface water could be changed to a mix of ground water and surface water, eliminating the risk of a large temperature drop. If this is not possible the water temperature could be monitored and pipes associated with risky areas of corrosive ground and large traffic loads could be targeted for replacement.

Analysis	Pipe type	Loading	Support	Defect	Major principal stress (N/mm^2)		Position of stress at mid section	Factor effect
					Bell & spigot	mid span		
1	2 Joints	Temperature	Uniform with end supports	None	54.46	24.06	Uniform	-
2	2 Joints	Temperature	Uniform with end supports	Slag void	54.44	30.72	At defect	1.28
3	2 Joints	Temperature	Uniform with end supports	Thin wall	52.55	34.13	At defect	1.42
4	2 Joints	Temperature	Uniform with end supports	Corrosion pit	54.48	43.18	At defect	1.79
5	2 Joints	Pressure	Uniform with end supports	None	8.71	7.72	In bell and spigot	
6	2 Joints	Pressure	Uniform with end supports	Slag void	8.87	8.05	At defect	1.06
7	2 Joints	Pressure	Uniform with end supports	Thin wall	11.56	10.56	At defect	1.37
8	2 Joints	Pressure	Uniform with end supports	Corrosion pit	12.15	12.15	At defect	1.57
9	2 Joints	Traffic load (1)	Uniform with end supports	None	1.01	0.65	At bottom inside pipe	
10	2 Joints	Traffic load (1)	Point supports only	Slag void	24.59	14.44	At bottom outside pipe	0.94
11	2 Joints	Traffic load (1)	Point supports only	Thin wall	23.98	21.44	At bottom outside pipe	1.4
12	2 Joints	Traffic load (1)	Point supports only	Corrosion pit	28.91	25.77	At defect	1.68
13	2 Joints	Traffic load (1)	Point supports only	None	24.64	15.36	At bottom inside pipe	
14	2 Joints	Traffic load (2)	Point supports only	Slag void	16.00	6.46	At bottom outside pipe	0.96
15	2 Joints	Traffic load (2)	Point supports only	Thin wall	15.28	8.71	At bottom outside pipe	1.3
16	2 Joints	Traffic load (2)	Point supports only	Corrosion pit	19.20	12.09	At defect	1.8
17	2 Joints	Traffic load (2)	Point supports only	None	15.98	6.70	At bottom inside pipe	
18	2 Joints	Combination	Point supports only	All	112.00	155.00	At concentration of defects	
	Average factor results	**Corrosion**	**Slag Void**	**Thin Wall**				
		1.71	**1.06**	**1.37**				

Table 5.1: Summary of maximum stress results for all models.

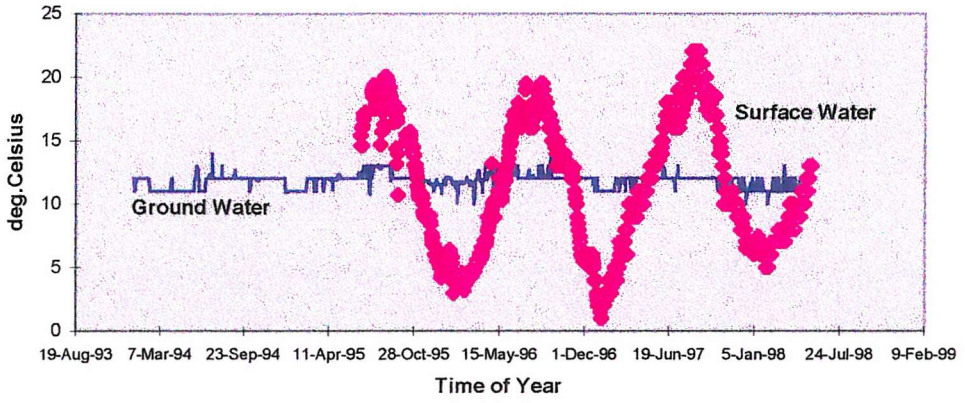

Figure 5.1: Graph to show water temperature variance over several years (courtesy: Thames Water Utilities).

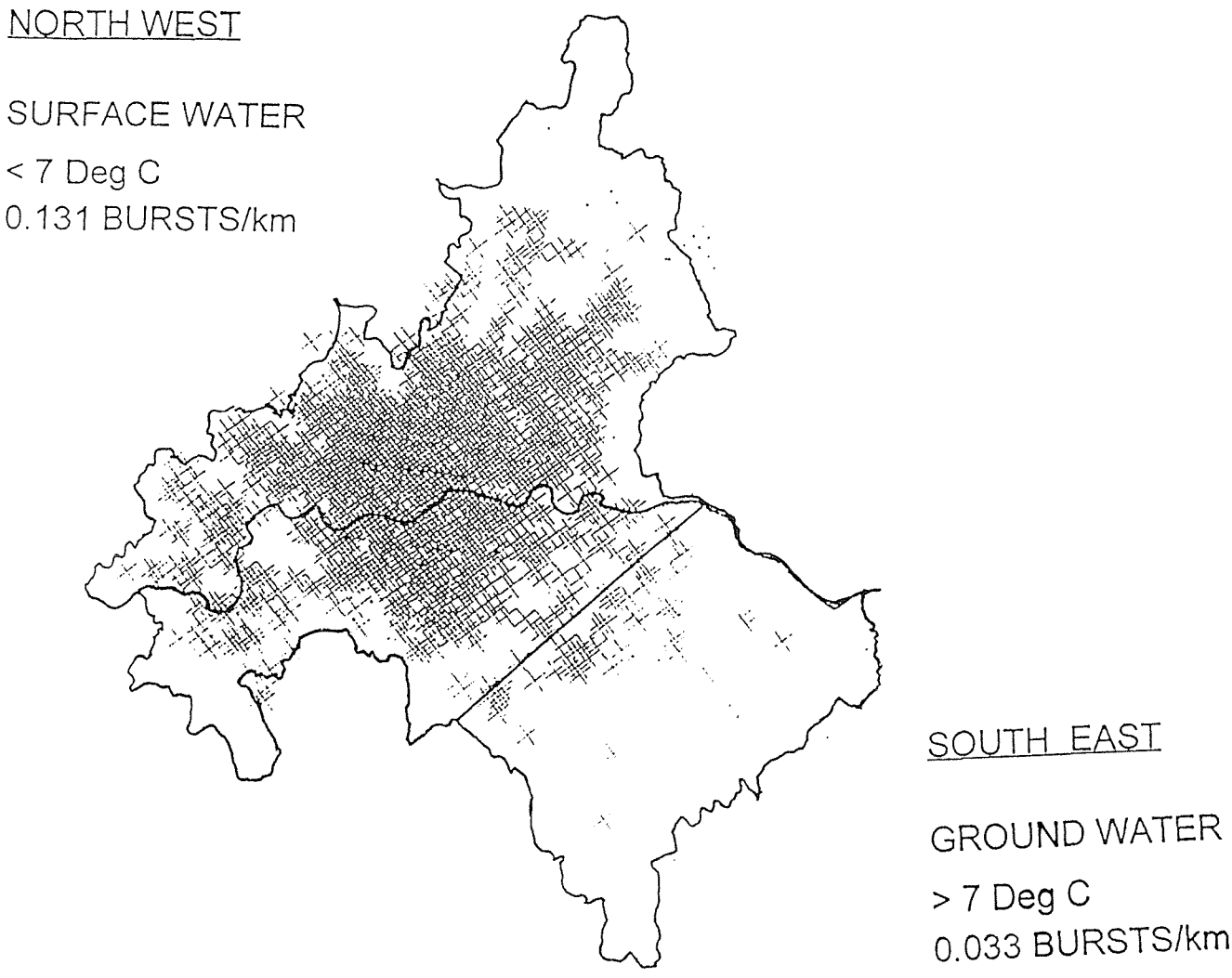

Figure 5.2: Regional map to show spread of pipe bursts to concentrate in surface water sourced areas (courtesy: Thames Water Utilities).

Figure 5.3 Average displacements of Embelton Road Joints, showing initial slip points

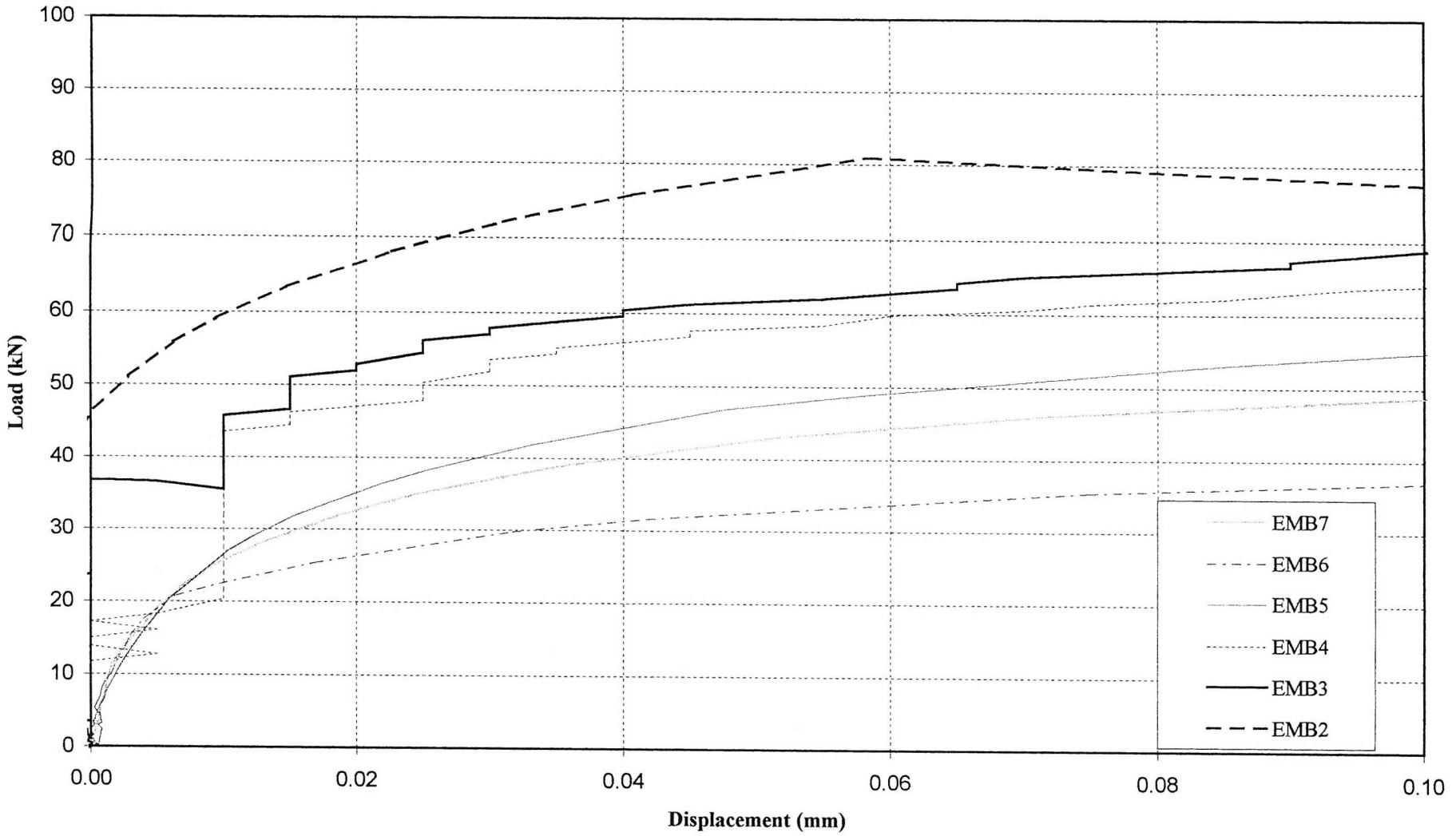

Figure 5.4 Graph to show initial slip loads for Embelton Joints 5, 6 & 7

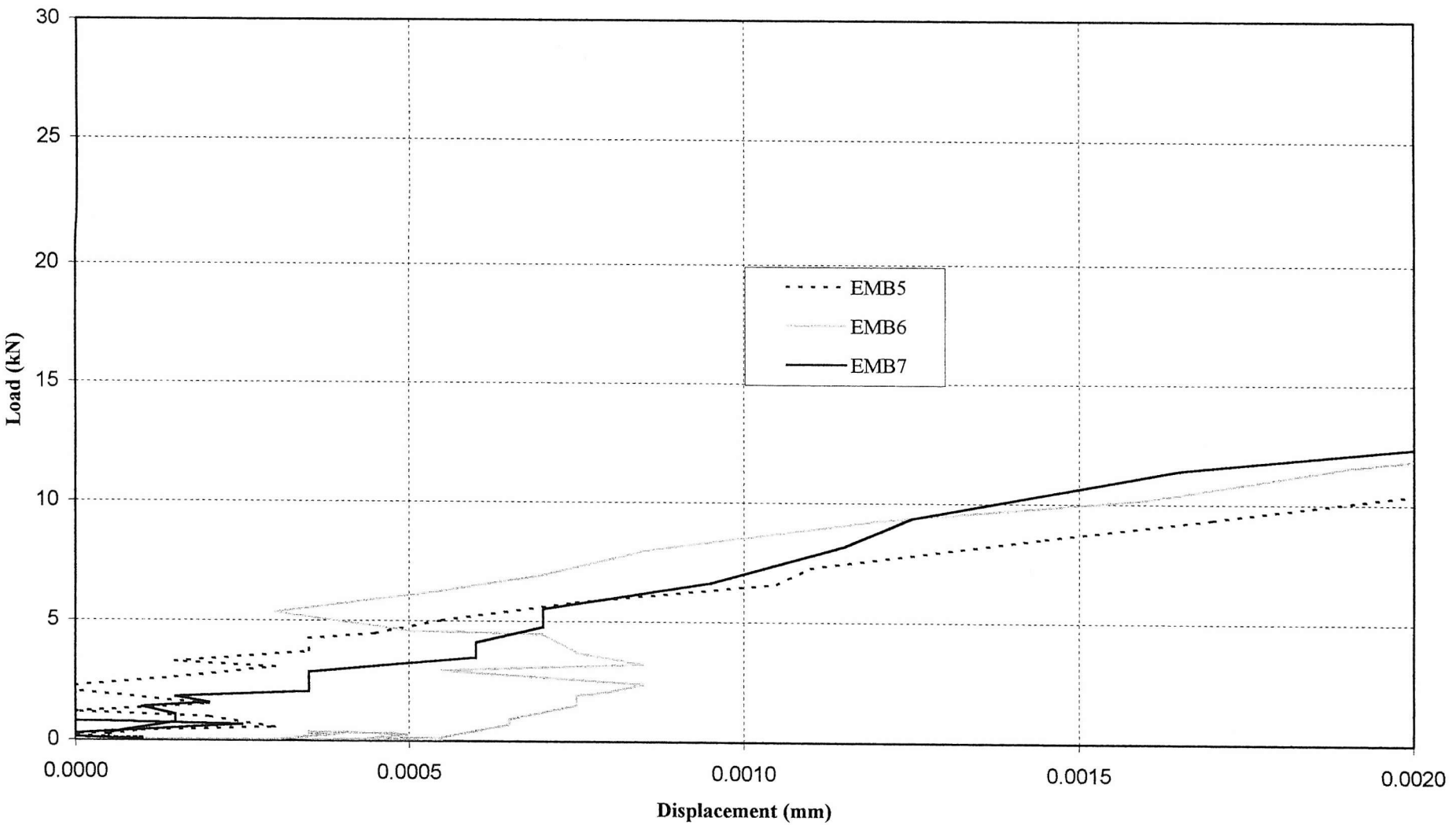

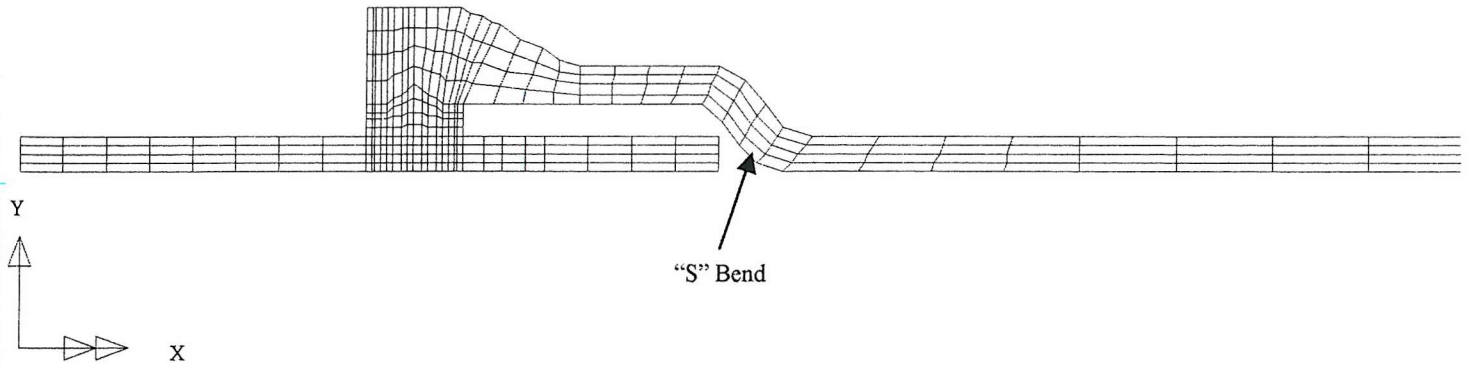

Figure 5.5: Profile of "S" bend joint

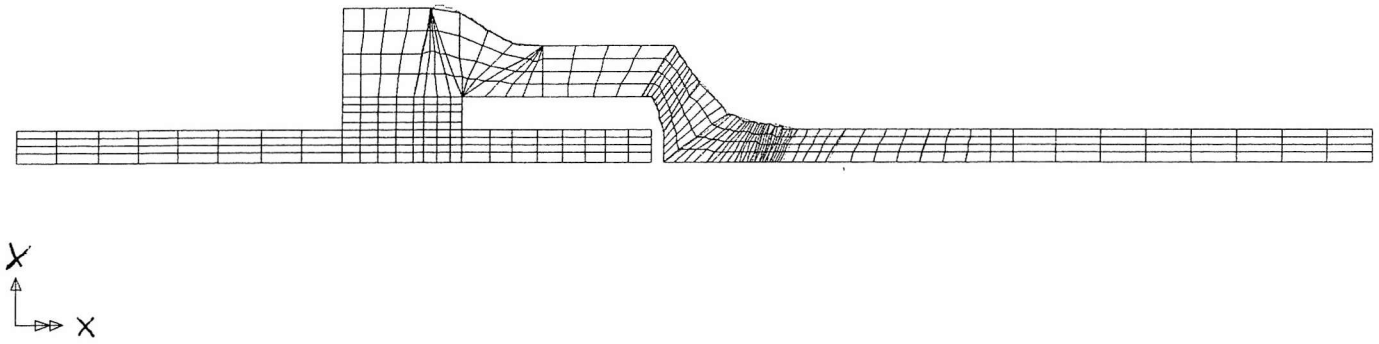

Figure 5.6: Profile of joint showing a 90° corner

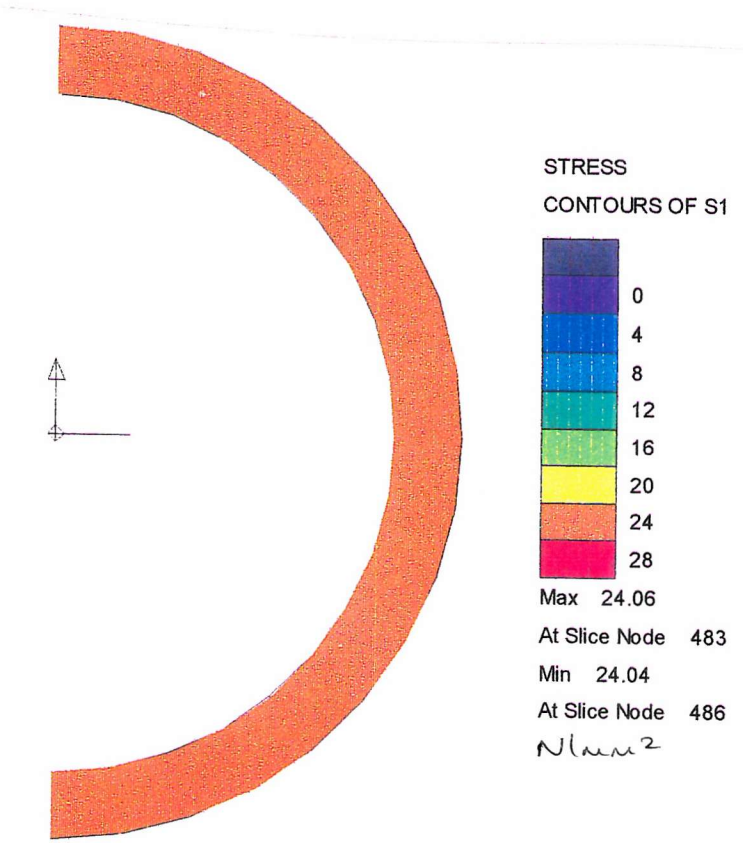

Figure 5.7: Section of 2 joint model showing stresses at mid span with temperature loading only.

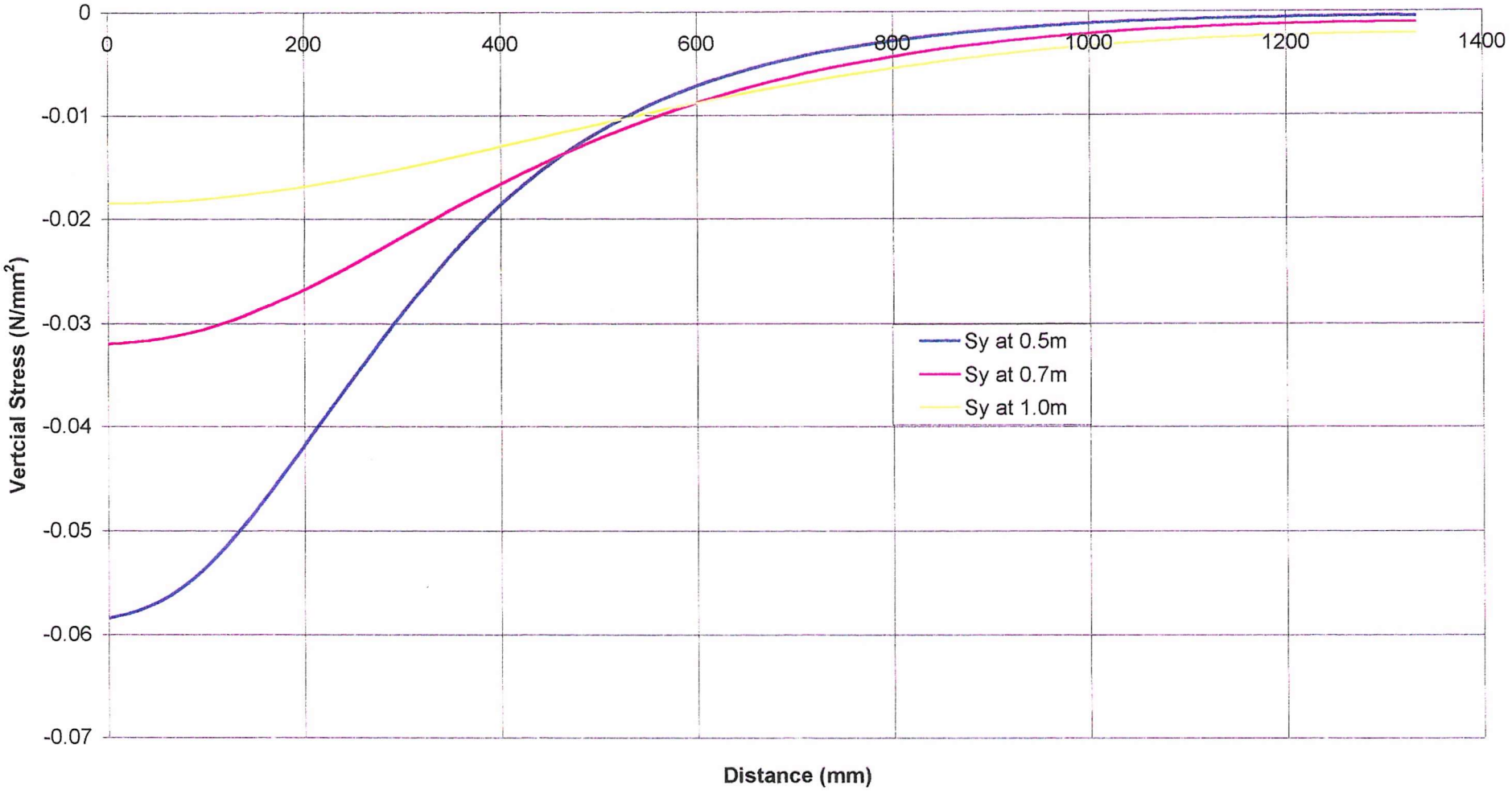

Figure 5.8: Stress distribution results of soil model.

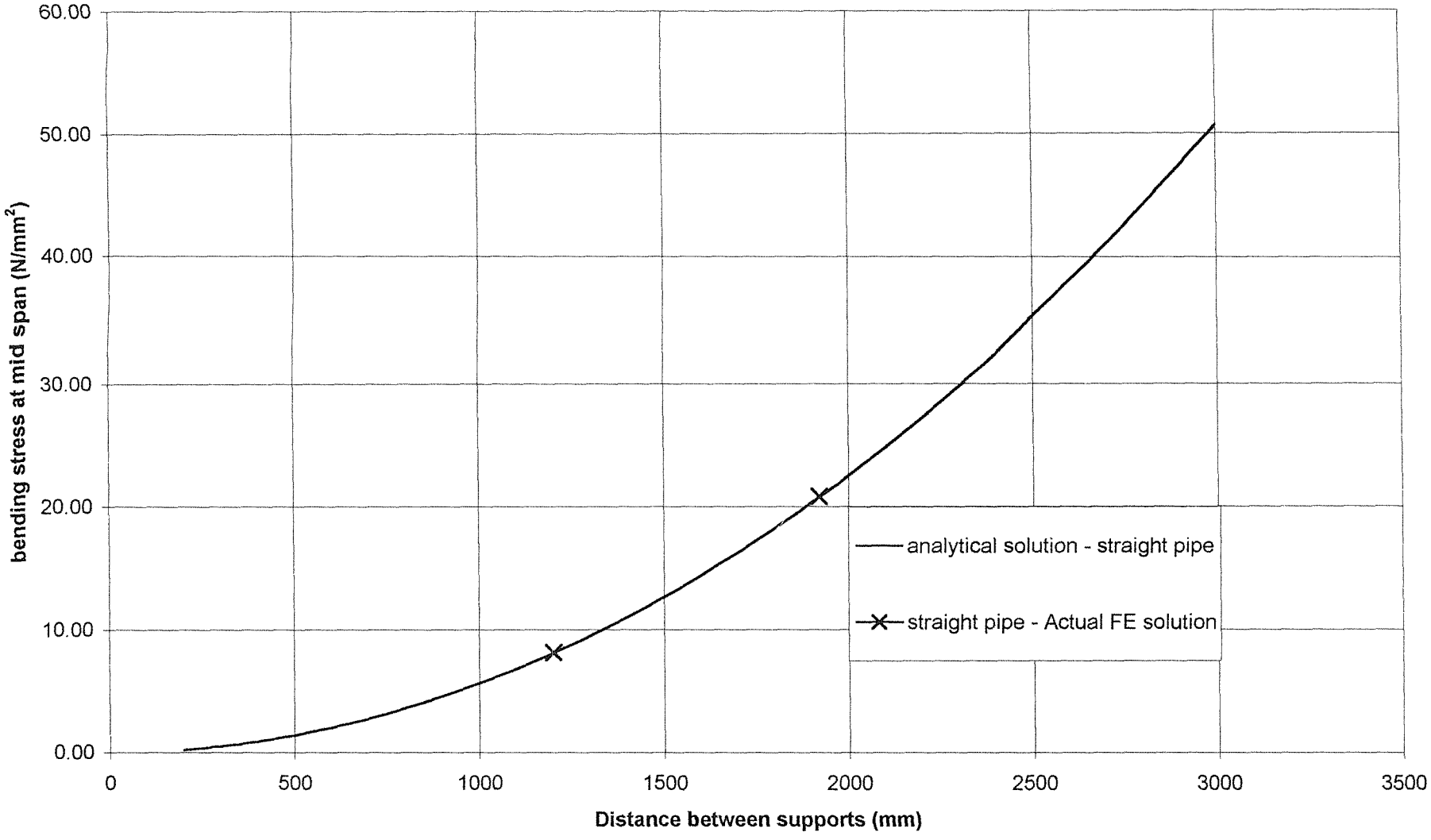

Figure 5.9: Graph comparing theoretical results with Lusas of a plain pipe length of approx. 3m, with uniform distributed, vertical load equivalent to 0.033N/mm^2.

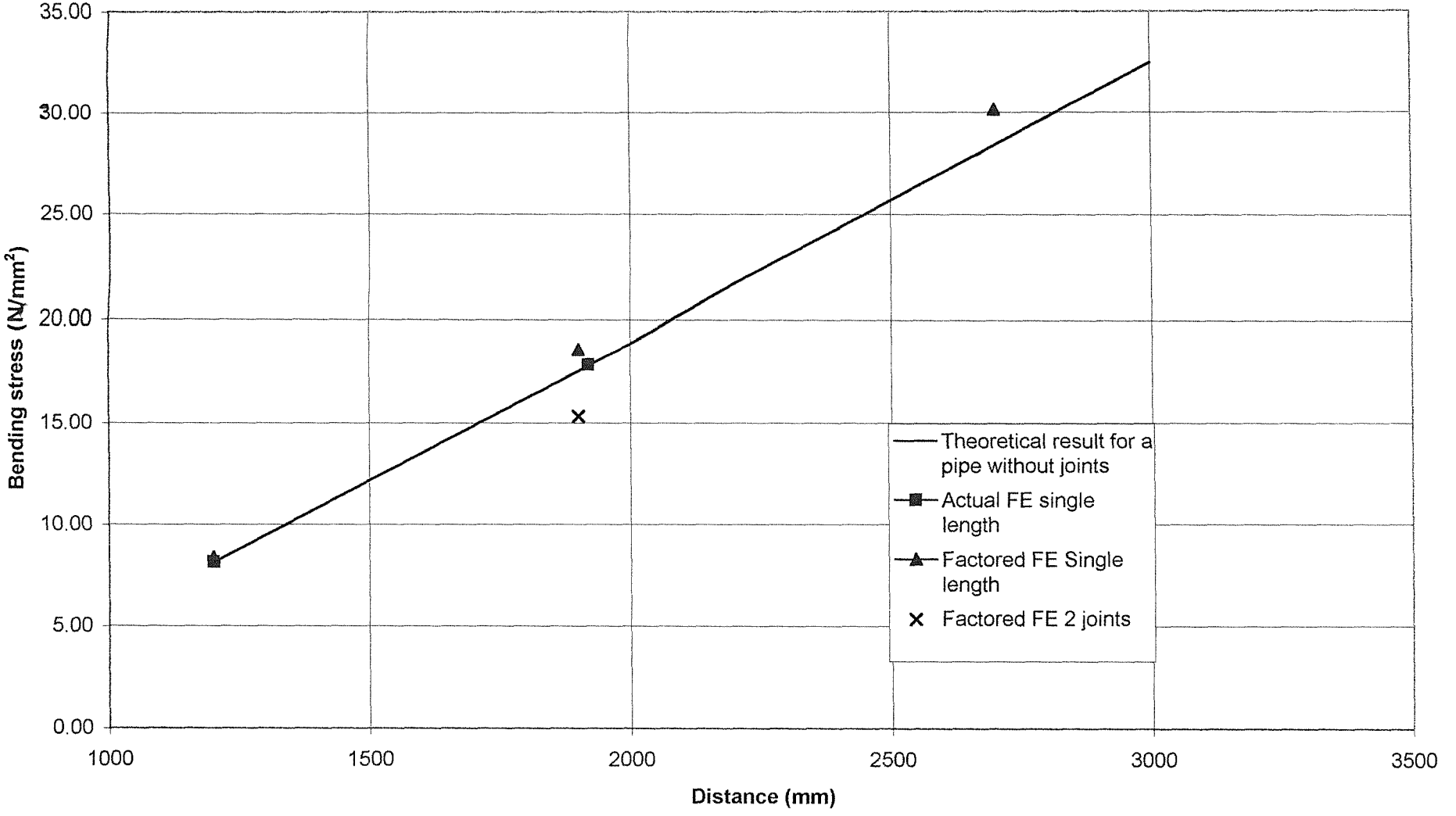

Figure 5.10: Graph comparing theoretical traffic load results to finite element results, of plain pipe pipe length approx. 3m and a 2 joint model, using a fixed width, vertical load equivalent to 0.033N/mm^2.

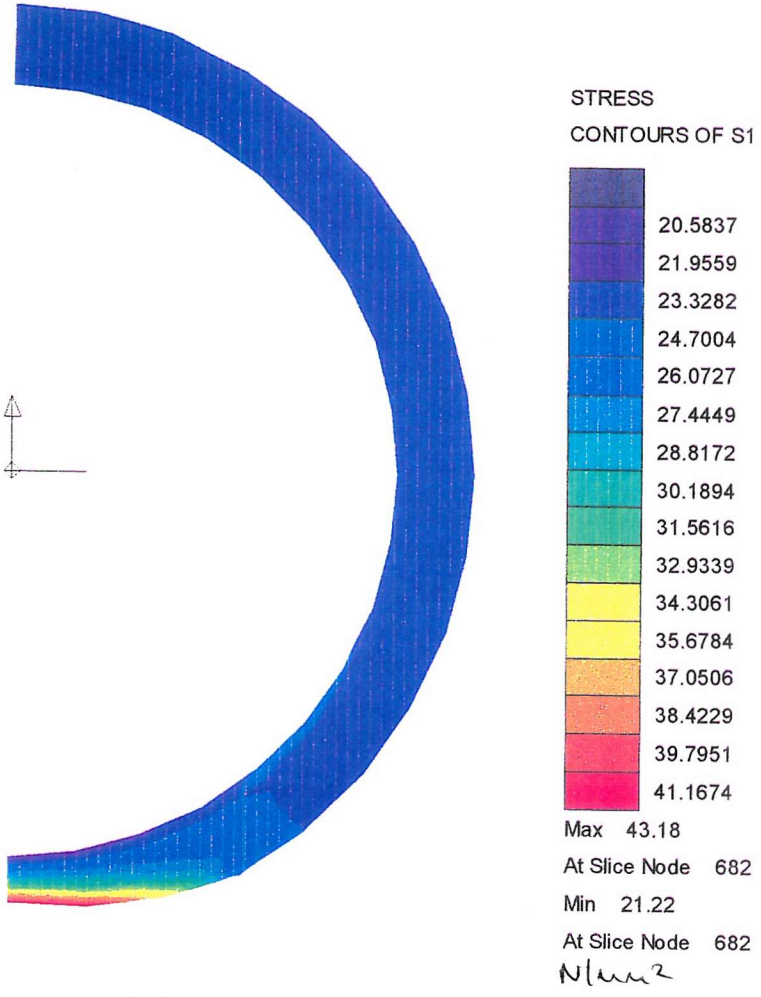

Figure 5.11: Section of 2 joint model showing stresses at mid span with temperature loading and Corrosion pit.

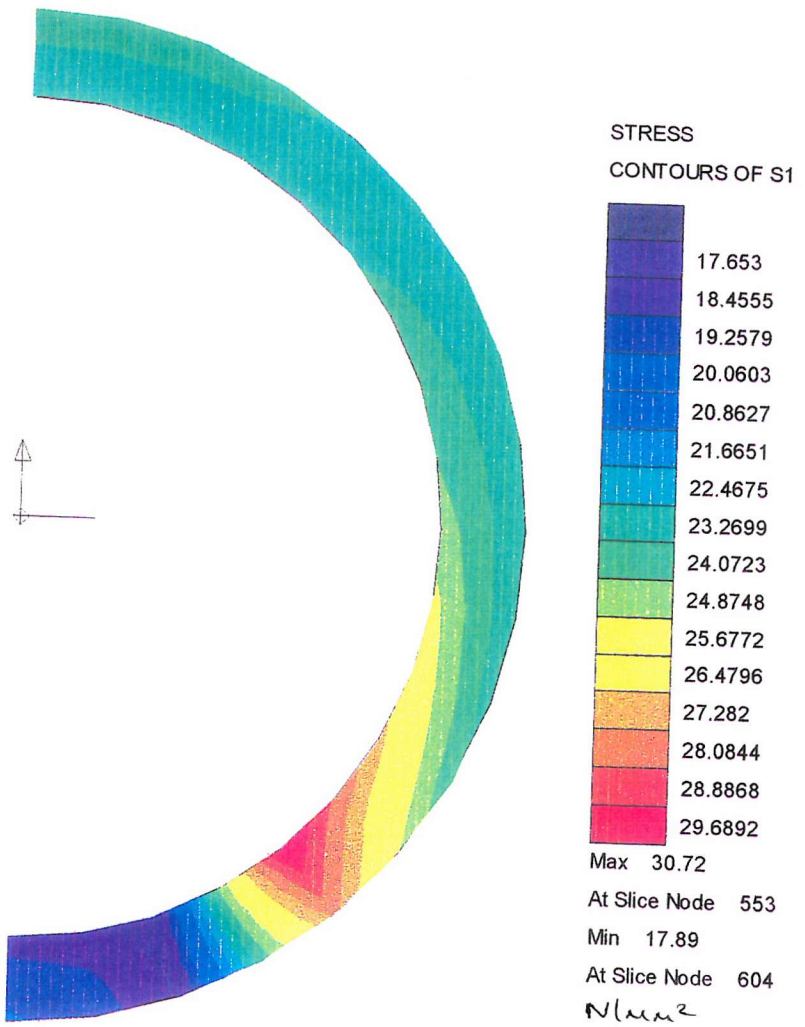

Figure 5.12: Section of 2 joint model showing stresses at mid span with temperature loading and slag void.

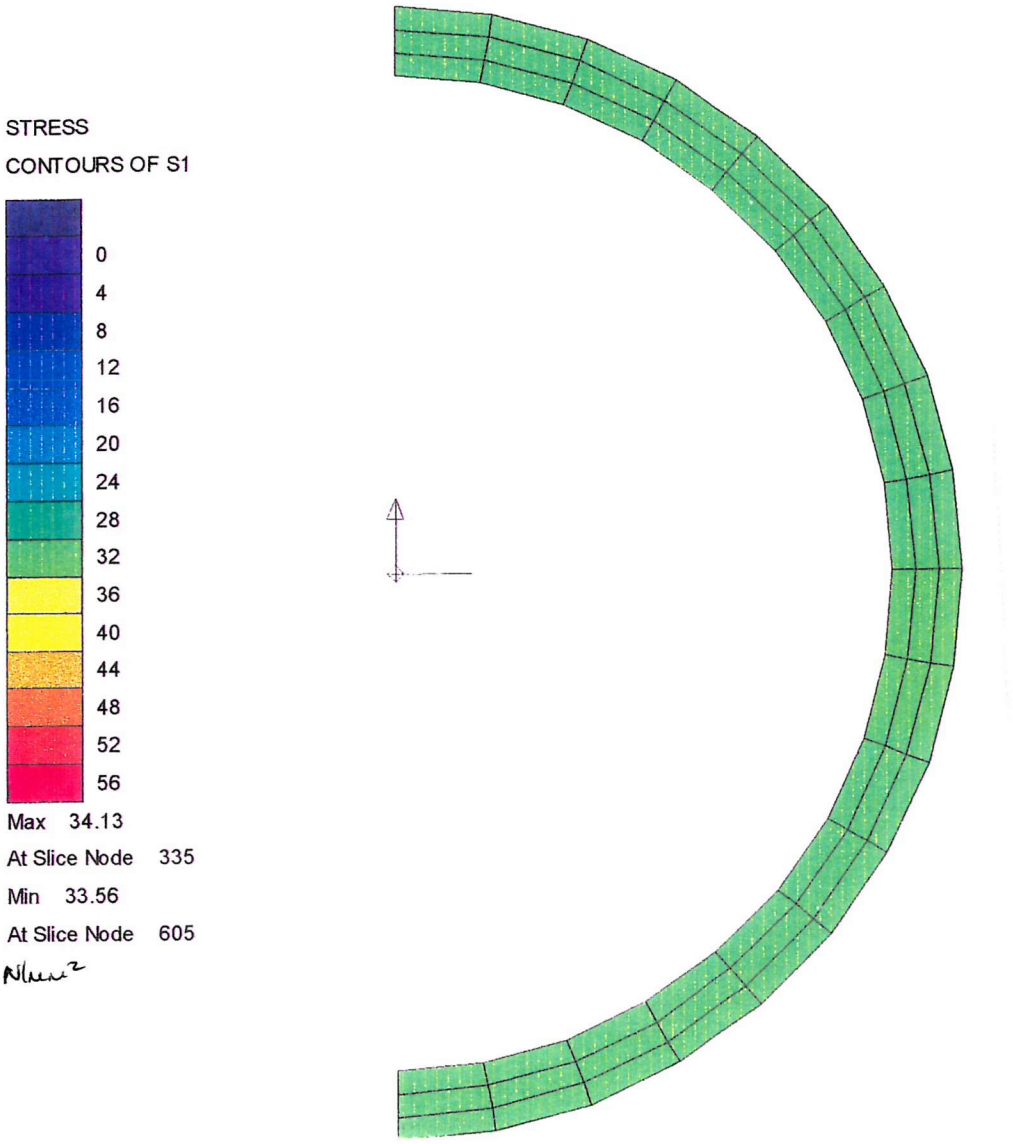

Figure 5.13: Section of 2 joint model showing stresses at mid span with temperature loading and thin wall.

CHAPTER 6

CONCLUSIONS

CHAPTER 6 - CONCLUSIONS

The large majority of bursts occur on small diameter cast iron pipes with lead run joints. These bursts frequently occur during the winter months and the type of fracture found is transverse, probably as a result of bending and/or axial tension. In contrast, large pipes fracture longitudinally or with blow holes resulting from excessive corrosion.

Historically, failure mechanisms research has been conducted in isolation. The combined effects of frost load, traffic loads, internal pressure and in-pipe water temperature have never been properly investigated for their combined loading effect.

In countries with more severe climates, frost loading has been shown to be a major factor in causing pipe failures. But in the UK the climate is far less severe, such that even during a severe winter significant loading would be unusual.

Cast iron pipes have inherent weaknesses introduced during the manufacturing processes, transportation and installation. Pipes that were laid between 50 and 100 years ago would not have had the benefit of precision pipe laying techniques of today. Weaknesses also result from corrosion, which can be caused in various ways.

Anecdotal evidence suggests that in-pipe water temperature fluctuations contribute to pipes bursts. Previously no research had been carried out to explain this mechanism. It has been shown that joint behaviour has a significant effect on the stresses induced by in-pipe water temperature changes. Rigid joints cause pipes to be subjected to high axial stress. This type of failure mechanism explains the transverse fractures on many pipes. In-pipe water temperature can vary by 20°C throughout the course of a year if fed by a surface water source. Pipes fed by surface water have a high number of bursts compared to pipes fed by ground water.

An in-pipe water temperature drop of 20°C can create an axial tensile stress of 24N/mm^2 (equivalent to a tensile load of 84kN) if the pipe if rigidly fixed. Joints tested had a wide variation of pull out forces (20-95kN). Corrosion encrusted joints required greater loads to produce significant displacement. Therefore corrosion encrusted jointed pipe that experience temperature fluctuations of up to 20°C are subjected to significant additional longitudinal tensile stress. The joint experiments were carried out at speeds greater than a pipe would experience for an equivalent temperature drop. Non-corroded joints are liable to give less resistance when pulled apart slowly as the tar coating would creep.

Traffic and frost loadings cause minimal stress when a pipe is laid in good bedding. Poor bedding is likely to produce point supports underneath the bell of the joints, as this point of the pipe has the larger diameter and hence meets the ground first. This condition increases the stress significantly. If the pipes are laid under uniform soil only, which has clay properties, the stress induced by severe traffic loading reaches 15N/mm^2 at mid span, when the joints act as point supports. If this same pipe is then laid under a road with point supports the induced stress reduces to 6N/mm^2. This clearly shows that pipes buried underneath roads have greater protection from failure compared to pipes buried under soil only. However, neither condition induces sufficient stress to cause pipe failure.

One average the effects of slag voids, thin wall and corrosion pits led to local increases in stress of 1.06, 1.37 and 1.71 times respectively, suggesting that defects play a significant part in pipe failure.

The overall results for the various load conditions showed that none of the load conditions were sufficient to fail the pipe on their own, even with uneven supports and defects present. Temperature loading alone could fail the pipe if the pipes were severely weakened. This weakening needed to consist of a corrosion pit, slag void and wall thinning due to graphitisation. Stresses induced by traffic load(1) and UK frost loading increased by 23 times when uneven supports were used. A combination of pressure; traffic; soil; frost and temperature loads was required, along with defects, to fail a cast iron pipe with lead run joints.

Of all the loading mechanisms described only in-pipe water temperature could come close to failing the pipe on its own, and then only with defects present. All of the other loading

conditions need the defects and other loading conditions working in combination. When all loads and defects are combined the maximum principal stress at mid span is 41% higher than an approximate ultimate tensile strength of 110N/mm^2. These stress levels are more than needed to fail the pipe with a transverse fracture, due to either bending or axial load.

RECOMMENDATIONS FOR FURTHER WORK

Research

Pipe and joint models should be analysed using finite element software that is capable of modelling soil properties realistically.

Once real soil behaviour can be modelled more closely, shear effects on the pipe and joint should be investigated.

If possible, further pipes and joints should be exhumed and tested to further quantify that corroded joints lead to locked joints and ultimately high longitudinal tensile loads.

Practice

The water feeding the distribution pipes should be mixed ground water and reservoir water. This could reduce the maximum temperature drop in in-pipe water temperature throughout the year, reducing the tensile loads.

Pipes fed by surface water, laid in corrosive soils should be rehabilitated first, or put on a "red alert" list when the water temperature drops below a certain level during the winter months. Water temperature should be monitored continually to predict the timing of burst events, to reduce the impact.

REFERENCES

REFERENCES

Arnold, G E (1960). "Experience with main breaks in four large cities", Annual Conference, Bal Harbour, Fla, *Journal AWWA,* 1041-1059

Argemt, C F, Furness, R R (1985). "Corrosion in Soils", *Soil Survey Technology,* Monograph 13, 135-146.

Bahmanyar, H, Edil, T (1982). "Cold weather effects on underground pipeline failures", *Proceedings on the American Society of cold regions science technology,* (2), 579-593.

Biddle, P G (1983). "Patterns of soil drying and moisture deficit in the vicinity of tress on clay soils", *Journal of Geotechnics*, 33 (2), 107-126.

Boden, W (1936). "A handbook on cast iron pipes and joints", *The Stanton Iron Works Company Limited.*

Bruzzone, A, Lonardo, P, M (1996). "Experimental assessment of traffic loads and cast iron joint escapes", *Trenchless Technology Research, Criteria for Gas Network Renewal*, 11 (2), 43-51.

Building Research Establishment (1980). "Low-Rise Buildings on Shrinkable Clay Soils: Part1 & 2", Digest 240 & 241.

Carder, D R & Taylor, M E (1983). "Modelling the effects of traffic loading on small-diameter rigid pipelines", *Pipe & Pipelines International*, March-April, 12-14.

Carder, D, R, Taylor, M, E, Pocock, R G (1982). "Response of a pipeline to ground movements caused by trenching in compressible alluvium", *TRRL*, (Report 047), 1-25.

Carder, D, R, Taylor, M, E (1983). "Response of a pipeline to nearby deep trenching in boulder clay", *TRRL*, (Report 1099).

Casson, D, R (1984). "Settlement loading on buried pipelines", *Ground Movements and Structures*, 3, 80-93.

Chard, B, M Symons, I F (1982). "Trial trench construction in London Clay: A ground movement study at Bracknell", *TRRL*, (1051).

Ciottoni, A S (1983). "Computerized data management in determining causes of water main breaks: The Philadelphia Case Study", *International Symposium on Urban*

Hydrology, Hydraulics and Sediment Control, University of Kentucky, Lexington, Kentucky, July 25-28, 323-329.

Clark, C M (1971). "Expansive-soil effect on buried pipe", *Journal AWWA*, 63, 424-427.

Crofts, J, E, Menzies, B, K, Tarzi, A, I (1977). "Lateral displacement of shallow buried pipelines due to adjacent deep trench excavations", *Geotechnique*, 27 (2), 162-179.

Driscoll (1983). "The Influence of Vegetation on the Swelling and Shrinking of Clay Soils in Britain", *Geotechnics Journal*, 33, 93-105.

Edil, T, Bahmanyar, G, H (1983). "Stresses in buried conduits caused by freezing front", *Cold Regions Science and Technology*, 8, 129-137.

Eigenbrod, K, D (1996). "Effects of cyclic freezing and thawing on volume changes and permeabilities of soft fine-grained soils", *Canandian Geotechnical Journal*, 33, 529-537.

Elder, W R (1966). "Movement in soils", *Journal AWWA*, 58 (11), 1462-1464.

Esparza, E (1985). "Trench Effects on blast-induced pipeline stresses", *Journal Geotechnical Engineering*, 3 (10), 1193-1210.

Fielding, M B & Cohen, A (1988). "Predicting Pipeline Frost Load", *Journal AWWA*, 80 (11), 62-69.

Fry, R, H, Rumsey, P, B (1983). "Prediction and control of ground movement associated with trench excavation", *Water Pollution Control*, 82 (2), 151-163.

Fry, R, Rumsey, P, B (1984). "Ground movements caused by trench excavation and the effect on adjacent buried pipelines", *Water Research Centre*, July, TR195.

Gagnebin, A, P, Millis, K, D, Pilling, N, B, (1949). "Ductile Cast Ion - A new engineering material", *The Iron Age*, 163, 77-84.

Habibian, A (1994). "Effect of Temperature Changes on Water-Main Breaks", *Journal of Transportation Engineering*, 120 (2), 312-321.

Howe, M (1984). "The protection of buried plant from adjacent deep works", *Ground Movements and Structures*, 3, 62-79.

Jarvis, M G (1997). "Factors affecting the risk of corrosion to iron pipes and pipe fracture potential in London", *Cornfield University*, 81/4096.

Jarvis, M G & Hedges, M R (1994). "Use of soil maps to predict the incidence of corrosion and the need for iron mains renewal", *Journal of Institution of Water and Environmental Management*, 8 (1), 68-75.

Jones, R (1983). "A review on buried pipelines and causes of failures with particular reference to ground movement", *MSc at the University of Surrey*, June.

Kassiff, G & Zeitlen, J G (1962). "Behaviour of pipes buried in expansive clays", *Journal of the Soil Mechanics and Foundations Division,* April, 133-148.

Kartvelishvili, N A (1983). "Internal Pressure Fluctuation in Pressure Pipes", *Hydrotechnical Construction*, 17 (8), 396-400.

Kirby, P, C (1978). "Internal corrosion and loss of strength of iron pipe", *Water Research Centre*, Paper 10.

Konrad, J (1994). "Frost heave in soils: concepts and engineering", *Canadian Geotechnical Journal Sixteenth, Canadian Geotechnical Colloquim*: 31, 223-245.

Konrad, J, Morgenstern, N R (1980). "A mechanistic theory of ice lens formation in fine-grained soils", *Canandian Geotechnical Journal*, 17, 473-486.

Kottmann, A (1995). "Pipe damage due to air pockets in low pressure piping", *3R International* 34, 11-16.

Lackington, D W & Burrows, B L (1994). "Criteria to determine appropriate levels of investment for rehabilitation", *Water Supply*, 12 (3/4), 21-32.

Legett, D (2000). Telephone communication with an ex-Ministry of Transport Inspector.

Lehmann, J A (1964). "Control of Corrosion in Water Systems", *Journal AWWA,* 56 (8), 1009-1018.

MacLeod, R D & Cram, W J (1996). "Forces Exerted by Tree Roots", *Arboriculture Research and Information Note,* 134/96/EXT.

Molin, J (1985). "Influence of frost action on load exerted on buried pipe", *Proceedings - International Conference on the advances in ground pipeline engineering*, 554-565.

Monie, W D, Clark, C M (1974). "Loads on underground pipe due to frost penetration", *JAWWA*, 66 (6), 353-358.

Morris, R E (1967). "Principal Causes and Remedies of Water Main Breaks", *Journal AWWA*, 54 (7), 782-798.

Morrogh, H, Williams, W (1947). "Graphite formation in cast irons and in nickel-carbon and cobalt-carbon alloys", *Journal of the Iron and Steel Institute*, 155, 321-371.

Needham, D & Howe, M (1981). "Why gas mains fail", *Pipeline Industry,* July.

Needham, D & Howe, M (1984). "Why pipes fail III", *Pipeline Industries Guils Scottish Branch Meeting,* 5 April, E419.

New, B M (1985). "The effect of increasing traffic on cast iron pipe breakage rates", *TRRL*, WP/2/85.

Newport, R (1981). "Factors Influencing the Occurrence of Bursts in Iron Water Mains", *Aqua*, (3) 274-278.

Needham, D, Howe, M (1979). "Why Pipes Fail", *Gas Research and Technology Centre*, E244 November.

Newman, G P, Wilson, G W (1997). "Heat and mass transfer in usaturated soils during freezing", *Canadian Geotechnical Journal*,34, 63-70.

Nixon, J F (1992). "Discrete ice lens theory for frost heave beneath pipelines", *Canadian Geotechnical Journal*, 29, 487-497.

O'Day, D K (1982). "Organising and analysing leak and break data for making main replacement decisions", *Journal of the American Water Works Association*, 74 (11), November, 588-594.

Page, J (1966). "Impact tests on pipes buried under roads", *RRL* Report 35.

Palmer, A C (1976). "Ice lensing, thermal diffusion and water migration in freezing soil", *Journal of Glaciology*, 6 (47), 681-694.

Peck, L, O'Neill, K (1997). "Frost penetration in soil with an inclusion of sand: dependence on soil moisture content and winter severity", *Canadian Geotechnical Journal*, 34, 368-383.

Prior, J C (1935). "Investigation of Bell and Spigot Joints in Cast Iron Water Pipes", *The Engineering Experiment Station, The Ohio Stata University*, January.

Rajani, B, Zhan, C & Kuruoka, S (1996). "Pipe-Soil Interaction Analysis of Jointed Water Mains", *Canadian Geotechnical Journal*, 33, 393-404.

Rajani, B, Zhan, C (1996). " On the estimation of frost loads", *Canadian Geotechnical Journal*, 33, 629-641.

Reedy, D R (1966). "Corrosion in the water works industry", *Materials Protection*, 5 (9), 55-59.

Rude, L C (1983). "Load Reductions on Buried Rigid Pipe", *Journal of Transportation Engineering*, 109, (1) January, 107-123.

Rumsey, P B (1982). "Construction and control of ground movement", *Ground Engineering*, 15 (8), p12-13..

Rumsey, P B, Dorking, C (1984). "The prediction of ground movement and induced pipe strain caused by trench excavation", *Ground Movements and Structures*, 3, 24-49.

Rumsey, P B, Cooper, I (1982). "Ground movements associated with trench excavation and their effect on adjacent services", *Ground Engineering*, 15, (2), 28-30, March.

Rumsey, P B, Cooper, I, Kyrou, K (1982). "Ground movement and pipe strain associated with trench excavation", *Restoration of sewerage systems, Thomas Telford Ltd, London,* 105-115.

Salvadori, M G, Singhal, A (1977). "Strength characteristics of jointed water pipelines", *National Science Foundation*, Report No. IR-3 June.

Scully, J C (1983). "Corrosion: Aqueous Processes and Passive Films", *Treatise on Materials Science and Technology,* Academic press, London, 23.

Singhal, A (1984). "Behaviour of jointed ductile iron pipelines", *Journal of Transportation Engineering*, 110, (2), 235-250

Singhal, A C (1980). "Experiments on Pipeline Joints", *Pressure Vessels and Piping Conference, San Francisco, California, ASME*, 12-15 August, 5-5.

Singhal, A ,Taylor, R, Deatherage, D (1979). "Experimental investigation of joint failure in pipelines", *Society for experimental stress analysis, San Francisco, California,* 20-25 May, 48-48.

Smith, W H (1976). "Frost Loadings on Underground Pipe", *Journal AWWA*, 68, (12), 673-674.

Stalder, F (1983). "The corrosion behaviour of cast iron pipes", *Aqua* (4) 183-187.

Stanton (1936). "Cast iron pipe: its life and service", *The Stanton Ironworks Company Limited,* 1-118.

Stanton, Stavelet (1997) "Stanton pipes", Stanton pipes (canada) limited.

Stanton PLC (1996). "Resistance of buried ductile iron to frost", *Product Design & Development Department Engineering Laboratory, PDD/N/96/2.*

Svensson, G (1990). "Methods of Identification and the Recording of Data", *Water Supply,* 8 (1/2), 163-166.

Symons, I F, Chard, B, Carder, D R (1981). "Ground movements caused by deep trench construction", *Restoration of sewerage systems*, June, 87-104.

Taber, S (1930). "Freezing and thawing of soils as factors in the destruction of road pavements", Public Roads, 11 (6), 113-132.

Takagi, N, Shimamura, K, Nishio, N (1984). "Buried pipe responses to adjacent ground movements associated with tunnelling and excavations", *Ground Movements and Structures*, 3, 97-112.

Taki, H, O'Rourke, D (1984). "Factors affecting the performance of cast iron pipe", *Geotechnical Engineering*, Report 84-1.

Talbot, A N (1926). "Strength properties of cast iron pipe made by different processes as found by tests", *Journal AWWA*, 16 (1), July, 1-44.

Tester, R E Gaskin, P N (1996). "Effect of fines content on frost heave", *Canadian Geotechnical Journal*, 33, 678-680.

Toombs, A F, McCaul, C Symons, I F (1982). "Ground movements caused by deep trench construction in an urban area", *TRRL* (1040), 1-8.

Tsytovich, N A (1975). *The Mechanics of Frozen Ground.* McGraw Hill Book Company.

Valliappan, S, Raja-Sekar, H L (1984). "Stability of buried pipes due to adjacent excavations", *Ground Movements and Structures*, 3, 50-61.Upshil, P (2000). Telephone communication with HGV driver.

Wettering, L A (1985). "Reusing Power Plant Cooling Water to Reduce Main Breaks", *Journal AWWA*, 77, (11), 42-52.

Yie, G G (1968). "Frost heaving in soils and the breakage of cast iron mains", *Institute of gas technology*, IIT centre, September (ID-4-7), 1-67.

Yevjevich, V, Starosolszky, O (1998). "Controversies between water resources development and protection of the environment", *Journal of Hydraulic Research*, 36 135-138.

Yoder, E J (1959). *Principles of Pavement Design*, John Wiley & Sons, INC, NY.

Zhan, C, Rajani, B, (1997). "Estimation of frost load in a trench: theory and experiment", *Canandian Geotechnical Journal*, 34, 568-579.

BIBLIOGRAPHY

BIBLIOGRAPHY

Anon (1995). "Water", *New Civil Engineer*, October.

Anon (1994). "New Light on the "black art " of predicting risk ", *Water Services*, June.

Anon (1980). "Low rise buildings on shrinkable clay soils: part 1", *BRE Digest*, August 240.

Anon (1995). "Pipeline Management", *Surveyor*, 9 November.

Anon (1984). "Water Practice Manuals", *Institution of Water Engineers and Scientists.*

Anon (1990). "Water Composition", *University of Surrey Library.*

Anon. "Corrosion detection and prevention", *Water Services.*

Anon. "Corrosion behaviour", *Properties of Cast Iron.*

Anon. "Pipe and pipelines - Improved production techniques for ductile iron pipe", *Water Services.*

Anand, S C (1974). "Stress distributions around shallow buried rigid pipes", *Journal of Structural Division*, 100 (ST1), 161-173.

Addis, R, R, Whitmarsh, R A (1981). "Relative Damaging Power of Wheel Loads in Mixed Traffic", *TRRL*, No 979.

Akagawa, S, Yamamoto, Y, Hashimoto, S (1985). "Frost heave characteristics and scale effect of stationary heave", *Ground Freezing - edited by Kinosita & Fukuda*, 5-7 August, 137-143.

Andreou, S, Marks, D (1987). "Maintenance decisions for deteriorating water pipelines", *Journal of Pipe Lines*, 7, 21-31.

Andreou, S, A, Marks, D, H, Clark, R, M (1987). "A new methodology for modelling break failure patterns in deteriorating water distribution system: Theory", *Adv. Water Resources*, 10, 2-10.

Andreou, S, A, Marks, D, H, Clark, R, M (1987). "A new methodology for modelling break failure patterns in deteriorating water distribution systems: Applications", *Adv. Water Resources*, 10, 11-20.

Argent, C, J, Furness (1979). "Corrosion in soils monograph 13", *Soil Survey Technology*, 135-146.

Arnold, G, E, Clark, E, J, Remas, G, J, Niemeyer, H, W (1960). "Experience with main breaks in four large cities", *Journal AWWA*, 52 (8), 1041-1059.

Arnold, J M, Todres, H A, Saha, N C (1985). "Alleviating the effects of frost action on gas distribution mains and regulator station piping", *Gas Research Institute*, Final Report, June, project no. 30554-03, 1-173.

Ashton, C (1998). "Modes of pipe failure", *MSC Paper University of Surrey.*

Atkins, R, T (1979). "Determination of Frost Penetration by Soil Resistivity Measurement", *Cold Regions Research and Engineering Lab (Hanover)*,July, Special Report 79/22.

Attewell, P B (1983). "Predicting the dynamics of ground settlement and its derivatives caused by tunnelling in soil", *Ground Engineering*, 15 (8), 13-22.

Azar, J, J, Bomba, J, G, Randolph, V, G (1975). "Pipeline Stress Analysis", *Transportation Engineering Journal*, 101 (TE1) February, 163-169.

Bacon, E, S, Langley, J, F, Roberts, N, P (1973). "Causes of Fractures in Cast Iron Water Mains, 2nd Edition", *The City University*, March.

Bahmanyar, G, H, Harrison, P, J (1985). "Pipelines surcharge by seasonally frozen soils", *Ground Freezing - edited by Kinosita & Fukuda*, 5-7 August, 291-246.

Baldock, B, T (1959). "The Organisation of Waste Detection", *Water and Water Engineering*, November, 509-514.

Banyard, J, K, Bostock, J, W 1998). "Investment planning for Utilities Asset Management", *Proceeding of the Institute of Civil Engineers*, 126 (May), 65-72.

Baracos, A, Hurst, W, D, Legget, R, F (1955). "Effects of physical environment on cast iron pipe", *Journal AWWA*, 47 (12), 1195-1206.

Barry, D, L (1983). "Material durability in aggressive ground", *Construction Industry Research and Information Association (CIRIA)*, 1-63.

Becher, A, E, Bizjak, G, J, Schulz, J, W (1972). "Computer Techniques for water distribution analysis", *Journal AWWA*, 64 (7), July, 410-466.

Benson, C, H, Othman, M, A (1993). "Hydraulic conductivity of compacted clay frozen and thawed in situ", *Journal of Geotechnical Engineering*, February 119 (2), 276-294.

Berggren, W, P (1943). "Prediction of Temperature distribution in frozen soils", *Transactions American Geophysical Union*, 71-71.

Bessey, S, G, Pinero, J, Cubillo, F, Schutte, C, F (1996). "Advances in the economics of leakage control and unaccounted for water", *Water Supply*, 14 (3/4) 487-500 .

Bland, C, E, G (1986). "Analysis of the results of loading tests", *Public Health Engineer,* 14 (1), 43-47.

Bland, C, E, G(1981). "Loads on Buried Rigid Pipes: Recent Research", *Public Health Engineer*, 159-166.

Bocock, C (1997). "An underground movement", *Water Bulletin,* No. 735, 17 January, 8-9.

Boden, J, B, Farrar, D, M Young, O, C. "Standards of site practice - implications for innovation in the design and construction of buried pipelines", *TRRL,* No. 345.

Bolton, J, W (1932). "Some notes on mechanism of deformations in gray iron", *Proceedings of the American Society for Material Testing*, June 32 (2), 477-487.

Booth, G, H, Cooper, A, W, Cooper, P, M (1967). "Criteria of Soil Aggressiveness Towards Buried Metals II, Assessment of Various Soils", *British Corrosion Journal*, 2, (May), 109-115 .

Booth, G, H, Cooper, A, W, Cooper, P, M Wakerley, D, S (1967). "Criteria of soil aggressiveness towards buried metals. I. Experimental methods", *British Corrosion Journal,* 2, (May), 104-108.

Booth, G, H, Cooper, A, W, Tiller, A, K (1967). "Criteria of Soil Aggressiveness Towards Buried Metals III, Verification of Predicted behaviour of Selected Soils", *British Corrosion Journal*, 2, (May), 116-118.

Brennan, G (1978). "A test to determine the bending moment resistance of rigid pipes", *TRRL,* No. 348, 1-19.

Brown, C, B (1967). "Forces on Rigid culverts under high fills", *Journal of the Structural Division ASCE,* 93 (ST5), Oct, 195-215.

Brown, S F (1998). "Developments in pavement structural design and maintenance", *Proceedings of Institute of Civil Engineers Transportation,* 129 (Nov), 201-206.

Brown, S F (1996). "Soil mechanics in pavement engineering", Geotechnique, 46 (3), 383-426.

Bughi, S, Aleotti, P, Bruschi, R, Andrei, G, Milani, G, Scarpelli, G & Sakellardi (1996). "Slow movements of slopes interfering with pipelines: modelling and monitoring", *Pipeline Technology*, 5, 363 – 372.

Butlin, K R, Vernon, W H. "Underground Corrosion of Metals: causes and prevention". *Journal of the Institute of Water Engineers,* 3 (8), 627-637.

Byatt, I (1997). "The sustainable and efficient use of water", OFWAT annual report, June.

Cabrera, E, Andres, M, Planells, F (1995). "Network Maintenance through analysis of the cost of water", *Journal AWWA*, 87 (7), 86-98.

Carder, D R, Nath, P, Taylor, M E (1981). "A method of modelling the effect of traffic on undermined buried pipelines", *TRRL*, 1028.

Carder, D, R, Nath, P, Taylor, M, E (1981). "A Method of Modelling the Effect of Traffic on Undermined Buried Pipelines", *TRRL*, (Report 1028)..

Carder, D, R, Ryley, M, D, Symons, I, F, (1984). "Ground movements caused by deep trench construction in boulder day and their effect on an adjacent service pipeline", *Ground Movements and Structures*, 3 (P3), 5-23.

Casagrande, A (1931). "Discussion, A new frost heave .", *Proceedings of Highway Research Board*, 11,168-172.

Ciottoni, A, S (1991). " Computerised data management in determining causes of 4 water main breaks: The Philadelphia Case Study", *NL of Indian Waterworks Association*, 23, 99-104.

Ciottoni, A, S (1985). "Updating the New York City Water System", *Proceedings of speciality conference on infrastructure for urban growth*, 69-77.

Clark, Stafford, Goodrich (1982). "Water distribution systems: A spatial & cost evaluation", *Journal of the water resources, planning and management division*, 3 (110), 243-256..

Clegg, B, G, H (1958). "Report on Broken Cast Iron Mains", *Institution of Gas Engineers*,1st January .

Chamberlian, E J (1987). "Freeze thaw test to determine the frost susceptibility of soils", *United States Army Corp of Engineers, The Cold Regions Research and Engineering Laboratory*, 1.

Chambers, G M (1983). "Analysis of Winnipeg's Watermain Failure Problem City of Winnipeg", *Works and Operations Division*, TD 491.W3.

Charles, E, A Parkins, R N (1995). "Generation of stress corrosion cracking environments at pipeline surfaces", *Corrosion Science*, July, 5 (7), 518-527.

Champoin, J, S, J (1990). "Rehabilitation Methods: Replacement and structural renovation", *Water Supply*, 8, 237-251.

Cohen, A, Fielding, M B (1979). "Predicting forst depth; protecting underground pipelines", *Journal AWWA*, 71 (2), 113-116, February.

Conlin, R, M, Baker, T J (1997). "Application of fracture mechanics to the failure behaviour of buried cast iron mains", *TRRL*, 266, 24 July, 1-20.

Conroy, P, J, Hall, M, J (1995). "Rehabilitation and Leakage - a joint approach", *Aqua*, 44 (4), 196-201.

Crabb, G, I, Carder, D, R (1985). "Loading tests on buried flexible pipes to validate a new design model", *TRRL*, (Report 28).

Creegan, P, J (1983). "Pipe Restraints: Design Fallacies", *Journal of Transportation Engineering*, 109 (6), Nov, 840-852.

Crilly, M, S, Driscoll, R, M, Chandler, R (1991). "Seasonal ground and water movement observations from an expansive clay site in the UK", *7th International Conference on Expansive Soils*, 313-318.

Coffin, L F, Schenectady, J R (1950). "The flow and fracture of brittle material", *Journal of Applied Mechanics*, 72 (Sept), 233-248.

Czurda, K, A, Wagner, J, F (1985). "Frost Heave and clay expansion in freshwater clays", *Ground Freezing - edited by Kinosita & Fukuda*, 5-7 August, 129-136.

D'Astous, A, Y, Ruland, W, W, Bruce, J, R, G, Cherry, J, A, Gillham, R W (1989). "Fracture effects in the shallow groundwater zone in the weathered Sarnia-area clay", *Canadian Geotechnical Journal*, 26, 43-56.

Davis, Bacher (1972). "Concrete Arch Culvert behaviour- phase 2", *Journal of the Structural Division M. ASCE*, 98 (ST11), 2329-2350.

Davis (1969). "Structural behaviour of concrete arch culvert", *Journal of the Structural Division M. ASCE*, 95 (ST12), December, 2665-2686.

Deacon, G, F (1982). "The Constant Supply and Waste of Water", *Journal of the Society of Art*, (May), 1-17.

Deb, A, K (1994). "Water distribution system performance indicators", *Water Supply*, 12 (3/4), 11-20.

DIPRA (1980). "Breaks in Cast Iron Pipe", *Ductile Iron Pipe Research Association.*

DIPRA (1998). "Ductile Iron Pipe", *Ductile Iron Pipe Research Association.*

Doleac, M, L, Lackey, S, L, Bratton, G. "Prediction of time-to-failure for buried cast iron pipe", 31-38.

Dolson, F, E (1954). "Factors Causing Main Failures" *JAWWA*, September, 465-469.

Duane, J (1892-93). "The effect of tuberculation on the delivery of a 48-inch water main", *Proceedings ICE*, CXIV (4).

Dyachkov, A (1994). "Rehabilitation of the water distribution network in the city of Moscow", *Water Supply*, 12, (3/4), 89-94.

Elhmadi, M, O'Rourke, M (1990). "Seismic damage to segmented buried pipelines", *Earthquake Engineering and Structural Dynamics*, 19, 529-539.

Evans, H (1996). "Biofilms, Filtration Theory and Particle Removal", *EngD Conference*, Thames Water Utilities, Kempton, Surrey, 1-11.

Ferguson *et al.* "Water Movement and Loss", *Proceedings of the American Soil Science Society*, 28, 700-703.

Fielding, M B & Cohen, A (1979). "Predicting Frost Depth; Protecting Underground Pipelines", *Journal AWWA*, 71 (2), 113-116.

Foriero, A, Ladanyi, B (1994). "Pipe uplift resistance in frozen soil and comparison with measurements", *Journal of Cold Regions Engineering*, 8, (3), September, 93-111.

Francis, C (1994). "Seiving the evidence on leakage", *WWT*, November, 18-18

Fredlund, D, G, Xing, A (1994). "Equations for the soil-water characteristic curve", *Canadian Geotechnical Journal*, 31 521-532.

Fredlund, D, G, Xing, A, Huang, S (1994). "Predicting the permeability function for unsaturated soils using the soil-water characteristic curve", *Canadian Geotechnical Journal*, 31, 533-546.

Fujiwara, O, Tung, H, D (1992). "Reliability improvement for water distribution networks through increasing pipe size", *Water Resources Journal*, 172, 29-36.

Fukuda, M, Nakagawa, S (1985). "Numerical analysis of frost heaving based upon the coupled heat and water flow model", *Ground Freezing - edited by Kinosita & Fukuda*, 5-7 August, 109-117.

Fuller, H (1940). "Studies of frost penetration", *Journal New England WWA*, 54, 275-281.

Gandahl, Bergan, (1957). "Two Methods of measuring the frozen zone in soil", *4th Conference Soil Mechanics and Foundation Eng.*, 1, 32-34.

Gaunt, J, Trott, J, J, Stevens, J, B (1976). "Static and dynamic loading tests on shallow-buried flexible pipes", *Ground Engineering*, April, 27-32.

Gemperline M,. C (1987). "Construction Equipment load on buried pipe", *Journal of Pipelines*, 3 (6), 283-290.

Globus, A, M, Nerpin, S V (1960). "On the mechanism of movement of soil moisture to the frozen ground level", *Dokl ACAD Nauk SSSR Earth Sciences*, 35, 795-796.

Goulter, I, Davidson, J, Jacobs, P (1993). "Predicting water-main breakage rates", *Journal Water Resources Planning and Management*, 119 (4), 419-436.

Goulter, I, C, Kazemi, A (1989). "Analysis of water distribution pipe failure types in Winnpeg, Canada", *Journal of Transportation Engineering*, 115 (2), 95-111.

Goulter, I, C (1990). "Methods of Identification and the recording of data", *Water Supply*, 8 (112), 175-179.

Goulter, I, C, Kazemi, A (1988). "Spatial and temporal groupings of water main pipe breakage in Winnipeg", *Canadian Journal of Civil Engineering*, 15, 91-97.

Graham, J, Au, V, C, S (1985). "Effects of freeze-thaw and softening on a natural clay at low stresses", *Canadian Geotechnical Journal*, 22, 69-78.

Hassan, J (1983). "Public ownership - its origins and growth", *Water Bulletin 14*, January, 12-15.

Hamilton, H, L (1960). "Effects of soil corrosion on cast iron pipe", *Journal AWWA*, 52 (5), 638-650.

Hardy, A (1984). "Water and the search for public health in London in the 18th &19th centuries", *Medical History*, 28, 250-282

Harrison, T (1875). "Constant and intermittent water supply", *Proceeding ICE*, XLII, 129-210.

Harrison, E, Patten (1909). "Heat transference in soils", *US Dept. Of Agriculture Bureau of Soils - Bulletin 59*, 1-54.

Herz, R, K (1996). "Aeging processes and rehabilitation needs of drinking water distribution networks", *Journal Water SRT – Aqua*, 45 (5), 221-231.

Herbert, H (1994). "Technical and economic criteria determining the rehabilitation and/or renewal of drinking water pipelines", *Water Supply*, 12 (3/4), 105-117.

Highland, S, G (1926). "Study of year round soil temperatures", *Journal AWWA*, 52 (5), 342-354

Hirner, W (1994). "Criteria for planning and establishing priorities for distribution network rehabilitation", *Water Supply*, 12 (3/4), 43-58.

Hoffman, J, M (1987). "Pipe materials usage for water distribution mains by the UK water industry", *Water Research (WRc)*, April, 1-29

Hope, W (1996). "The waste water in public supplies and its prevention", *Proceeding ICE*, 115 (2), 68-75.

Hudson, J, C, Acock, G, P (1951). "Tests on the Corrosion of Buried Iron and Steel Pipes", *National Gas Archive Special report 45.*

Hunter, P, McCaffrey, R, G (1984). "Blasting adjacent to buried cast iron pipes", *Ground Movements and Structures*, 3, 677-693.

Ishizaki, T Nishio, N (1985). "Experimental study of final ice lens growth in partially frozen saturated soil", 4th International Symposium on Ground Freezing, Sapporo, 5-7 August, 71-78.

Israel, T, D, Viraraghavan, T (1991). "Ananalysis of Water-main failures", *Journal of the Indian Water Works Association*, 23 (2), 99-104.

Jacobs, P, Goulter, I, C, Davidson, J (1993). "Water-Distribution GIS from fragmented and incomplete information", *Journal of Computing in Civil Engineering*, 7 (3), 372-386.

Johnston, T C, Berg, R C *et al.* (1956). "Frost action predictive techniques for roads and airfields", *United States Army Corp of Engineers, The Cold Regions Research and Engineering Laboratory*, 1.

Jones, R (1983). "A review on buried pipelines and causes of failures with particular refence to ground movement", *Msc dissetation, University of Surrey*, June.

Jowitt, P, W, Xu, C, C (1993). "Predicting pipe failure effects in water distribution networks", *Journal Water Resources Planning and Management*, 119 (1), 18-31.

Katoh, J (1972). "Systematic stress analysis of circular pipe", *Transportation Engineering Journal*, 98 (TE4), November, 1039-1063.

Kettler, A, J, Goulter, I, C (1985). "An analysis of pipe breakage in urban water distribution networks", *Canadian Journal of Civil Engineering*, 12 (2), 286-293.

Kirmeyer, J, Logsdon, G (1983). "Principles of internal corrosion and corrosion monitoring", *Journal AWWA*, 72 (2), 78-83.

Knutsson, S, Domaschuk, L, Chandler, N (1985). "Analysis of large scale laboratory and in situ frost heave tests", *4th International Symposium on Ground Freezing, Sapporo*, 5-7 August, 65-70.

Koelle, W (1977). "Corrosion in Drinking Water systems", *European Conference on Metal Corrosion, London*, (77), 421-429.

Konrad, J, Morgenstern, N R (1981). "The segregation potential of a freezing soil", *Canadian Geotechnical Journal*, 18, 482-491.

Kottmann, A, Fojtu, P(1978). "Carrying capacity of pipes made from different materials", *GWF-Das Gas und Wasserfach*, 119 (6), 225-233.

Kowalewski, P (1976). "Rohrbruchuntersuchungen", *GWF-Wasser/Abwasser*, 117 (8), 358-363.

Kuroda, T (1985). "Theoretical study of frost heaving - kinetic process at water layer between ice lens and soil particles", *4th International Symposium on Ground Freezing, Sapporo,* 5-7 August, 39-45.

Lackington, D, W (1991). "Leakage control, reliability and quality of supply", *Civil Engineering Systems*, 8, 219-229.

Lambert, A (1994). "Accounting for losses:- The bursts and backgroung concept", *J. IWEM*, 8, 205-205.

Lambert, A (1995). "An international model for leakage management - the bursts and background losses concept", *Water Supply,* 13 (3/4), 251-255.

Lambert, A, Morrison, J, A, E (1996). "Recent developments in application of "Bursts and Background Estimates" concepts for leakage management", *J. CIWEM*, 10, 100-104.

Lambert, A, Morrison, J A E (1988). "Leakage: Setting leakage targets in rural areas", *Journal of Associate Water Officers*, April, 59-67.

Larson, T, E (1966). "Chemical Control of Corrosion", *Journal AWWA*, 58 (3P), 354-362.

Lawrence, C, Rude. M (1983). "Load reductions on buried rigid pipes", Journal of Transportation Engineering, 109 (1).

Lloyd-Davies, D, E (1922-23). "The works for the Augmentation of the supply of water to the city of Cape Town, South Africa", *Proceeding of Institute of Civil Engineering*, CCXVI (II), 338-371.

Lyon, S (1997). "Relationships between pipe breaks in the water distribution system, soil type and other factors", *Environmental Science at University College London.*

Lyon, S (1997). "Relationships between pipe breaks and factors including soil type", *Thames Water Plc, Group Research & Development*, R9750 Oct, 1-24.

Mahmood, P (1970). "Effect of Coating on Thermal Conductivity of Pipes", *Transportation Engineering Journal*, 96 (TE1), Feb, 71-78.

Manger, R (1986). "Cushioning stress and strain in pipe systems", *Water/Engineering and Management,* November, 133, (11), 28-29.

McCabe, E Y, Kettle, R J, (1985). "Thermal aspects of frost action", *4th International Symposium on Ground Freezing, Sapporo,* 5-7 August, 47-54.

Meyer, A, F (1960). "Effect of temperature on ground water levels", *Journal of Geophysical Research,* 65, (6), 1747-1752

McCormick, G (1971). "Estimation of Design Freezing Indices", *Transportation Engineering Journal*, 97 (TE3), August, 401-409.

McKenna, R (1996). "Mathematical Modelling of water distribution networks", *Engineers Journal*, 51 (1).

Michyalik, P (1994). "Status and rehabilitation of the distribution newtwork in Dresden", *Water Supply*, 12 (3/4), 81-87.

Mikasinovic, M, Marcucci, P (1984). "Sizing Pipe for external pressure", *Chemical Engineering*, 91 (9), 61-64.

Millward, R, Sheard, S (1995). "The urban fiscal problem, 1870-1914: goverment expenditure and finance in England and Wales", *Economic History Review*, XLVIII (3), 502-535.

Miller, R D, Baker, J H, Kolaian, J H (1960). "Particle size, over burden pressure, pore water pressure and freezing temperature of ice lenses in soil", *7th International Congress of Soil Science, Madison, Wisconsin*, 1, 122-129.

Millette, J, R, Hammonds, A, F, Pansing, M, F Hansen, E, C Clark, P, J (1980). "Aggressive water: assessing the extent of the problem", *JAWWA*, (May), 262-266.

Mingzhu, G, Huaguang, H (1985). "Calculation of normal frost heave force", *4th International Symposium on Ground Freezing, Sapporo*, 5-7 August, 119-177.

Mitchell, G (1924-25). "The water-supply of the city of Aberdeen", *Proceedings of the Insitute of Civil Engineering*, 220 (2), 209-248.

Monro, M, Martin, A (1986). "Water distribution network analysis", *Water/Engineering and Management*, 133 (11), 28-29.

Moore, I D, Booker, J R (1987). "Ground Failure Around Buried Tubes", *Rock Mechanics and Rock Engineering*, 20 (4), 243-260.

Moulton, L K, Schaub, J H (1969). "Estimation of Climatic Parameters for Frost Depth Prediction", *Transportation Engineering Journal*, 95 (TE4) November, 605-616.

Moulton, L K, Schaub, J H (1969). "Estimation of Pavement Surface Freezing Indices", *Transportation Engineering Journal*, 95 (TE4) November, 587-604

Muleski, G E, Ariman, T (1984). "Fracture of Buried Pipelines", *5th International Conference on Pressure Fracture of Buried Pipelines, San Francisco, ASME, New York*, (2), 997-1010.

Nath, P (1981). "Pressures on buried pipes due to revised HB Loading", *TRRL*, (977).

Needham, D, Howe, M (1982). "Why Pipes Fail - Again?", *Gas Research and Technology Centre*, E315 February.

New Scientist (1997). 19 April, P22

Newport, R (1981). "Factors influencing the occurrence of bursts in iron water mains", *Aqua*, 3, 274-278.

Nielsen, K (1996). "National Report Denmark", *Water Supply*, 14 (3/4), 267-268.

Obrecht, M F, Pourbaix, M (1967). "Corrosion of Metals in Potable Water Systems", *JAWWA*, 977-992.

O'Day, D K (1989). "External Corrosion on Distribution Systems", *Journal AWWA*, 81 (10), 45-52.

Oliphant, R J (1987). "Causes and Cures of Corrosion on Iron Water Mains", *Corrosion*, 29-33.

Ohrai, T, Yamamoto, H (1985). "Growth and migration of ice lenses in partially frozen soil", *4th International Symposium on Ground Freezing, Sapporo*, 5-7 August, 79-84.

O'Rourke, T D (1978). "Discussion - lateral displacement of shallow buried pipelines due to adjacent deep trench excavation", *Geotechnique*, 28 (2), 214-217.

O'Rourke, M, Elhmadi, K, Bouabid, J (1989). "Seismic Responce and vunerability of water delivery systems", *5th International conference on - Structural Safety and Reliability*, (1989), 493-500.

Owen, R C (1984). "Vegetation and Seasonal Ground Movement Effect on Buried Mains", *Ground Movements and Structures*, 3, 145-160.

Palmer, A C (1972). "Settlement of Pipeline on Thawing Permafrost", *Transportation Engineering Journal*, 98 (TE3) August, 472-491.

Palmer, A C (1967). "Ice Lensing, Thermal Diffusion and Water Migration in Freezing Soil", *Journal of Glaciology*, 6 (47), 681-694.

Paterson, A M (1924-25). "Bristol Waterworks: Cheddar Supply", *Proceeding ICE*, 220 (2), 192-207.

Paula, A D, Fialho, J F (1977). "Influence of Inocluants on large diameter centrifugally cast ductile iron pipe", *AFS International Cast Metals Journal*, 2 (2), 39-46.

Pchelintsev, A M (1960). "Anisotropy in the swelling of freezing dispersed soil", *Dokl Akad Nauk SSSR Earth Sciences*, 134, 1038-1040.

Pearson, F H.(1977). "Beam Behavior of Buried Rigid Pipelines", *Journal of the Environmental Engineering Division*, 103 (EE5), 767-783.

Pierce, J W (1961). "Fundamentals of Cathodic protection", *Journal of the Pipeline Division*, 87 (PL2) September, 35-51.

Pilcher, R P. "Leakage Control Practice in the 1990's", *Institute of Water Offices Journal*, 30 (3), 30-31.

Philip, J R, Vries, D A (1957). "Moisture Movement in Porous Materials under Temperature Gradients", *Transactions of American Geophysical Union*, 38, 222-232.

Pludek, V R (1977). "Design and Corrosion Control", *The Macmillan Press 1st Edition.*

Pocock, R G, Lawrence, G J L, Taylor, M E (1980). "Behaviour of a shallow buried pipeline under static and rolling wheel loads", *TRRL*, (954).

Potter. J (1985). "Effects of vehicles on buried high pressure pipes", *Journal of Transportation Engineering M. ASCE*, 111 (3), 224-236.

Raymond, J, Krizeh, M, Paul, V (1978). "Behaviour of buried concrete pipe", *Journal of the Geotechnical Eng. Division*, 104.

Ryder, R A (1980). "The costs of internal corrosion in water systems", *JAWWA*, (May), 267-279.

Ryokai, K (1985). "Frost heave theory of saturated soil coupling water/heat flow and its application", *4th International Symposium on Ground Freezing, Sapporo*, 5-7 August, 101-108.

Saad, M, Turgeon, A, Pbigras Duquette, R. "Learning disaggregation technique for the operation of long -term hyroeletric power systems", *Water Resources research* 30 (11), 3195-3202 .

Saul , G M (1979). "The water supply in 19th Century London", *The University of Brunel - Brunel Bulletin*, 3-7.

Schmulevich Galili (1986). "Deflections and bending moments in buried pipes", *Journal of Transportation Engineering*, 112.

Schlick, W J, Moore, B A (1936). "Strength and elastic properties of cast iron", *Bulletin 127, IOWA engineering experiment station, IOWA state college*, June.

Scotland G Highland (1926). "Study of year round soil temperatures", *Journal AWWA*, 16, 342-354.

Selig, E T, McVay, M C, Chang, C S (1982). "Finite-element modeling of buried concrete pipe installations", *Transportation Research Record*, (878), 17-23.

Selvadurai, A P S, Shinde, S B (1993). "Frost Heave Induced Mechanics of buried pipelines", *Journal of Geotechnical Engineering*, 119 (12), December, 1929-1951.

Shamir, U, Howard, C D (1979). "An Analytical approach to scheduling pipe replacement", *Journal of the American Water Works Association*, 71, (5), 248-258.

Shannon (1945). "Prediction of Frost Penetration", *Journal NEWWA*, 59, 356-363.

Shen, M, Ladanyi, B (1991). "Soil-pipe interaction during frost heaving around a buried chilled pipeline ", *Proceedings of 6th International Cold Regions Science and Technology*, 11-21.

Sheer, D P (1980). "Analysing the risk of drought: the occoquan experience", *JAWWA*, May .

Shmulevich, I, Galili, N, Foux, A (1986). "Soil stress distribution around buried pipes", *Journal of Transportation Engineering*, 112 (5), 481-494.

Shmulevich, I, Galili, N (1986). "Deflections and bending moments in buried pipes", *Journal of Transportation Engineering*, 112 (4), 345-357.

Shreir, L L . "Metal/Environment Reactions", *Corrosion, Newnes-Butterworths, London*, 1 (8), 3-46.

Singhal (1983). "Junction stresses in buried pipelines", *Journal of Transportation Engineering*, 109.

Singhal, A, Meng, C (1983). "Junction Stresses in Buried Jointed Pipelines", *Journal of Transportation Engineering*, 109, (3) May, 450-461.

Singhal, A C (1980). "Strength Characteristics of buried cast iron pipes", *Arizona State University*, ERC-R-80027 August.

Singley, J E (1978). "Principles of Corrosion", *Corrosion*, 1-11.

Skarda, B C (1994). "Water pipe network future strategy detection and prevention of external corrosion in Zruich", 12 (3/4), 139-150.

Slipper, M J (1994). "Pipeline rehabilitation - Challenges and innovations", *Water Supply*, 12 (¾), 59-67.

Smith, M W, Dallimore, S R, Kettle, R J (1985). "Observations and prediction of frost heave of an experimental pipeline", *4th International Symposium on Ground Freezing, Sapporo*, 5-7 August, 247-304.

Smith, E (1982). "Application of the Net section stress approach to pipe failure", *Internal Journal of Pressure Vessels and Piping*, 10, 81-92.

Smith, T R (1976). "The significance of soil conditions and trench preparation in relation to pipeline performance", *Ground Eningeering*, April, 33-38.

Smith, W H (prior 1976). "Breaks in cast iron pipe", *Cast Iron Pipe Research Association, Illinois, 60521.*

Smolyakov, A N, Korenyako, V A (1986). "Quality control test for cast iron pipes using acoustic emissions", *Soviet Castings Technology- Liteinoe Proizvodstvo*, (2), 70-71.

Staff (1980). "Internal Corrosion", *JAWWA*, May, 245-253.

Stephens, J W, Gill, B W (1982). "Service failure experience of uPVC pressure pipes in the water industry", *Plastic Pipes*, 5, 33.1-33.15.

Steverding, B, Nieberlein, V A (1974). "Fluid Interaction with Fracture Propagation in Pipelines", *Transportation Engineering Journal*, 100 (TE3) August, 583-592.

Srinivasan, P Lakshminarayanan, V (1970). "Vibration of Pipe Carrying Flowing Fluid", *Transportation Engineering Journal,* Vol 96 (TE2) May, 165-174.

Su-Won Kim P (1989). "Leakage control practice in distribution network", *Water Nagoya*, 707-715.

Subhash. C Anand. M (1974). "Stress distributions around shallow buried rigid pipes", *Journal of the Structural Division*, 100.

Sullivan J. P, (1982). "Maintaining aging systems - Boston's approach", *Journal of the American Water Works Association*, 74, (11), 554-559.

Taber, S (1929). "Frost Heaving", *Journal of Geology*, 37, (5), 428-461.

Taber, S (1930). "The mechanics of frost heaving", *Journal of Geology*, 38, (303-317).

Tarzi, A I, Menzies, B K, Crofts, J E (1979). "Bending of jointed pipelines in laterally deforming soil", *Geotechnicque*, 29 (2), 203-206.

Taylor, G S, Luthin, J N (1978). "A model for coupled heat and moisture transfer during soil freezing", *Canadian Geotechnical Journal*, School of CEE, University of Ithaca, NY, 15, 548-555.

Taylor, M E, Lawrence, G J L, Carder, D (1984). "Behavior of shallow buried pipeline under impact and abnormal loads", *TRRL* Crowthorne, U.K. Laboratory, Report 1129.

Terzaghi K. Peck R. B. *Soil Mechanics in Engineering Practice Book*, 2nd edition, 149-151.

Thames Water Utilities (1983). "Land evaluation for corrosivity -The assessment of soil-based factors as a cause of mains failures", *Soil Survey and Land Research Centre,* Doc CIS 139 Version 2

Thames Water. "A literature Review of work relating to bursts".

Thames Water. "Presentation slides on London cold temperature events"

Thames Water Authority. "Fractures in Water Mains".

The Institution of Gas Engineers (1958). "Report on Broken Cast Iron Mains", *National Gas Archive.*

UK Water Industry (1994). "Managing Leakage", *WRc*, Summary Report A October.

Van der Zwan, J T (1987). "Causes of pipe damage", *Water Supply* 5 (3/4).

Vasudev, S (1984). "Pipeburst flow analysis", *Journal of Transportation Engineering*, 110, (3), May, 309-323.

Versanne, D (1987). "Causes of water main damage", *Water Supply*, 5 (¾), 8-13.

Vuorinen, A, Carlson, L, Tuovien, O H, (1985). "Surface Characteristics of tubercule mass and graphitc residue in cast iron water pipelines", *Materials Chemistry and Physics*, 12 (3), 275-285.

Water Practice Manuals (1984). "Water Distribution System", *Institution of Water Engineers and Scientist*, 4.

WRc (1994). "Damage to highways by leaks and bursts", *UK Water Industry Research Limited*, WM-01/E Highway Reinstatement. 1-4.

Weronski, A (1977). "Bursting of steel moulds for centrifugal casting of cast iron pipes", *Archiwum Hutnictwa*, 22, (1), 133-154.

Williams, S M, Ainsworth, R G A, Elvidge, A F (1998). "Method of assessing the corrosivity of water towards iron", *Water Research (WRc)*, February, 1-35.

Willis *et al.*, (1964). "Water table changes", *Soil Science*, 98, 224-248.

Willis, W O, Carlson, C W, Alessi, J, Haas, H J (1961). "Depth of Freezing and Spring Run-off as Related to Fall Soil-moisture level", *Canadian Journal of Soil Science*, 41, 115-123.

Winn H. F (1940). "Soil Mechanics and its applications; symposium of frost action", *Proceedings of the Purdue Conference*, Iowa State College September 2-6, 444-482.

Wood, J A, Williams, P J (1985). "Stress distribution on frost heaving soils", *4th International Symposium on Ground Freezing, Sapporo,* 5-7 August, 165-171.

Yanagisawa, E, Yao, Y J (1985). "Moisture movement in freezing soils under constant temperature condition", *4th International Symposium on Ground Freezing, Sapporo,* 5-7 August, 85-91.

Yong, R N, Boonsinsuk, P, Yin, C W (1985). "Alteration of soil behaviour after cyclic freezing and thawing", *4th International Symposium on Ground Freezing, Sapporo,* 5-7 August, 187-195.

Young, O C, Smith, J H (1970). "Simplified tables of external loads on buried pipelines", *Building Reseacrh Station,* Minstry of Public Building and Works, 1-14.

Young, R N, Osler, J C (1971). "Heave and Heaving Pressures in Frozen Soil", *Canadian Geotechnical Journal*, 8, 272-282.

APPENDIX A – SITE INVESTIGATIONS

PIPE and JOINT EXHUMATION

CEDARS ROAD (London, E15)

30th July 1998

PIPE and JOINT EXHUMATION
CEDARS ROAD LONDON E15, 30th July 1998

INTRODUCTION

This report presents a factual summary of the pipe exhumation at Cedars Road, on 30th July 1998. It is intended for use as a reference by all the groups involved in research linked to the site:— Thames Water Utilities, the University of East London (pipeline technology and geotechnics groups) and the University of Surrey (materials and geotechnics groups).

A section of Cedars Road has been fenced off and is to be developed as student accommodation for the University of East London. The west side of the street consists of an unoccupied terrace of two storey housing, which is believed to date from the inter-war period. Within the fenced compound, the east side of the street is wasteground.

On 29th July 1998, a trench along the axis of the pipe was excavated (Figure 1). In the morning of 30th July, the mains supply through the pipe was interrupted and a section of approximately 10 metres of the pipe was removed. Samples of the pipe, joints and soil were taken. A new section of MDPE pipe was then fitted between the remaining iron main (Figure 2), permitting resumption of water supply. The site work was carried out by Total Pipeline Solutions, which is a subsidiary of Thames Water.

IN-SITU OBSERVATIONS

The trench (11.6 m long, 0.6 m wide, 1 m deep) was excavated along the axis of a 3″ internal diameter iron main. The trench was located approximately 1 m west of the centre line of Cedars Road, and ran north-south (bearing 157°).

Figures 3a and 3b presents a sketch of the features and dimensions observed in the east wall of the trench, and notes the joint locations.

The invert of the pipe was 0.76 to 0.80 m below the road surface. The asphalt was 10 cm thick and was underlain by 25-26 cm thickness of sub-base (Figure 4). The pipe was laid in made ground. (Disturbed, bag samples of the material have been acquired.) Two small diameter pipes crossed the pipe transversely, about 20 cm above crown level, at 4 and 4.6 m, respectively, from the south end of the trench (Figure 5). There were two disconnected tapped ferrules and two plugged ferrules (see Figure 5) in the midsection of the pipe (between 3.8 and 6.3 m from the south end). At the north end of the trench, two conduits for cable utilities had been installed in a backfilled trench (Figure 6). The base of the cable trench was 10-15 cm above the level of the pipe crown. A patch repair to the road surface in the vicinity of the ferrules and transverse pipes (Figure 7), had been backfilled with Type 1 backfill and pea gravel.

PIPE and JOINT SAMPLES

The pipe was detached from the network in three parts. The pipe segments were removed by cutting a slot through the pipe and by hammering a wedge into the slot (Figure 8).

The pipe included five joints (A, B, C, D, E) and four pipe sections (1, 2, 3, 4). The details of the pipe and joint samples obtained, and the destination of the samples, are:

University of Surrey (materials research)
Pipe section 1 (2.11 m length, from north end of trench)
Pipe section 2 (2.19 m; includes one tapped and two plugged ferrules)
Pipe section 3 (2.30 m)
Pipe section 4 (1.52 m, from south end of trench)

University of Surrey (geotechnics group)
Joint A (24 cm long), between southernmost unexhumed pipe and pipe section 4 (Figure 9)
Joint B (11 cm), between pipe sections 3 and 4 (Figure 10)
Joint D (12 cm), between pipe sections 1 and 2 (Figure 11)
Joint E (12 cm), between the northernmost unexhumed pipe and pipe section 1 (Figure 12)

University of East London
Joint C (11 cm), between pipe sections 2 and 3 (includes one tapped ferrule)

SOIL SAMPLES

Six disturbed, large bag samples were obtained from the base of the trench immediately beneath the pipe (Figure 13). Additional, small bag samples were taken of other materials encountered in the trench. The samples have been delivered to the University of Surrey (geotechnics group).

Details of the samples are:
Bag 1 (TWUL code 4312) large bag sample from beneath pipe (made ground)
Bag 2 (TWUL code 4310) large bag sample from beneath pipe (made ground)
Bag 3 (TWUL code 4308) large bag sample from beneath pipe (made ground)
Bag 4 (TWUL code 4307) large bag sample from beneath pipe (made ground)
Bag 5 (TWUL code 4304) large bag sample from beneath pipe (made ground)
Bag 6 (TWUL code 4302) large bag sample from beneath pipe (made ground)
Bag 7 (TWUL code 4309) sample from vicinity of ferrules (pea gravel)
Bag 8 (TWUL code 4306) sample from beneath Joint A (wood)
Bag 9 (TWUL code 4313) material scraped from underside of pipe section
Bag 10 (TWUL code 4314) sample from below sub-base layer from vicinity Joint B
Bag 11 (TWUL code 4311) sample from vicinity ferrules, depth 15-20 cm (Type 1 fill)

The trench was dry when the samples were taken (Figure 14). This is in contrast with the condition of pipe trench excavations for burst repair. Figure 15, taken after the pipe was cut and the water in the shut-off pipe escaped, shows the typical condition of a wet trench. It should be noted that soil samples from wet trenches would be affected by loss of fine material.

Figure 1 View of excavated trench, from north

Figure 2 View of replaced pipe

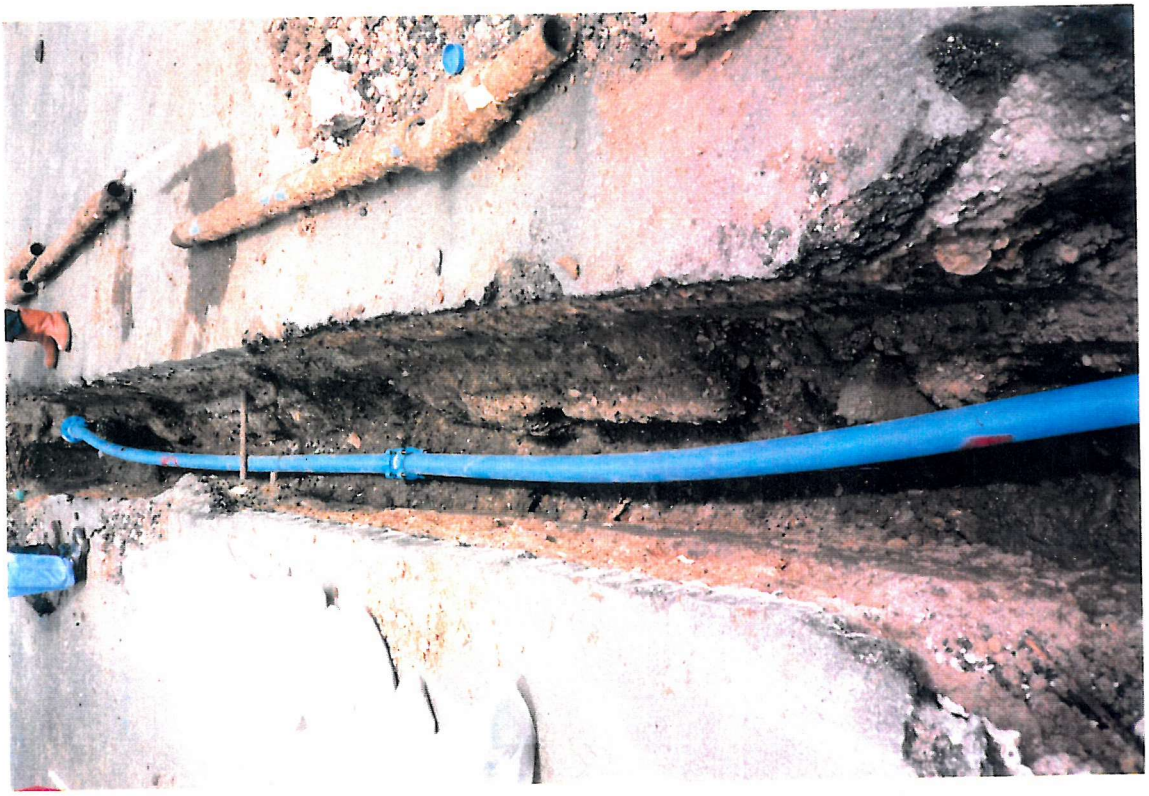

FIGURE 3A - Plan of trench showing joint locations

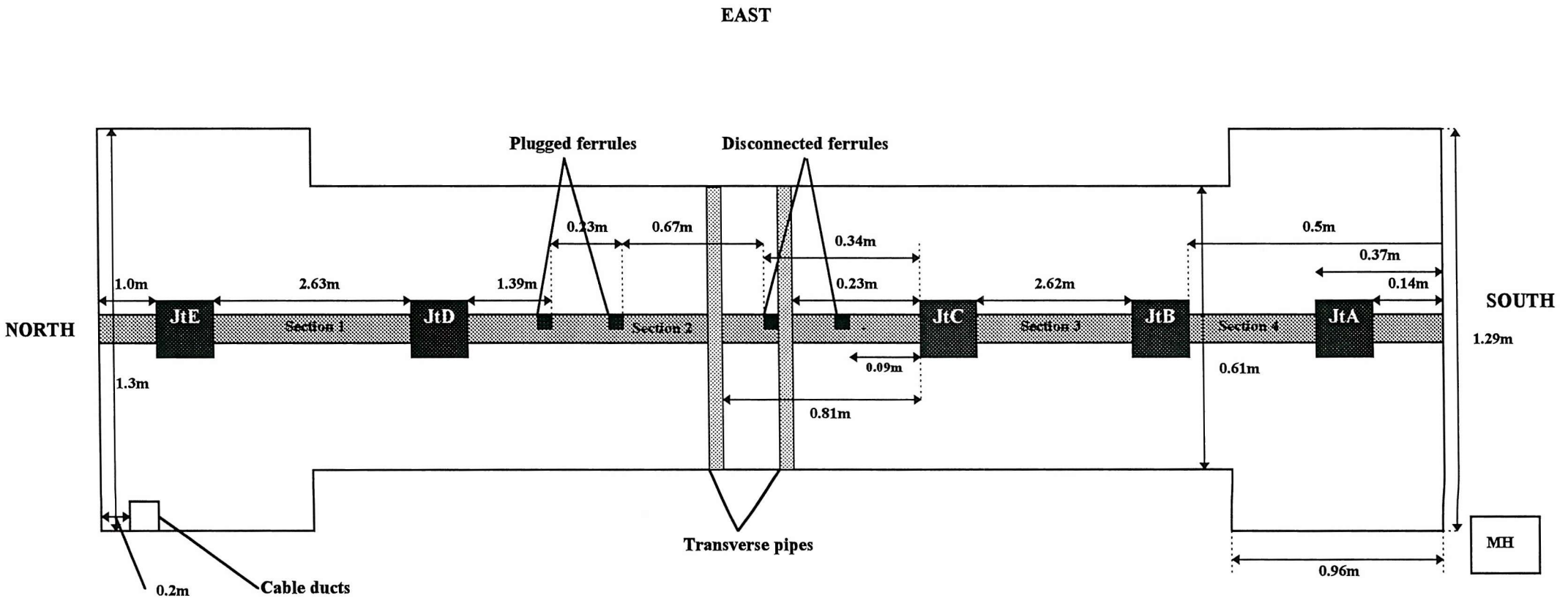

FIGURE 3B -Elevation veiw of east side of trench

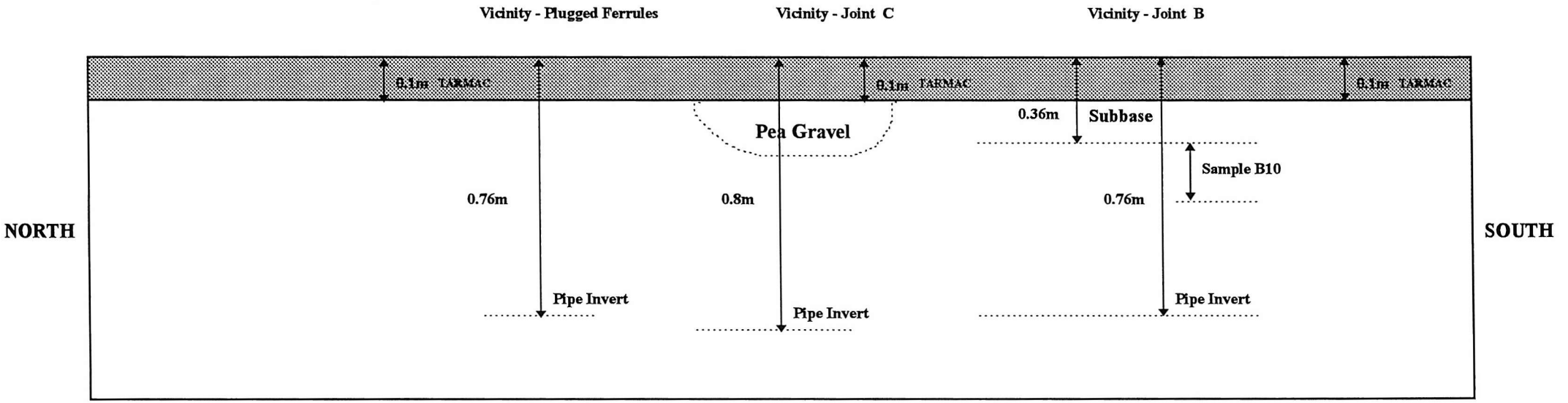

Figure 4 Side wall of trench, showing asphalt, road sub-base layer and pipe backfill

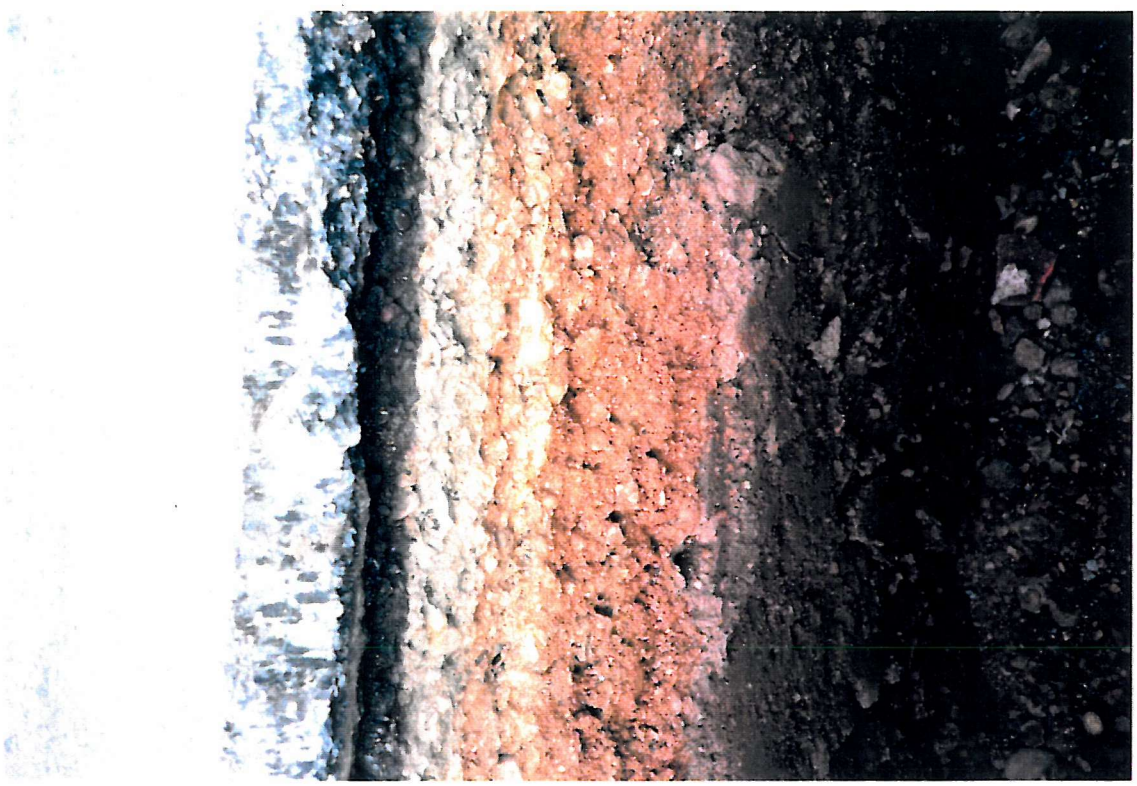

Figure 5 Small diameter pipes crossing path of 3″ pipe; also Joint C and capped ferrules.

Figure 6 Cable conduits with backfill (north end of trench)

Figure 7 Patch repair, showing pea gravel

Figure 8 Use of wedge in removal of pipe segments

Figure 9 Joint A

Figure 10 Joint B

Figure 11 Joint D

Figure 12 Joint E

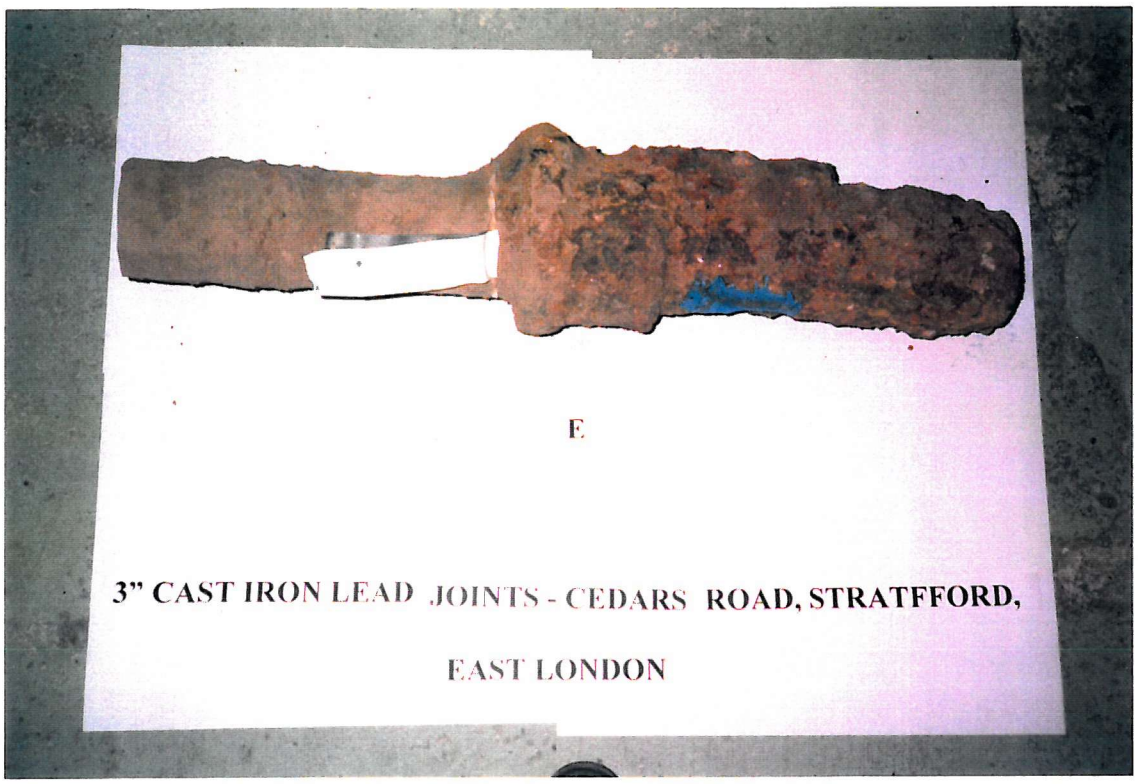

Figure 14 Dry trench conditions

Figure 15 Wetted trench conditions, after cutting pipe

<END>

FIGURE 13 - Plan view showing position of soil samples (large bags)

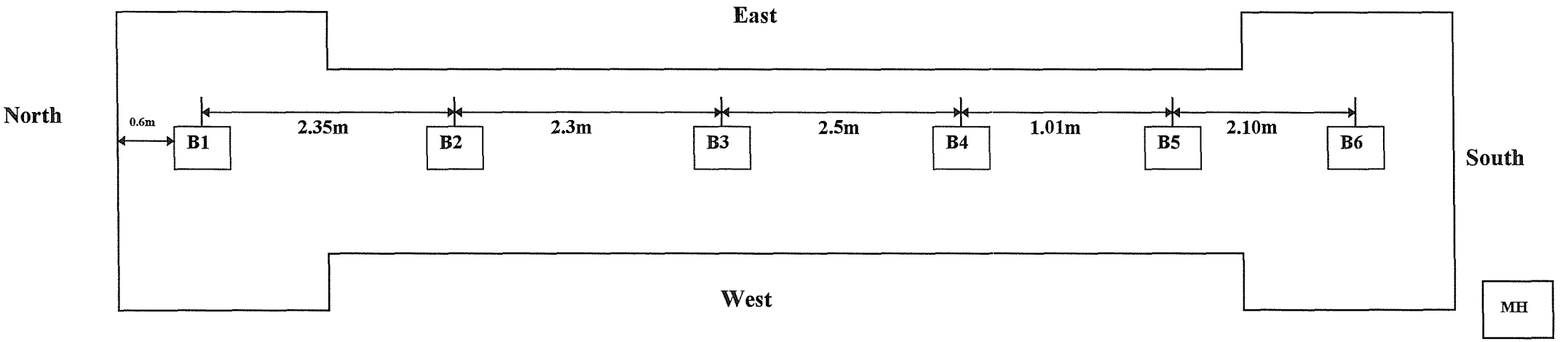

PIPE and JOINT EXHUMATION

EMBLETON ROAD (London, SE13)

23rd September 1998

PIPE and JOINT EXHUMATION
EMBLETON ROAD LONDON SE13, 23rd September 1998

INTRODUCTION

This report presents a factual summary of the pipe exhumation at Embleton Road in Ladywell (SE13), on 23rd September 1998. It is intended for use as a reference by the groups involved in research linked to the site, Thames Water Utilities and the University of Surrey (materials and geotechnics groups).

A section of Embleton Road was fenced off to replace the existing cast iron pipe with MDPE pipe, as this area was thought to have few service connections. On 23rd September 1998, a trench along the axis of the pipe was excavated (Figure 1). In the morning of the 23rd September, the mains supply through the pipe was interrupted and a section of approximately 20m of the pipe was removed. Samples of the pipe, joints and soil were taken. A new section of MDPE pipe was then fitted between the remaining iron main permitting resumption of water supply. The site work was carried out by Morrisons.

IN-SITU OBSERVATIONS

The trench (19 m long, 1.2 m wide, 1.2 m deep approximately) was excavated along the axis of a 4" internal diameter iron main. The trench was located approximately 1m west of the kerb of Embleton road, and ran north-south.

Figures 2 presents a sketch of the features and dimensions observed in the east wall of the trench, and notes the joint locations.

The invert of the pipe was 0.82 to 0.89 m below the road surface. Along the 20m length of the trench the backfill was varied ranging from sand at one end to clay at the other. At the south end of the trench the asphalt was 5 cm thick and was underlain by 30 cm of sub-base, 40-50 cm sand and then the remainder was clayey sand (Figure 13).

(Disturbed, bag samples of the material have been acquired). At the north end of the trench (from between joints 5 and 6) the asphalt was 5 cm thick and was underlain by 30 cm sub-base underlain by sand (Figure 12). (Disturbed, bag samples of the material have been acquired).

The surrounding housing had a Victorian style, three storey with a mixture of deattached and terraced houses. At the north end of the trench on the road above was a stop clock cover marked "MWB", Metropolitan Water Board. The joints had a date of 1910 stamped onto the rim of the bell. These three observations suggest the age of the pipes and joints to be in the early 1900's.

PIPE and JOINT SAMPLES

The pipe was detached from the network in seven parts. One pipe segment was removed using a pipe cutter, to prevent the joint from experiencing excessive stress (Figure 3). One of the blades of the pipe cutter failed and therefore the rest of the pipe segments had to be removed by cutting a slot through the pipe with a disc cutter and hammering a wedge into the slot (Figure 4).

The pipe included seven pipe joints (1, 2, 3, 4, 5, 6, 7) and seven pipe sections (1, 2, 3, 4, 5, 6, 7). The pipes and joints were numbered in situ. Each pipe section was marked on the crown and also on the southern most end. The details of the pipe and joint samples obtained, and the destination of the samples, are:

University of Surrey (materials research)
Pipe section 1 (1.99 m length, from south end of trench)
Pipe section 2 (2.11 m)
Pipe section 3 (2.13 m)
Pipe section 4 (2.17 m)
Pipe section 5 (2.15 m)
Pipe section 6 (2.13 m)
Pipe section 7 (0.98 m, from north end of trench)

University of Surrey (geotechnics group)

Joint 1 (0.64 m long), between pipe sections 1 and 2 (Figure 5)

Joint 2 (0.63 m long), between pipe sections 2 and 3 (Figure 6)

Joint 3 (0.63 m long), between pipe sections 3 and 4 (Figure 7)

Joint 4 (0.61 m long), between pipe sections 4 and 5 (Figure 8)

Joint 5 (0.59 m long), between pipe sections 5 and 6 (Figure 9)

Joint 6 (0.59 m long), between pipe sections 6 and 7 (Figure 10)

Joint 7 (0.59 m long), between pipe section 7 and the northernmost unexhumed pipe (Figure 11)

SOIL SAMPLES

Seven disturbed bag samples were obtained from the base of the trench immediately beneath the joints. Additional, small bag samples were taken of other materials encountered in the trench. Three disturbed, large bag samples were taken from the kerb where the backfill had been deposited in digging the trench. The trench was dry when the samples were taken. The samples have been delivered to the University of Surrey (geotechnics group).

Details of the samples are:

Bag 4433 small bag sample from beneath joint 1

Bag 4435 small bag sample from beneath joint 2

Bag 4436 small bag sample from beneath joint 3

Bag 4437 small bag sample from beneath joint 4

Bag 4438 small bag sample from beneath joint 5

Bag 4439 small bag sample from beneath joint 6

Bag 4440 small bag sample from beneath joint 7

Bag 4429 large bag sample of excavated material from south end (see Figure 2)

Bag 4430 large bag sample of excavated material from mid section (see Figure 2)

Bag 4431 large bag sample of excavated material from north end (see Figure 2)

Bag 4434 small bag sample around pipe section between joints 5 and 6

Bag 4432 small bag sample encrustation from pipe between joints 5 and 6

FIGURE 2 - Plan of trench showing joint locations and excavation sample locations

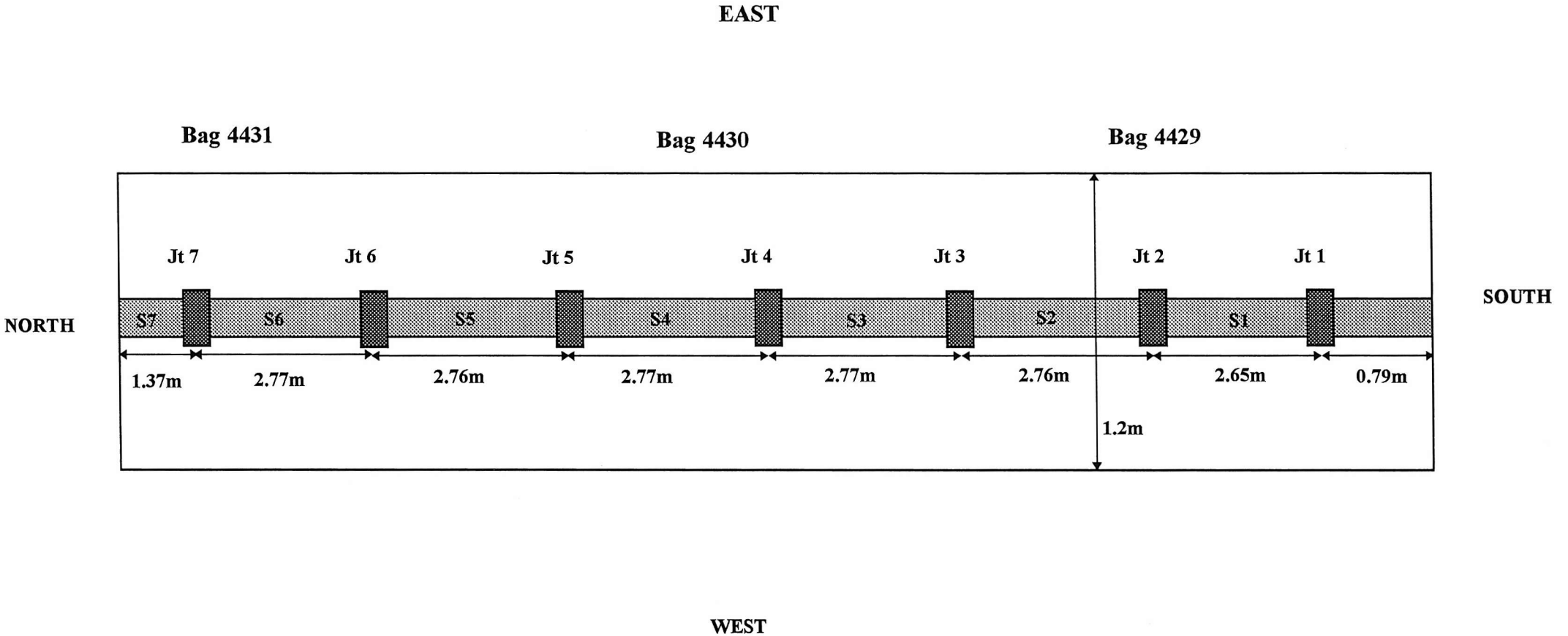

Figure 1 View of excavated trench, from north end

Figure 3 Use of pipe cutter in removal of pipe segments

Figure 4 Use of wedge in removal of pipe segments

Figure 5 Joint 1

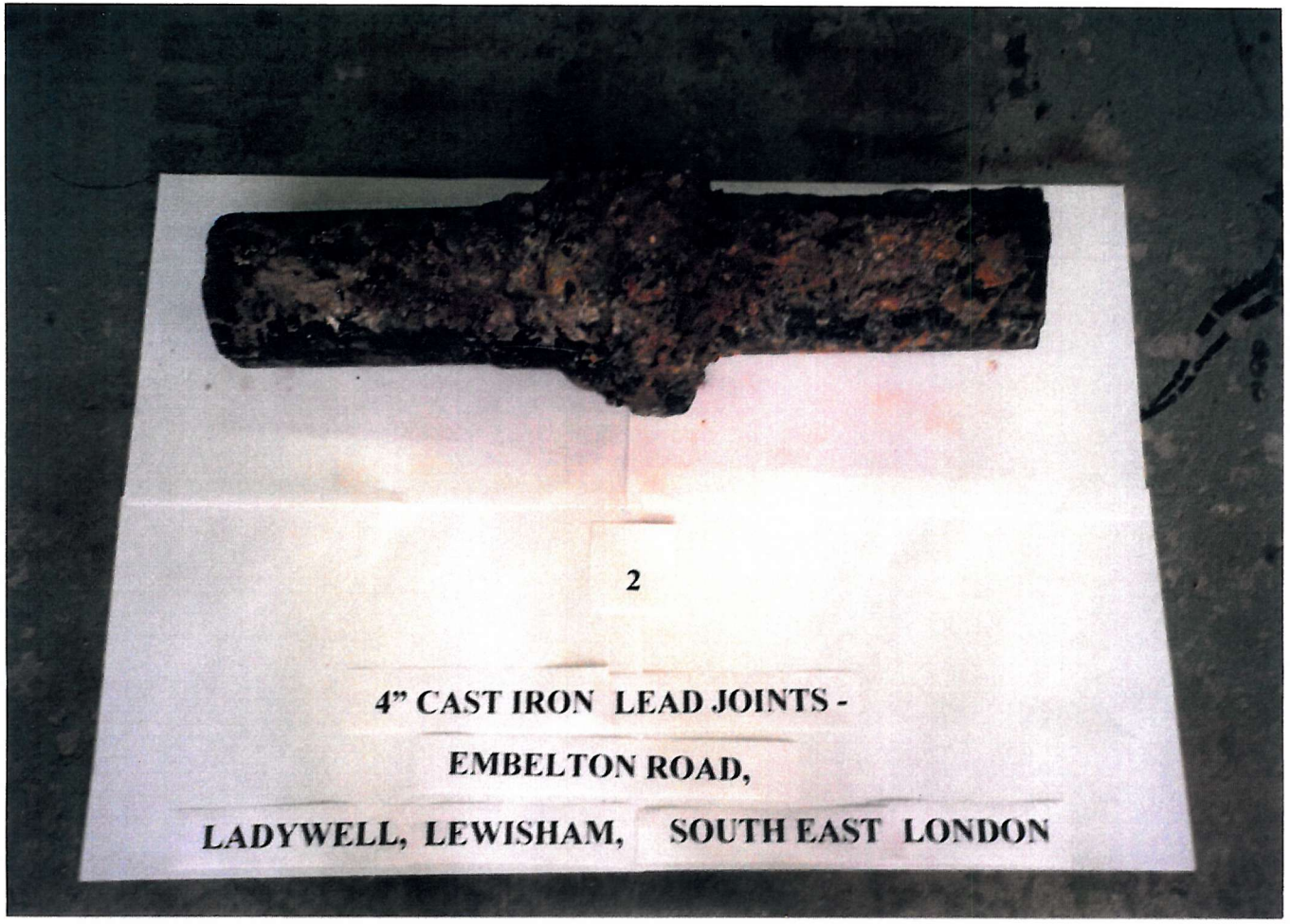

Figure 6 Joint 2

Figure 7 Joint 3

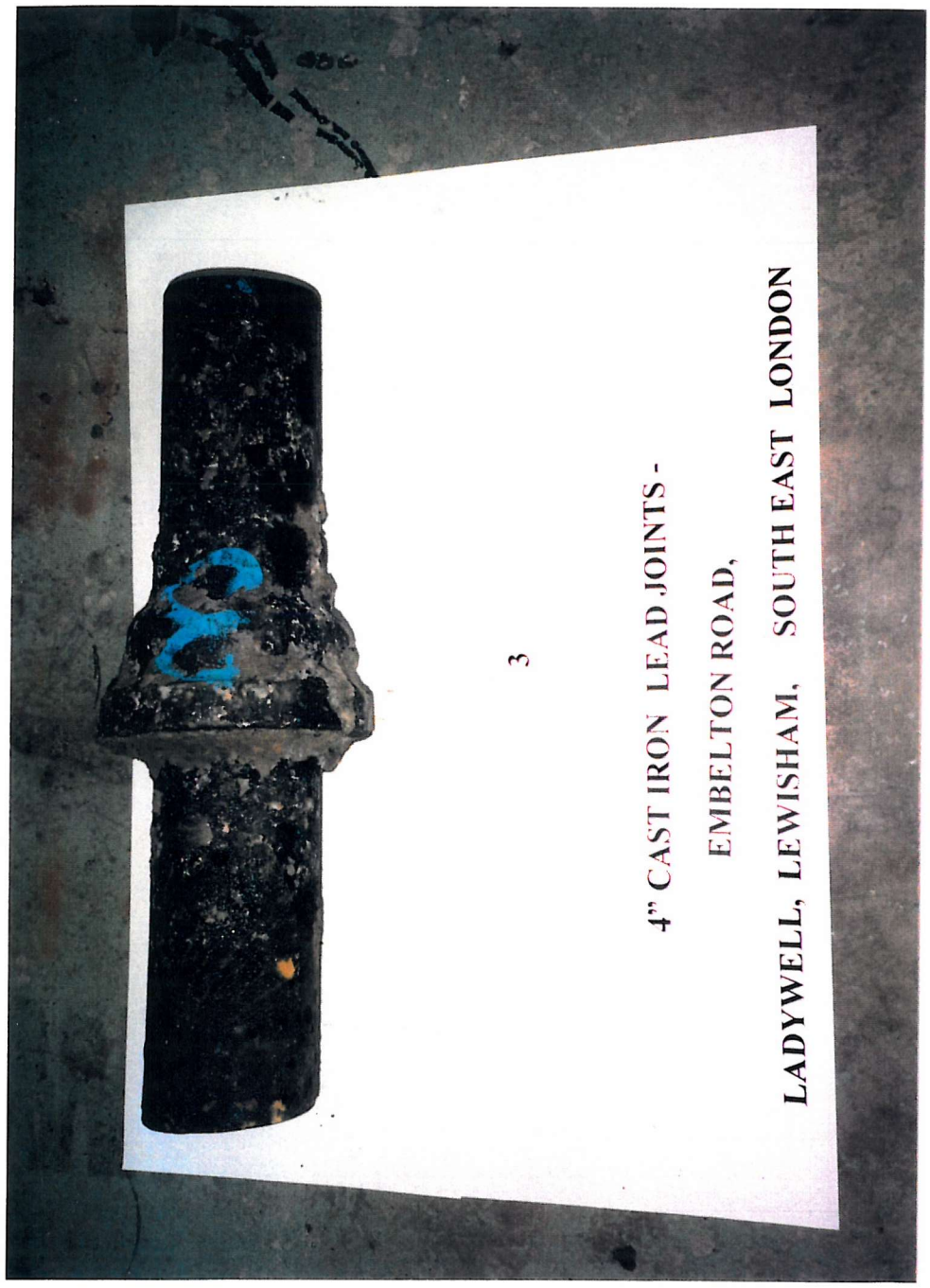

Figure 8 Joint 4

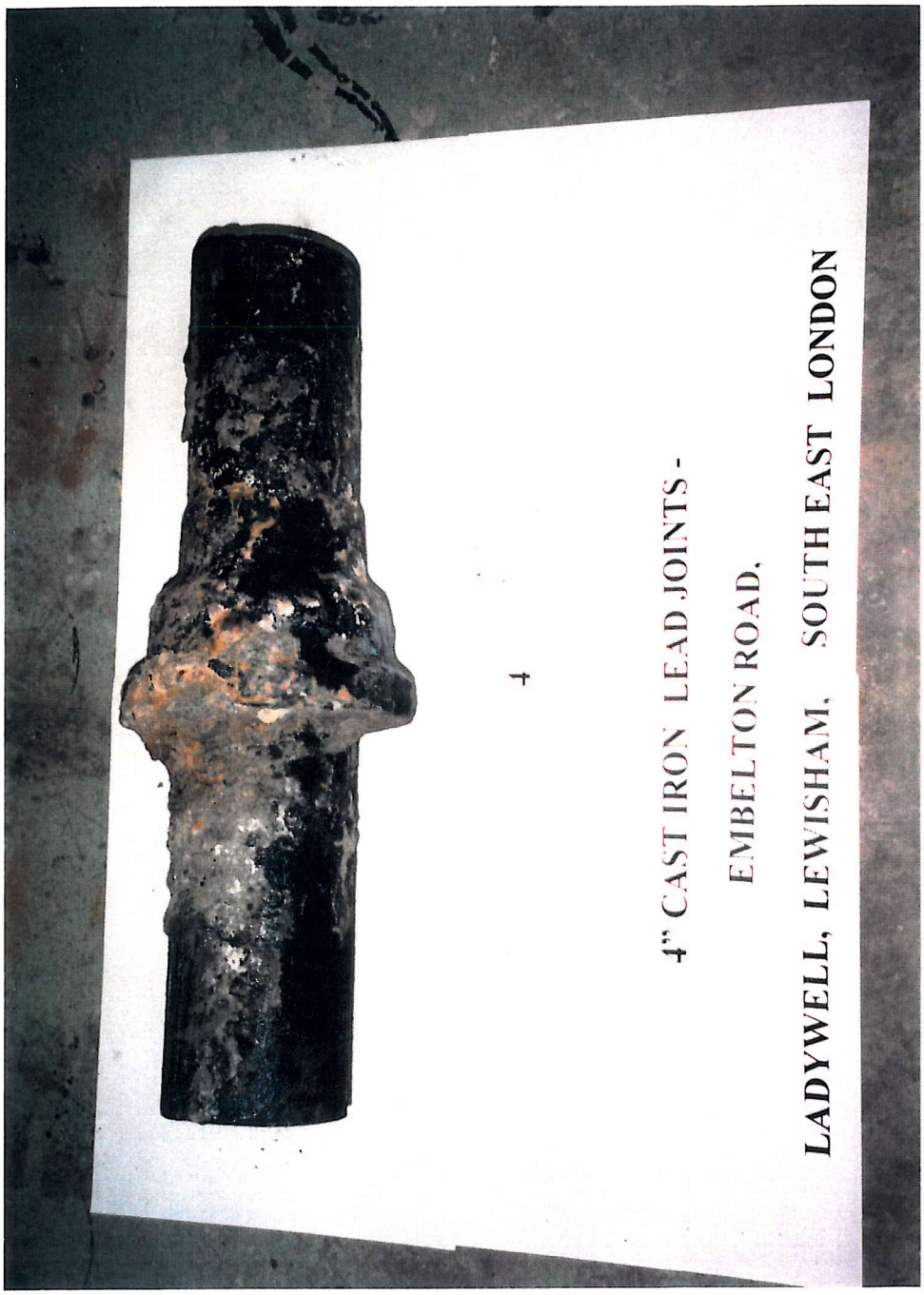

Figure 9 Joint 5

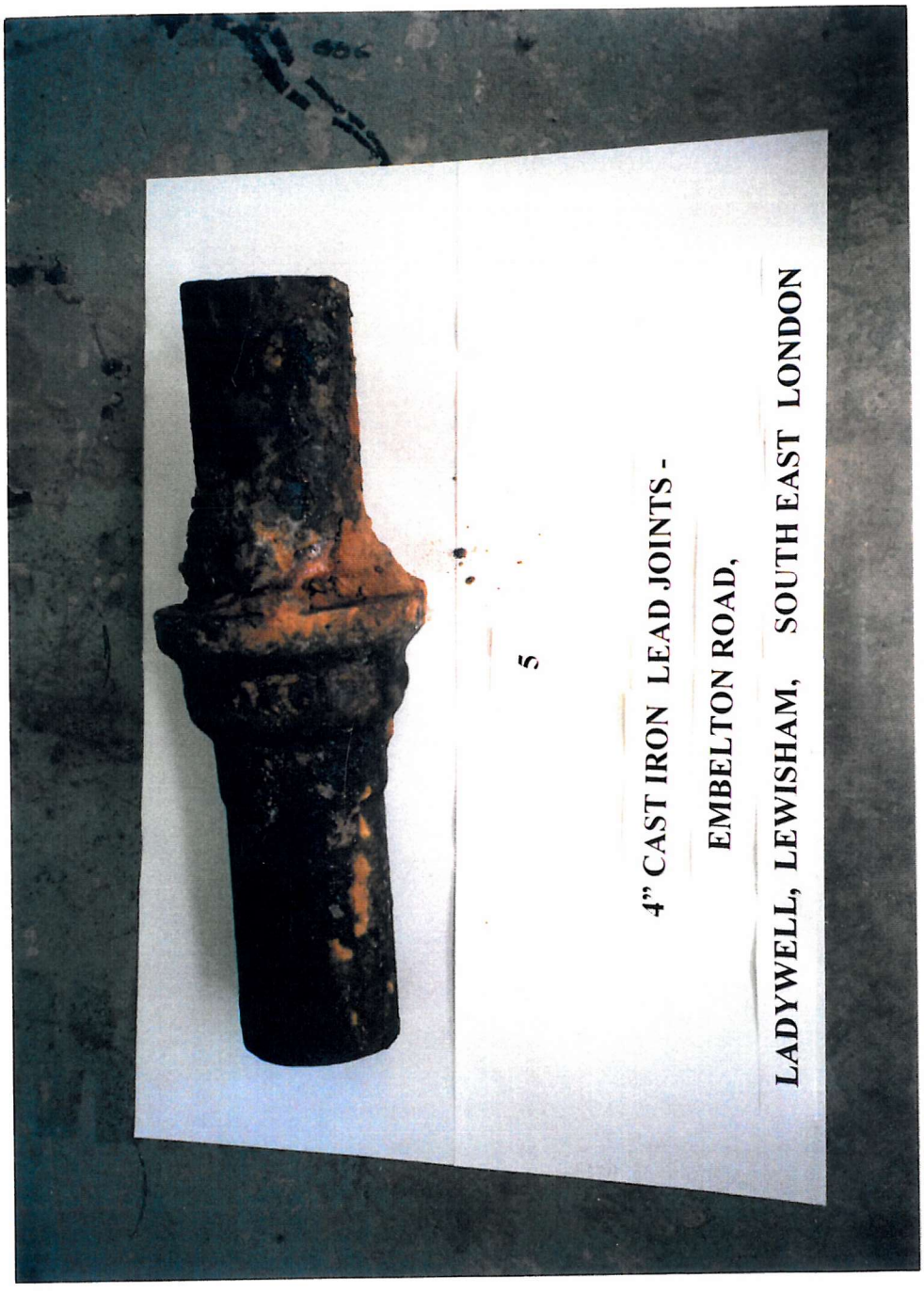

Figure 10 Joint 6

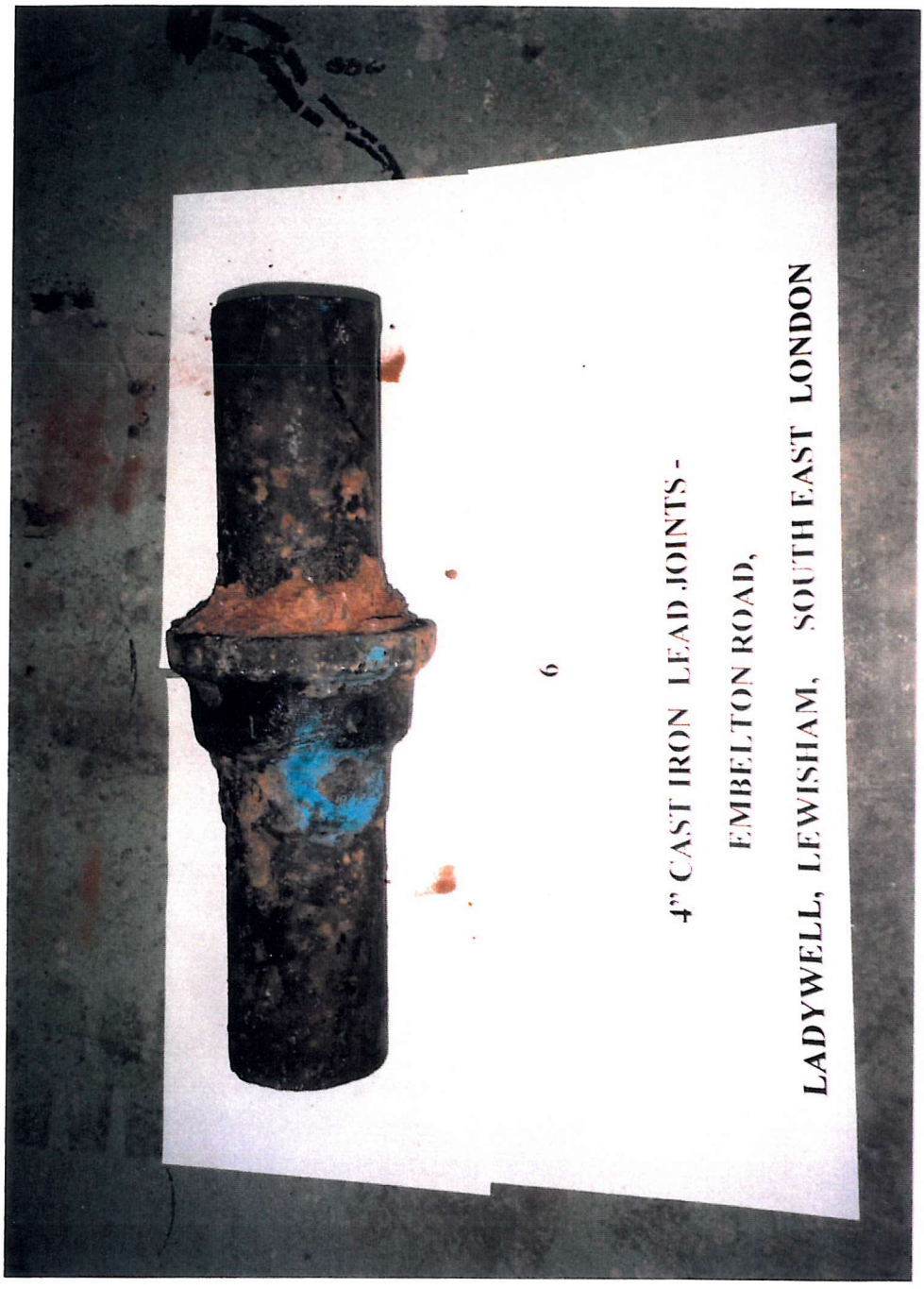

Figure 11 Joint 7

Figure 12 North end of trench, showing asphalt, sub-base and pipe backfill (sand)

Figure 13 South end of trench, showing asphalt, sub-base and pipe backfill (clayey sand)

PIPE and JOINT EXHUMATION

THEED/ROUPELL STREET
(London, SE1)

2nd December 1998

PIPE and JOINT EXHUMATION
THEED/ROUPELL STREET LONDON SE1, 2nd December 1998

INTRODUCTION

This report presents a factual summary of the pipe exhumation at Theed/Roupell Street in Waterloo (SE1), on 2nd December 1998. It is intended for use as a reference by the groups involved in research linked to the site, Thames Water Utilities and the University of Surrey (materials and geotechnics groups).

A section of Theed/Roupell Street was fenced off to replace the existing cast iron pipe with MDPE pipe, as this area was thought to have previous failure history. On 2nd December 1998, a trench (A) along the axis of the pipe was excavated (Figure 1). In the morning of the 2nd December, the mains supply through the pipe was interrupted and a section of approximately 10m of the pipe was removed (3 inch diameter cast iron pipe from Theed Street). Samples of the pipe, joints and soil were taken. A new section of MDPE pipe was then fitted between the remaining iron main permitting resumption of water supply. The site work was carried out by Morrisons.

A second section of pipe was removed from Theed Street on the 17 December 1998. This work was not carried out during the first excavation, as the direction of the pipe deviated into the centre of the road, and would therefore result in a road closure.

On 16 December 1998 the area was fenced off and trench (B) was excavated. The mains supply was shut off and pipe removal was carried out on the 17 December 1998. The pipe section was replaced with 125mm diameter MDPE. The layout of the pipe section can be seen in Figure 3.

IN-SITU OBSERVATIONS

Trench (A), (10 m long, 1.2 m wide, 0.76 m deep approximately) was excavated along the axis of a 3" internal diameter cast iron main. The trench was located approximately 1m east of the kerb of Theed Street, and ran north-south.

Figures 2 presents a sketch of the features and dimensions observed in the east wall of the trench (A), and notes the joint locations.

The invert of the pipe was 0.7 to 0.8 m below the road surface. Along the 10m length of the trench the backfill was varied, consisting of soil, rubble, sticks, bricks etc. (Disturbed, bag samples of the material have been acquired). Half way along the trench a repair collar could be seen, here the surrounding soil support was gravel, disturbed bag samples were taken.

The surrounding housing had a Victorian style, three storey, terraced houses. At the north end of the trench on the road above was a stop clock cover marked "MWB", Metropolitan Water Board.

Trench (B) (12.3m long, 1.2m wide and 0.75m deep approximately) was excavated along an axis of 3" cast iron pipe (Figure 3). The soil type appeared to be made up ground with the exception of two isolated areas, both approximately 0.3m in diameter where a clayey soil was present. Soil samples were taken at both these locations from underneath the pipe.

PIPE and JOINT SAMPLES

The pipe was detached from the network in four parts. All pipe segment were removed by cutting a slot through the pipe with a disc cutter and hammering a wedge into the slot.

In trench (A) the pipe included three pipe joints, one cast iron collar and repair collar (2, 3, 4) and four pipe sections (1, 2, 3, 4). The pipes and joints were numbered in

situ. Each pipe section was marked on the crown and also on the southern most end. The details of the pipe and joint samples obtained, and the destination of the samples, are:

University of Surrey (materials research)

Trench (A)

Pipe section 2 (1.07 m length, from south end of trench)

Pipe section 3 (2.00 m)

Pipe section 4 (2.10 m, from north end of trench)

Trench (B)

Pipe section 0 (0.38 m length, from south end of trench)

Pipe section 1 (1.66 m)

Pipe section 2 (2.1 m)

Pipe section 3 (1.94 m)

Pipe section 4 (1.9 m)

University of Surrey (geotechnics group)

Trench (A)

Joint A2 (0.61 m long), between pipe sections 2 and 3 (Figure 4)

Joint A3 (0.60 m long), between pipe sections 3 and 4 (Figure 5)

Joint A4 (0.71 m long), between pipe sections 4 and end of trench (Figure 6)

Trench (B)

Joint B1• (0.89 m long), between pipe sections 1 and 2

Joint B2• (0.61 m long), between pipe sections 2 and 3

Joint B3• (0.51 m long), between pipe sections 3 and 4

Joint B4• (0.64 m long), between pipe sections 4 and end of trench

SOIL SAMPLES

Four disturbed bag samples were obtained from the base of the trench immediately beneath the three joints and the repair collar. Trench (A) was dry when the samples were taken. Three soil samples were taken from trench (B). The samples have been delivered to the University of Surrey (geotechnics group).

Details of the samples are:

Trench (A)

Bag 0495 small bag sample from beneath repair collar

Bag 0494 small bag sample from beneath joint A3

Bag 0493 small bag sample from beneath joint A1 (cast iron collar)

Bag 0496 small bag sample from beneath joint A2

Trench (B)

Soil sample S1 small bag sample just right from joint B1•, 0.75m deep

Soil sample S2 small bag sample just right from joint B3•, 0.7m deep

Soil sample S3 small bag sample from underneath parallel main, 0.75m deep

Unfortunately photographs of trench (B) were not available.

Figure 1 View of excavated trench, from north end

FIGURE 2 - Plan of trench (A) showing joint locations and excavation sample locations

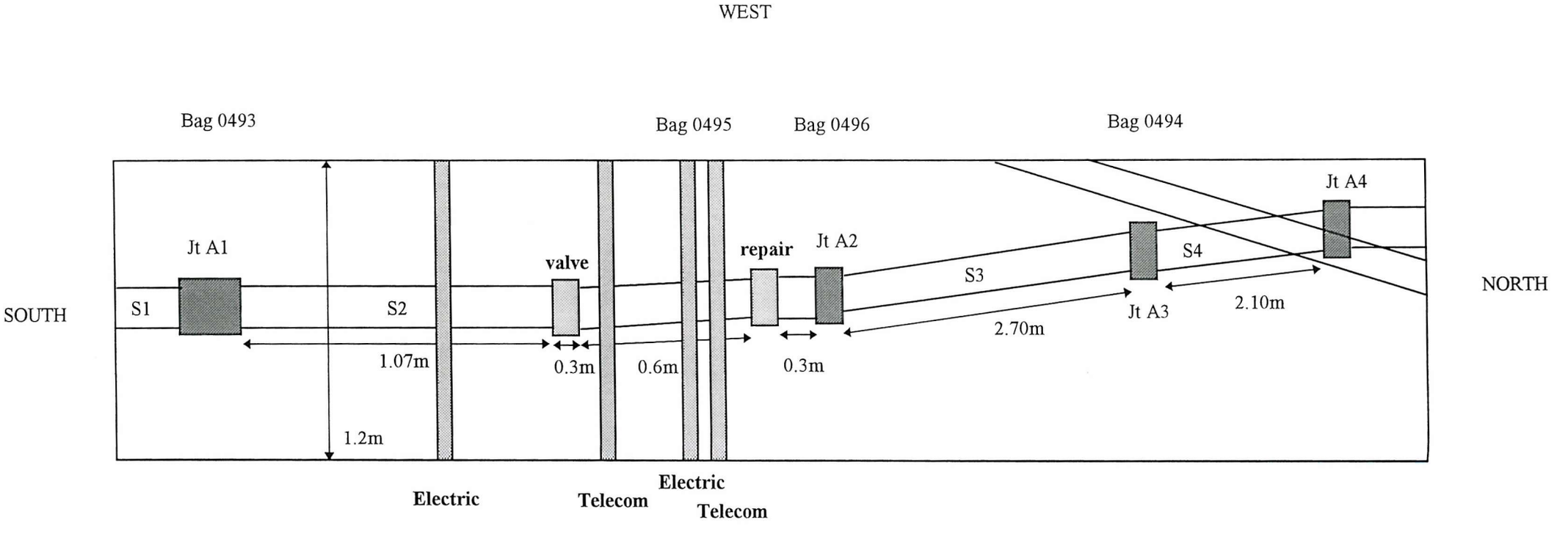

FIGURE 3 - Plan of trench (B) showing joint locations and excavation sample locations

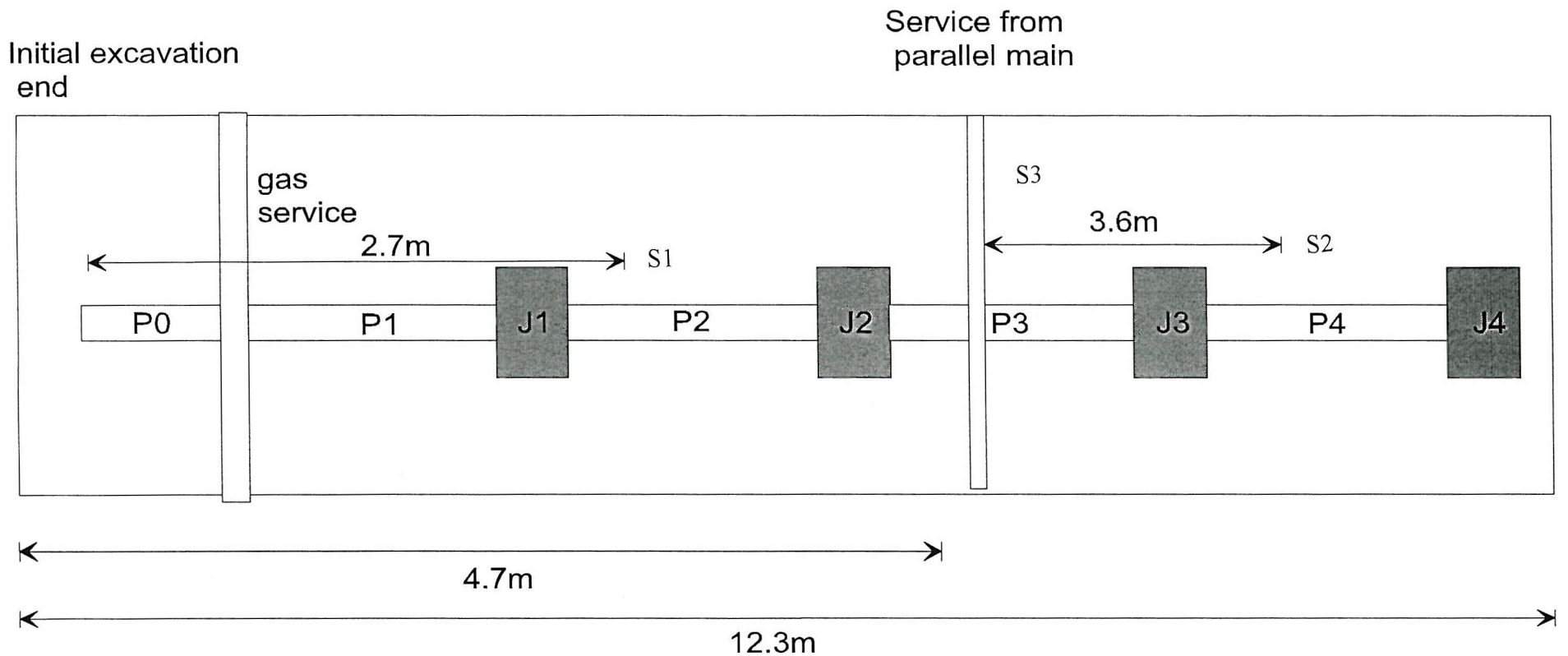

P = pipe section
J = joint section
s = soil sample taken

Figure 4 Joint A2

Figure 5 Joint A3

Figure 6 Joint A4

Figure 7 North end of trench (A)

Figure 8 South end of trench (A)

APPENDIX B – CALCULATIONS

APPENDIX B

Temperature load

The following calculation estimate the effect that a temperature drop could have on a fixed rigid pipe:

Cast Iron Pipes

Outside radius, r_1	= 60 mm
Inside radius, r_2	= 50 mm
Coefficient of thermal expansion, α	= 11 x 10^{-6}/°C
Design tensile strength	= 110 GPa
Young's Modulus, E	= 110 kN/mm^2
Change in temperature, Δt	= 20°C

Combining the equations for Young's Modulus ($E = \sigma/\varepsilon$) and strain due to temperature change ($\varepsilon = \alpha.\Delta t$) yields the stress induced when a temperature change is applied to a fixed pipe:

$$\sigma = E.\Delta t.\alpha \qquad (1)$$

Substituting the values above leads to:

$$\sigma = 11 \times 10^{-6}. 20 .110 \times 10^{3} = 24.2 \text{ N/mm}^2 \qquad (2)$$

The axial tensile load induced depends upon the cross-sectional area. For a pipe with an outside radius of 60mm and an inside radius of 50 mm the tensile load (R) equals:

$$R = \sigma.A = 24.2.\pi\left[60^2 - 50^2\right] = 84kN \qquad (3)$$

Traffic Load

According to the Ministry or Transport, the maximum load that a HGV may carry today falls into four categories: 38, 40, 41 and 44 tonnes. Each vehicle weight uses a different number of axles and varying number of wheels.

Legally, the worst case of loading results from a 38 tonne HGV, with 5 axles and 12 wheels.

$$\text{Load per wheel} = 38 \cdot 9.81 / 12 = 31.1 \text{ kN}$$

The load per wheel should be multiplied by an impact factor of 1.3 (BS153:1954) to simulate the effects of speed and average road surface, and therefore the maximum wheel load (F) = 40.4 kN

The amount of stress this wheel load could cause on a pipe crown depends on how much surface area of the tyre is in contact with the ground. Three different types of wheels can be used to carry lorry loads; single, twin and super single. The inflation pressures of these wheels are 120, 100 and 125 lb/in^2 respectively.

In reality a pressure of $120lb/in^2$ is generally used by HGV drivers for all tyres. Again taking the worst case scenario, a single wheel with a pressure of $120lb/in^2$ has a contact pressure (P) of approximately:

$$P = 120 \text{ lb/in}^2 = 0.827 \text{ N/mm}^2.$$

Therefore the contact area, A

$$A = \frac{F}{P} = \frac{40.4}{0.827} = 48851 \text{ mm}^2$$

This contact area is equivalent to a 0.22 m x 0.22 m square or a 0.125 m radius circle.

Soil Spring Supports

Using an approximation of the elastic solution for soils:

$$\rho = \frac{1.5 * q * B}{E} \qquad (1)$$

Where q is the stress, B is the width of loaded area, E is the Young's modulus and ρ is the settlement.

$$k = \frac{q}{\rho} \qquad (2)$$

Rearranging equation (1) and (2)

$$k = \frac{E}{1.5B} \qquad (3)$$

For an average soil E = 50Mpa, B=0.1m, assuming an infinitely long pipe

Therefore k = 0.3 $N/mm^2/mm$

APPENDIX C

APPENDIX C

Lusas version 13 was used for the analyses carried out in this thesis. Lusas is an associative feature-based Modeller. The model geometry is entered in terms of features which are sub-divided into finite elements in order to perform the analysis. The features in Lusas form a hierarchy, that is Volumes are comprised of surfaces, which in turn are made up of Lines or Combined Lines, which are defined by Points.

Some basic assumptions were made about the material in order to carry out this analysis. Cast iron was assumed to be elastic: this was due to lack of resources and time required to carry out elastoplastic analyses. The calculated stresses were compared with the ultimate tensile strength of the material to establish when the model was close to failure. Only the principal stress was reported as, due to the nature of the loading conditions, the failure modes were associated with the direct stress in the longitudinal direction.

The soil was modelled by means of applied pressures and linear elastic springs. This approach is somewhat simplistic and crude, but was a consequence of the programme used and constraints on the time and resources available. It was considered reasonable to focus on the pipe in this study, as it was the interaction of various loads on the pipe and the behaviour of the joint that were the main areas of uncertainty.